

OPTIMAL CONTROL, SELF-TUNING TECHNIQUES AND
THEIR APPLICATIONS TO DYNAMICALLY POSITIONED VESSELS

by

PATRICK TZE-KWAI FUNG

A thesis submitted to the Council For
National Academic Awards in partial fulfillment
of the requirements for the degree of
Doctor of Philosophy

The research was conducted at Sheffield City
Polytechnic in collaboration with GEC Electrical
Projects Ltd., Rugby

OCTOBER 1983

OPTIMAL CONTROL, SELF-TUNING TECHNIQUES AND
THEIR APPLICATIONS TO DYNAMICALLY POSITIONED VESSELS

Patrick T K Fung

ABSTRACT

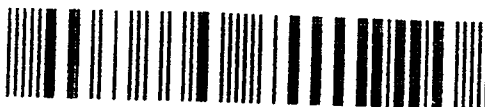
This thesis consists of two parts. The development of a self-adaptive stochastic control system for dynamically positioned vessels is described in Part One. Part Two is the investigation and the development of self-tuning control techniques.

In Part One, the dynamic ship positioning control problems and basic components are described. The modelling techniques of low frequency ship motions and wave motions are given. The various Kalman filtering methods are appraised. An optimal state feedback control with integral action for the ship positioning system is proposed, followed by the simplification of the complex control structure to allow easy implementation. A self-tuning Kalman filter is proposed for systems which have low frequency outputs corrupted by high frequency disturbances. This filter is used in the ship positioning system. Simulation results of scalar, multivariable and non-linear cases are given.

Part Two begins with the development of an adaptive tracking technique for slowly varying processes with coloured noise disturbances. Estimated results for various wave signals are given. The self-tuning control techniques are overviewed, followed by the development of an explicit multivariable weighted minimum variance controller. Simulation results including the estimation of system time delay are given. Finally, an implicit weighted minimum variance controller for single input-single output system is developed.

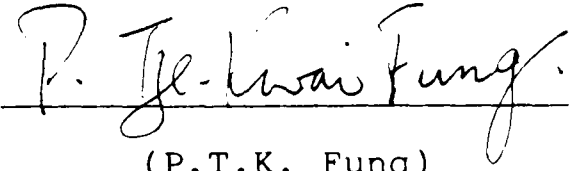
793290501 X

TELEPEN



DECLARATION

This is to declare that the author, while registered as a candidate for the degree for which the submission of this thesis is made, has not been a registered candidate for another award of CNAA or of a university during the research program.


(P.T.K. Fung)

This thesis is dedicated to my beloved wife, Kam,
and daughter, Ruth, who fill my life with joy and
many blessings.

ACKNOWLEDGEMENTS

The work presented in this thesis was basically completed at the end of 1981. However, a series of exciting events happened thereafter: the removal of the research team from Sheffield City Polytechnic to the University of Strathclyde; the coming of the author's daughter to his family; immigration to Canada and taking up a new appointment at Spar Aerospace. The author is indebted to Professor Mike J. Grimble for his encouragement, inspiration and guidance throughout the project, particularly for his patience to this belated presentation.

The author would also like to express his sincere gratitude to the following:

Dr. P.J. Gawthrop, for his advice on self-tuning techniques.

Mr. D. Wise and Mr. P. Urry, for their technical supervision.

Dr. T.J. Moir and Dr. A. Al-Takie for their helpful discussions throughout the research work.

Mr. N. Roger and Mr. Apperly, both with Spar Aerospace Ltd., for reviewing the manuscript.

Mrs. P. Cheung, the author's Godmother, for her support and encouragement during his study in Britain.

British Science and Engineering Research Council, for their financial support of the project.

GEC Electrical Projects Ltd., for their technical support of the project on dynamic ship positioning.

Department of Electrical and Electronic Engineering of Sheffield City Polytechnic and of the University of Strathclyde, for providing the facilities for the research work.

Spar Aerospace Ltd., RMS Division, for providing the typing facility.

Mrs. Cathy Nowik, Mrs. Cathy Atkins and Barbara Parkin for their excellent typing of a difficult manuscript.

Finally, but not least, Brothers and Sisters-in-Christ, particularly in Sheffield Chinese Christian Fellowship, whose faith, prayer, support and practical help throughout this study are gratefully acknowledged.

C O N T E N T S

	<u>Page</u>
ACKNOWLEDGEMENTS	iii
ABSTRACT	xiv
CONTRIBUTIONS AND PUBLICATIONS	xvi
INTRODUCTION	xx
PART I	
CHAPTER ONE	
DYNAMIC SHIP POSITIONING SYSTEM	1
1.1 Introduction	1
1.2 Control Problems	2
1.3 Basic Components	5
1.3.1 Sonar Measurement System	5
1.3.2 Taut Wire Measurement System	8
1.3.3 Radio Measurement System	8
1.3.4 Thrusters	11
1.3.5 Wind Speed/Direction Measurement System	11
CHAPTER TWO	
DYNAMIC MODELLING OF VESSEL MOTIONS	14
2.1 The Motions of Vessels	14
2.2 The Non-Linear Low Frequency Ship Model	17
2.3 The Linearized Low Frequency Ship Model	19

Contents (continued)	Page
2.4 Thruster Allocation Logic	21
2.5 The Non-Linear Thruster Model	22
2.6 The Linear Thruster Model	29
2.6.1 First Order Approximation	29
2.6.2 Second Order Approximation	29
2.7 The Dynamic Models of Wimpey Sealab	30
2.7.1 The Low Frequency Model	32
2.7.2 The Noise Covariance Specifications	37
2.8 High Frequency Models	38
2.8.1 Rational Proper Transfer Function Model	39
2.8.2 Auto-Regressive Moving Average Model	45
2.8.3 Harmonic Oscillation Model	46
2.8.4 Simulation of High Frequency Motions	48

Contents (continued)

Page

2.9	The Linear State Space Equations for Ship Motions	49
		52
CHAPTER THREE	THE KALMAN FILTERING PROBLEMS OF DYNAMIC SHIP POSITIONING SYSTEMS	52
3.1	The Estimation Structure	55
3.2	Extended Kalman Filter Using Harmonic Wave Model	59
3.3	Constant Gain Linear Kalman Filter	60
3.4	Extended Kalman Filter Using Four Order Wave Models	61
CHAPTER FOUR	THE STOCHASTIC OPTIMAL CONTROL PROBLEM IN DYNAMIC POSITIONING SYSTEMS	61
4.1	Introduction	61
4.2	Optimal Controller Design Philosophy	63
4.3	Optimal Controller with Integral Action	65

Contents (continued)		Page
4.3.1	System Description	65
4.3.2	Optimal Regulating Problem	69
4.3.3	Control Problem	74
4.3.4	Filtering Problem	90
4.3.5	Stability of Closed Loop Output Feedback System	97
4.3.6	Implementation on the Dynamic Ship Positioning System	100
4.4	Simplified DP Integral Control Systems	103
4.4.1	System Models	103
4.4.2	Control System Design One and Simulation Results	107
4.4.3	Control System Design Two and Simulation Results	111
4.4.4	Control System Design Three	116

Contents (continued)	Page
4.5 Summary of Results	116
CHAPTER FIVE THE SELF-TUNING KALMAN FILTER	119
5.1 Introduction	119
5.2 The System Description	121
5.3 The Low Frequency Motion Estimator	125
5.4 The High Frequency Motion Estimator	127
5.5 Modified Estimation Equations	129
5.6 Kalman and Self-Tuning Filter Algorithms	133
5.7 Discussion	137
5.8 Summary of Results	140
CHAPTER SIX THE USE OF SELF-TUNING KALMAN FILTERING TECHNIQUES IN DYNAMIC SHIP POSITIONING SYSTEMS	142
6.1 Introduction	142
6.2 Linear System Implementation	143
6.2.1 Single Input - Single Output Systems	143

Contents (continued)	Page
6.2.2 Multi Input - Multi Output Systems	157
6.3 Non-linear System Implementation	175
6.4 Self-Tuning Kalman Filter with Integral Control	189
6.5 Summary of Results	194

PART II

CHAPTER SEVEN THE ADAPTIVE TRACKING OF SLOWLY VARYING PROCESSES WITH COLOURED NOISE DISTURBANCES	195
7.1 Introduction	195
7.2 System Description	196
7.3 Tracking and Filtering Problems	199
7.4 The Design of Adaptive Estimator	200
7.5 Simulation Results	206
7.6 Summary of Results	213

Contents (continued)

Page

CHAPTER EIGHT	SELF-TUNING CONTROL AND WEIGHTED MINIMUM VARIANCE SELF-TUNERS	214
8.1	Introduction	214
8.2	Self-Tuning Control Overview	214
8.2.1	The Self-Tuning Control	214
8.2.2	The Development	217
8.2.3	Implementation, Advantages and Disadvantages	222
8.3	Explicitly Multivariable Weighted Minimum Variance Self-Tuning Controller	226
8.3.1	IntroductionSystem	226
8.3.2	Description	227
8.3.3	The Cost Function	229
8.3.4	Multivariable Weighted Minimum Variance Controller	230
8.3.5	Explicit Self-Tuning Control	234

Contents (continued)

Page

8.3.6	Discussion	237
8.3.7	Industrial Applications	240
8.4	Implicit Weighted Minimum Variance Self-Tuner	241
8.4.1	Introduction	241
8.4.2	Plant Description	241
8.4.3	Weighted Minimum Variance Controller	243
8.4.4	Implicit Self-Tuning Control	245
8.4.5	Discussion	251
CHAPTER NINE	OVERALL CONCLUSIONS AND FUTURE WORK	252
9.1	Overall Conclusions	252
9.2	Future Work	254

Contents (continued)

Page

REFERENCES	256
APPENDIX A TRANSFER FUNCTION WAVE MODELS FOR VARIOUS SEA CONDITIONS	285
APPENDIX B WIMPEY SEALAB PER UNIT SYSTEM SPECIFICATIONS	293
APPENDIX C DISCRETE KALMAN GAIN MATRIX COMPUTATION	295
APPENDIX D A RECURSIVE ALGORITHM FOR SMOOTHING AND PREDICTING OF A SIGNAL	298
APPENDIX E WEIGHTED MINIMUM VARIANCE CONTROLLER DERIVATION	300
APPENDIX F PUBLISHED PAPER	307

OPTIMAL CONTROL, SELF-TUNING TECHNIQUES AND
THEIR APPLICATIONS TO DYNAMICALLY POSITIONED VESSELS

Patrick T K Fung

ABSTRACT

This thesis consists of two parts. The development of a self-adaptive stochastic control system for dynamically positioned vessels is described in Part One. Part Two is the investigation and the development of self-tuning control techniques.

In Part One, the dynamic ship positioning control problems and basic components are described. The modelling techniques of low frequency ship motions and wave motions are given. The various Kalman filtering methods are appraised. An optimal state feedback control with integral action for the ship positioning system is proposed, followed by the simplification of the complex control structure to allow easy implementation. A self-tuning Kalman filter is proposed for systems which have low frequency outputs corrupted by high frequency disturbances. This filter is used in the ship positioning system. Simulation results of scalar, multivariable and non-linear cases are given.

Part Two begins with the development of an adaptive tracking technique for slowly varying processes with coloured noise disturbances. Estimated results for various wave signals are given. The self-tuning control techniques are overviewed, followed by the development of an explicit multivariable weighted minimum variance controller. Simulation results including the estimation of system time delay are given. Finally, an implicit weighted minimum variance controller for single input-single output system is developed.

CONTRIBUTIONS AND PUBLICATIONS

Main Contributions

1. The developmment of the dynamic models and the analysis of the control design philosophy of ship positioning systems.
2. The analysis of the Kalman Filter problem and structures for ship positioning systems.
3. The development of stochastic optimal control systems including integral actions for dynamically positioned vessels.
4. The development of a self-tuning Kalman filter for systems with unknown high frequency disturbances.
5. The use of self-tuning Kalman filter for dynamically positioned vessels, which includes single input-single output, multivariable and non-linear cases.
6. The extension of the dynamic models for dynamic positioning control and filtering to include a second order linear thruster model.

7. The development of an adaptive tracking technique for slowly varying systems with coloured noise disturbances.
8. The development of an explicit multivariable weighted minimum variance controller.
9. The development of an implicit single input-single output weighted minimum variance controller.

Publications

1. Fung, P.T.K. and Grimble M.J. 1981, "Self-Tuning Control of Ship Positioning Systems" IEE Workshop on Self-Tuning and Adaptive Control, March, Oxford University, U.K. Also published by Peter Peregrinus Ltd. and edited by C.J. Harris and S.A. Billings.
2. Grimble M.J. and Fung P.T.K. 1981, "The Application of Kalman Filters and Self-Tuning Filters to Dynamic Ship Positioning Systems" Science and Engineering Research Council Vacation School, University of Warwick, U.K.

3. Grimble M.J. and Fung P.T.K. 1981 "Explicit Weighted Minimum Variance Self-Tuning Controllers" IEEE Conf. on Decision and Control, December, San Diego, Calif., U.S.A.
4. Grimble M.J. Johnson M.A. and Fung P.T.K. 1980 "Optimal Self-Tuning Control Systems: Theory and Application, Part I Introduction Controller Design", Trans. Inst. Measurement and Control, Vol. 2, No. 3, p115-119.
5. Grimble M.J., Fung P.T.K. and Johnson M.A. 1982, "Optimal Self-Tuning Control Systems: Theory and Application, Part II, Identification and Self-Tuning" Trans. Inst. Measurement and Control, Vol. 4, No. 1, p25-36.
6. Grimble M.J. Moir T.J. and Fung P.T.K. 1982, "Comparison of WMV and LQG Self-Tuning Controllers", IEEE Symposium on Multivariable and Stochastic Control Theory, Hull, U.K.
7. Fung P.T.K., Chen Y.L. and Grimble M.J., 1982, "Dynamic Ship Positioning Control Systems Design Including Non-linear Thrusters and Dynamics", NATO Advanced Study Institute on Non-linear Stochastic Problems, May, Algarve, Portugal. Also published in "Nonlinear

Stochastic Problems", NATO ASI series on Mathematical and Physical Sciences No. 104, Edited by R.C. Bucy and J.M.F. Moura, published by Reidel, 1983.

8. Fung P.T.K. and Grimble M.J. 1983 "Dynamic Ship Positioning Using a Self-Tuning Kalman Filter", IEEE Trans AC-28, No. 3, March, Special Issue on Applications of Kalman Filtering, p339-350.
9. Fung P.T.K. Chen X.P. and Grimble M.J. 1982", The Adaptive Tracking of Slowly Varying Processes with Coloured Noise Disturbances", Submitted Trans. Inst. Measurement and Control.

Reports

1. Fung P.T.K., 1980, "Optimal and Self-Tuning of Dynamically Positioned Vesels", Sheffield City Polytechnic Research Report, EEE/64.
2. Fung P.T.K. and Grimble M.J. 1982 "Dynamic Ship Positioning Using a Self-Tuning Kalman Filter", University of Strathclyde, Research Report No. EE/8/March.

INTRODUCTION

Objectives

The contents of this thesis are separated into two main parts. Part I involves the solution of the dynamic ship positioning control problem using optimal and self-tuning techniques. This is the main theme of the thesis. Part II is concerned with the development of adaptive and self-tuning control theory.

Introduction to Part I

The abundant deposits in the ocean seabed have become the targets for energy and mineral searches. The development is progressing towards deeper seas. Thence the demand for technical support by way of dynamically positioned vessels is increasing and the performance specifications are becoming tightened. Basically, the position control of a vessel must only allow for a maximum certain radial position error. The control system must avoid high frequency fluctuations in the thruster demands. Moreover, the controller must be capable of eliminating any offset due to constant disturbances.

In the conventional dynamic system using Proportional- Integral-Derivative (PID) controllers and notch filters, the wave filter imposes a phase lag on the position error signals. This phase lag restricts the allowable bandwidth that can be used for the controller, whilst still maintaining the stability margins required for satisfactory controller performance; hence an inevitable conflict arises between bandwidth and filter attenuation. The more effective the wave filter becomes in reducing the thruster oscillations due to the waves, the more restriction is placed on the controller bandwidth and hence on the position holding accuracy. These considerations have led to the development of a second generation of dynamic positioning systems, designed using optimal stochastic control theory and employing the Kalman filter.

The non-linearity and the uncertainty of ship parameters and weather conditions are the main obstacles in achieving a good performance for the control system. The recent development of the self-tuning control theory has encouraged the author to investigate the use of self-tuning techniques in dynamic ship positioning systems. Self-tuning of dynamically positioned vessels can be classified as the third generation in this development.

Introduction to Part II

When the author was solving the dynamic ship positioning control problem, he was encouraged by Professor M.J. Grimble to work on self-tuning control as well. This attempt led to the development of a self-adaptive tracker for slow varying processes with coloured noises and weighted minimum variance self-tuning controllers.

Self-tuning control, because of its practical utility, has received much attention since it was first developed in the early seventies. The self-tuning algorithms vary according to the controller design criteria used. Usually, several self-tuning algorithms may be generated using the same control criterion. The weighted minimum self-tuner is one example based on the weighted minimum variance control criterion and was developed particularly for the non-minimum phase system.

The self-adaptive tracker was primarily developed to estimate slowly varying signals with coloured noises. The approach was to gather as much information as possible based on the observed signal, and then estimate the remnant using recursive parameter identification techniques.

Outline of the Thesis

Chapter One is an introduction to dynamic ship positioning control problems and a description of the basic components for the control system. The dynamic models for controller and filter design are developed in Chapter Two. The fundamental dynamic positioning control problem consists of controller design and filtering. The Kalman filtering techniques are described in Chapter Three. In Chapter Four, an optimal and three sub-optimal schemes of stochastic control with integral action are developed. Chapter Five consists of the self-tuning Kalman filtering theory. The applications and results of self-tuning Kalman filter to DP (Dynamic Positioning) control system are discussed in Chapter Six. This includes single input/single output, multivariable and non-linear cases.

Chapter Seven is the development of an adaptive tracker for slowly varying processes corrupted by coloured noises, followed by simulation results. The self-tuning control techniques are surveyed in Chapter Eight, followed by the development of an explicit multivariable weighted minimum variance self-tuning controller and an implicit version for single input/single output systems. Finally, an overall conclusions and suggestions for future work are described in Chapter Nine.

CHAPTER ONE

DYNAMIC SHIP POSITIONING SYSTEMS

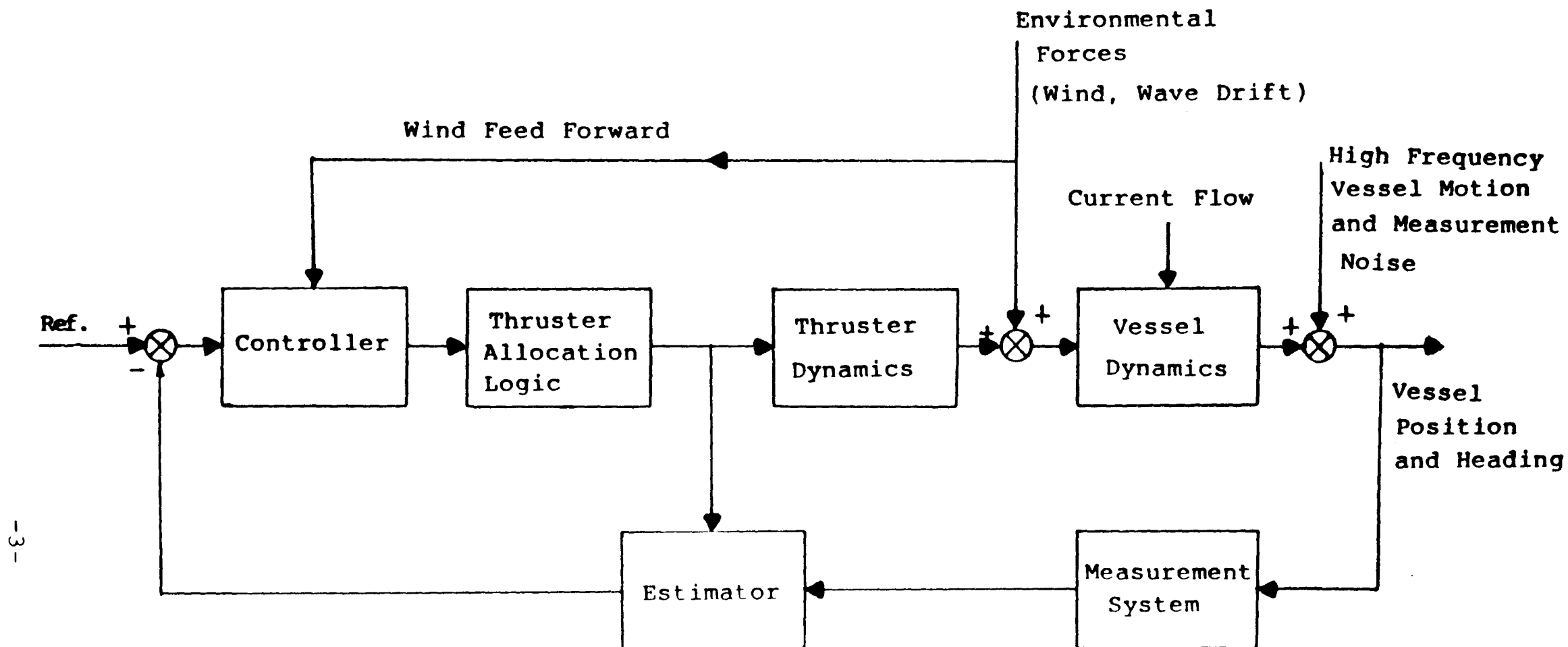
1.1 INTRODUCTION

The philosophy of dynamic ship positioning control is to maintain the position and heading of a ship or a floating platform above a pre-selected fixed position over the seabed by using the vessel's thrusters. It can be extended to include the tracking problem of a vessel at fixed speed. Its superiority over conventional positioning control technique is that the dynamic positioning (DP) system does not need anchor or mooring. It is particularly suitable for operation in deep seas such as the North Sea. The operation is efficient since there is no delay due to setting up and dismantling the anchors. It causes no damage to existing constructions on the seabed such as oil pipe lines. This type of vessel is used for several applications in the survey and development of off-shore mineral and oil resources and in oceanography. The number of countries involved in off-shore exploration is increasing rapidly. The manufacturers competing against GEC in the United Kingdom are mainly from Norway, United States and Japan.

1.2 THE POSITION CONTROL PROBLEMS

A DP system should be able to keep a vessel within specified position limits, with minimum energy consumption and with minimum wear and tear on the thrusters. The DP system should also cope with the time delay in the measurement system and the errors in the propulsion devices.

The control loops (Figure 1-1) for dynamically positioned vessels include filters to remove the high frequency wave induced motion signals. This is necessary because the thruster devices are not intended and are not rated to suppress wave induced motions greater than 0.3 radians per second. High frequency motions are generally tolerable in ship position control. The position control system must only respond to the low frequency forces on the vessel. The filtering problem is one of estimating the low frequency motions so that control can be applied. Notice that even though the position measurement includes a noise component, this does not cause the filtering problem. If the total position of the vessel were known exactly, there would still be a need to estimate the low frequency motions. A typical GEC duplex DP control system is shown in Figure 1-2.



- 3 -

FIGURE 1-1 The Main Elements of DP Systems

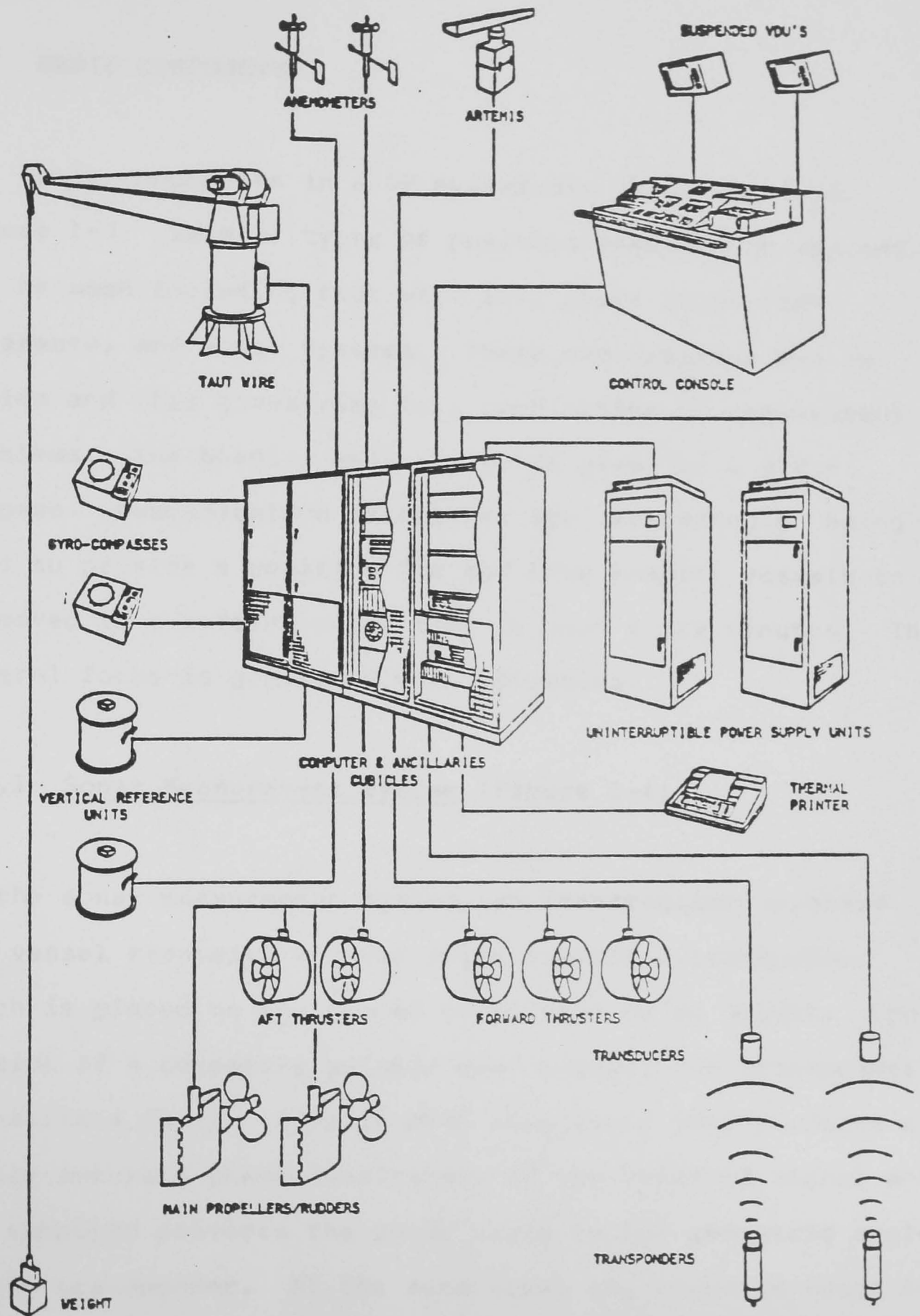


FIGURE 1-2

Typical GEC Duplex DP Control System

1.3 BASIC COMPONENTS

The basic components in a DP system are illustrated in Figure 1-3. Several types of position measurement systems can be used including taut wire [1], short range radio reference, and sonar systems. These measurements can be pooled and this gives rise to a combination of measurement problems. The heading measurement is given by a gyro-compass. Communication satellites are increasingly being used to provide a position fix and this enables vessels to be moved to a reference position in just a few minutes. The control force is generated from thrusters.

1.3.1 Sonar Measurement System (Figure 1-4)

In the sonar measurement system, an interrogator on board the vessel transmits a sound pulse towards a transponder which is placed on the seabed or mounted on an object. Upon receipt of a correctly pulsed/coded signal, the transponder transmits a reply. A split beam transducer then performs a highly accurate phase measurement of the received signal and the computer converts the phase angle to the geometric angle of the transponder. At the same time, the accurate range to the transponder is measured, which enables this system to determine the water depth.

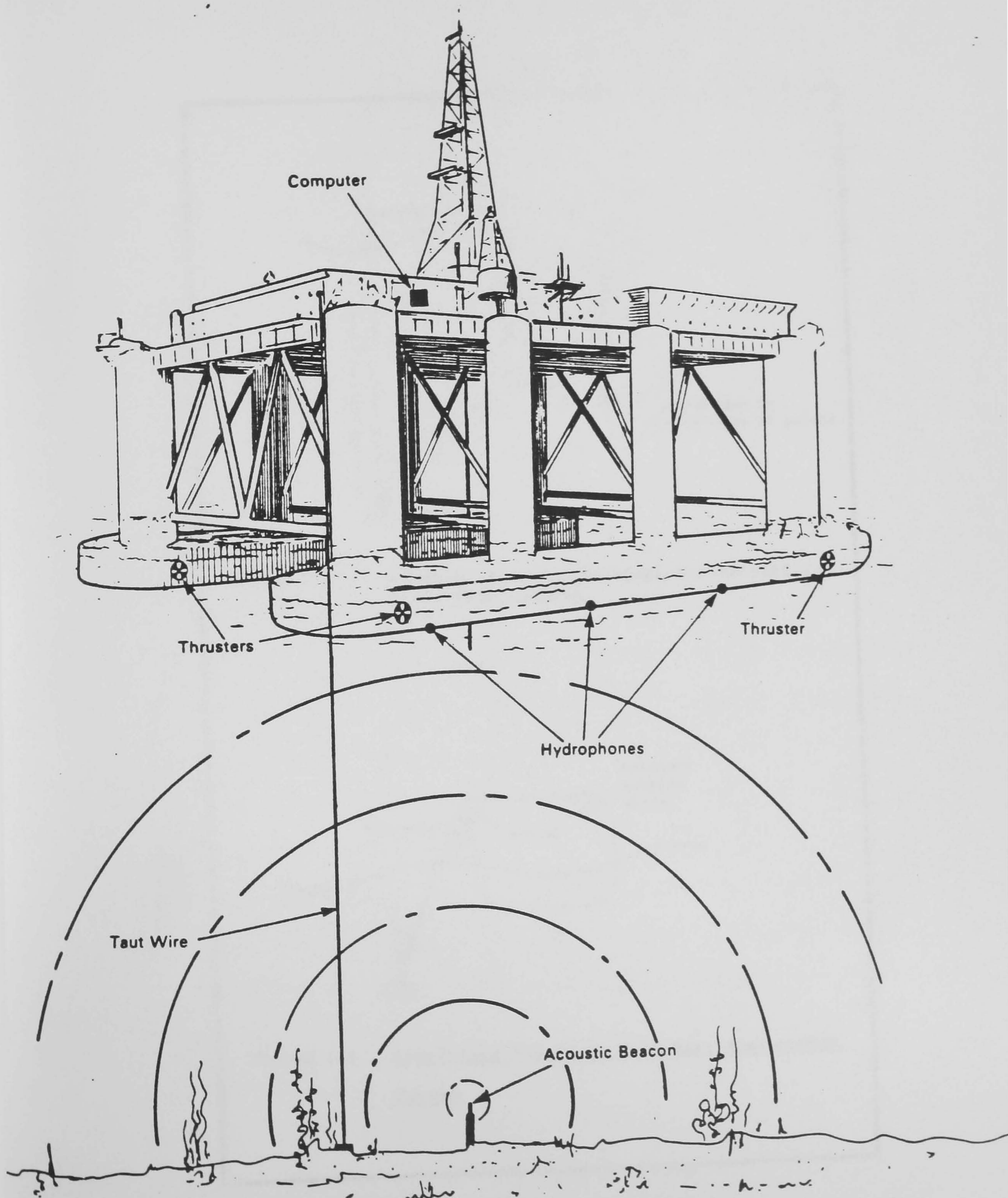


FIGURE 1-3 BASIC COMPONENTS IN DYNAMIC SHIP POSITIONING SYSTEM

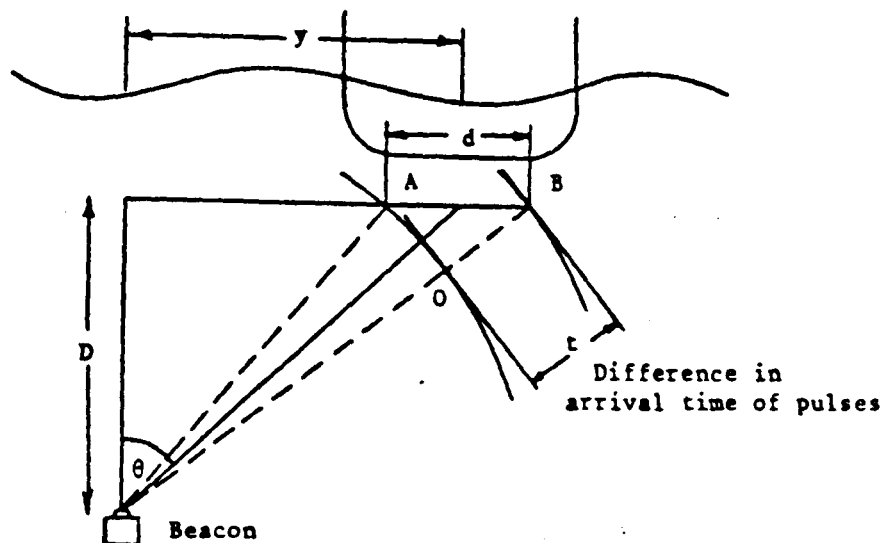


FIGURE 1-4 Simplified Two Dimensional Representation of Acoustic System

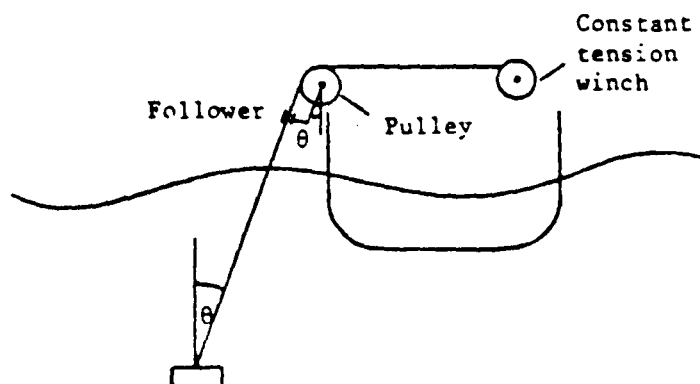


FIGURE 1-5 Simplified Diagram of Taut Wire Measurement System

There are many types of acoustic position measurement systems but the GEC/Marconi system was a single beacon on the seabed with a multi-head transponder on a pod beneath the vessel. The signals can be upset by gas bubbles from divers or from the ocean bottom. However, vessels often use more than one position reference system including taut wire, rig mounted radio beacons and satellite fixes.

1.3.2 Taut Wire Measurement System (Figure 1-5)

The taut wire system is a well established and reliable method of determining the horizontal position of a vessel relative to a fixed point on the seabed. The required seabed reference point is marked by a sinker weight lowered on a steel wire rope from the vessel. To sense the location of the vessel relative to the sinker weight, the rope is maintained under constant tension and the angle of rope from the vertical is measured in two orthogonal axes. The horizontal displacement of the vessel from the seabed reference point is the tangent of these angles multiplied by the water depth.

1.3.3 Radio Measurement System (Figure 1-6)

The position of off-shore vessels can also be measured by radio, satellite navigation, and inertial navigation

systems. These systems are used extensively for navigation and survey purposes. However, their position accuracy is not suitable for dynamic positioning. These measurement systems are suitable for applications such as mining and pipelaying. Nevertheless, the short range radio position reference system has a potential for future development. Its operating range is 50 Km with accuracy from 2 m to 20 m at a frequency of 3000 MHz. Basically, it has three modes:

- (a) circular,
- (b) range/bearing,
- (c) hyperbolic.

GEC adopts the Artemis range/bearing system (Figure 1-6). The artemis measuring system has the following advantages:

- (a) The fixed station equipment is portable and can be set up in approximately half an hour.
- (b) One fixed station is sufficient for position fixing of a vessel within line of sight.
- (c) The angular accuracy is independent on azimuth.
- (d) A very low radiated power.
- (e) A data channel is available for numerical data and voice communication.

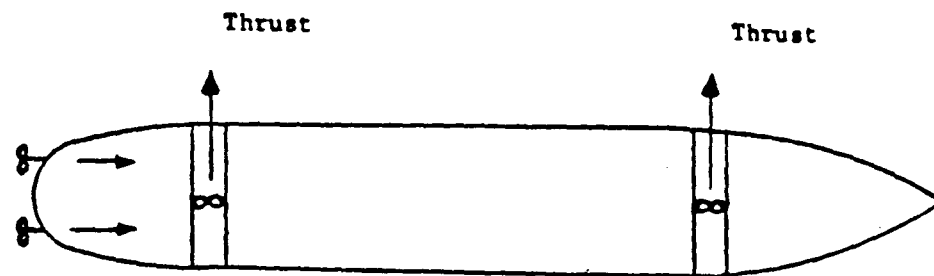
1.3.4 Thrusters

The thruster devices for positioning the vessel can take several forms (Figure 1-7) but the ship model used in the following analysis is based upon Wimpey Sealab which has retractable ac motor driven thrusters with variable pitch propellers. The vessel has two rotatable bow and two rotatable stern thrusters, capable of 360 degrees rotation and each rated at 12.5 tonnes. The detailed model of the thruster will be discussed in the next chapter.

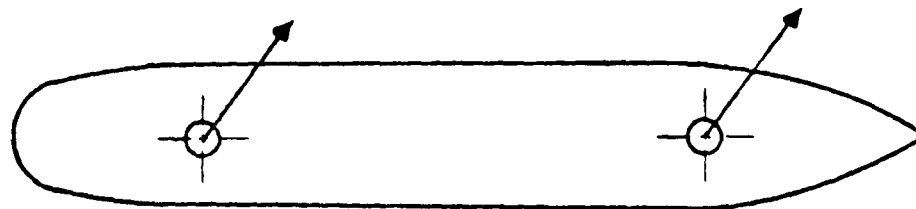
1.3.5 Wind Speed/Direction Measurement System

The wind force is normally regarded as an environmental disturbance. However, this force can be used in the feed forward loop, which has been shown to improve the control responses significantly. Wind speed and direction are measured by different sensors. However, a package unit consisting of the two sensors is available, which simplifies the installation and ensures these two parameters are measured at the same location.

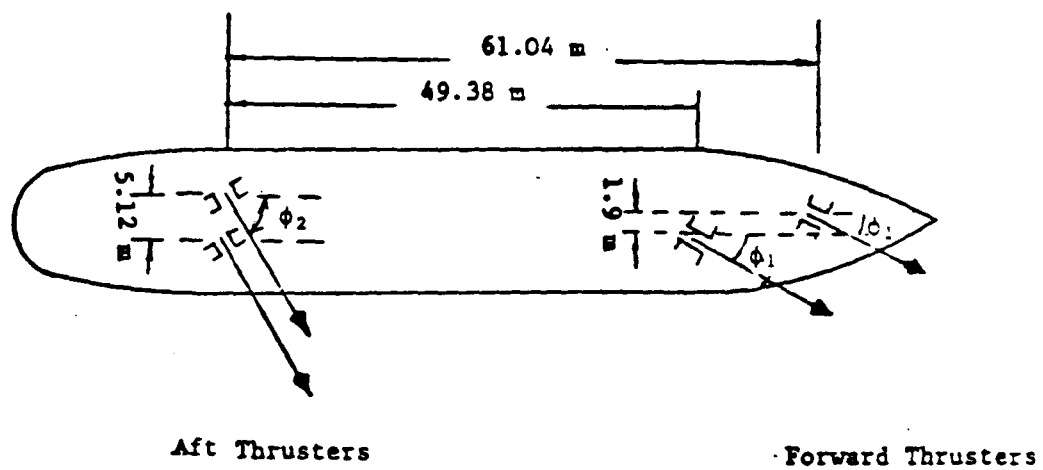
The most commonly used wind speed sensor employs a propeller to drive a small dc voltage generator. The voltage generated is approximately directly proportional to the speed of



(a) Fixed Transverse Tunnel Thrusters and Main Propellers



(b) Cycloidal Propellers



(c) Steerable Thruster Configuration for Wimpey Sealab

FIGURE 1-7 Possible Thruster Configurations

the wind. The output voltage can be calibrated as the measurement of the wind speed.

The wind direction sensor consists of a vane which rotates to track the direction of flow of the wind. Attached to the vane is an angle measuring device which exerts minimum drag on the vane. Commonly used wind sensors are linear potentiometer and synchro transmitters. The latter has the advantages over the former of avoiding discontinuity and wearing of the components.

CHAPTER TWO

DYNAMIC MODELLING OF VESSEL MOTIONS

2.1 THE MOTIONS OF VESSELS

The environmental forces acting on a vessel induce motions in six degrees of freedom (shown in Figure 2-1). In a dynamic positioning system, only vessel motions in the horizontal plane (surge, sway and yaw) are controlled. All the motions will be referred to the body axes of the vessel (shown in Figure 2-2). The assumption will be made that the low and high frequency vessel motions (Figure 2-3) can be determined separately and that the total motion is the sum of each of them. This is the usual assumption made by a marine engineer because the analysis is simplified and the low frequency motions can be predicted with more accuracy than the high frequency motions.

The low frequency motions are mainly due to thruster, current, wind and second order wave forces. These are normally less than 0.25 radians per second. The last three forces can cause the vessel to drift from its station, therefore, they must be counteracted by using the vessel's thrusters.

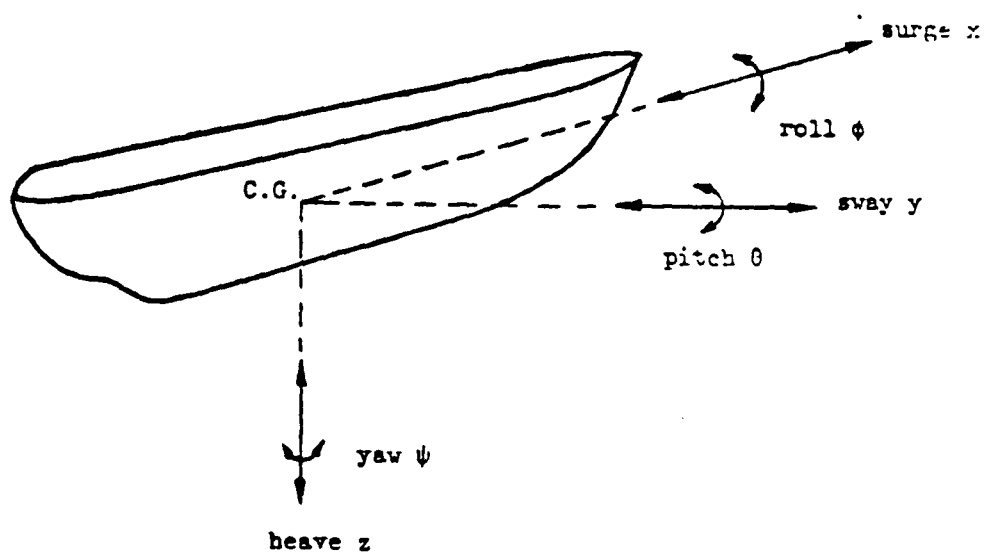


FIGURE 2-1 The Motions of Vessel on Sea.

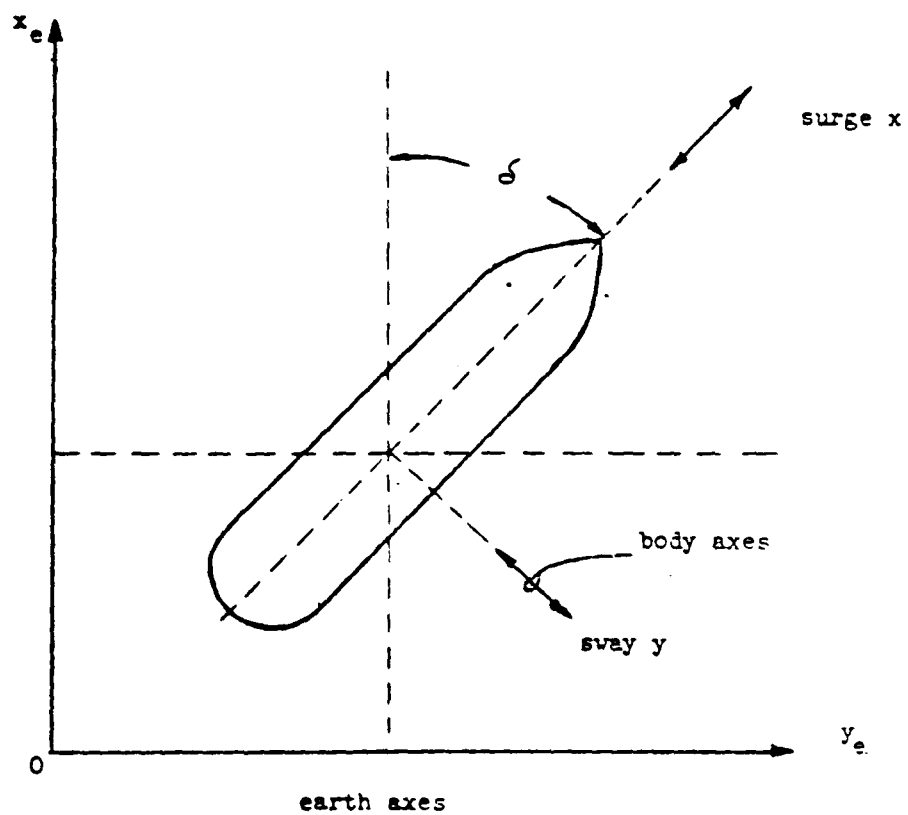


FIGURE 2-2 Earth and Body Axes Systems

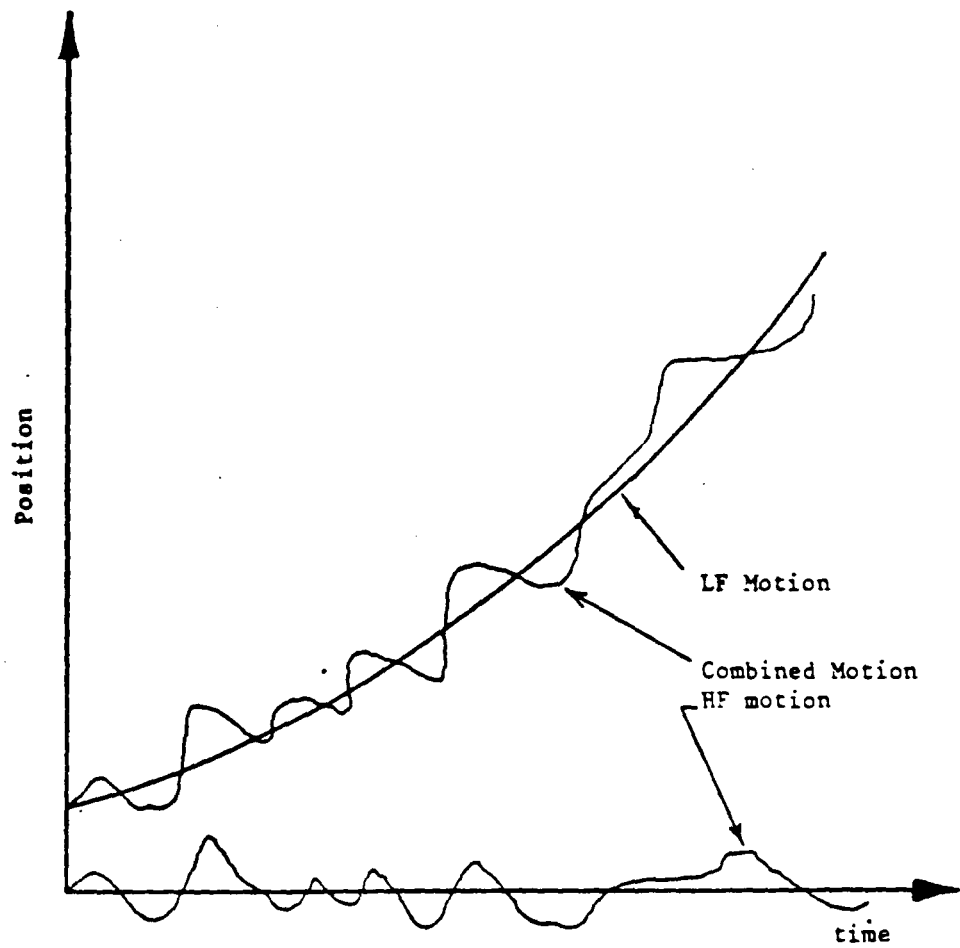


FIGURE 2-3 The Low and High Frequency Components of
Ship Motion

The first order high frequency wave induced motions are normally oscillating between 0.3 to 1.6 radians per second. These motions are not controlled because the existing thrusters cannot counteract them effectively. Any attempt will cause unnecessary wear and use extra energy.

In practice, most applications can allow such errors in the controlled variables, particularly in calm sea conditions.

2.2 THE NON-LINEAR LOW FREQUENCY SHIP MODEL

The forces which produce the low frequency (LF) motions are listed as follows:

- (a) Forces generated by the thrusters and propellers.
- (b) Wind forces. The horizontal wind speed can be resolved into a component in the average wind direction and a component perpendicular to this direction with zero mean. Both components can be modelled by a random variable with a Gaussian probability distribution.
- (c) Wave induced drift forces. These second order wave forces are relatively steady and are assumed to be unaffected by the current forces which are almost constant.
- (d) Hydrodynamic forces, caused by the vessel's motion relative to the water. These forces are due to add-

mass, wave generation, viscous drag and hydrostatic buoyancy.

The non-linear differential equation relating surge, sway and yaw velocities are represented by the following form [2,3].

$$\begin{aligned} (M-X_{\dot{u}})\dot{u} - (M-Y_{\dot{v}})rv &= X_A + X_H(u,v,r) \\ (M-Y_{\dot{v}})\dot{v} + (M-X_{\dot{u}})ru &= Y_A + Y_H(u,v,r) \\ (I^2_{zz} - N_{\dot{r}})\dot{r} &= N_A + N_H(u,v,r) \end{aligned} \quad (2.1)$$

where

u: surge velocity

v: sway velocity

r: yaw velocity

X_A : applied surge direction force due to the thruster and the environment

Y_A : applied sway direction force due to the thruster and the environment

N_A : applied turning moment on the vessel

X_H, Y_H, N_H : the hydrodynamic forces and moment due to relative motion between the vessel and water

$X_{\dot{u}}, Y_{\dot{v}}, N_{\dot{r}}$: add masses and add inertia which depend on the nature of the body motion and the resulting flow pattern.

M: mass of vessel
 I_{zz} : radius of gyration

The coefficients of this non-linear model are to be determined by a combination of theoretical analysis and model tank tests [4]. The thruster force \underline{f} is a function of the control signal in the linearized model. The thruster dynamics will be discussed later in this section.

2.3 THE LINEARIZED LOW FREQUENCY SHIP MODEL

The linear LF ship model is determined by linearizing the non-linear model about an operating point of assumed current flow. This model and the linearized thruster model will be used in system design. The linear model has very little interaction between surge motion and sway/yaw motions, thence, surge motion control will be treated as a separate entity.

The state space equation for the surge motion is:

$$\begin{bmatrix} \dot{x}_1^{su} \\ \dot{x}_2^{su} \end{bmatrix} = \begin{bmatrix} a_{11}^{su} & 0 \\ 1 & 0 \end{bmatrix} \begin{bmatrix} x_1^{su} \\ x_2^{su} \end{bmatrix} + \begin{bmatrix} \beta^{su} \\ 0 \end{bmatrix} F^{su} \quad (2.2)$$

$$+ \begin{bmatrix} \beta^{su} \\ 0 \end{bmatrix} \omega^{su} + \begin{bmatrix} \beta^{su} \\ 0 \end{bmatrix} \eta^{su}$$

The sway and yaw state space equations are:

$$\begin{bmatrix} \dot{x}_1 \\ \dot{x}_2 \\ \dot{x}_3 \\ \dot{x}_4 \end{bmatrix} = \begin{bmatrix} a_{11} & 0 & a_{13} & 0 \\ 1 & 0 & 0 & 0 \\ a_{31} & 0 & a_{33} & 0 \\ 0 & 0 & 1 & 0 \end{bmatrix} \begin{bmatrix} x_1 \\ x_2 \\ x_3 \\ x_4 \end{bmatrix} + \begin{bmatrix} \beta_1 & 0 \\ 0 & 0 \\ 0 & \beta_2 \\ 0 & 0 \end{bmatrix} \begin{bmatrix} F_1 \\ T_1 \end{bmatrix} \quad (2.3)$$

$$+ \begin{bmatrix} \beta_1 & 0 \\ 0 & 0 \\ 0 & \beta_2 \\ 0 & 0 \end{bmatrix} \begin{bmatrix} \omega_1 \\ \omega_2 \end{bmatrix} + \begin{bmatrix} \beta_1 & 0 \\ 0 & 0 \\ 0 & \beta_2 \\ 0 & 0 \end{bmatrix} \begin{bmatrix} \eta_1 \\ \eta_2 \end{bmatrix}$$

where

- x_1^{su} : surge velocity
- x_2^{su} : surge position
- x_1 : sway velocity
- x_2 : sway position
- x_3 : yaw angular velocity
- x_4 : yaw angle
- F^{su} : achieved thrust in surge direction
- F_1 : achieved thrust in sway direction
- T_1 : achieved torque in yaw direction
- ω^{su} : random force applied to surge direction
- ω_1 : random force applied to sway direction
- ω_2 : random torque applied to yaw direction

The disturbances such as wave drift and current forces are considered to produce an unknown mean value on the random forces. The parameters in the system matrices resulted from linearization.

2.4 THRUSTER ALLOCATION LOGIC

The function of the thruster allocation logic is to operate on the demands for thrust in the three axes from the state feedback control to:

- (a) Set the thrusters so that the demands are met as closely as possible.
- (b) Produce an achieved thrust command signal in each of the three axes for the input into the estimator.

The inputs to the thruster logic are:

- (a) F_{\max} : maximum achieved thrust of the thrusters.
- (b) l_1, l_2 : the distances of the thrusters from the vessel's center of gravity.
- (c) X_u, Y_u, N_u : the demanded forces and moment from the state feedback controller.

The outputs are:

- (a) F_1, F_2 : the achieved thrust command signals of the thrusters.
- (b) ϕ_1, ϕ_2 : the angle setting of the thrusters.
- (c) X_F, Y_F, N_F : the achieved forces and moment in surge, sway and yaw direction.

The configuration is illustrated in Figure 2-4.

The thruster allocation logic is a static optimization problem, where minimum fuel consumption is the target. It will be treated as a separate entity and will not be included in the Kalman filter model. The Kalman filter and the state feedback controller will be concerned only with the thrust in surge and sway axes and moment about the yaw axis. The detailed thruster algorithm is very complicated and it will not be discussed in this report.

2.5 THE NON-LINEAR THRUSTER MODEL [4]

The thruster devices for dynamic positioning of a vessel can take several forms, but the ship model used in the following is based upon Wimpey Sealab which has retractable ac motor driven thrusters with variable pitch propellers (Figure 2-5). The vessel has two rotatable bow and two

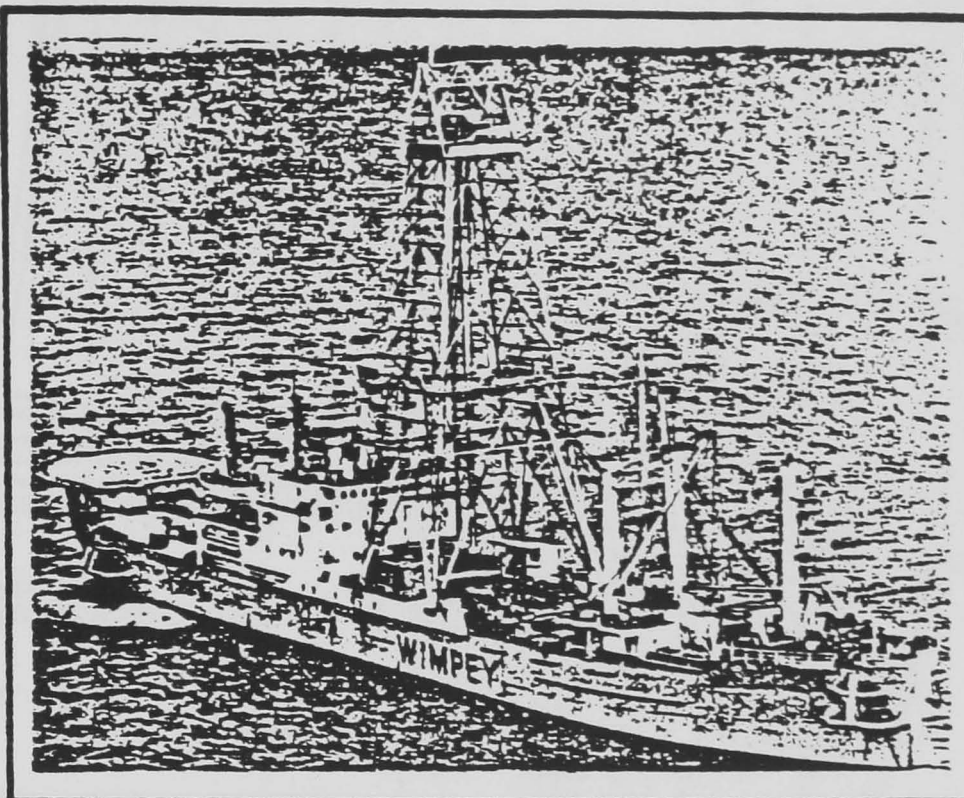


FIGURE 2-4a The 5674 tonne Multi-Purpose Ocean Engineering
Vessel Wimpey Sealab

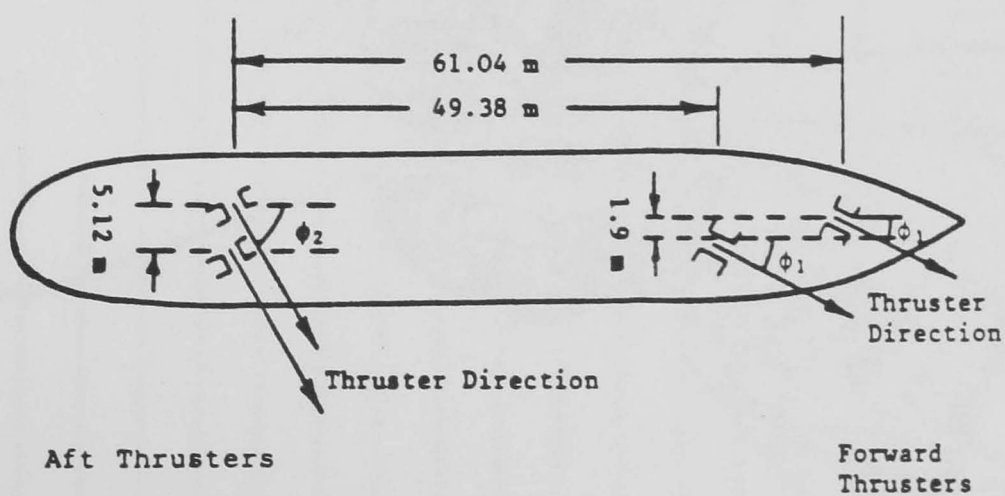


FIGURE 2-4b Wimpey Sealab's Bow and Stern
Rotable Thrusters

1 TUNNEL SECTION
2 STAINLESS STEEL LINER
3 PROPELLER BLADE
4 FLANGE PROTECTION RING
5 SHAFT-FLANGE BOLT
6 BLADE BOLT

7 BLADE CARRIER
8 HUB COVER
9 MOVING CYLINDER-YONE
10 CAP
11 HUB BODY
12 SLIDING BLOCK

13 ORIGIN PIN
14 BLADE SEAL
15 PROPELLER SHAFT SEAL
16 BEAR POD COVER
17 PINION SHAFT SEAL
18 ISOLATING RING

19 LUB OIL RETURN PIPE
20 HYDRAULIC PRESSURE OIL PIPE
21 UPPER PINION SHAFT BEARING
22 PINION SHAFT
23 FAIRING CONE
24 PITCH CONTROL ROD

25 BEAR POD
26 LOWER PINION SHAFT BEARING
27 SPIRAL BEVEL PINION
28 THRUST BEARING ASSEMBLY
29 GEAR POD CAP
30 OIL DISTRIBUTION VALVE

31 PIPING INSERT
32 HYDRAULIC CONTROL UNIT
33 HEAD OIL PIPE
34 PROPELLER SHAFT
35 SPIRAL BEVEL WHEEL
36 PROPELLER SHAFT BEARING

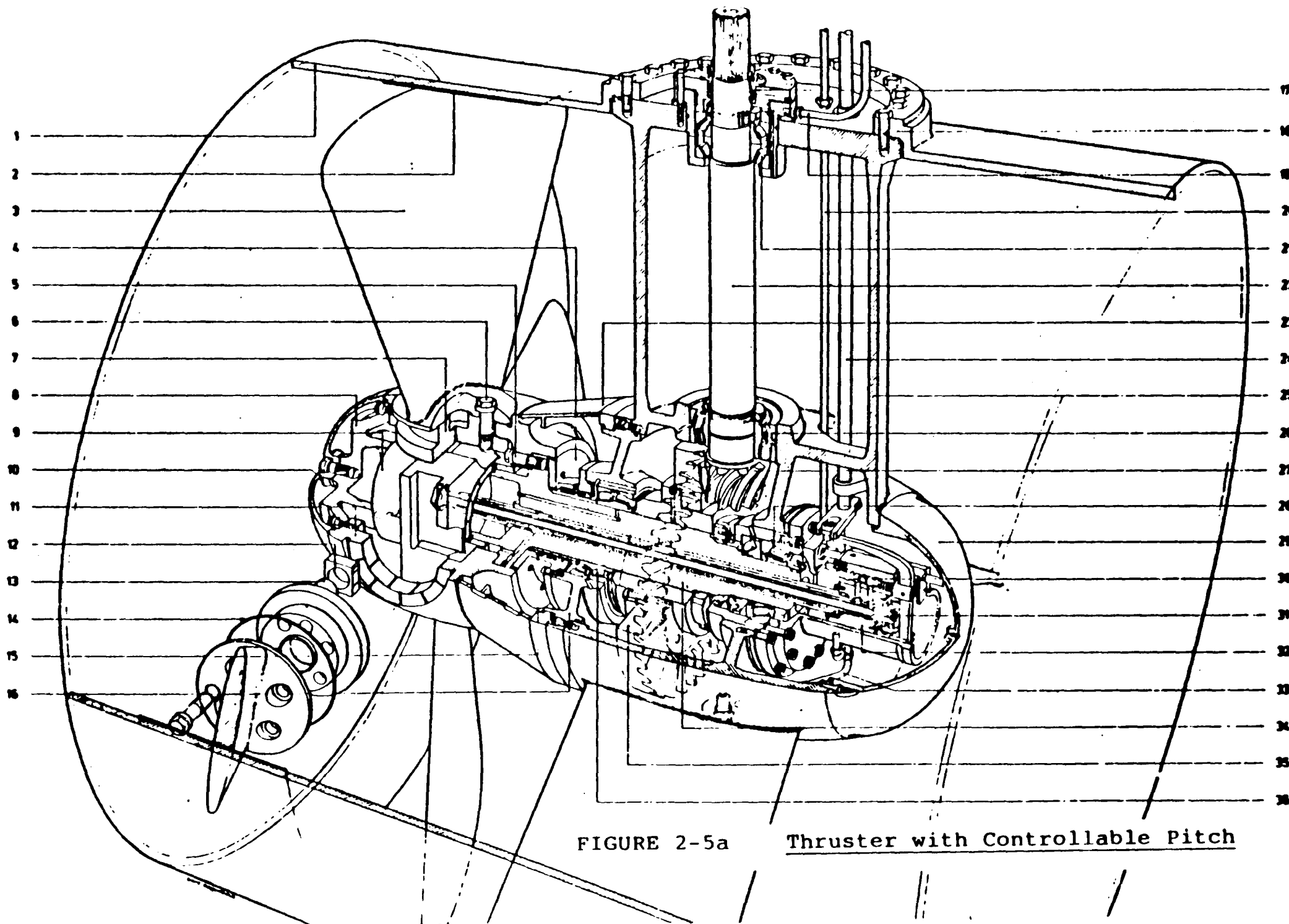


FIGURE 2-5a

Thruster with Controllable Pitch

rotatable stern thrusters which can rotate 360 degrees and are each rated at 12.5 tonnes. The non-linear model is shown in Figure 2-6. The detailed thruster model is very complicated [10]. However, this simplified model is adequate for the purpose of control analysis.

The input servo is of bang-bang type. It has an electrical input circuit which compares a reference voltage against an electrical feedback from potentiometers measuring the moment of the ram. The error signal is applied to comparators which switch the forward or reverse solenoid valves when the error exceeds a predetermined deadband. This deadband is set to stop the servo from hunting.

The spring box between the input servo and output servo restricts the force exerted on the mechanical linkage between the two servos. This is approximated by a saturation non-linearity.

The non-linearity between the spring box and the input to the main servo is not great for the angular movement is small, thence, it is assumed to be linear.

The model of the main servo consists of a three position switch with a small dead zone at zero. The output from the

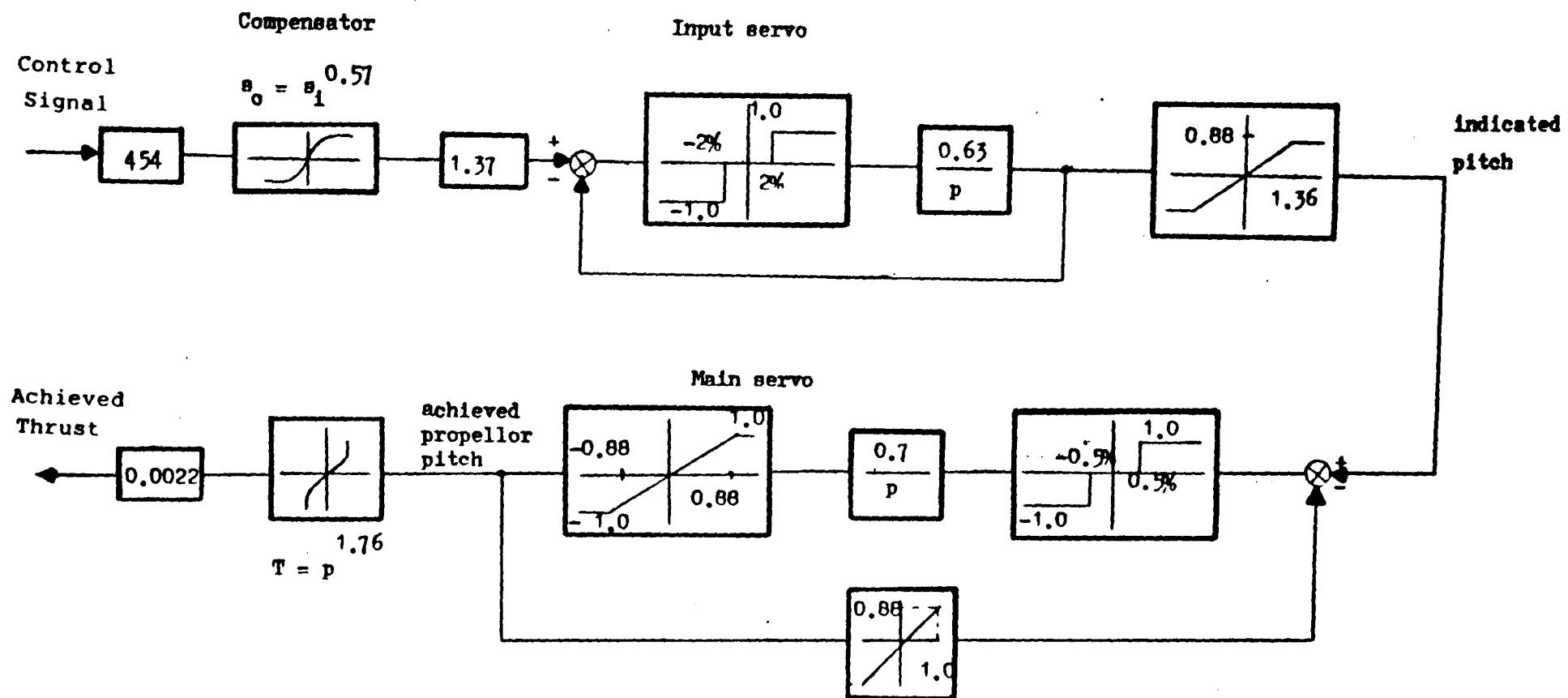


FIGURE 2-6 The Non-Linear Thruster Model

switch is passed through an integrator and then a saturation non-linearity. The scale factor inserted in the feedback loop is the inverse of this saturation element. In practice, the output servo is faster than the input servo, so the steady state loop gain should be greater than that in the input servo. The ram should move to 100 percent in less than 5 seconds. The actual non-linearities in the forward path and feedback path are not known but can be seen from the experimental curves, that, they can be either compensated or neglected if small.

The most severe non-linearity is at the thrust and pitch relationship:

$$\text{Thrust} = (\text{pitch})^m \quad m = 1.76 \quad (2.4)$$

It is usual to compensate for this non-linearity using an input compensator of the form:

$$S_o = (S_i)^{\frac{1}{m}} \quad (2.5)$$

The parameters at the input and the output of the thruster model are scaling factors which normalize the model with reference to the ship model.

2.6 THE LINEAR THRUSTER MODELS

2.6.1 First Order Approximation

The linear model is a fundamental requirement for linear Kalman filter and state feedback controller design. The order of the linear model is quite critical to the computing load and accuracy of the model. A first order lag approximation was proposed by Grimbale et. al. [5,6,7]. For the i th thruster, it takes the following form:

$$\dot{x}_i^t(t) = -b_i x_i^t(t) + b_i u_i(t) \quad (2.6)$$

where $1/b_i$ is the time constant of the thruster and u_i is the control signal from the controller. $x_i^t(t)$ is the achieved thrust.

The parameter b_i is the input amplitude and is frequency dependent. The usual modelling technique is first to estimate the current and wind forces as well as the operating frequency range. The time constant is then estimated by frequency response or step response techniques.

2.6.2 Second Order Lag Approximation

Fung et. al. [8] proposed a second order linear model to the non-linear thruster. It is well known that a high order

linear model is usually a better approximation to the non-linear model. On the other hand, it will increase the computing load. Then, the choice of the order should depend on these two factors: complexity and accuracy. In the dynamic ship positioning system, a second order linear thruster model would only place a small increase on the computing load when using a fixed Kalman filtering scheme yet it has been shown that it gives better estimation [9] of the states and improve the robustness of the control system. The state equation of the second order linear model has the following form:

$$\begin{bmatrix} \dot{x}_1^t(t) \\ \dot{x}_2^t(t) \end{bmatrix} = \begin{bmatrix} -b_1 & -b_2 \\ 1 & 0 \end{bmatrix} \begin{bmatrix} x_1^t(t) \\ x_2^t(t) \end{bmatrix} + \begin{bmatrix} b_2 \\ 0 \end{bmatrix} u(t) \quad (2.7)$$

Where $x_1^t(t)$ is the thrust rate, $x_2^t(t)$ is the achieved thrust, $u(t)$ is the demand control signal, b_1 and b_2 are the linearized parameters. The method to estimate these parameters is the same as that described in Section 2.6.1.

2.7 THE DYNAMIC MODEL OF WIMPEY SEALAB

Wimpey Sealab is a dynamically positioned vessel for a variety of operational duties in off-shore exploration operated by Wimpey Laboratories Ltd. It was converted from a Cargo Ship to a drilling ship in 1974. The vessel has an

overall length of 99.11 metres, a beam of 15.24 metres and a displacement of 5674 tonnes. The position is automatically controlled by a computer which controls the operation of four 1,000 HP (746 Kw) retractable thrusters, each fitted with variable pitch propellers [10] and capable of 360° rotation. The vessel is equipped with acoustic and taut wire position reference systems. Wimpey Sealab also has a satellite navigation system which enables the vessel to position itself accurately at predetermined locations and has an integrated Doppler Sonar System for traversing predetermined paths to very high orders of accuracy. The specifications of the vessel for control system analysis are listed in Appendix B.

GEC Electrical Projects Ltd. is responsible for the control system design.

Dynamic positioning for Wimpey Sealab is required in water depths between 30 and 300 metres. The ship must be held within a circle of 7 metres radius (or 3% of water depth, whichever is the greater) in a steady wind of up to 12.87 m/sec. with waves of significant height, 3.54 metres and significant length 91.44 metres and with a steady sea current up to 1.54 m/sec. Under the above conditions, but with the wind gusting up to 20.50 m/sec, the ship position

must be held within a circle of 11 metres radius. Ship heading is allowed to vary.

2.7.1 The Low Frequency Model

The normalized non-linear differential equation reference of the vessel are [11]:

$$\begin{aligned} 1.044 \dot{u} &= X_A + 0.092 v^2 - 0.138 uU + 1.84 rv \\ 1.840 \dot{v} &= Y_A - 2.580 vU - 1.840 v^3/U + 0.068 r|r| - rU \\ 0.1021 \dot{r} &= N_A - 0.764 uv + 0.258 vU - 0.162 r|r| \end{aligned} \quad (2.8)$$

The variables are defined in equation 2.1. U is the vector sum of u and v.

The linear LF model, under zero current flow, is:

$$\begin{aligned} 1.044 \dot{u} &= X_A - 0.0159 u \\ 1.840 \dot{v} &= Y_A - 0.1004 v + 0.002981 r \\ 0.1022 \dot{r} &= N_A - 0.007101 r + 0.005859v \end{aligned} \quad (2.9)$$

The linearized model shows very little interaction between surge (u) and sway (v)/yaw (r), thence, the research into the control system for Wimpey Sealab in this project is concentrated in sway and yaw multivariable control. Surge control is treated as a single input and single output

case. It can be solved easily once the control system for the multivariable case is established.

The linearized state equation of the ship model, together with the thrusters, is of the following form:

$$\begin{aligned}\dot{\underline{x}}_l(t) &= A_l \underline{x}_l(t) + B_l \underline{u}_l(t) + D_l \underline{\omega}_l(t) + E_l \underline{\eta}_l(t) \\ \underline{y}_l(t) &= C_l \underline{x}_l(t)\end{aligned}\tag{2.10}$$

Where $\underline{u}_l(t) \in \mathbb{R}^2$ is the control input to the thrusters, $\underline{\omega}_l(t) \in \mathbb{R}^2$ is a white noise sequence representing the random forces applied to the vessel and $\underline{\eta}_l \in \mathbb{R}^2$ is the wind force disturbances. Other disturbance forces, such as wave drift and current forces cannot be measured but can be considered to produce an unknown mean value on the signal $\underline{\omega}_l(t)$, the vector $\underline{y}_l(t) \in \mathbb{R}^2$ represents the position outputs: sway and yaw.

In Section 2.6, the linear thruster model can be either first order or second order, thence state vector $\underline{x}_l(t)$ and the system matrices are different in each case. Model A and Model B given below represent two different models for control system design. Let the system matrices be partitioned into the following forms:

$$\begin{aligned}
A_l &= \begin{bmatrix} A_l^{11} & A_l^{12} \\ 0 & A_l^{22} \end{bmatrix}, \quad B_l = \begin{bmatrix} 0 \\ B_l^{21} \end{bmatrix}, \quad D_l = \begin{bmatrix} D_l^{11} \\ 0 \end{bmatrix} \\
E_l &= \begin{bmatrix} E_l^{11} \\ 0 \end{bmatrix}, \quad C_l = \begin{bmatrix} C_l^{11} \\ 0 \end{bmatrix} \\
\dot{x}_l(t) &= \begin{bmatrix} \dot{x}_l^{11}(t) \\ \dot{x}_l^{21}(t) \end{bmatrix}
\end{aligned} \tag{2.11}$$

$x_l^{11}(t) \in \mathbb{R}^4$, $x_l^{21}(t)$ is dependent on the model used. Matrices A_l^{11} , A_l^{12} , D_l^{11} , E_l^{11} , C_l^{11} and vector $\dot{x}_l^{11}(t)$ are the same for both models. Matrices A_l^{22} and B_l^{21} are dependent on the thruster model selected. All linearized equations have been time scaled with 3.104 as a time normalization factor.

$$\dot{x}_l^{11}(t) = \begin{bmatrix} x_1 \\ x_2 \\ x_3 \\ x_4 \end{bmatrix} \begin{array}{l} \text{sway velocity} \\ \text{sway position} \\ \text{yaw angular velocity} \\ \text{yaw angle} \end{array} \tag{2.12}$$

$$A_l^{11} = \begin{bmatrix} -0.0546 & 0 & 0.0016 & 0 \\ 1.0 & 0 & 0 & 0 \\ 0.0573 & 0 & -0.0695 & 0 \\ 0 & 0 & 1.0 & 0 \end{bmatrix}$$

$$A_l^{12} = \begin{bmatrix} 0.5435 & 0 \\ 0 & 0 \\ 0 & -1.6340 \\ 0 & 0 \end{bmatrix}, \quad D_l^{11} = \begin{bmatrix} 0.5435 & 0 \\ 0 & 0 \\ 0 & 9.785 \\ 0 & 0 \end{bmatrix}$$

$$E_l^{11} = \begin{bmatrix} 0.384 & 0 \\ 0 & 0 \\ 0 & 6.92 \\ 0 & 0 \end{bmatrix} \quad C_l^{11} = \begin{bmatrix} 0 & 1 & 0 & 0 \\ 0 & 0 & 0 & 1 \end{bmatrix} \quad (2.13)$$

There are two linear ship models to be used in the simulation analysis. The difference between these models is in the thruster subsystems only.

Model A

$$\begin{bmatrix} x_5 \\ x_6 \end{bmatrix} \begin{array}{l} \text{thruster one} \\ \text{thruster two} \end{array} \quad (2.14)$$

$$A_l^{22} = \begin{bmatrix} -1.55 & 0 \\ 0 & -1.55 \end{bmatrix} \quad B_l^{21} = \begin{bmatrix} 1.55 & 0 \\ 0 & 1.55 \end{bmatrix} \quad (2.15)$$

In this model, the time constants of the thrusters are all 2 seconds (0.644 per unit).

Model B

$$\begin{bmatrix} x_5 \\ x_6 \\ x_7 \\ x_8 \end{bmatrix} \begin{array}{l} \text{thrust rate of thruster one} \\ \text{thrust of thruster one} \\ \text{thrust rate of thruster two} \\ \text{thrust of thruster two} \end{array} \quad (2.16)$$

The time constants obtained by fitting the best second order linear model to the non-linear thrusters using frequency tests and Bode diagrams are:

TABLE 2-1

<u>PEAK SINE WAVE INPUT</u>	<u>TIME CONSTANTS (PER UNIT)</u>	
	T_1	T_2
0.0002	0.3981	0.3055
0.0005	0.7244	0.4266
0.001	1.059	0.6918
0.0022	1.585	0.861

Note that one unit is equivalent to input amplitude of 0.0022. The time constants used in the linear model were taken as $T_1 = 1.059$ and $T_2 = 0.6918$ seconds which corresponds with a mid-range input signal. The system matrices for the thrusters are:

$$\begin{aligned}
 A_l^{22} &= \begin{bmatrix} -2.3895 & -1.3646 & 0 & 0 \\ 1.0 & 0 & 0 & 0 \\ 0 & 0 & -2.3895 & -1.3646 \\ 0 & 0 & 1.0 & 0 \end{bmatrix} \\
 B_l^{21} &= \begin{bmatrix} 1.3646 & 0 \\ 0 & 0 \\ 0 & 1.3646 \\ 0 & 0 \end{bmatrix}
 \end{aligned} \tag{2.17}$$

In the full LF model, two zero columns should be added to the RHS of matrix A_l^{12} to complete a square matrix A_l .

2.7.2 The Noise Covariances Specifications

The process noise in the dynamic positioning problem can be partitioned into two parts: high frequency model and low frequency model. Let Q_h and Q_l be their covariance matrices respectively. Q_h is assumed to be unity. The Q_l covariance matrix is dependent on the mean wind force level. In Wimpey Sealab tests, the following values have been taken:

$$\begin{aligned}
 Q_{l1} &= \text{sway per unit force covariance} \\
 &= (0.00228)^2 = 5.2 \times 10^{-6} \simeq 4 \times 10^{-6}
 \end{aligned}$$

$$\begin{aligned}
 Q_{l2} &= \text{yaw per unit torque covariance} \\
 &= (0.00031)^2 = 9.6 \times 10^{-8} \simeq 9 \times 10^{-8}
 \end{aligned}$$

Thence the process noise covariance matrix for the total system is:

$$Q_f = \begin{bmatrix} 4 \times 10^{-6} & 0 & \vdots & 0 & 0 \\ 0 & 9 \times 10^{-8} & \vdots & 0 & 0 \\ \hline 0 & 0 & \vdots & 1 & 0 \\ 0 & 0 & \vdots & 0 & 1 \end{bmatrix} \quad (2.18)$$

The position measurement error is assumed to be 0.333 metre. In the normalized unit, it is 0.0033. Therefore, the noise variance for sway motion is $R_{11} \approx 10^{-5}$. The yaw standard deviation is assumed to be 0.2 degrees, so that $R_{22} \approx 1.22 \times 10^{-5}$. Thence, the measurement noise covariance matrix is:

$$R_f = \begin{bmatrix} 10^{-5} & 0 \\ 0 & 1.22 \times 10^{-5} \end{bmatrix} \quad (2.19)$$

2.8 HIGH FREQUENCY MODEL

The high frequency motions of the vessel are in sympathy with the wave frequencies, and are assumed to be linearly related to the wave forces. The spectrum of the high frequency vessel motion is obtained from a standard sea spectrum and the vessel dynamics. It is assumed that in the worst case, the high frequency motions are determined by the

sea spectrum alone which means the wave motions are not attenuated by the vessel dynamics.

Several sea wave spectra [12] have been proposed. A commonly used one is the Pierson-Moskowitz model [13] which is expressed by:

$$S_n(\omega) = \frac{A}{\omega^5} e^{-B/\omega^4} \quad (2.20)$$

where ω is the angular frequency in radians per second. $A = 4.894$, $B = 3.1094/(h_{1/3})^2$. The term $h_{1/3}$ is defined as the significant wave height in metres. By finding the stationary point for $S_n(\omega)$, the resonant frequency of the spectrum is found to be:

$$\omega_n = (4B/5)^{1/4} \quad (2.21)$$

The wave spectra of several sea conditions (identified by Beaufort Numbers) are shown in Figure 2-7.

There are three types of models used in state estimation using Kalman filter.

2.8.1 Rational Proper Transfer Function Model

Kostecki [14] suggested the sea spectrum can be approximated by a rational proper transfer function presented by:

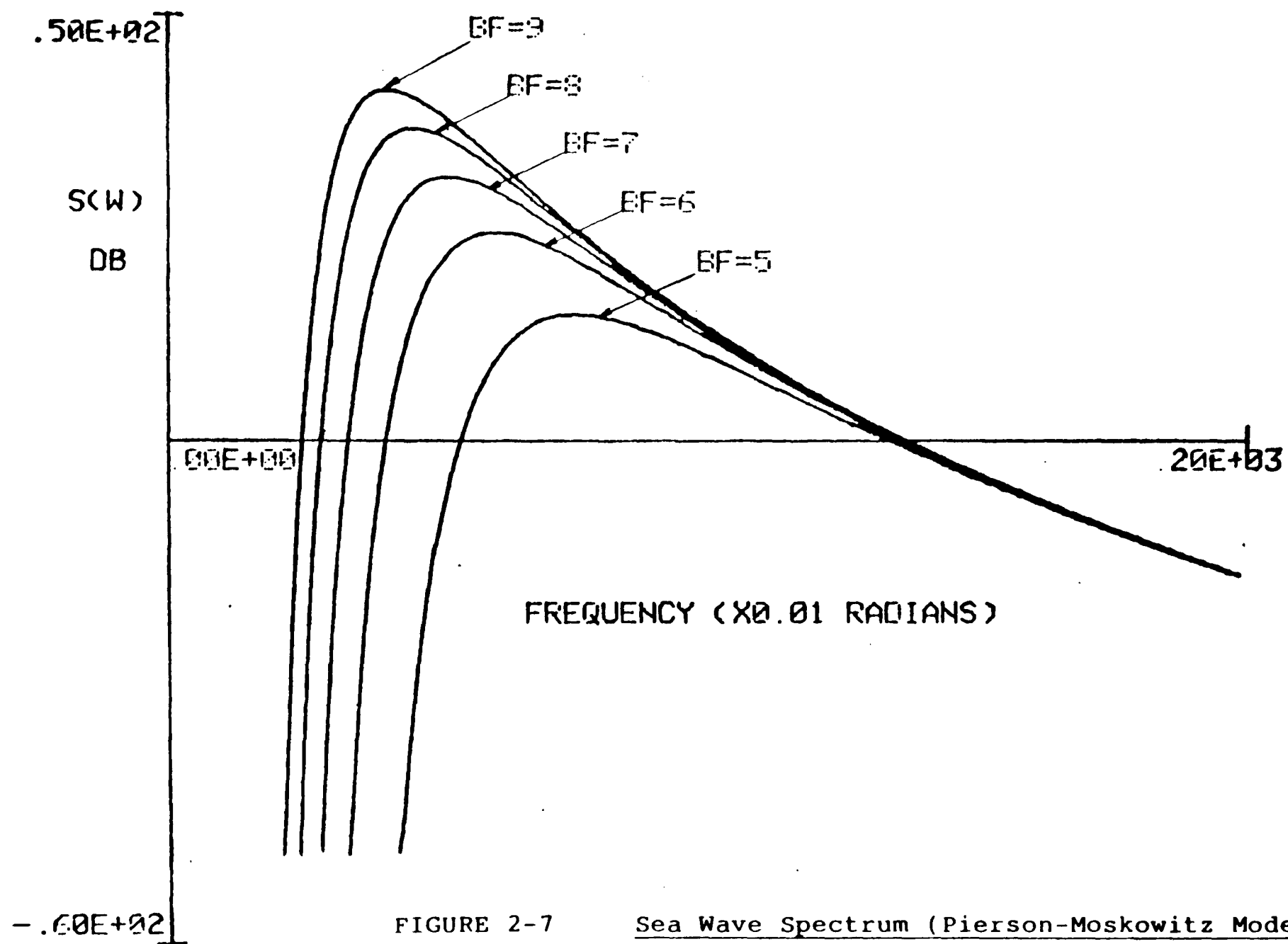


FIGURE 2-7

Sea Wave Spectrum (Pierson-Moskowitz Model)

$$S_o(\omega) = |G(j\omega)|^2 S_i(\omega) \quad (2.22)$$

Where $S_i(\omega)$ is the wind spectrum density which is assumed to be stationary and has unit value. $S_o(\omega)$ is the approximated spectrum and $G(j\omega)$ is the transfer function. A single section of the transfer function may be expressed as:

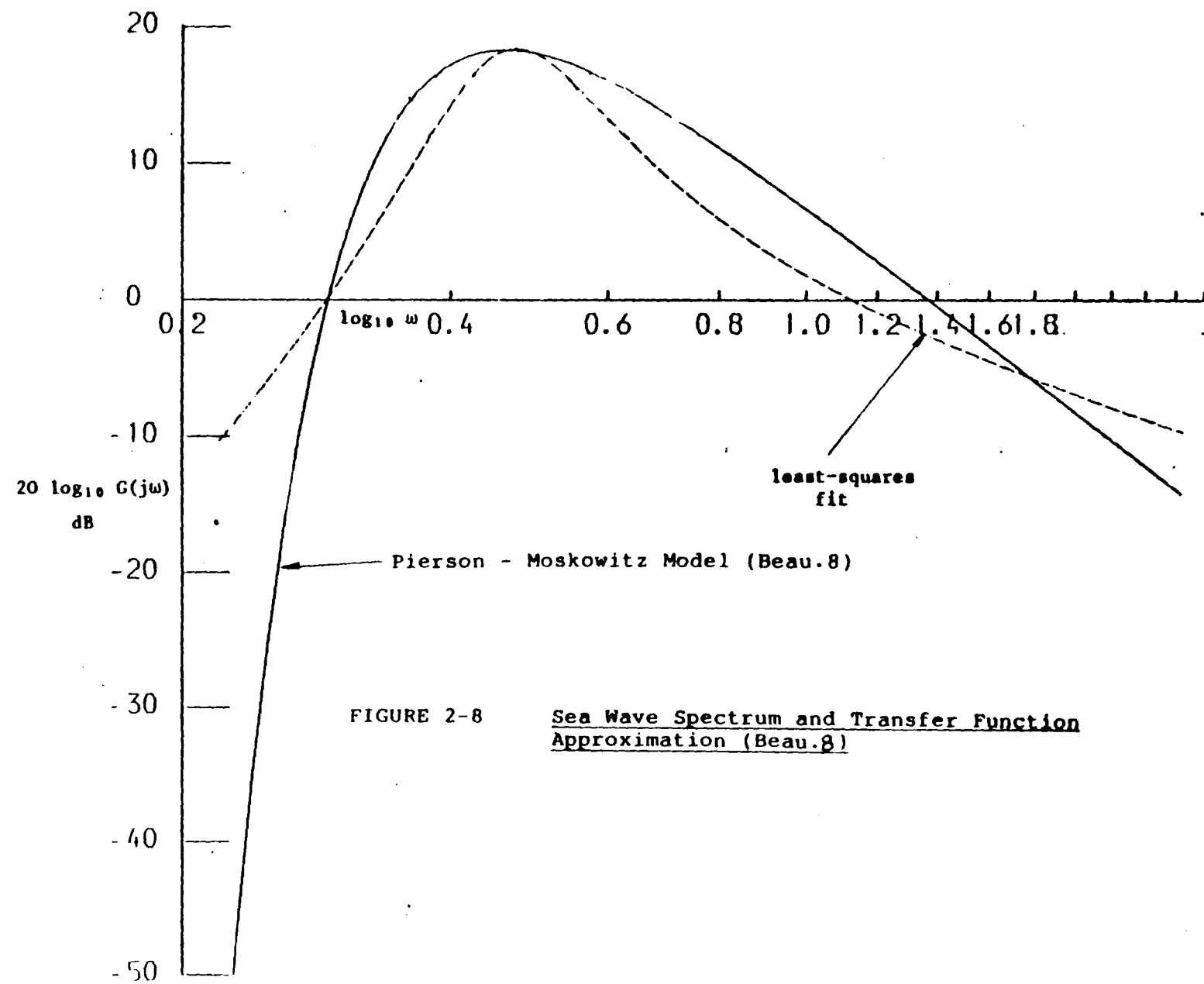
$$G_i(s) = \frac{2b_i\zeta_i s}{s^2 + 2\zeta_i\omega_{ni}s + \omega_{ni}^2} \quad (2.23)$$

Two sections of $G_i(s)$ are chosen [15]. The parameters of the transfer function are estimated using the criterion:

$$\Delta S(\omega) = \min \left\{ \int_0^{\omega_g} [S_n(\omega) - S_o(\omega)]^2 d\omega \right\}^{1/2} \quad (2.24)$$

Where $S_n(\omega)$ is defined in the frequency interval $(0, \omega_g)$ and n is typically 250. Two typical examples are shown in Figure 2-8 and Figure 2-9. The high frequency model, for one degree of freedom, therefore has the form:

$$G(s) = \frac{Ks^2}{s^4 + a_3s^3 + a_2s^2 + a_1s + a_0} \quad (2.25)$$



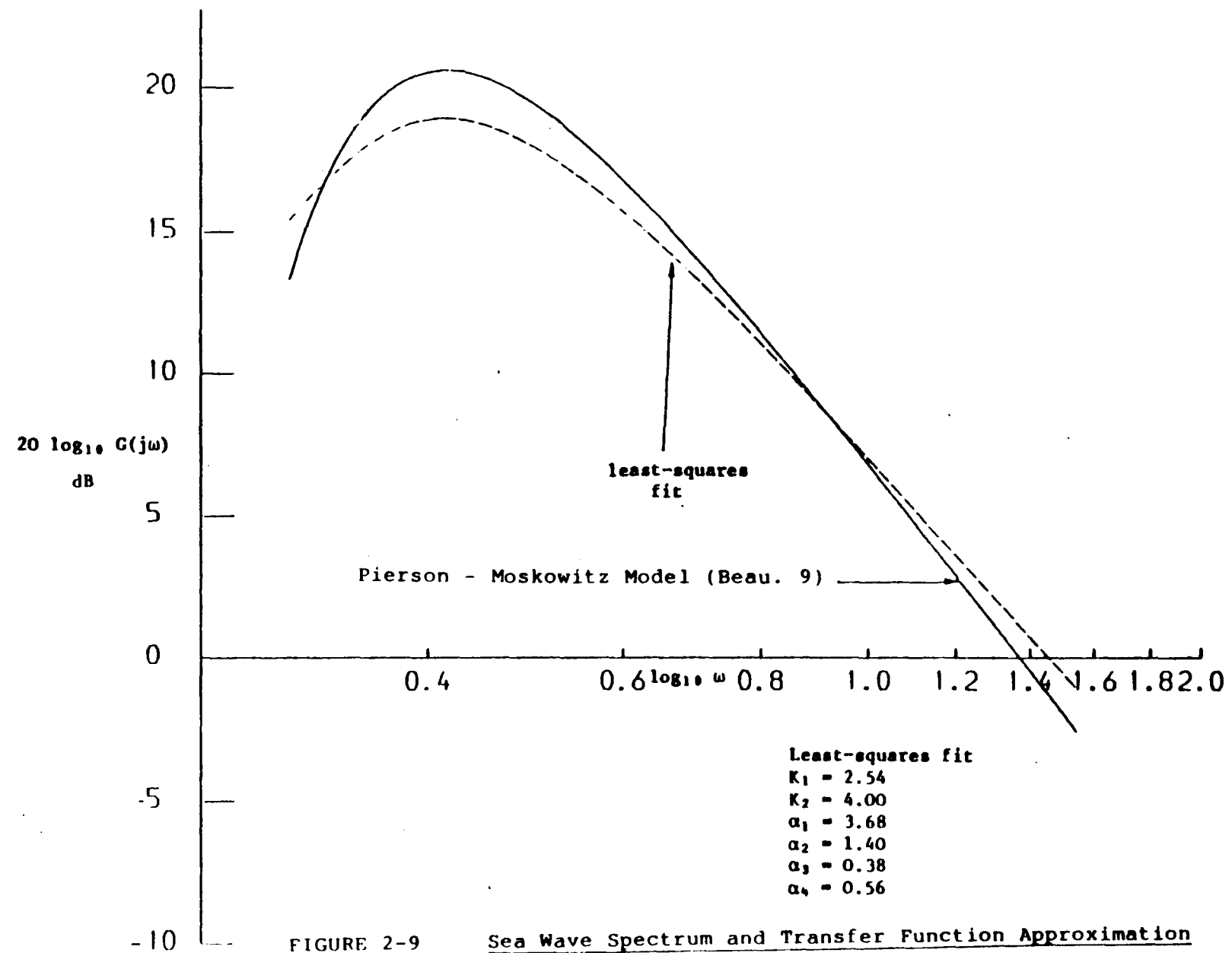


FIGURE 2-9

Sea Wave Spectrum and Transfer Function Approximation
(Beau. 9)

In state space form:

$$\begin{aligned}\dot{\underline{x}}_h(t) &= F_h \underline{x}_h(t) + G_h \underline{\omega}_h(t) \\ \underline{y}_h(t) &= H_h \underline{x}_h(t)\end{aligned}\tag{2.26}$$

Where:

$$\underline{x}_h(t) \in R^{12}, \underline{\omega}_h(t) \in R^3$$

$$\begin{aligned}F_h &= \begin{bmatrix} F_h^{su} & 0 & 0 \\ 0 & F_h^s & 0 \\ 0 & 0 & F_h^y \end{bmatrix}, \quad G_h = \begin{bmatrix} G_h^{su} & 0 & 0 \\ 0 & G_h^s & 0 \\ 0 & 0 & G_h^y \end{bmatrix} \\ H_h &= \begin{bmatrix} H_h^{su} & 0 & 0 \\ 0 & H_h^s & 0 \\ 0 & 0 & H_h^y \end{bmatrix}\end{aligned}\tag{2.27}$$

The sub-matrices for surge, sway and yaw each has the following form:

$$F_h^S = \begin{bmatrix} 0 & 1 & 0 & 0 \\ 0 & 0 & 1 & 0 \\ 0 & 0 & 0 & 1 \\ -f_0^S & -f_1^S & -f_2^S & -f_3^S \end{bmatrix} \quad G_h^S = \begin{bmatrix} 0 \\ 0 \\ 0 \\ g_4^S \end{bmatrix}$$

$$H_h^S = [0 \quad 0 \quad h_3^S \quad 0]$$

2.8.2 Auto-Regressive Moving Average (ARMA) Model

This model was first used in the DP Kalman filter estimation by Fung and Grimble [16]. It is assumed that the high frequency disturbance can be represented by the following multivariable ARMA model:

$$A_h(z^{-1}) \underline{y}_h(t) = C_h(z^{-1}) \underline{\xi}_h(t) \quad (2.29)$$

which is assumed to be asymptotically stable and $y_h(t) \in R^3$ and $\underline{\xi}_h(t) \in R^3$. Here, $\underline{\xi}_h(t)$ represents an independent zero mean random vector which is uncorrelated with the low frequency disturbances and the measurement noise. The covariance matrix of $\underline{\xi}_h(t)$ is denoted by Σ_{ξ_h} . The polynomial matrices $A_h(z^{-1})$ and $C_h(z^{-1})$ are assumed to be square and of the form:

$$A_h(z^{-1}) = I_3 + A_1 z^{-1} + \dots + A_{n_a} z^{-n_a} \quad (2.30)$$

$$C_h(z^{-1}) = C_1 z^{-1} + C_2 z^{-2} + \dots + C_{n_c} z^{-n_c} \quad (2.31)$$

where z^{-1} is the backward shift operator. The matrix $A_h(z^{-1})$ is assumed to be regular (that is A_{n_a} is non-singular). The zeros of $\det(A_h(x))$ and $\det(C_h(x))$ are assumed to be strictly outside the unit circle. The order of the polynomial matrices are known but the coefficients $\{A_i\}$ and $\{C_j\}$, $i=1, \dots, n_a$, $j=1, \dots, n_c$, are treated as constant or slow varying unknowns since in practice, the wave spectrum varies slowly with weather conditions. It is also assumed that the disturbances in each observed channel are uncorrelated so that the matrices $\{A_i\}$ and $\{C_j\}$ have diagonal form.

2.8.3 Harmonic Oscillation Model

The harmonic oscillation model for high frequency motions of a vessel for dynamic control system was discussed in [17,18]. The surge, sway and yaw motions are modelled by three separate harmonic oscillators. Each oscillator has a variable frequency, a white noise input representing the modelling error and unpredictable wave noise. The state space representation of HF motions becomes:

$$\begin{aligned}\dot{\bar{x}}_h(t) &= \bar{F}_h \bar{x}_h(t) + \bar{G}_h \bar{\omega}_h(t) \\ \bar{y}_h(t) &= \bar{H}_h \bar{x}_h(t)\end{aligned}\quad (2.32)$$

where:

$$\begin{aligned}\bar{x}_h(t) &= \begin{bmatrix} \bar{x}_{h1}(t) \\ \bar{x}_{h2}(t) \\ \bar{\omega}_1 \\ \bar{x}_{h3}(t) \\ \bar{x}_{h4}(t) \\ \bar{\omega}_2 \\ \bar{x}_{h5}(t) \\ \bar{x}_{h6}(t) \\ \bar{\omega}_3 \end{bmatrix} \quad \begin{array}{l} \text{HF surge position} \\ \text{HF surge velocity} \\ \text{HF surge frequency} \\ \text{HF sway position} \\ \text{HF sway velocity} \\ \text{HF sway frequency} \\ \text{HF yaw angle} \\ \text{HF yaw angular velocity} \\ \text{HF yaw frequency} \end{array} \\ \bar{F}_h &= \begin{bmatrix} \bar{F}_{h1} & 0 & 0 \\ 0 & \bar{F}_{h2} & 0 \\ 0 & 0 & \bar{F}_{h3} \end{bmatrix} \quad \bar{G}_h = \begin{bmatrix} \bar{G}_{h1} & 0 & 0 \\ 0 & \bar{G}_{h2} & 0 \\ 0 & 0 & \bar{G}_{h3} \end{bmatrix} \\ \bar{H}_h &= \begin{bmatrix} \bar{H}_{h1} & 0 & 0 \\ 0 & \bar{H}_{h2} & 0 \\ 0 & 0 & \bar{H}_{h3} \end{bmatrix} \\ \bar{F}_{hi} &= \begin{bmatrix} 0 & 1 & 0 \\ -\bar{\omega}_i^2 & 0 & 0 \\ 0 & 0 & 0 \end{bmatrix} \quad \bar{G}_{hi} = \begin{bmatrix} 0 & 0 \\ 1 & 0 \\ 0 & 1 \end{bmatrix}, \quad \bar{H}_{hi} = \begin{bmatrix} 1 & 0 & 0 \end{bmatrix} \\ i &= 1, 2, 3\end{aligned}\quad (2.34)$$

$\bar{x}_h(t) \in R^9$ is the state variable $\bar{y}_h(t) \in R^3$ is the high frequency motions, $\bar{\omega}_h(t) \in R^6$ is the process white noise sequence.

2.8.4 Simulation of High Frequency Motions

Method 1

The first order wave induced HF motions can be simulated using the following expression [19] (in one direction with unit in metre):

$$y_h(t) = \sum_{i=1}^M y_0 \sin(\omega_i t + \theta_i) \quad (2.35)$$

where θ_i are random numbers lying in $(0, 2\pi)$, y_0 and ω_i are selected to approximate the Pierson-Moskowitz wave spectrum. M is the number of equal parts (in terms of energy) into which the wave spectrum is divided. A typical value of M is 20.

For a fully developed sea [16]:

$$\omega_i = \frac{0.6990525}{\sqrt{h_{1/3}}} \times \ln\left(\frac{2M}{2i-1}\right)^{1/4} \quad \text{rad/sec} \quad (2.36)$$

$$y_0 = h_{1/3} (M/2)^{-1/2} \quad \text{metres} \quad (2.37)$$

where $h_{1/3}$ is defined as the significant wave height. Other terms such as wind speed and Beaufort number are also used to characterize the sea conditions.

Method 2

This method uses the rational proper transfer function of HF motions described in Section 2.8.1 to simulate sea waves. For each weather condition, the parameters of the model are estimated using least squares technique. The state space representation of the model is used to generate the HF motions. Since the model is assumed to be linear, a discrete model is more appropriate for updating the states. A set of values for some typical weather conditions are given in Appendix A.

2.9 THE LINEAR STATE SPACE EQUATIONS FOR SHIP MOTIONS

The state equations for the low and high frequency models of the ship can be combined into the form:

$$\begin{aligned}
\begin{bmatrix} \dot{\underline{x}}_l(t) \\ \dot{\underline{x}}_h(t) \end{bmatrix} &= \begin{bmatrix} A_l & 0 \\ 0 & F_h \end{bmatrix} \begin{bmatrix} \underline{x}_l(t) \\ \underline{x}_h(t) \end{bmatrix} + \begin{bmatrix} B_l \\ 0 \end{bmatrix} \underline{u}_l(t) + \\
&\quad \begin{bmatrix} E_l \\ 0 \end{bmatrix} \underline{\eta}_t(t) + \begin{bmatrix} D_l & 0 \\ 0 & G_h \end{bmatrix} \begin{bmatrix} \underline{\omega}_l(t) \\ \underline{\omega}_h(t) \end{bmatrix}
\end{aligned} \tag{2.38}$$

The position of the vessel is given by the sum of the low and high frequency motions:

$$\underline{y}(t) = \underline{y}_l(t) + \underline{y}_h(t) \tag{2.39}$$

The position measurement $Z(t)$ sway and yaw is therefore:

$$\begin{aligned}
\begin{bmatrix} \underline{z}_1(t) \\ \underline{z}_2(t) \end{bmatrix} &= [C_l \quad H_h] \begin{bmatrix} \underline{x}_l(t) \\ \underline{x}_h(t) \end{bmatrix} + \underline{v}(t) \\
&= \underline{y}_l(t) + \underline{y}_h(t) + \underline{v}(t)
\end{aligned} \tag{2.40}$$

where $\underline{v}(t) = [v_1 \ v_2]^T$ is a white noise signal representing measurement system noise. The above equations can be written more concisely as:

$$\dot{\underline{x}}(t) = A\underline{x}(t) + B\underline{u}(t) + E\underline{\eta}(t) + D\underline{\omega}(t) \tag{2.41}$$

$$\underline{z}(t) = C\underline{x}(t) + \underline{v}(t) \tag{2.42}$$

where $\underline{u}(t)$ includes the control signals, $\underline{\eta}(t)$ includes the measurable disturbances inputs, $\underline{\omega}(t)$ represents the white process noise input and $\underline{v}(t)$ represents the white measurement noise signal. These equations are in the standard form associated with the Kalman filtering and optimal stochastic control problem.

CHAPTER THREE

KALMAN FILTERING PROBLEM OF DYNAMIC SHIP POSITIONING SYSTEMS

3.1 THE ESTIMATION STRUCTURE

The stochastic model of the vessel is defined by the state equation in Section 2.9, and now the estimation problem can be considered. Recall that for control purposes, it is not simply the total position $y(t)$ of the vessel that is to be estimated, but rather the low frequency component $y_l(t)$. That is, the position control problem must only respond to the low frequency position error signal. The estimator is therefore required to provide an estimate $\hat{y}_l(t)$. If a state feedback controller is to be implemented, the states in the low frequency model must be estimated. If a stochastic model of a system is formed the Kalman filtering solution is quite standard nowadays [20, 21]. The Kalman filter includes a model of the total system and can therefore provide the high and low frequency motion estimates. The DP Kalman filter structure is shown in Figure 3-1 and is defined by the equation:

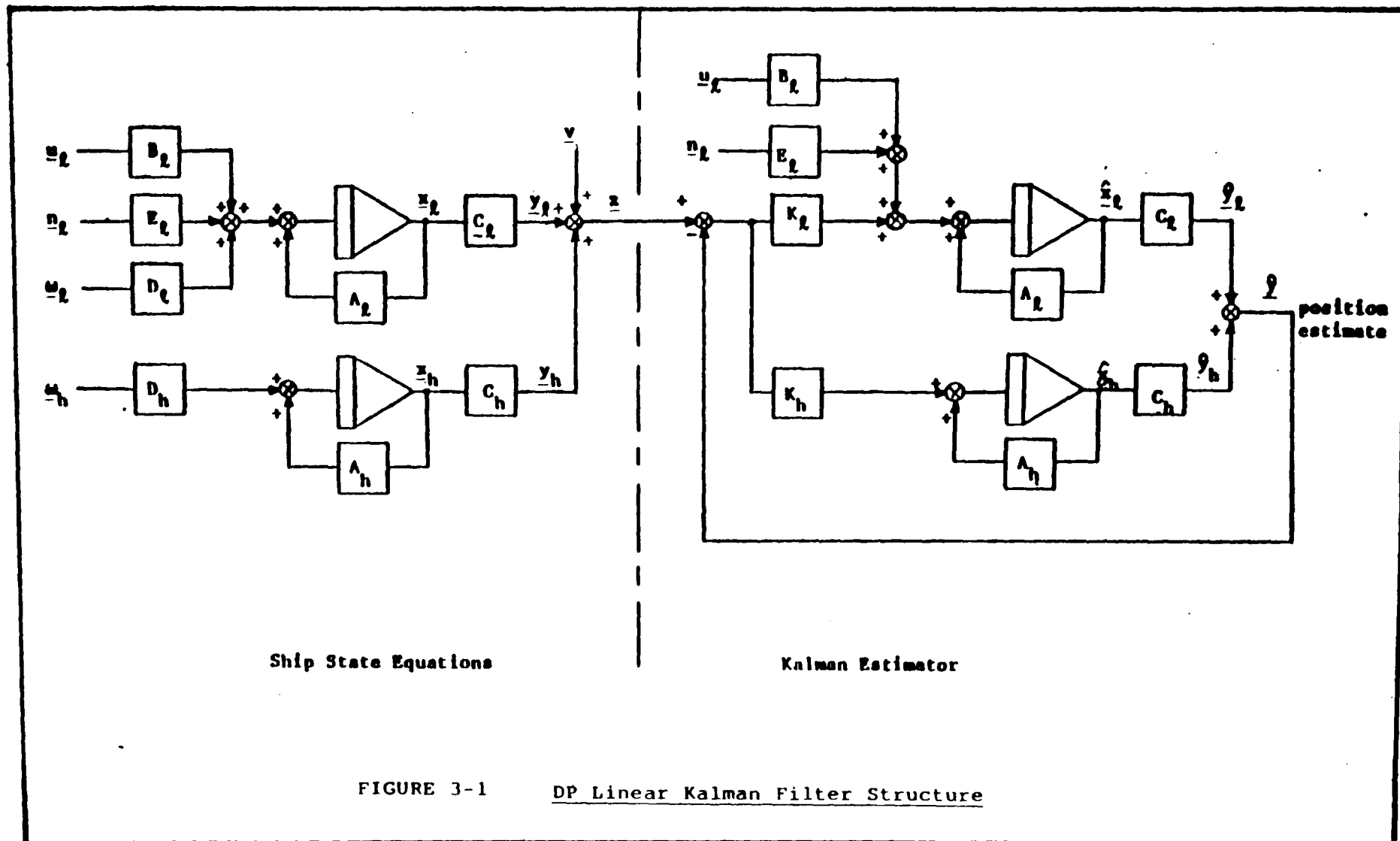


FIGURE 3-1 DP Linear Kalman Filter Structure

$$\begin{aligned} \dot{\underline{\hat{x}}}(t) = & A\underline{\hat{x}}(t) + K(t)[\underline{z}(t) - C\underline{\hat{x}}(t)] \\ & + Bu(t) + E\underline{\eta}(t) \end{aligned} \quad (3.1)$$

$$\underline{\hat{y}}(t) = C\underline{\hat{x}}(t) \quad (3.2)$$

The Kalman gain matrix $K(t)$ can be partitioned into low and high frequency matrices as follows:

$$K(t) = \begin{bmatrix} K_l(t) \\ K_h(t) \end{bmatrix} \quad (3.3)$$

This matrix can be calculated for given noise covariance matrices by using standard results (Appendix C). The measurement noise covariance can be defined relatively accurately from the knowledge of the position measurement system and using manufacturers data. The process noise covariance matrix is less well defined (Section 2.7).

In practice, the process noise of the LF model and the measurement noise can be assumed stationary. The LF linear model with respect to a current force can be assumed constant. However, the HF model is based upon sea spectra which vary with sea conditions. The variations may be very slow but nevertheless, the Kalman gain $K_h(t)$ and the parameters in the model vary with the weather conditions. To implement an optimal Kalman filter, the Kalman gains and the parameters in the models need updating, that means the

Riccati equation must be solved in real time. In order to reduce the computer load the following techniques can be used.

3.2 ^{ADAPTIVE} EXTENDED KALMAN FILTER USING HARMONIC WAVE MODELS

When the harmonic oscillation models described in Section 2.8.3 are used for high frequency motions of a vessel, the dominant frequency ω_i is treated as the only unknown parameter in the system matrices [17,18]. It was observed in simulation results that:

- (a) After a short initial period, the LF filter gains for estimation of positions and velocities vary within 2 to 3%.
- (b) The filter gains for estimation of the HF motion frequencies ω_i , oscillate with the same frequency as the HF motions and with zero mean value.

The following simplifications were made in the estimation algorithms:

- (a) The filter gains for updating of LF positions and LF velocities are assumed to be constant.
- (b) The filter gains for updating the HF motion frequencies are assumed to be a linear combination of the high frequency position and velocity estimates.

Simulation results shows that the Kalman gain of the high frequency subsystem can be expressed as [17]:

$$K_i^H(t) = k_i \hat{x}_i^H(t) \quad (3.4)$$

where K_i^H is the Kalman gain for the HF frequency ω_i , k_i is the modulation factor and \hat{x}_i^H is the position estimate of HF motion.

Alternatively, the high frequency ω_i can be estimated in the following technique.

Consider the state estimator in the i th channel.

$$\dot{\hat{x}}_l(t) = f_l(.) + K_l \xi_i(t) \quad (3.5)$$

$$\dot{\hat{x}}_{h1}(t) = \hat{x}_{h2}(t) + K_{h1} \xi_i(t) \quad (3.6)$$

$$\dot{\hat{x}}_{h2}(t) = -\hat{\omega}_i^2 \hat{x}_{h1}(t) + K_{h2} \xi_i(t) \quad (3.7)$$

where $f(.)$ is a vector function which generates the predicted states. ξ_i is the prediction error and $\hat{\omega}_i$ is the sea wave dominant frequency.

If $\hat{\omega}_i$ varies away from its initial value, the covariance of the innovation process will increase.

The algorithm to track the $\hat{\omega}_i$ is:

$$\begin{aligned}\dot{\hat{\omega}}_i &= \frac{k}{2} \frac{\partial}{\partial \hat{\omega}_i} (\varepsilon_i^2(t)) \\ &= -k \frac{\partial \varepsilon_i(t)}{\partial \hat{\omega}_i} \cdot \varepsilon_i(t)\end{aligned}\quad (3.8)$$

$\hat{\omega}_i$ is adjusted in the negative gradient direction of ε_i^2 .

The constant k is chosen to be small so that the influence of the measurement and process noises are kept small.

It can be shown that:

$$\frac{\partial \varepsilon_i(t)}{\partial \hat{\omega}_i} = -[\partial \hat{x}_{h1}(t)/\partial \hat{\omega}_i + \partial \hat{x}_{l1}(t)/\partial \hat{\omega}_i] \quad (3.9)$$

and

$$\frac{\partial \hat{x}_{l1}(t)}{\partial \hat{\omega}_i} \ll \frac{\partial \hat{x}_{h1}}{\partial \hat{\omega}_i} \quad (3.10)$$

Differentiating equations (3.6) and (3.7) gives:

$$\dot{r} = s - K_{h1}r \quad (3.11)$$

$$\dot{s} = -\hat{\omega}_i^2 r - 2\hat{\omega}_i \hat{x}_{h1}(t) - K_{h2}r \quad (3.12)$$

where $r = \partial \hat{x}_{h1}/\partial \hat{\omega}_i$ and $s = \partial \hat{x}_{h2}/\partial \hat{\omega}_i$. Differentiating equation (3.11) and substituting into equation (3.12):

$$\ddot{r} + K_{h1}\dot{r} + (\hat{\omega}_i^2(t) + K_{h2})r = -2\hat{\omega}_i \hat{x}_{h1}(t) \quad (3.13)$$

Assume that the HF estimate is given by:

$$\hat{x}_{h1}(t) = \bar{\rho} \sin \hat{\omega}_i t \quad (3.14)$$

$$\hat{x}_{h2}(t) = \bar{\rho} \hat{\omega}_i \cos \hat{\omega}_i t \quad (3.15)$$

The steady state solution to equation (3.13) is given by:

$$\begin{aligned} r &= \frac{-\partial \xi_i(t)}{\partial \hat{\omega}_i} \\ &= \frac{2\hat{\omega}_i}{(K_{h1}\hat{\omega}_i)^2 + K_{h2}^2} [K_{h1}\hat{x}_{h2}(t) - K_{h2}\hat{x}_{h1}(t)] \end{aligned} \quad (3.16)$$

This substituted into equation (3.8) yields the algorithm for tracking $\hat{\omega}_i$.

To select the value of k , introduce the first order approximation

$$\xi_i(t) = \xi_{i0}(t) + \frac{\partial \xi_i(t)}{\partial \hat{\omega}_i} \Delta \omega_i \quad (3.17)$$

in equation (3.8), where $\xi_{i0}(t)$ is the innovation signal when $\hat{\omega}_i = \omega_i$ and where $\Delta \omega_i = \hat{\omega}_i - \omega_i$.

If ω_i is assumed to be constant, the following result is obtained:

$$\Delta \dot{\omega}_i = -k \left(\frac{\partial \xi_i(t)}{\partial \hat{\omega}_i} \right)^2 \Delta \omega_i - k \frac{\partial \xi_i(t)}{\partial \hat{\omega}_i} \xi_{i0} \quad (3.18)$$

This yields an approximate time constant for the estimation of ω_i given by:

$$T_\omega = \frac{(K_{h1}\hat{\omega}_i)^2 + K_{h2}^2}{2k\hat{\omega}_i^2\bar{\rho}^2} \quad (3.19)$$

If the variance of $\partial \xi_i(t)/\partial \hat{\omega}_i$ is small compared to the variance of $\xi_i(t)$, the variance of $\hat{\omega}_i$ is approximately given by [18]:

$$\text{Cov}(\hat{\omega}_i) = \frac{1}{2} k \text{Cov}(\xi_{i0}) \quad (3.20)$$

3.3 CONSTANT GAIN LINEAR KALMAN FILTER

In the fourth order transfer function model approach [5], the models discussed in Section 2.8.1 are selected for the HF motions. The on-line computation of Kalman gains and the estimation of parameters in the HF wave model is very complicated and cumbersome. A simplified algorithm is to choose a particular sea state say Beaufort 8, for filter design. The filter gain matrix is computed off-line based upon the linear LF model and the selected HF model. It is then used constantly for any sea state. Experimental results showed that in most cases, the constant gain filter is noticeably slower in reaching the steady state than the corresponding time varying filter. However, it may be acceptable in some operational conditions in which the accuracy is not so critical.

CHAPTER FOUR

THE STOCHASTIC OPTIMAL CONTROL PROBLEM IN DYNAMIC POSITIONING SYSTEM

4.1 INTRODUCTION

Recall that the control system must respond to the low frequency vessel motions but not high frequency motions. In the classical design of dynamic positioning control systems, a notch filter is cascaded with a PID controller. The notch filter is therefore an integral part of the control loop. In designing the notch filter, it is important that the phase shift introduced by the filter is small at the control loop unity gain crossover frequency, otherwise it may destabilize the control loop. The filter design always includes this compromise between good filtering (suppression of thruster modulation) and good regulating actions. The basic criteria for such a design given by Sorheim and Galtung [22] are:

- (a) The wave filter center frequency should be chosen equal to the maximum amplitude frequency response of the vessel for the chosen wave conditions.
- (b) The phase shift introduced by the filter at one decade below the center frequency should be less than 10 degrees.

- (c) The notch depth should be the maximum attainable consistent with hardware limitations.

The control frequencies normally lie in the range of 0 to 0.3 radians per second and the wave frequencies lie in the range 0.3 to 1.6 radians per second.

The PID controller approach has several disadvantages. Due to the couplings between the controlled motions, the integral action of the controller must be slow enough to reduce the excessive overshoots in the other controlled variables. The second disadvantage is due to the phase lag introduced in the control loops by the notch filters. These disadvantages led research engineers [6, 7, 8, 17, 18] to investigate the use of Kalman filtering and optimal control techniques in dynamic positioning systems.

Section 4.2 describes the optimal controller design criterion. In the dynamic ship positioning system, there are slowly varying disturbances such as current and wind. It is essential that the offsets due to such disturbances are eliminated. The technique to include integral action in the optimal controller is described in Section 4.3. Simplified schemes are given in Section 4.4.

4.2 OPTIMAL CONTROLLER DESIGN

The dynamic positioning control system and the state estimator is shown in Figure 4-1. The controller uses state feedback from the low frequency Kalman estimator. If the estimator works efficiently, the control system will respond only to the low frequency position error signal. Thence, the thruster modulation will be reduced. The wind force can be measured separately. It is a usual practice to feed this disturbance forward to minimize any undesirable effect.

The controller gain matrices can be determined using optimal control techniques. However, a suitable design must also satisfy classical design criteria. The performance criterion to be minimized may be defined as:

$$J(u) = E \left\{ \lim_{T \rightarrow \infty} \frac{1}{2T} \int_{-T}^T [\underline{x}_l^T Q_c \underline{x}_l + \underline{u}^T R_c \underline{u}] dt \right\} \quad (4.1)$$

where $\underline{x}_l(t)$ is the low frequency state vector, $\underline{u}(t)$ is the control signal, Q_c and R_c are weighting matrices and are positive definite and semi-positive definite respectively. E is the expectation operator. The optimal control gain matrix $K_c(t)$ may be calculated using well known Riccati equation techniques. The selection of the weighting matrices needs experience and judgement from the designer.

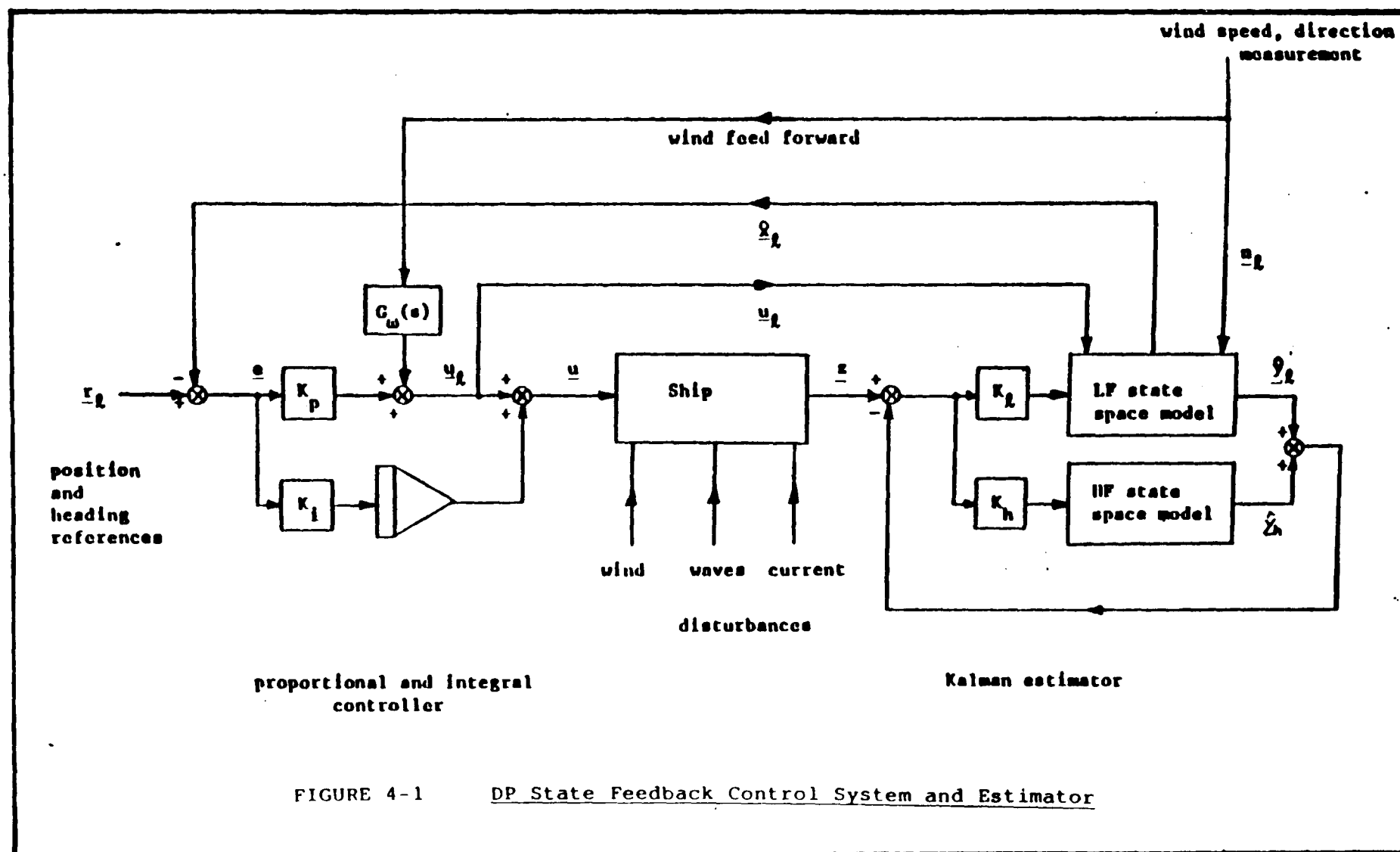


FIGURE 4-1 DP State Feedback Control System and Estimator

It may be useful to use the guidelines proposed by researchers such as Chang [23], Tyler and Tutem [24], Chen and Shen [25], Melheim [26] and Grimble [27].

4.3 OPTIMAL CONTROLLER WITH INTEGRAL ACTION

4.3.1 System Description

The dynamic ship positioning control problem is more complicated than that considered in the simple white noise LQG stochastic optimal control problem [28] (Section 4.2). The DP system has both slowly varying and high frequency disturbance inputs and the measurements are contaminated by both white and coloured noise. It is desirable to use integral control to offset slowly varying unmodelled disturbances, so the system can regulate about the given references. The system to be controlled is shown in Figure 4-2. The plant is assumed to be completely controllable and observerable and is represented by the time invariant state equations:

$$\dot{\underline{x}}_l(t) = \underline{A}_l \underline{x}_l(t) + \underline{B}_l \underline{u}(t) + \underline{D}_l \underline{\omega}_l(t) \quad (4.2)$$

$$\underline{y}_l(t) = \underline{C}_l \underline{x}_l(t) \quad (4.3)$$

where $\underline{x}_l(t) \in \mathbb{R}^h$, $\underline{u}(t) \in \mathbb{R}^r$, $\underline{\omega}_l(t) \in \mathbb{R}^q$ and $\underline{y}_l(t) \in \mathbb{R}^m$. The observed plant output $\underline{z}(t)$ is corrupted by an additive noise

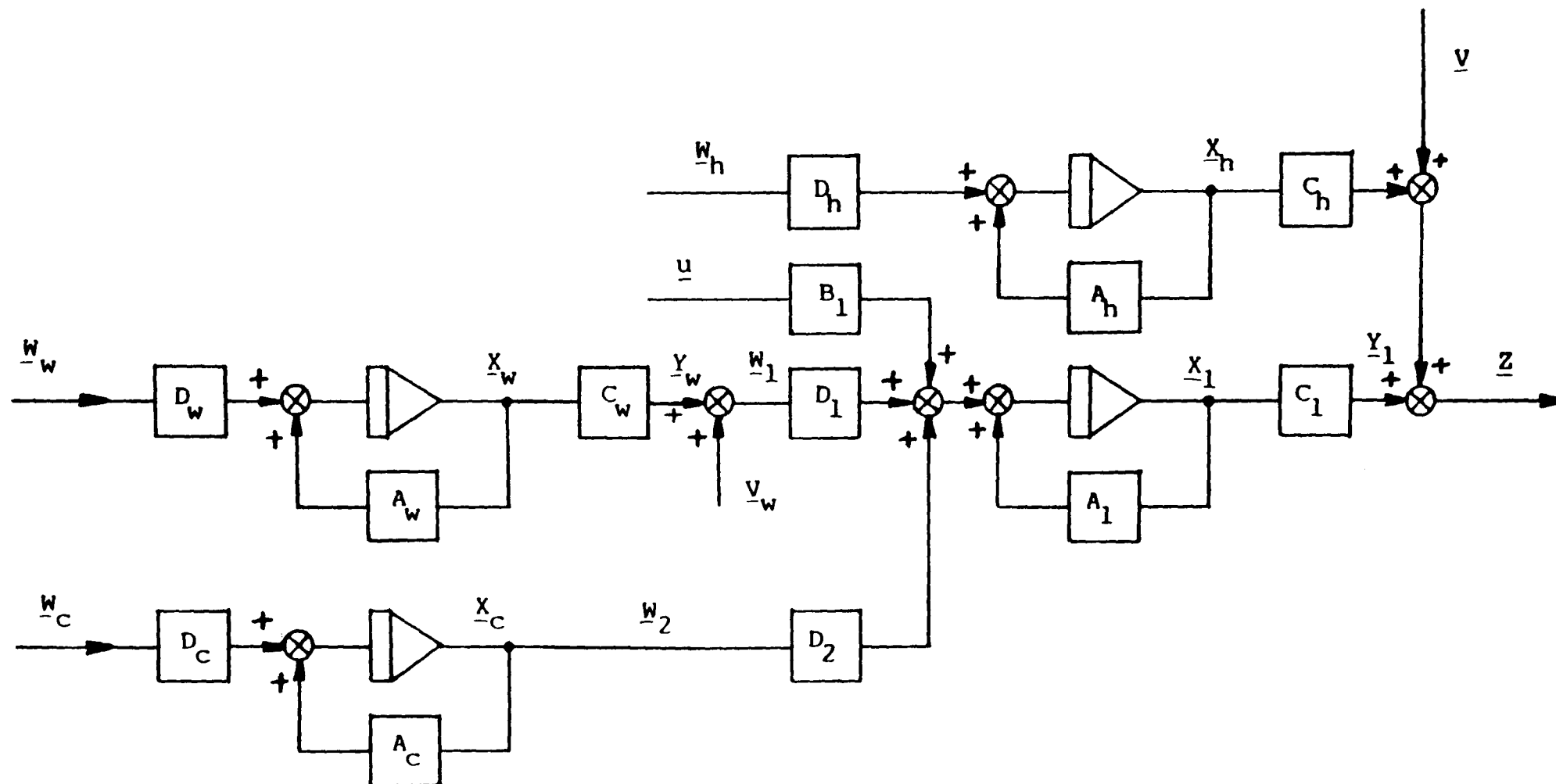


FIGURE 4-2 Stochastic Ship Positioning System (Complicated Model)

signal $\underline{v}'(t)$ containing both coloured $\underline{y}_h(t)$ and white $\underline{v}(t)$ noise components. The coloured output noise is generated by the following dynamical system which assumed to be asymptotically stable:

$$\dot{\underline{x}}_h(t) = A_h \underline{x}_h(t) + D_h \underline{\omega}_h(t) \quad (4.4)$$

$$\underline{y}_h(t) = C_h \underline{x}_h(t) \quad (4.5)$$

$\underline{v}(t)$ is the actual measurement noise where $\underline{y}_h(t)$ is the high frequency motion.

The output noise and the observation vectors are given by:

$$\underline{v}'(t) = \underline{y}_h(t) + \underline{v}(t) \quad (4.6)$$

$$\underline{z}(t) = \underline{y}_l(t) + \underline{v}'(t) \quad (4.7)$$

the input disturbances consist of current disturbances and wind gust disturbances. These can be separated into two groups, $\underline{\omega}_1$ and $\underline{\omega}_2$ where:

$$D_l \underline{\omega}_l(t) = D_1 \underline{\omega}_1(t) + D_2 \underline{\omega}_2(t) \quad (4.8)$$

and

$$\underline{\omega}_1(t) = \underline{y}_\omega(t) + \underline{v}_\omega(t) \quad (4.9)$$

$$\underline{\omega}_2(t) = \underline{x}_c(t) \quad (4.10)$$

The white noise input $\underline{y}_\omega(t)$ may allow for modelling errors, and the coloured noise $\underline{y}_\omega(t)$ represents the relatively fast

plant disturbances (e.g. wind gust). Disturbances which are slowly varying can be represented by the signal $\underline{x}_C(t)$ (current). The system modelling the disturbances is assumed to be asymptotically stable. The system representing the fast input disturbances is modelled by the state equations:

$$\dot{\underline{x}}_\omega(t) = A_\omega \underline{x}_\omega(t) + D_\omega \underline{\omega}_\omega(t) \quad (4.11)$$

$$\underline{y}_\omega(t) = C_\omega \underline{x}_\omega(t) \quad (4.12)$$

and similarly, the low frequency disturbances are modelled by the system.

$$\underline{x}_C(t) = A_C \underline{x}_C(t) + D_C \underline{\omega}_C(t) \quad (4.13)$$

The white noise signals $\underline{\omega}_h(t)$, $\underline{\omega}_\omega(t)$ and $\underline{\omega}_C(t)$ driving the disturbance models are assumed to have known constant variance matrices Q_v , Q_ω and Q_C respectively. Similarly, the signals $\underline{v}_\omega(t)$ and $v(t)$ are assumed to have covariance matrices Q_v and R_v respectively. The noise sources are assumed to be mutually independent and the noises are assumed to be Gaussian and stationary.

The above equations may be written in the augmented matrix form:

$$\dot{\underline{\tilde{x}}}(t) = \tilde{A} \underline{\tilde{x}}(t) + \tilde{B} \underline{\tilde{u}}(t) + \tilde{D} \underline{\tilde{\omega}}(t) \quad (4.14)$$

$$\underline{z}(t) = \tilde{C} \underline{\tilde{x}}(t) + \underline{v}'(t) \quad (4.15)$$

where the augmented state vector is defined as:

$$\begin{aligned}\tilde{\underline{x}}(t) &= \text{Col}\{\underline{x}_h(t) \quad \underline{x}_c(t) \quad \underline{x}_\omega(t) \quad \underline{x}_l(t)\} \quad \tilde{\underline{x}}(t) \in \mathbb{R}^P \\ \tilde{\underline{\omega}}(t) &= \text{Col}\{\underline{\omega}_h(t) \quad \underline{\omega}_c(t) \quad \underline{\omega}_\omega(t) \quad \underline{v}_\omega(t)\}\end{aligned}$$

and the system matrices become:

$$\tilde{\underline{A}} = \begin{bmatrix} A_h & 0 & 0 & 0 \\ 0 & A_c & 0 & 0 \\ 0 & 0 & A_\omega & 0 \\ 0 & D_2 & D_1 C_\omega & A_l \end{bmatrix} \quad \tilde{\underline{B}} = \begin{bmatrix} 0 \\ 0 \\ 0 \\ B_l \end{bmatrix} \quad (4.16)$$

$$\tilde{\underline{D}} = D_h \oplus D_c \oplus D_\omega \oplus D_l, \quad \tilde{\underline{C}} = [C_h \quad 0 \quad 0 \quad C_l] \quad (4.17)$$

In the dynamic ship positioning problem, it is important that a constant disturbance should not produce a constant position offset in a calm sea. Thus, as in the usual industrial control situation, integral control must be used to ensure that constant disturbances do not produce steady state errors. The way in which integral action is introduced is discussed in the following section.

4.3.2 Optimal Regulating Problem

Assuming that the set point vector $\underline{x}_0(t)$ to be constant the optimal controller must bring the system states to the corresponding non-zero set points, which means the expected value of the steady state error between the states and their

set points, must be zero. To achieve this condition, an integral operator L will be introduced into the performance criterion, where the operator L is defined as:

$$(L\tilde{x})(t) \triangleq \int_0^T A_I \tilde{x}(t) dt \quad (4.18)$$

Where A_I is a constant $r \times p$ matrix with elements equal to zero or unity. The unity element corresponds to the state which should have zero steady state value under constant disturbance. Since only plant states are to be controlled, the matrix A_I has the block form:

$$A_I = [0 \quad 0 \quad 0 \quad A_{24}] \quad (4.19)$$

Matrix A_{24} has the elements corresponding to sway position and yaw angle equal to unity. The other elements are zero. The performance criterion may now be defined as:

$$\begin{aligned} J(t_0, T) = E \left\{ \int_{t_0}^T [< \tilde{x}(t) - \tilde{x}_0(t), Q_1 \tilde{x}(t) - \tilde{x}_0(t) > E_p \right. \\ & + < L \{ \tilde{x}(t) - \tilde{x}_0(t) \}, Q_2 L \{ \tilde{x}(t) - \tilde{x}_0(t) \} > E_p \\ & \left. + < \underline{u}(t), R_1 \underline{u}(t) > E_r] dt \right\} \quad (4.20) \end{aligned}$$

Where $\tilde{x}_0(t) = [0 \quad 0 \quad 0 \quad \underline{x}_0^T(t)]^T$, $Q_1 \succ 0$, $Q_2 \succ 0$ and $R_1 \succ 0$. The reason behind the introduction of the integral operator terms is that, when T becomes large, the cost will tend to infinity, unless the mean error $A_I \{ \tilde{x}(t) - \tilde{x}_0(t) \}$ is zero.

This performance specification therefore ensures that the controller includes integral action.

The above problem is not the usual form for the linear quadratic stochastic control problem. To transform the problem into the required form so that the standard results may be used, define:

$$\tilde{\underline{x}}_1(t) = \begin{bmatrix} \tilde{\underline{x}}(t) \\ (L\tilde{\underline{x}})(t) \end{bmatrix} \quad (4.21)$$

$$\tilde{\underline{x}}_2(t) = \begin{bmatrix} \tilde{\underline{x}}_0(t) \\ (L\tilde{\underline{x}}_0)(t) \end{bmatrix} \quad (4.22)$$

Notice that:

$$\dot{\tilde{\underline{x}}}_1(t) = \begin{bmatrix} \dot{\tilde{\underline{x}}}(t) \\ A_I \tilde{\underline{x}}(t) \end{bmatrix} \quad (4.23)$$

and

$$\dot{\tilde{\underline{x}}}_2(t) = \begin{bmatrix} \dot{\tilde{\underline{x}}}_0(t) \\ A_I \tilde{\underline{x}}_0(t) \end{bmatrix} \quad (4.24)$$

The reference signal $\underline{x}_0(t)$ is assumed constant. An additional assumption will now be made, namely that $\underline{x}_0(t)$ is a solution of the plant state space equation. Thus, $\tilde{\underline{x}}_0(t)$ is assumed to be a solution of the augmented state space equation.

$$\dot{\tilde{\underline{x}}}_0(t) = A_I \tilde{\underline{x}}_0(t) = 0 \quad (4.25)$$

The subspace spanned by the reference signal is therefore assumed to be in the Kernel of matrix \tilde{A} . To understand the implications of this assumption, the second and fourth state variable represent the position of the vessel in sway and yaw. These position signals are obtained by integrating the ship velocities. Thus, if there are no disturbances, the plant state vector, in steady state, will have the form:

$$\underline{x}_p(t) = [0 \quad \underline{x}_s \quad 0 \quad \underline{x}_y \quad 0, \dots, 0]^T \quad (4.26)$$

The reference signal $\underline{x}_o(t)$ will have a similar form and $\underline{x}_o(t)$ will span the corresponding two dimensional subspace of the p-dimensional state space. That is, the only reference signals which are allowed are those whose non-zero entries correspond to a particular set of plant states. These states correspond to integrators, and are at the output of the state space model of the system. These are also the states to be controlled to the set point and may be recognized by the zero columns of the system A_p -matrix.

The state equations now become:

$$\dot{\tilde{\underline{x}}}_1(t) = \begin{bmatrix} \tilde{\underline{A}} & 0 \\ \underline{A}_I & 0 \end{bmatrix} \tilde{\underline{x}}_1(t) + \begin{bmatrix} \tilde{\underline{B}} \\ 0 \end{bmatrix} \underline{u}(t) + \begin{bmatrix} \tilde{\underline{D}} \\ 0 \end{bmatrix} \tilde{\underline{\omega}}(t) \quad (4.27)$$

$$\dot{\tilde{\underline{x}}}_2(t) = \begin{bmatrix} \tilde{\underline{A}} & 0 \\ \underline{A}_I & 0 \end{bmatrix} \tilde{\underline{x}}_2(t) \quad (4.28)$$

The performance criterion and state equations may now be rewritten in the form:

$$\dot{\underline{\bar{x}}} = \underline{\bar{A}} \underline{\bar{x}}(t) + \underline{\bar{B}} \underline{\bar{u}}(t) + \underline{\bar{D}} \underline{\bar{\omega}}(t) \quad (4.29)$$

$$\underline{z}(t) = \underline{\bar{C}} \underline{\bar{x}}(t) + \underline{v}(t) \quad (4.30)$$

$$J(t_0, T) = E \left\{ \int_{t_0}^T \langle \underline{\bar{x}}(t), \underline{\bar{Q}}_1 \underline{\bar{x}}(t) \rangle_{E_P} + \langle \underline{u}(t), \underline{R} \underline{u}(t) \rangle_{E_R} dt \right\} \quad (4.31)$$

Where

$$\underline{\bar{x}}(t) \triangleq \begin{bmatrix} \tilde{\underline{x}}_1(t) \\ \tilde{\underline{x}}_2(t) \end{bmatrix} \quad (4.32)$$

$$\underline{\bar{A}} \triangleq \begin{bmatrix} \tilde{\underline{A}}_1 & 0 \\ 0 & \tilde{\underline{A}}_2 \end{bmatrix}, \quad \underline{A}_1 = \begin{bmatrix} \tilde{\underline{A}} & 0 \\ \underline{A}_I & 0 \end{bmatrix}, \quad \underline{A}_2 = \begin{bmatrix} \tilde{\underline{A}} & 0 \\ \underline{A}_I & 0 \end{bmatrix} \quad (4.33)$$

$$\underline{\bar{B}} \triangleq \begin{bmatrix} \tilde{\underline{B}}_1 \\ 0 \end{bmatrix}, \quad \tilde{\underline{B}}_1 \triangleq \begin{bmatrix} \tilde{\underline{B}} \\ 0 \end{bmatrix}, \quad \underline{\bar{D}} \triangleq \begin{bmatrix} \tilde{\underline{D}}_1 \\ 0 \end{bmatrix}, \quad \tilde{\underline{D}}_1 \triangleq \begin{bmatrix} \tilde{\underline{D}} \\ 0 \end{bmatrix} \quad (4.34)$$

$$\underline{\bar{C}} \triangleq [\tilde{\underline{C}}_1, 0], \quad \underline{C}_1 \triangleq [\tilde{\underline{C}}, 0] \quad (4.35)$$

$$\underline{\bar{Q}}_1 \triangleq \begin{bmatrix} \tilde{\underline{Q}}_1 & -\tilde{\underline{Q}}_1 \\ -\tilde{\underline{Q}}_1 & \tilde{\underline{Q}}_1 \end{bmatrix}, \quad \tilde{\underline{Q}}_1 = \begin{bmatrix} \underline{Q}_1 & 0 \\ 0 & \underline{Q}_2 \end{bmatrix} \quad (4.36)$$

The effect of the equivalence on the matrix caused by the assumption $\tilde{A}_1 = \tilde{A}_2$ will be discussed in the following section.

The above problem may now be solved by considering the individual subsystems. This has the advantage that the structure of the optimal system can be identified, and the role of individual blocks can be analyzed. The order of the Riccati equations which must be solved can also be reduced.

4.3.3 Control Problem

It is well known [29] that the solution to the linear stochastic control problem may be obtained by considering the equivalent deterministic optimal control problem and the Kalman filtering problem. This result follows from the separation principle [30] of stochastic optimal control theory.

Consider the partitioned system described by equations (4.29) to (4.31). The control matrix Riccati differential equation for the system becomes:

$$\dot{\bar{P}}_1(t) = -\bar{P}_1\bar{A} - \bar{A}^T\bar{P}_1 + \bar{P}_1\bar{B}R^{-1}\bar{B}^T\bar{P}_1 - \bar{Q}_1 \quad (4.37)$$

$$\begin{aligned}
\begin{bmatrix} \dot{\bar{P}}_{11} & \dot{\bar{P}}_{12} \\ \dot{\bar{P}}_{21} & \dot{\bar{P}}_{22} \end{bmatrix} &= - \begin{bmatrix} \bar{P}_{11} & \bar{P}_{12} \\ \bar{P}_{21} & \bar{P}_{22} \end{bmatrix} \begin{bmatrix} \tilde{A}_1 & 0 \\ 0 & \tilde{A}_2 \end{bmatrix} \\
&- \begin{bmatrix} \tilde{A}_1^T & 0 \\ 0 & \tilde{A}_2^T \end{bmatrix} \begin{bmatrix} \bar{P}_{11} & \bar{P}_{12} \\ \bar{P}_{21} & \bar{P}_{22} \end{bmatrix} + \begin{bmatrix} \bar{P}_{11} & \bar{P}_{12} \\ \bar{P}_{21} & \bar{P}_{22} \end{bmatrix} \begin{bmatrix} \tilde{B}_1 R^{-1} \tilde{B}_1^T & 0 \\ 0 & 0 \end{bmatrix} \\
&\begin{bmatrix} \bar{P}_{11} & \bar{P}_{12} \\ \bar{P}_{21} & \bar{P}_{22} \end{bmatrix} - \begin{bmatrix} \tilde{Q}_1 & -\tilde{Q}_1 \\ -\tilde{Q}_1 & \tilde{Q}_1 \end{bmatrix} \quad (4.38)
\end{aligned}$$

The individual equations become:

$$\begin{aligned}
\dot{\bar{P}}_{11}(t) &= -\bar{P}_{11}(t)\tilde{A}_1 - \tilde{A}_1^T \bar{P}_{11}(t) \\
&+ \bar{P}_{11}(t)\tilde{B}_1 R^{-1} \tilde{B}_1^T \bar{P}_{11}(t) - \tilde{Q}_1 \quad (4.39)
\end{aligned}$$

$$\begin{aligned}
\dot{\bar{P}}_{12}(t) &= -\bar{P}_{12}(t)\tilde{A}_2 - \tilde{A}_1^T \bar{P}_{12}(t) \\
&+ \bar{P}_{11}(t)\tilde{B}_1 R^{-1} \tilde{B}_1^T \bar{P}_{12}(t) + \tilde{Q}_1 \quad (4.40)
\end{aligned}$$

$$\begin{aligned}
\dot{\bar{P}}_{22}(t) &= -\bar{P}_{22}(t)\tilde{A}_2 - \tilde{A}_2^T \bar{P}_{22}(t) \\
&+ \bar{P}_{21}\tilde{B}_1 R^{-1} \tilde{B}_1^T \bar{P}_{12}(t) - \tilde{Q}_1 \quad (4.41)
\end{aligned}$$

When $\bar{P}_1(T)=0$, the optimal control feedback gain matrix is given by:

$$\bar{K}_1(t) = R^{-1} \tilde{B}_1^T \bar{P}_1 \quad (4.42)$$

$$= [R^{-1} \tilde{B}_1^T \bar{P}_{11}(t), R^{-1} \tilde{B}_1^T \bar{P}_{12}(t)] \quad (4.43)$$

In this particular case, $\tilde{A}_1 = \tilde{A}_2$. It follows that the above Riccati equations become identical, giving the solutions:

$$\bar{P}_{11}(t) = \bar{P}_{22}(t) = -\bar{P}_{12}(t) \quad (4.44)$$

and thus the gain matrix becomes:

$$\bar{K}_1(t) = [\bar{K}_{11}(t) \quad -\bar{K}_{11}(t)] \quad (4.45)$$

where

$$\bar{K}_{11}(t) \triangleq R^{-1} \tilde{B}_1^T \tilde{P}_{11}(t) \quad (4.46)$$

Thus, for the system where the assumption made in the last section holds, using the equation (4.45), the control signal is obtained by multiplying the gain matrix $\bar{K}_{11}(t)$ by the signal $\tilde{x}_1(t) - \tilde{x}_2(t)$, which gives:

$$\underline{u}^*(t) = -\bar{K}_{11}(t) \{ \tilde{x}_1(t) - \tilde{x}_2(t) \} \quad (4.47)$$

$$= K_{11}^c(t) \{ \tilde{x}_0(t) - \tilde{x}(t) \} + K_{12}^c(t) \{ L(\tilde{x}_0 - \tilde{x}) \}(t) \quad (4.48)$$

where

$$\bar{K}_{11}(t) = [K_{11}^c(t) \quad K_{12}^c(t)] \quad (4.49)$$

The optimal control signal $\underline{u}^*(t)$ is clearly the sum of a state tracking error term and an integral of the state tracking error term. The integral term only involves a subset of the state variables which are determined by A_I .

The matrix Riccati equation (4.39) can be expanded to obtain an expression of the gain matrices $K_{11}^C(t)$ and $K_{12}^C(t)$.

$$\begin{aligned}\bar{K}_{11}(t) &= R^{-1}\tilde{B}_1^T\bar{P}_{11}(t) \\ &= [K_{11}^C(t) \quad K_{12}^C(t)] \\ &= [R^{-1}\tilde{B}^T\tilde{P}_{11}(t) \quad R^{-1}\tilde{B}^T\tilde{P}_{12}(t)]\end{aligned}\tag{4.50}$$

where $\tilde{P}_{11}(t)$ and $\tilde{P}_{12}(t)$ are the solutions of the following matrix Riccati equations with $\bar{P}_{11}(T)=0$.

$$\begin{aligned}\dot{\tilde{P}}_{11}(t) &= -\tilde{P}_{11}\tilde{A} - \tilde{P}_{12}A_I - \tilde{A}^T\tilde{P}_{11} - A_I^T\tilde{P}_{21} \\ &\quad + \tilde{P}_{11}\tilde{B}R^{-1}\tilde{B}^T\tilde{P}_{11} - Q_1\end{aligned}\tag{4.51}$$

$$\dot{\tilde{P}}_{12}(t) = -\tilde{A}^T\tilde{P}_{12} - A_I^T\tilde{P}_{22} + \tilde{P}_{11}\tilde{B}R^{-1}\tilde{B}^T\tilde{P}_{12}\tag{4.52}$$

$$\dot{\tilde{P}}_{22}(t) = \tilde{P}_{21}\tilde{B}R^{-1}\tilde{B}^T\tilde{P}_{12} - Q_2\tag{4.53}$$

An alternative partition of the state vector will be used below. It will further simplify the equations. The system matrices \tilde{A}_1 and \tilde{B}_1 in equation (4.33) and (4.34) have the form:

$$\tilde{A}_1 = \begin{bmatrix} A_h & 0 & 0 & 0 & 0 \\ 0 & A_c & 0 & 0 & 0 \\ 0 & 0 & A_w & 0 & 0 \\ 0 & D_2 & D_1C_w & A_l & 0 \\ 0 & 0 & 0 & A_I & 0 \end{bmatrix}, \tilde{B}_1 = \begin{bmatrix} 0 \\ 0 \\ 0 \\ B_l \\ 0 \end{bmatrix}\tag{4.54}$$

and

$$\tilde{Q}_1 = 0 \oplus 0 \oplus 0 \oplus Q_l \oplus Q_2, \quad (Q_l \geq 0, Q_2 \geq 0) \quad (4.55)$$

where Q_l is the optimal control weighting matrix corresponding to the plant states. Note that the state associated with the output noise subsystem and the disturbance subsystem A_c and A_w have zero weighting in the cost function. These states are uncontrollable and thus, it is reasonable to set their weighting matrices Q_v , Q_c and Q_w to zero. Note that if non-zero values have been assigned to these matrices, they would not affect the gain calculation.

It may now be shown that there is no feedback from the output noise states $\underline{x}_h(t)$, for these states do not affect the plant states. Let the state vector $\tilde{\underline{x}}_1(t)$ be partitioned as follows:

$$\tilde{\underline{x}}_1 = \begin{bmatrix} \underline{x}_h(t) \\ \underline{x}_3(t) \end{bmatrix} \quad (4.56)$$

The above matrices may then be written in the form:

$$\tilde{A}_1 = \begin{bmatrix} A_h & 0 \\ 0 & A_3 \end{bmatrix}, \quad \tilde{B}_1 = \begin{bmatrix} 0 \\ B_3 \end{bmatrix}, \quad \tilde{Q}_1 = \begin{bmatrix} 0 & 0 \\ 0 & Q_3 \end{bmatrix} \quad (4.57)$$

Matrix Riccati equation (4.39) is expanded and the individual equations become:

$$\dot{P}_{11}(t) = -P_{11}A_h - A_h^T P_{11} + P_{12}B_3 R^{-1} B_3^T P_{21} \quad (4.58)$$

$$\dot{P}_{12}(t) = -P_{12}A_3 - A_h^T P_{12} + P_{12}B_3 R^{-1} B_3^T P_{22} \quad (4.59)$$

$$\dot{P}_{22}(T) = -P_{22}A_3 - A_3^T P_{22} + P_{22}B_3 R^{-1} B_3^T P_{22} - Q_3 \quad (4.60)$$

where $P_{22}(T)=0$. The third equation above is independent of the first two equations and the latter have the following solutions:

$$P_{11}(t) = 0, \quad P_{12}(t) = P_{21}^T(t) = 0 \quad (4.61)$$

$$\forall t \in [t_0, T]$$

The optimal control feedback gain matrix is given by:

$$\begin{aligned} \bar{K}_{11}(t) &= R^{-1} \tilde{B}_1^T \bar{P}_{11}(t) \\ &= [0, \quad R^{-1} B_3^T P_w(t)] \end{aligned} \quad (4.62)$$

where $P_w(t) \triangleq P_{22}(t)$. Note that the matrix $P_{11}(t)$ does not affect the gain calculation and also that $P_{12}(t)$ and $P_{21}(t)$ will be non-zero if \tilde{Q}_1 has a non-zero off diagonal block.

In such a case, the first entry in the gain matrix $R^{-1} B_3^T P_{21}(t)$ becomes non-zero.

As would be expected, there is state feedback from the disturbance states $x_c(t)$ and $x_w(t)$, which affect the plant states $\underline{x}_l(t)$. This may be shown by partitioning the state vector $\underline{x}_3(t)$ into the form:

$$\underline{x}_3(t) = \begin{bmatrix} \underline{x}_c(t) \\ \underline{x}_w(t) \\ \underline{x}_4(t) \end{bmatrix} \quad (4.63)$$

The submatrices A_3 and B_3 occurring in equation (4.57) may now be partitioned as follows:

$$A_3 = \left[\begin{array}{cc|cc} A_c & 0 & 0 & 0 \\ 0 & A_w & 0 & 0 \\ \hline D_2 & D_1 C_w & A & 0 \\ 0 & 0 & A_I & 0 \end{array} \right] \quad B_3 = \begin{bmatrix} 0 \\ 0 \\ B_l \\ 0 \end{bmatrix} \quad (4.64)$$

and

$$Q_3 = \left[\begin{array}{cc|cc} 0 & 0 & 0 & 0 \\ 0 & 0 & 0 & 0 \\ \hline 0 & 0 & Q_l & 0 \\ 0 & 0 & 0 & Q_2 \end{array} \right] \quad (4.65)$$

These matrices may therefore be written in the form:

$$A_3 = \begin{bmatrix} A_{cw} & 0 \\ A_a & A_4 \end{bmatrix} \quad B_3 = \begin{bmatrix} 0 \\ B_4 \end{bmatrix} \quad Q_3 = \begin{bmatrix} 0 & 0 \\ 0 & Q_4 \end{bmatrix} \quad (4.66)$$

The matrix Riccati equation (4.60) is expanded and the individual equations become as follows (note that $P_w(t) = P_{22}(t)$):

$$\begin{aligned} \dot{P}'_{11}(t) = & -P'_{11}(t)A_{cw} - P'_{12}(t)A_a - A_{cw}^T P'_{11}(t) \\ & - A_a^T P'_{21}(t) + P'_{21}(t)B_4 R^{-1} B_4^T P'_{21}(t) \end{aligned} \quad (4.67)$$

$$\begin{aligned} \dot{P}'_{21}(t) = & -P'_{21}A_{cw} - P'_{22}A_a - A_4^T P'_{21}(t) \\ & + P'_{22}(t)B_4 R^{-1} B_4^T P'_{21}(t) \end{aligned} \quad (4.68)$$

$$\begin{aligned} \dot{P}'_{22}(t) = & -P'_{22}(t)A_4 - A_4^T P'_{22}(t) \\ & + P'_{22}(t)B_4 R^{-1} B_4^T P'_{22}(t) - Q_4 \end{aligned} \quad (4.69)$$

where $P_w(T)=P_{22}(T)=0$. The optimal control feedback gain matrix is given by:

$$K_w(t) \triangleq R^{-1} B_3^T P_w(t) \quad (4.70)$$

$$= [R^{-1} B_4^T P'_w(t) \quad R^{-1} B_4^T P_a(t)] \quad (4.71)$$

where $P'_w(t)=P'_{21}(t)$ and $P_a(t)=P'_{22}(t)$. Notice that the solution to equation (4.67) need not be calculated since this does not enter into the calculation of the optimal feedback gain $K_w(t)$.

Let the solutions to equations (4.68) and (4.69) be:

$$P'_w(t) = \begin{bmatrix} P_{11}^w(t) & P_{12}^w(t) \\ P_{21}^w(t) & P_{22}^w(t) \end{bmatrix}, \quad P'_w(t) = P'_{21}(t) \quad (4.72)$$

and

$$P_a(t) = \begin{bmatrix} P_{11}^a(t) & P_{12}^a(t) \\ P_{11}^a(t) & P_{22}^a(t) \end{bmatrix}, \quad P_a(t) = P_{22}^a(t) \quad (4.73)$$

respectively.

The system matrices involved in the equations have the form:

$$A_4 = \begin{bmatrix} A_l & 0 \\ A_I & 0 \end{bmatrix}, \quad B_4 = \begin{bmatrix} B_l \\ 0 \end{bmatrix}, \quad Q_4 = \begin{bmatrix} Q_l & 0 \\ 0 & Q_2 \end{bmatrix} \quad (4.74)$$

Thus, the total feedback gain matrix is obtained in the simplified form:

$$\bar{K}_{11}(t) = [0, K_w(t)] \quad (4.75)$$

$$= R^{-1} B_4^T [0, P_{11}^w(t), P_{12}^w(t), P_{11}^a(t), P_{12}^a(t)] \quad (4.76)$$

where $\{P_{11}^a(t), P_{12}^a(t)\}$ and $\{P_{11}^w(t), P_{12}^w(t)\}$ are the solutions of the linear differential equations:

$$\dot{P}_a(t) = -P_a A_4 - A_4^T P_a + P_a B_4 R^{-1} B_4^T P_a - Q_4 \quad (4.77)$$

and

$$\dot{P}_w(t) = -P_w A_{cw} - A_{cw}^T P_w - P_a A_a + P_a B_4 R^{-1} B_4^T P_w \quad (4.78)$$

respectively. The optimal control signal can be calculated using equation (4.47)

$$\begin{aligned}
 \underline{u}^*(t) &= -\bar{K}_{11}(t) \{ \tilde{x}_1(t) - \tilde{x}_2(t) \} \\
 &= \bar{K}_{11}(t) \begin{bmatrix} \tilde{x}_0(t) - \tilde{x}(t) \\ L(\tilde{x}_0 - \tilde{x})(t) \end{bmatrix}
 \end{aligned}
 \tag{4.79}$$

The matrix $\bar{K}_{11}(t)$ has been partitioned in a simple form as shown in equation (4.75). There is no feedback from the output noise states. Proportional feedback is present both in the input disturbance model states and the plant states. In addition, there is an integral feedback term from a subset of the plant states which must have zero steady state error. Finally, it should be noted that the weighting matrix Q_1 was assumed to be block diagonal. If this is not the case, the above feedback gains have to be modified.

Infinite Time Solution to Control Problem

The most important practical solution to the control problem is often the limiting case in which the final T tends to infinity. It will now be shown that the matrix Riccati equations considered previously should yield a unique solution for the optimal feedback gain matrix in steady state. Let the state vector $\tilde{x}_1(t)$ be partitioned in such a way that the second vector contains the plant and integral states only, that is:

$$\begin{aligned} \tilde{\underline{x}}_1(t) = & \{ \underline{x}_h^T(t), \underline{x}_c^T(t), \underline{x}_w^T(t) \}, \\ & \{ \underline{x}_l^T(t), (L\tilde{\underline{x}})^T(t) \} \}^T \end{aligned} \quad (4.80)$$

The system matrices in (4.64) may also be partitioned in the same manner:

$$\tilde{\underline{A}}_1 = \begin{bmatrix} \tilde{A}_{11} & 0 \\ \tilde{A}_{21} & A_4 \end{bmatrix}, \quad \tilde{\underline{B}}_1 = \begin{bmatrix} 0 \\ B_4 \end{bmatrix}, \quad \tilde{\underline{Q}}_1 = \begin{bmatrix} 0 & 0 \\ 0 & Q_4 \end{bmatrix} \quad (4.81)$$

The matrix Riccati equation (4.39) may be expanded to obtain the following equations in the steady state:

$$\begin{aligned} 0 = & -P_{11}\tilde{A}_{11} - P_{12}\tilde{A}_{21} - \tilde{A}_{11}^T P_{21} - \tilde{A}_{21}^T P_{21} \\ & + P_{12}B_4R^{-1}B_4^T P_{21} \end{aligned} \quad (4.82)$$

$$\begin{aligned} 0 = & -P_{21}\tilde{A}_{11} - P_{22}\tilde{A}_{21} - A_4^T P_{21} \\ & + P_{22}B_4R^{-1}B_4^T P_{21} \end{aligned} \quad (4.83)$$

$$Q_4 = -P_{22}A_4 - A_4^T P_{22} + P_{22}B_4R^{-1}B_4^T P_{22} \quad (4.84)$$

The feedback gain matrix is given by equation (4.46) as:

$$\bar{K}_{11}(t) = R^{-1}B_4^T [P_{21} \quad P_{22}] \quad (4.85)$$

Note that only the steady state matrices P_{21} and P_{22} enter the gain calculation, thence equation (4.82) may be

neglected. Also notice that given P_{22} , equation (4.83) is linear in P_{21} .

The condition under which equation (4.84) has a unique solution will now be discussed [29, 31]. Assume Q_4 is of rank r_1 , where $r_1 \leq n+r$, Q_4 may be expressed as:

$$Q_4 = H^T H \quad (4.86)$$

where H is a constant $r_1 \times (n+r)$ matrix [32]. It is well known that if (A_4, H) is completely observable, and (A_4, B_4) is completely controllable, then equation (4.84) has a unique positive definite solution. Furthermore, all the eigenvalues of the resulting closed loop system matrix

$$A_f \triangleq A_4 - B_4 R^{-1} B_4^T P_{22} \quad (4.87)$$

have negative real parts and A_f is an asymptotically stable matrix [33]. In this case, equation (4.83) may be written as:

$$A_f^T P_{21} + P_{21} \tilde{A}_{11} = -P_{22} \tilde{A}_{21} \quad (4.88)$$

This equation has a unique solution if and only if A_f^T and $-\tilde{A}_{11}$ have no eigenvalues in common [34, 35]. That is, the equation has a unique solution provided that:

$$\lambda_i(A_f^T) + \lambda_j(\tilde{A}_{11}) \neq 0, \quad \forall i, j \quad (4.89)$$

The eigenvalues corresponding to the matrix A_f are all negative and thus equation (4.89) will be satisfied provided the eigenvalues of \tilde{A}_{11} are all negative too.

The subsystem matrix $\tilde{A}_{11} = A_h \oplus A_c \oplus A_w$ is, by previous assumptions, stable and hence equation (4.88) has a unique solution. Note that in the case of constant disturbances, $A_c = 0$ and the above condition still holds.

To show that the above system with state feedback is stable, let $\tilde{x}_1(t)$ given by equation (4.80) be written in the form:

$$\tilde{x}_1(t) = \begin{bmatrix} \underline{x}_5(t) \\ \underline{x}_4(t) \end{bmatrix} \quad (4.90)$$

The state trajectory $\underline{x}_5(t)$ will clearly be bounded, since $\underline{x}_5(t)$ satisfies:

$$\dot{\underline{x}}_5(t) = \tilde{A}_{11} \underline{x}_5(t) \quad (4.91)$$

and \tilde{A}_{11} is assumed stable. The control signal which determines the zero input response of the system is given by equation (4.48) and (4.85) as:

$$u^*(t) = -R^{-1}B_4^T P_{21} \underline{x}_5(t) - R^{-1}B_4^T P_{22} \underline{x}_4(t) \quad (4.92)$$

and thus $\underline{x}_4(t)$ satisfies:

$$\dot{\underline{x}}_4(t) = A_f \underline{x}_4(t) + (\tilde{A}_{21} - B_4 R^{-1} B_4^T P_{21}) \underline{x}_5(t) \quad (4.93)$$

The matrix A_f has eigenvalues with negative real parts and the state trajectory $\underline{x}_5(t)$ is bounded, which implies that the response $\underline{x}_4(t)$ will also be bounded. It follows that the system is stable. However, for a constant input disturbance (modelled by setting $A_C=0$), the plant states may not all tend asymptotically to the set point. The plant states which must be driven to the set point values are, of course, included in the integral term. The disturbance system A_C was in fact, assumed to be asymptotically stable. It therefore follows that both \tilde{A}_{11} and the closed loop system are asymptotically stable.

The above uniqueness and stability arguments depend upon the assumption that the A_4 subsystem is controllable and observable. The latter assumption may be easily justified, since both the weighting matrix H and the integral control matrix A_I are selected by the designer. The conditions under which the subsystem is controllable have been established by Porter and Power [36-39]. They are:

- (a) If A_l is non-singular (A_l, B_l) must be a controllable pair, and

$$\text{rank}(A_I A_l^{-1} B_l) = r \quad (4.94)$$

(b) If A_l is singular (A_l, B_l) must be a controllable pair and

$$\text{rank} \{ A_I (A_l + B_l F)^{-1} B_l \} = r \quad (4.95)$$

where r is the rank of the matrix A_I and F is any matrix for which $(A_l + B_l F)$ is non-singular.

In ship positioning control problems, the matrix A_l is singular, but the second condition may be satisfied since an appropriate F matrix may be defined.

The equivalent state feedback scheme for deterministic systems is shown in Figure 4-3. Usually, an alternative way to obtain integral control action may be by introducing an additional derivative term of $\underline{u}(t)$ in the cost function. This is often used in deterministic optimal control systems [40-42]. However, the optimal control signal in the stochastic control problem will include the filtered noise input signals. Thus, if the cost is to be calculated from the plant measurements, the cost function should not include a term which depends upon the derivative of this control signal. Fuller [43] has found that it is difficult to find an appropriate justification for this type of technique. This does not apply to the introduction of an integral

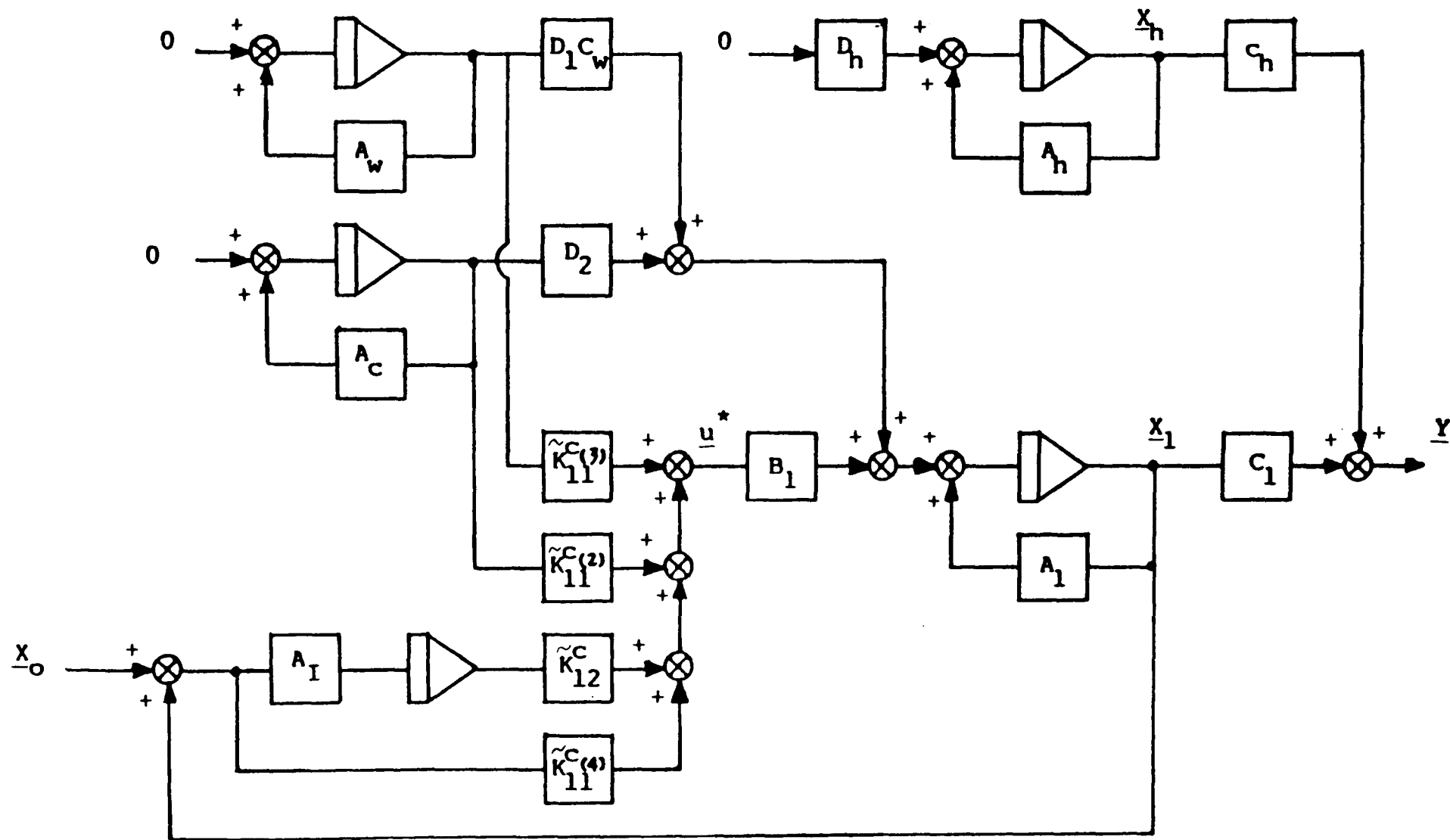


FIGURE 4-3

Deterministic Optimal Regulation of DP System

operator into the cost function, since this clearly ensures that the steady state regulating error is zero.

4.3.4 Filtering Problem

It is not intended to include the details of the filtering problem in this section since this has been discussed in the previous chapter. However, it has been shown that due to the optimal control problem which includes the integral action, some adjustments have been made in the system model. It is desirable that the filter should be adjusted to give consistent estimates for feedback purposes.

As in the control problem, the filtering problem may be simplified by considering the individual subsystems. The filter matrix Riccati equation corresponding to the system equations (4.29) and (4.30) is given by:

$$\begin{aligned} \dot{\bar{P}}_f(t) = & \bar{A}\bar{P}_f(t) + \bar{P}_f(t)\bar{A}^T - \bar{P}_f(t)\bar{C}^T R_f^{-1} \bar{C}\bar{P}_f(t) \\ & + \bar{D}\bar{Q}_f\bar{D}^T \end{aligned} \quad (4.96)$$

where \bar{Q}_f is the covariance matrix of driving noises of the input disturbance models and R_f is the covariance matrix of the driving noises of the output disturbance models.

The equation may be expanded using the system matrices defined in equations (4.33) to (4.35). The individual equations become:

$$\begin{aligned} \dot{\bar{P}}_{11}^f(t) = & \tilde{A}_1 \bar{P}_{11}^f(t) + \bar{P}_{11}^f(t) \tilde{A}_1^T \\ & - \bar{P}_{11}^f(t) \tilde{C}_1^T R_f^{-1} \tilde{C}_1 \bar{P}_{11}^f(t) + \tilde{D}_1 \tilde{Q} \tilde{D}_1^T \end{aligned} \quad (4.97)$$

$$\begin{aligned} \dot{\bar{P}}_{12}^f(t) = & \tilde{A}_1 \bar{P}_{12}^f(t) + \bar{P}_{12}^f(t) \tilde{A}_2^T \\ & - \bar{P}_{11}^f(t) \tilde{C}_1^T R_f^{-1} \tilde{C}_1 \bar{P}_{12}^f(t) \end{aligned} \quad (4.98)$$

$$\begin{aligned} \dot{\bar{P}}_{22}^f(t) = & \tilde{A}_2 \bar{P}_{22}^f(t) + \bar{P}_{22}^f(t) \tilde{A}_2^T \\ & - \bar{P}_{21}^f(t) \tilde{C}_1^T R_f^{-1} \tilde{C}_1 \bar{P}_{12}^f(t) \end{aligned} \quad (4.99)$$

where $\bar{P}_{11}^f(0) = \tilde{\Sigma}_0$, $\bar{P}_{12}^f(0) = 0$, $\bar{P}_{22}^f(0) = 0$. The latter two initial covariances are zero because the initial state of the reference (second) subsystem is completely determined. Thence, the solutions of equations (4.98) and (4.99) are obviously zero (i.e. $\bar{P}_{12}^f(t) = 0$ and $\bar{P}_{22}^f(t) = 0, \forall t \geq 0$). The gain matrix is then given by:

$$\bar{K}^f(t) = \bar{P}^f(t) \bar{C}^T R_f^{-1} = \begin{bmatrix} \bar{P}_{11}^f(t) \tilde{C}_1^T R_f^{-1} \\ 0 \end{bmatrix} \quad (4.100)$$

It follows that the filter subsystem generating the estimates of the reference signal $\tilde{x}_2(t)$ is completely separate from the other filter subsystems.

The filter state variables associated with the integral control action may now be considered. These states form the second subsystem in the following partition of the state vector $\tilde{\underline{x}}_1(t)$.

$$\tilde{\underline{x}}_1(t) = [\underline{x}_h(t) \quad \underline{x}_c(t) \quad \underline{x}_w(t) \quad \underline{x}_l(t) \quad (L\tilde{\underline{x}})^T(t)]^T \quad (4.101)$$

The system matrices in equation (4.54) may now be partitioned as in equations (4.33) to (4.35).

$$\tilde{\underline{A}}_1 = \begin{bmatrix} \tilde{\underline{A}} & 0 \\ \underline{A}_I & 0 \end{bmatrix} \quad \tilde{\underline{D}}_1 = \begin{bmatrix} \tilde{\underline{D}} \\ 0 \end{bmatrix} \quad \tilde{\underline{C}}_1 = [\tilde{\underline{C}} \quad 0] \quad (4.102)$$

The filter matrix Riccati equation corresponding to the system equation (4.27) is given by equation (4.97). The equation may be expanded using the system matrices defined in equation (4.102). The individual equations become:

$$\begin{aligned} \dot{\tilde{\underline{P}}}_{11}^f(t) = & \tilde{\underline{A}}\tilde{\underline{P}}_{11}^f(t) + \tilde{\underline{P}}_{11}^f\tilde{\underline{A}}^T - \tilde{\underline{P}}_{11}^f\tilde{\underline{C}}^T\tilde{\underline{P}}_{11}^f(t) \\ & + \tilde{\underline{D}}\tilde{\underline{Q}}\tilde{\underline{D}}^T \end{aligned} \quad (4.103)$$

$$\begin{aligned} \dot{\tilde{\underline{P}}}_{21}^f(t) = & \underline{A}_I\tilde{\underline{P}}_{11}^f(t) + \tilde{\underline{P}}_{21}^f\tilde{\underline{A}}^T \\ & - \tilde{\underline{P}}_{21}^f\tilde{\underline{C}}^T\tilde{\underline{R}}_f^{-1}(t)\tilde{\underline{C}}\tilde{\underline{P}}_{11}^f(t) \end{aligned} \quad (4.104)$$

$$\begin{aligned} \dot{\tilde{P}}_{22}^f(t) = & A_I \tilde{P}_{12}^f(t) + \tilde{P}_{21}^f(t) A_I^T \\ & - \tilde{P}_{21}^f(t) \tilde{C}^T R_f^{-1} \tilde{C} \tilde{P}_{12}^f(t) \end{aligned} \quad (4.105)$$

Where $\tilde{P}_{11}^f(0) = \tilde{\Sigma}_0$, $\tilde{P}_{12}^f(0) = 0$, $\tilde{P}_{22}^f(0) = 0$. The latter two covariances are zero, for the integral control subsystem has a known (zero) initial state. The Kalman gain matrix is given by:

$$\begin{aligned} \tilde{K}^f(t) = & \begin{bmatrix} \tilde{K}_{11}^f(t) \\ \tilde{K}_{21}^f(t) \end{bmatrix} = \bar{P}_{11}(t) \tilde{C}_1^T R_f^{-1} \\ & = \begin{bmatrix} \tilde{P}_{11}(t) \tilde{C}^T R_f^{-1} \\ \tilde{P}_{21}(t) \tilde{C}^T R_f^{-1} \end{bmatrix} \end{aligned} \quad (4.106)$$

The gain matrix depends only upon the solutions of the equations (4.103) and (4.104).

The integral control subsystem has input from the plant state estimates $A_I \tilde{x}(t)$ and from the innovation process via the filter gain $\tilde{K}_{21}^f(t)$. Also note that the structure of the Kalman filter [44] depends upon the output matrix \tilde{C}_1 ($= [C_h \ 0 \ 0 \ C_l \ 0]$), and thus state estimate feedback within the filter only comes from the output noise and the plant model subsystems. The structure of the filter is shown diagrammatically in Figure 4-4.

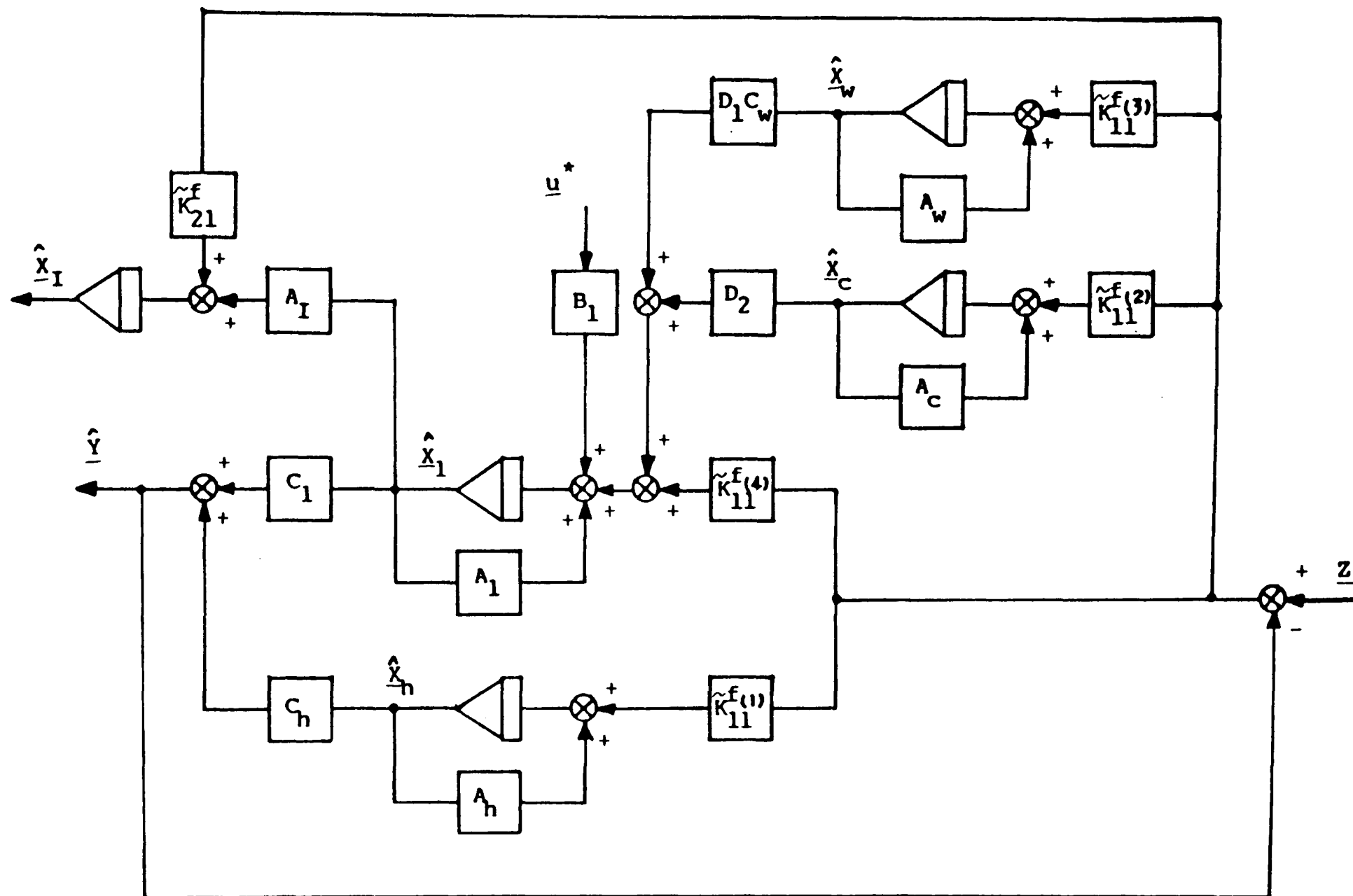


FIGURE 4-4 Kalman Filter Section for DP Stochastic System

Infinite-Time Solution of Filtering Problem

The disturbance and output noise subsystems are assumed to be asymptotically stable and the plant is assumed to be controllable and observable. Thus, the system \tilde{A} may be assumed to be stabilizable and detectable [29]. It then follows that the solution of the equation (4.103) approaches a unique positive semi-definite solution [29] as $t \rightarrow -\infty$, for every $\tilde{\Sigma}_0 \succ 0$. The resulting steady state optimal observer follows as:

$$\frac{d\hat{\tilde{x}}(t)}{dt} = \tilde{A}\hat{\tilde{x}}(t) + \tilde{K}_{11}\{z(t) - \tilde{C}\hat{\tilde{x}}(t)\} + \tilde{B}u^*(t) \quad (4.107)$$

and is asymptotically stable. The section of the filter concerned with the integral action may now be considered. In steady state, equation (4.104) becomes:

$$\tilde{P}_{21}^f(t) \tilde{A}_f^T = -A_I \tilde{P}_{11}^f(t) \quad (4.108)$$

where the steady state value of $\tilde{p}_{11}^f(t)$ is given by equation (4.103) and the closed loop filter matrix is defined as:

$$\tilde{A}_f = \tilde{A} - \tilde{K}_{11}^f \tilde{C} \quad (4.109)$$

Equation (4.108) is based only upon the assumption that R_f and $\tilde{P}_{11}(t)$ are both symmetric.

The eigenvalues of the matrix \tilde{A}_f have all negative real parts and thus $(\tilde{A}_f^T)^{-1}$ exists, so the unique solution for \tilde{P}_{21}^f is:

$$\tilde{P}_{21}^f = -A_I \tilde{P}_{11}^f (\tilde{A}_f^T)^{-1} \quad (4.110)$$

The corresponding gain matrix may be calculated using equation (4.106) and the filter subsystem becomes:

$$\frac{d}{dt} \hat{\underline{x}}_I(t) = A_I \hat{\underline{x}}(t) + \tilde{K}_{21}^f(t) \{ \underline{z}(t) - \tilde{C} \hat{\underline{x}}(t) \} \quad (4.111)$$

where $\hat{\underline{x}}_I(t)$ is the state estimate of $(L\tilde{\underline{x}})(t)$. This subsystem consists of a number of integrators whose inputs are given in equation (4.111). The filter shown in Figure 4-4 is therefore stable. The integral control subsystem must also be used for generating the signal $(L\tilde{\underline{x}}_0)(t)$ contained in the $\tilde{\underline{x}}_2(t)$ subsystem. Equations (4.106), (4.110) and (4.111) then give the modified subfilter as:

$$\begin{aligned} \frac{d\hat{\underline{x}}_I(t)}{dt} &= A_I \left\{ \hat{\underline{x}}(t) - \hat{\underline{x}}_0(t) \right. \\ &\quad \left. - \tilde{P}_{11}^T (\tilde{A}_f^T)^{-1} \tilde{C}^T R^{-1} \{ \underline{z}(t) - \tilde{C} \hat{\underline{x}}(t) \} \right\} \end{aligned} \quad (4.112)$$

Recall that A_I is the matrix which selects the subset of

the plant states to be driven to their set point values. In steady state, $\hat{\underline{x}}_I(t)$ should tend to a constant value.

4.3.5 Stability of Closed Loop Output Feedback System

In the last two sections, the closed-loop state feedback system with constant gains was shown to be asymptotically stable, and the Kalman filter (with the exception of the integral control system) was also shown to be asymptotically stable. In this section, the stability problem of the closed loop system with state feedback and including integral action will be investigated.

Let the white noise inputs to the system be assumed to be zero and let the following state tracking error vectors and reconstruction error vector be defined as:

$$\underline{\tilde{x}}'(t) = \underline{\tilde{x}}(t) - \underline{\tilde{x}}_0(t) \quad (4.113)$$

$$\underline{\tilde{x}}'_I(t) = \left\{ L(\underline{\tilde{x}} - \underline{\tilde{x}}_0) \right\}(t) \quad (4.114)$$

$$\underline{e}(t) = \underline{\tilde{x}}(t) - \hat{\underline{x}}(t) \quad (4.115)$$

The optimal control signal is then given by the separation principle and equation (4.48) becomes:

$$u^*(t) = -\tilde{K}_{11}^c \hat{\underline{\tilde{x}}}'(t) - \tilde{K}_{12}^c \hat{\underline{\tilde{x}}}_I(t) \quad (4.116)$$

From equations (4.14) and (4.15), the system equations become:

$$\dot{\underline{\hat{x}}}(t) = \tilde{A}\underline{\hat{x}}(t) + \tilde{B}u^*(t) \quad (4.117)$$

and

$$\underline{z}(t) = \tilde{C}\underline{\hat{x}}(t) \quad (4.118)$$

The filter equations follow from equations (4.107) and (4.111).

$$\frac{d}{dt} \underline{\hat{x}}(t) = \tilde{A}\underline{\hat{x}}(t) + \tilde{K}_{11}^f \{ \underline{z}(t) - \tilde{C}\underline{\hat{x}}(t) \} + \tilde{B}u^*(t) \quad (4.119)$$

$$\frac{d}{dt} \underline{\hat{x}}_I(t) = A_I \underline{\hat{x}}(t) + \tilde{K}_{21}^f \{ \underline{z}(t) - \tilde{C}\underline{\hat{x}}(t) \} \quad (4.120)$$

From equations (4.115), (4.117) and (4.119), yield:

$$\dot{\underline{e}}(t) = (\tilde{A} - \tilde{K}_{11}^f \tilde{C}) \underline{e}(t) \quad (4.121)$$

and from equations (4.25), (4.113), (4.117) and (4.118), yield:

$$\dot{\underline{\hat{x}}}'(t) = \tilde{A}\underline{\hat{x}}'(t) + \tilde{B}u^*(t) \quad (4.122)$$

Also note that:

$$\underline{\hat{x}}'(t) = \underline{\hat{x}}(t) - \underline{\hat{x}}_O(t) \text{ and } \underline{\hat{x}}'_I(t) = \underline{\hat{x}}_I(t) - \underline{x}_{IO}(t)$$

so

$$\underline{\hat{x}}'(t) = \underline{\hat{x}}(t) - \underline{e}(t) \quad (4.123)$$

and

$$\dot{\tilde{\underline{x}}}(t) = (\tilde{\underline{A}} - \tilde{\underline{B}}\tilde{\underline{K}}_{11}^c)\tilde{\underline{x}}(t) - \tilde{\underline{B}}\tilde{\underline{K}}_{12}^c\hat{\underline{x}}_I'(t) + \tilde{\underline{B}}\tilde{\underline{K}}_{11}^c\underline{e}(t) \quad (4.124)$$

Similarly, from equation (4.114), (4.115) and (4.120)

$$\dot{\hat{\underline{x}}}_I'(t) = \hat{\underline{x}}_I(t) - \underline{A}_I\tilde{\underline{x}}_0(t) \quad (4.125)$$

and

$$\dot{\tilde{\underline{x}}}_I'(t) = \underline{A}_I\tilde{\underline{x}}_I'(t) - (\underline{A}_I - \tilde{\underline{K}}_{21}^f\tilde{\underline{C}})\underline{e}(t) \quad (4.126)$$

Equations (4.121), (4.124) and (4.126) may now be put into the form:

$$\begin{bmatrix} \dot{\tilde{\underline{x}}}(t) \\ \dot{\tilde{\underline{x}}}_I'(t) \\ \dot{\underline{e}}(t) \end{bmatrix} = \begin{bmatrix} \tilde{\underline{A}} - \tilde{\underline{B}}\tilde{\underline{K}}_{11}^c & -\tilde{\underline{B}}\tilde{\underline{K}}_{12}^c & \tilde{\underline{B}}\tilde{\underline{K}}_{11}^c \\ \underline{A}_I & 0 & -(\underline{A}_I - \tilde{\underline{K}}_{21}^f\tilde{\underline{C}}) \\ 0 & 0 & \tilde{\underline{A}} - \tilde{\underline{K}}_{11}^f\tilde{\underline{C}} \end{bmatrix} \begin{bmatrix} \tilde{\underline{x}}(t) \\ \hat{\underline{x}}_I'(t) \\ \underline{e}(t) \end{bmatrix} \quad (4.127)$$

The eigenvalues of the closed loop system [29] may be found using the matrix equation (4.127). This matrix has the form:

$$\underline{F} = \begin{bmatrix} (\tilde{\underline{A}}_1 - \tilde{\underline{B}} \tilde{\underline{K}}_{11}^c) & \underline{F}_{12} \\ 0 & (\tilde{\underline{A}} - \tilde{\underline{K}}_{11}^f\tilde{\underline{C}}) \end{bmatrix} \quad (4.128)$$

where

$$\tilde{\underline{A}}_1 \triangleq \begin{bmatrix} \tilde{\underline{A}} & 0 \\ \underline{A}_I & 0 \end{bmatrix} \quad \tilde{\underline{K}}_{11}^c \triangleq \begin{bmatrix} \tilde{\underline{K}}_{11}^c \\ \tilde{\underline{K}}_{12}^c \end{bmatrix}$$

and

$$F_{12} = \begin{bmatrix} \tilde{B}\tilde{K}_{11}^C \\ -(A_I - \tilde{K}_{21}\tilde{C}) \end{bmatrix}$$

Thence, the closed loop eigenvalues are determined by the zeros of the polynomial.

$$\rho_C(s) = \det(sI - \tilde{A}_1 + \tilde{B}\tilde{K}_{11}^C) \det(sI - \tilde{A} + \tilde{K}_{11}^f\tilde{C}) \quad (4.129)$$

and clearly, these include the state regulator and the Kalman filter poles. The state regulator and Kalman filter have both been shown to be asymptotically stable. It therefore follows that the optimal stochastic regulator with integral control is also asymptotically stable. If the reference state vector $\tilde{x}_0(t)$ is different from zero, the plant states will be driven asymptotically to the non-zero set point values. The integral term will ensure that any unmodelled constant disturbances are offset, without producing a steady state tracking error, which is based on the assumption that a steady state solution exists for such an input.

4.3.6 Implementation on the Dynamic Ship Positioning System

The optimal stochastic regulating system which is a combination of the deterministic regulator and Kalman filter

is shown in Figure 4-5. The controller includes the state estimate feedback from each of the input disturbance subsystems and proportional plus integral feedback from the plant regulating error. The integral control term enables unmodelled low frequency disturbances to be offset to maintain zero steady state regulating errors. However, even when the disturbances are modelled accurately, the integral action is desirable. Consider, for example, the situation where the low frequency disturbance $\underline{x}_c(t)$ is almost constant. Assuming for the time being that the integral control is not being used ($A_I=0$), then $\underline{u}^*(t)$ will include terms in both $\hat{\underline{x}}_c(t)$ and $\{\underline{x}_o(t) - \hat{\underline{x}}(t)\}$. The latter term will not be zero in steady state because the cost function includes the regulating error and the control signal. The error will of course be smaller than it would have been had the disturbances been modelled. However, the integral control term ensures that even these small errors are driven to zero.

In the dynamic ship positioning problem, the input disturbances are usually not modelled in the Kalman filter to be implemented. The details will be discussed in the next section. In this case, the stochastic optimal control scheme is of roughly the same complexity as one based on PID [45, 46] controllers and notch filters [22, 47]. Similarly, the transportation delay of the measurement system is

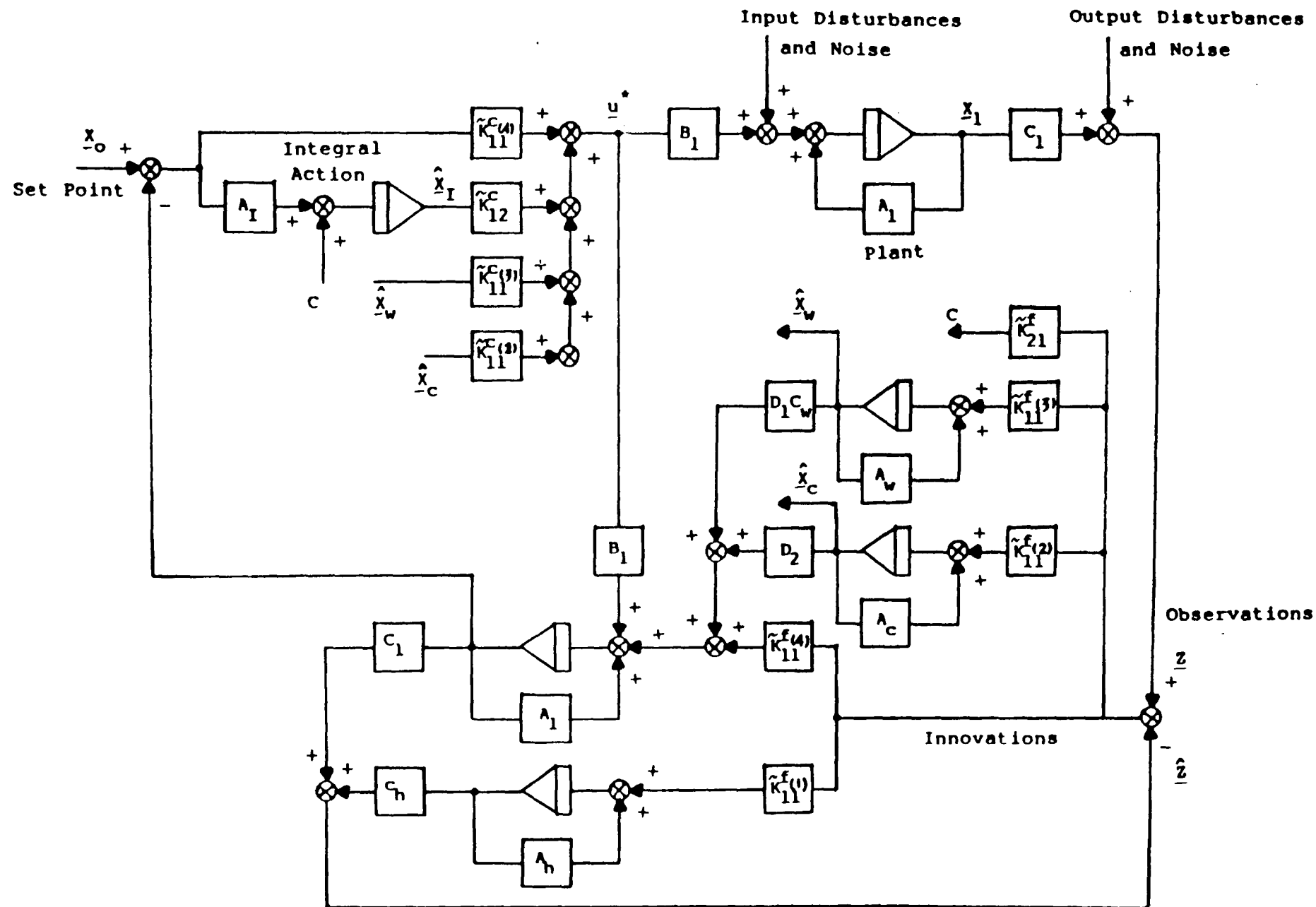


FIGURE 4-5 DP Optimal Stochastic Regulating System with Integral Control

usually neglected. However, if necessary, the above scheme can be modified to allow for such delays [48, 49].

Belanger [50] has proposed a scheme based upon Johnson's [51] work involving an observer for the control of linear systems with constant output disturbances. This scheme has an integral feedback from the innovation signals in the observer (equivalent to $A_I=0$). Thus, the input disturbances, for example, can still produce steady state offsets in the states being controlled. This may not be observed in the measured outputs. Smith and Davidson [52, 53] also describe an integral control system which uses an observer. However, the optimal stochastic control system was not considered in their work.

4.4 SIMPLIFIED DP INTEGRAL CONTROL SYSTEMS

4.4.1 System Model

The original theory of the stochastic optimal control scheme given in Section 4.3 assumes that the constant input disturbances can be modelled. Usually the steady current forces in DP problems are difficult to measure. The simulations shown in this section are based on unknown constant disturbance, which means that the constant

disturbance state equation (4.13) is not included in the Kalman filter. However, in the ship dynamics simulation a constant input disturbance, which represents the current force and steady state wind force, is purposely injected into the dynamical equations.

The dynamic models of Wimpey Sealab are given in Chapter 2, Section 2.7. In the application of integral control to the DP (dynamic positioning) problems, two integral states are added to form a state vector of eight dimensions. The high frequency motions are not controlled, theoretically they have no direct effect on the performance of the integral controller, therefore the high frequency motions are not considered here.

Define the state vector and observed output vector:

$$\underline{\bar{x}}(t) = \begin{bmatrix} x_1 \\ x_2 \\ x_3 \\ x_4 \\ x_5 \\ x_6 \\ x_7 \\ x_8 \end{bmatrix} \begin{array}{l} \text{sway velocity} \\ \text{sway position} \\ \text{yaw angular velocity} \\ \text{yaw angle} \\ \text{thruster one} \\ \text{thruster two} \\ \text{integral state (sway)} \\ \text{integral state (yaw)} \end{array} \quad (4.130)$$

$$\underline{z}(t) = \begin{bmatrix} z_1 \\ z_2 \end{bmatrix} \begin{array}{l} \text{observed sway position} \\ \text{observed yaw angle} \end{array} \quad (4.131)$$

The system matrices are given in Section 2.7, except for A_I . The thruster model is a first order model. With reference to the state vector $\bar{x}(t)$, the unity elements in A_I can be assigned. They should correspond to sway position and yaw angle so that their offsets are eliminated. Therefore,

$$A_I = \begin{bmatrix} 0 & 1 & 0 & 0 & 0 & 0 \\ 0 & 0 & 0 & 1 & 0 & 0 \end{bmatrix} \quad (4.132)$$

The weighting matrices, optimal gains, noise covariance and Kalman gains are given below:

State Weighting Matrix

$$Q_C = \begin{bmatrix} 3.0 & 0 & 0 & 0 & 0 & 0 & 0 & 0 \\ 0 & 500.0 & 0 & 0 & 0 & 0 & 0 & 0 \\ 0 & 0 & 3.0 & 0 & 0 & 0 & 0 & 0 \\ 0 & 0 & 0 & 500.0 & 0 & 0 & 0 & 0 \\ 0 & 0 & 0 & 0 & 10.0 & 0 & 0 & 0 \\ 0 & 0 & 0 & 0 & 0 & 10.0 & 0 & 0 \\ \hline 0 & 0 & 0 & 0 & 0 & 0 & 0.05 & 0.025 \\ 0 & 0 & 0 & 0 & 0 & 0 & 0.025 & 0.05 \end{bmatrix} \quad (4.133)$$

Control Weighting Matrix

$$R_C = \begin{bmatrix} 500.0 & 0 \\ 0 & 500.0 \end{bmatrix} \quad (4.134)$$

Optimal State Feedback Gains (computed from Matrix Riccati equation)

$$K_C = \begin{bmatrix} 2.333678 & -0.8974105E-1 \\ 1.017820 & -0.9651867E-2 \\ 0.940621E-2 & -2.052542 \\ 0.5321420E-2 & -1.596670 \\ 0.6298736 & -0.1424548E-1 \\ 0.5698193E-2 & 1.318934 \\ \hline 0.7199648E-2 & -0.4749765E-2 \\ 0.2967002E-2 & -0.1147172E-1 \end{bmatrix} \quad (4.135)$$

Process Noise Co-variance Matrix

$$Q_F = \begin{bmatrix} 4 \times 10^{-6} & 0 \\ 0 & 9 \times 10^{-8} \end{bmatrix} \quad (4.136)$$

Measurement Noise Co-variance Matrix

$$R_F = \begin{bmatrix} 10^{-5} & 0 \\ 0 & 1.22 \times 10^{-5} \end{bmatrix} \quad (4.137)$$

Kalman Gains (computed from matrix Riccati equation)

$$K_F = \begin{bmatrix} 0.3013153 & 0.7578478E-2 \\ 0.7761472 & 0.1344847E-1 \\ 0.2410643E-1 & 0.7459922 \\ 0.1681059E-1 & 1.221376 \\ 0 & 0 \\ 0 & 0 \\ \hline 1.0 & 0 \\ 0 & 1.0 \end{bmatrix} \quad (4.138)$$

4.4.2 Control System Design One and Simulation Results

Figure 4-6 shows the step time responses of sway and yaw motions. The constant disturbance came in at the 80th second. Both the real states $\underline{x}_l(t)$ and estimated states $\hat{\underline{x}}_l(t)$ were deviated from the set position. The constant bias between $\underline{x}_l(t)$ and $\hat{\underline{x}}_l(t)$ was due to the fact that the constant disturbances did not go into the Kalman filter directly.

The structure of the state feedback control with integral action is shown in Figure 4-7. Figure 4-8 shows the time responses of the system. The real steady errors were driven to zero by the integral controllers. As before, the bias between $\underline{x}_l(t)$ and $\hat{\underline{x}}_l(t)$ remained. The overall system was overdamped with settling time about 60 seconds. It should be emphasized that the stability and optimality of this control scheme are guaranteed. The constant control forces were built up to balance the steady disturbances.

Linear Analysis of Constant Error in Estimation

Assume the system output (single input single output case) due to the constant disturbance $x_c(t)$ is in the form (see Figure 4-2):

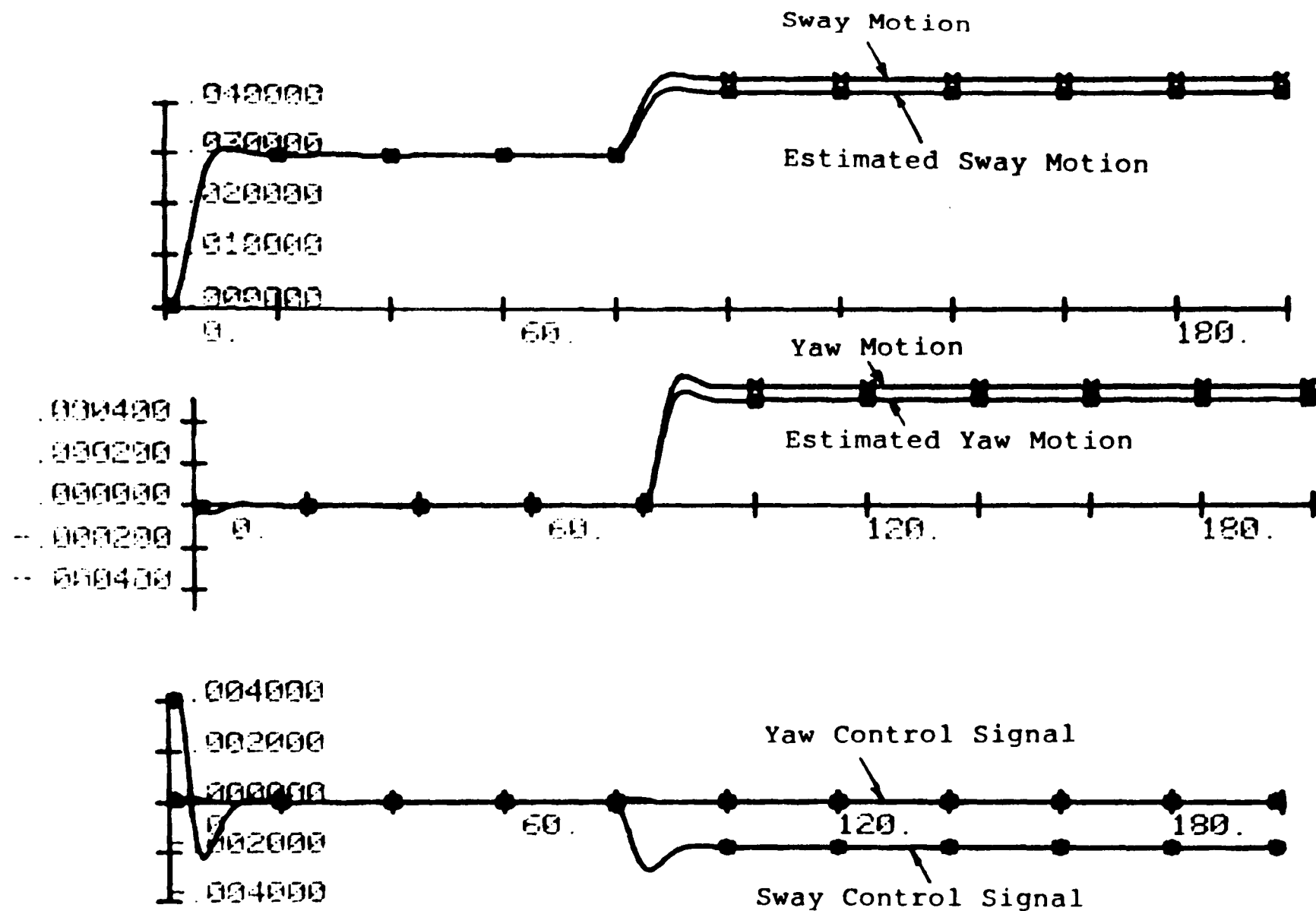


FIGURE 4-6

Ship Motions without Integral Control(Deterministic Case)

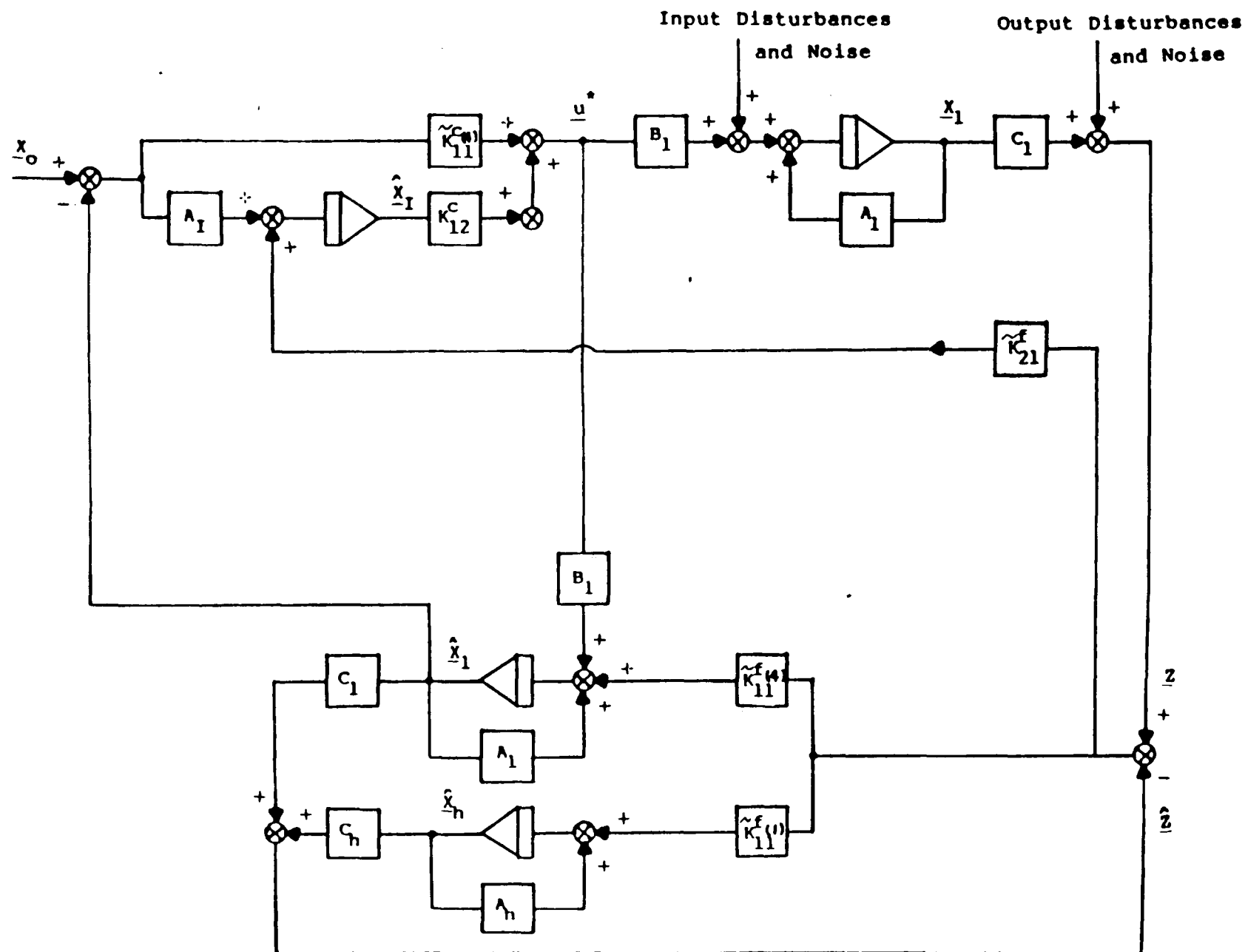


FIGURE 4-7 DP Regulating System with Integral Control
(Design One)

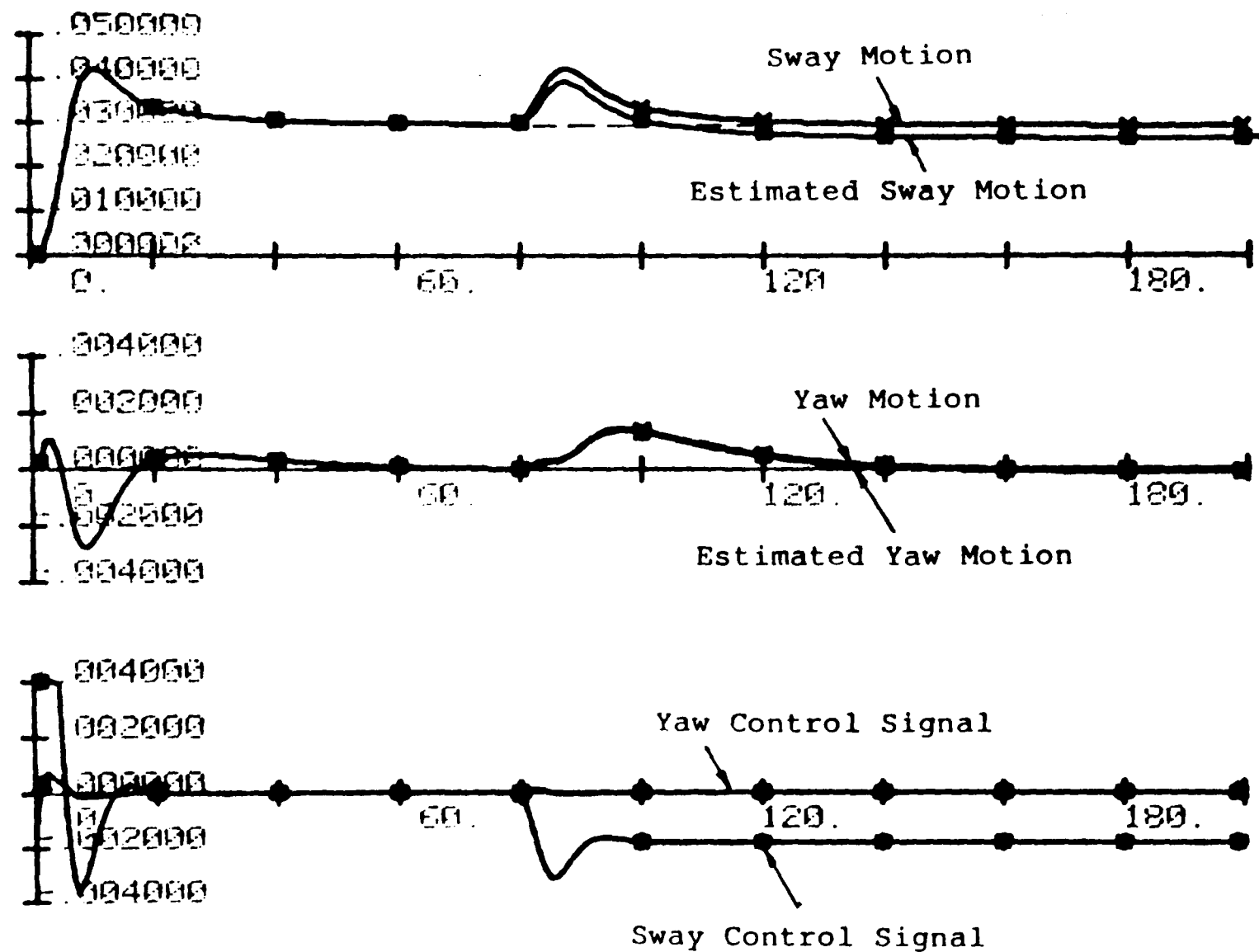


FIGURE 4-8 Ship Motions with Integral Control (Design One)

$$y^c(t) = G^c(s)x_c(t) \quad (4.139)$$

where:

$$G^c(s) = C_l (sI - A_l)^{-1} D_2 \quad (4.140)$$

Since $x_c(t)$ is not estimated, the LF filter output due to x_c can be shown to be:

$$\hat{y}^c(t) = \hat{G}^c(s)y^c(t) \quad (4.141)$$

where:

$$\hat{G}^c(s) = (C_l (sI - A_l)^{-1} \tilde{K}_{11}^f) \quad (4.142)$$

Therefore, the constant estimation error in position, in steady state, is:

$$\begin{aligned} e^c(t) &= y^c(t) - \hat{y}^c(t) \\ &= G^c(o)x_c(t) - \hat{G}^c(o)y^c(t) \end{aligned} \quad (4.143)$$

It will be shown in Section 6.4 that this quantity can be estimated using self-tuning techniques.

4.4.3 Control System Design Two and Simulation Results

There are two ways of overcoming the bias between $\underline{x}_l(t)$ and $\hat{\underline{x}}_l(t)$ observed in the last section:

- (a) include the constant disturbance forces in the filter,
- (b) disconnect the integral control signal from the filter.

Since the system matrix A_1 is singular and the constant forces cannot be measured directly, thus method (a) may not be applicable. Method (b) is an intuitive technique. The argument is: the integral control signal is used to eliminate the offset due to the constant disturbance, since the constant disturbance is not modelled in the filter. Thus, this additional driving force should naturally be disconnected from the filter.

The disadvantage of this design is that stability and optimality will no longer be guaranteed. Improper weighting factors of the integral states may lead to an unstable control system.

Figure 4-9 shows the layout of this design. The time responses show that the bias has vanished (Figure 4-10). It is always a problem that an integral controller may produce an underdamped response. The underdamped problem has been improved by reducing the weighting on the integral states.

Figure 4-11 shows the time responses with random noise disturbances. The constant disturbance appeared at the 200th second. The Kalman filter performed very well and the system was stable. Note that this test was with input disturbance, measurement noise and HF output disturbance

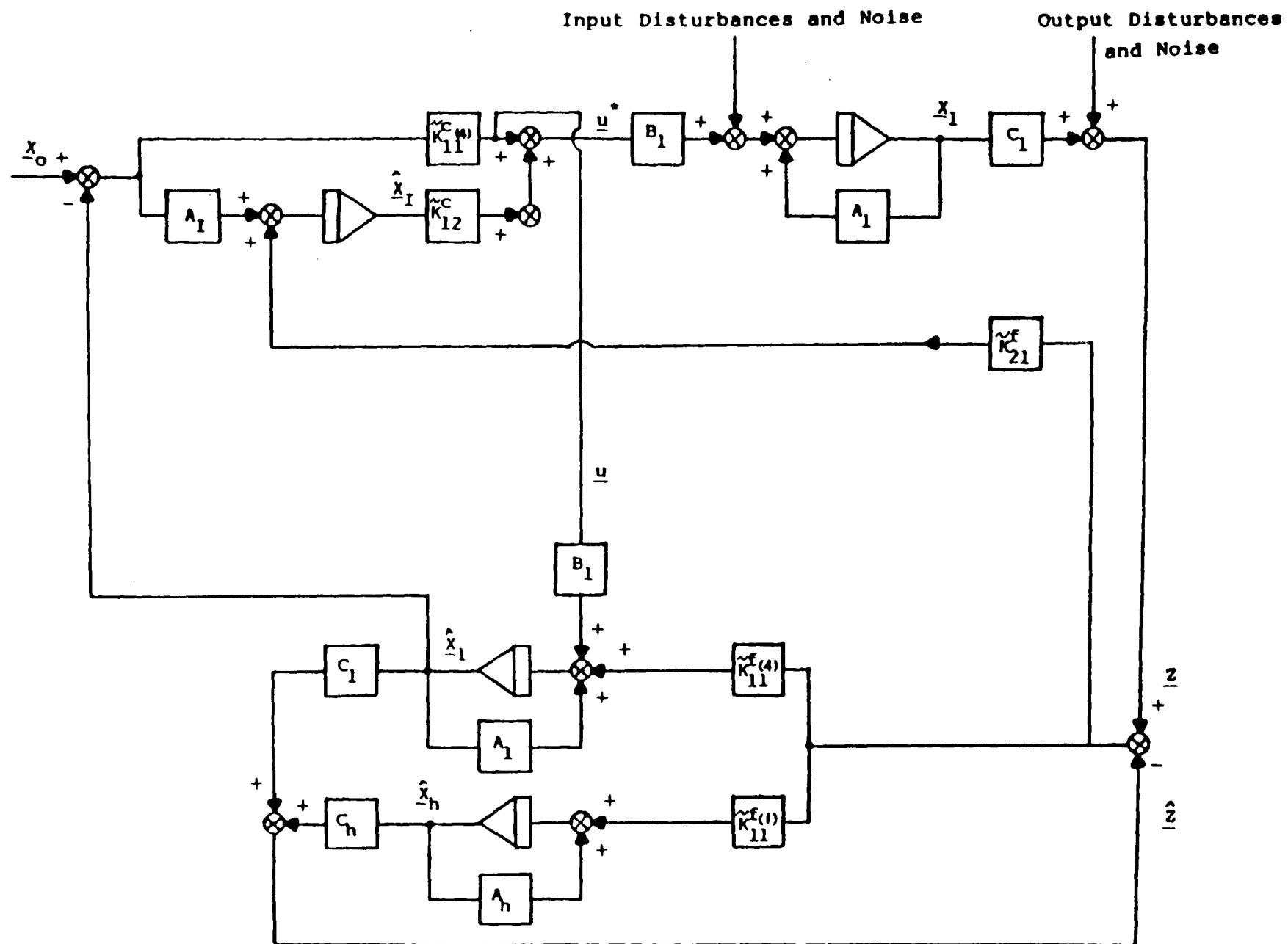


FIGURE 4-9 DP Regulating System with Integral Control (Design Two)

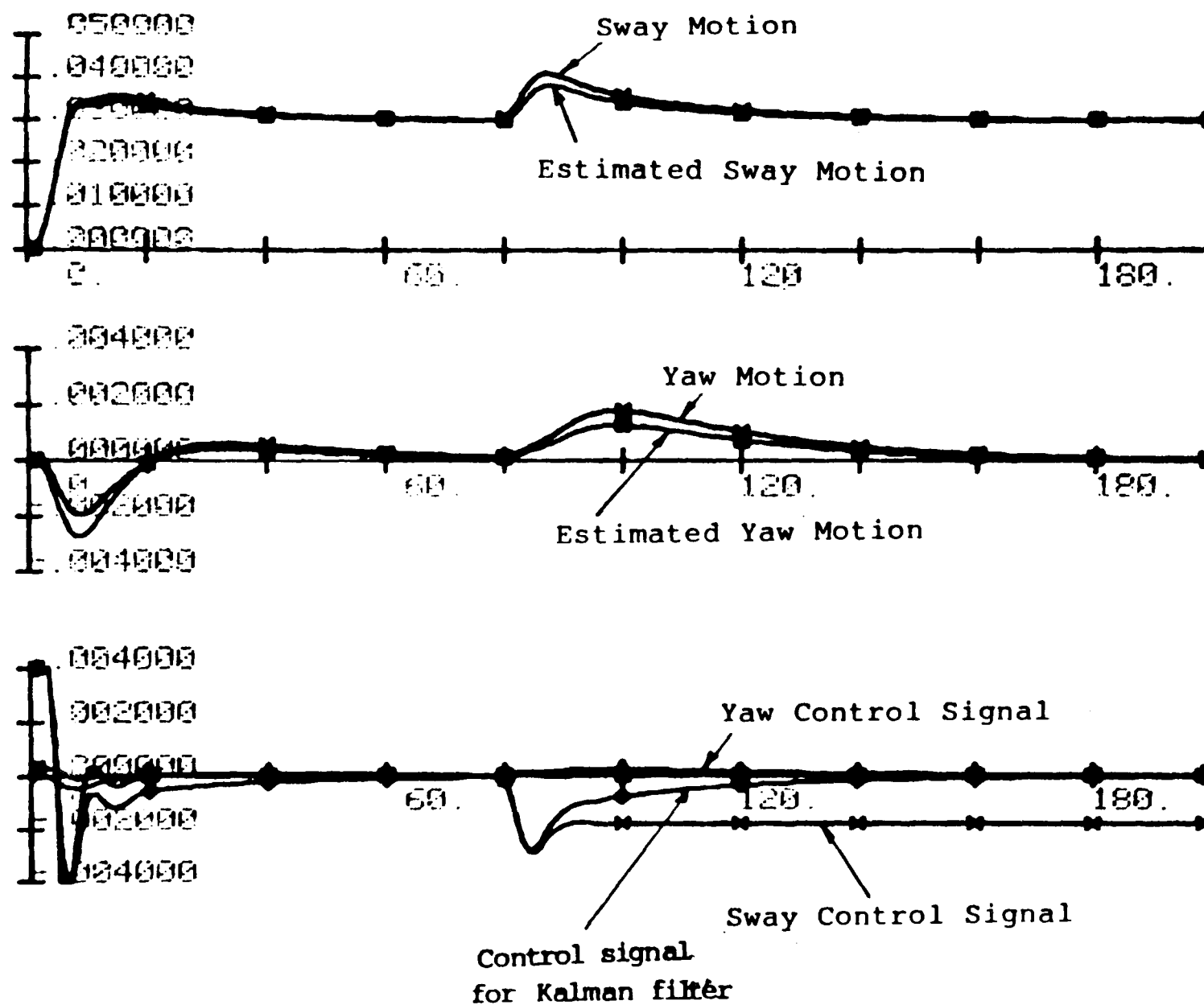


FIGURE 4-10 Ship Motions with Integral Control (Design Two)

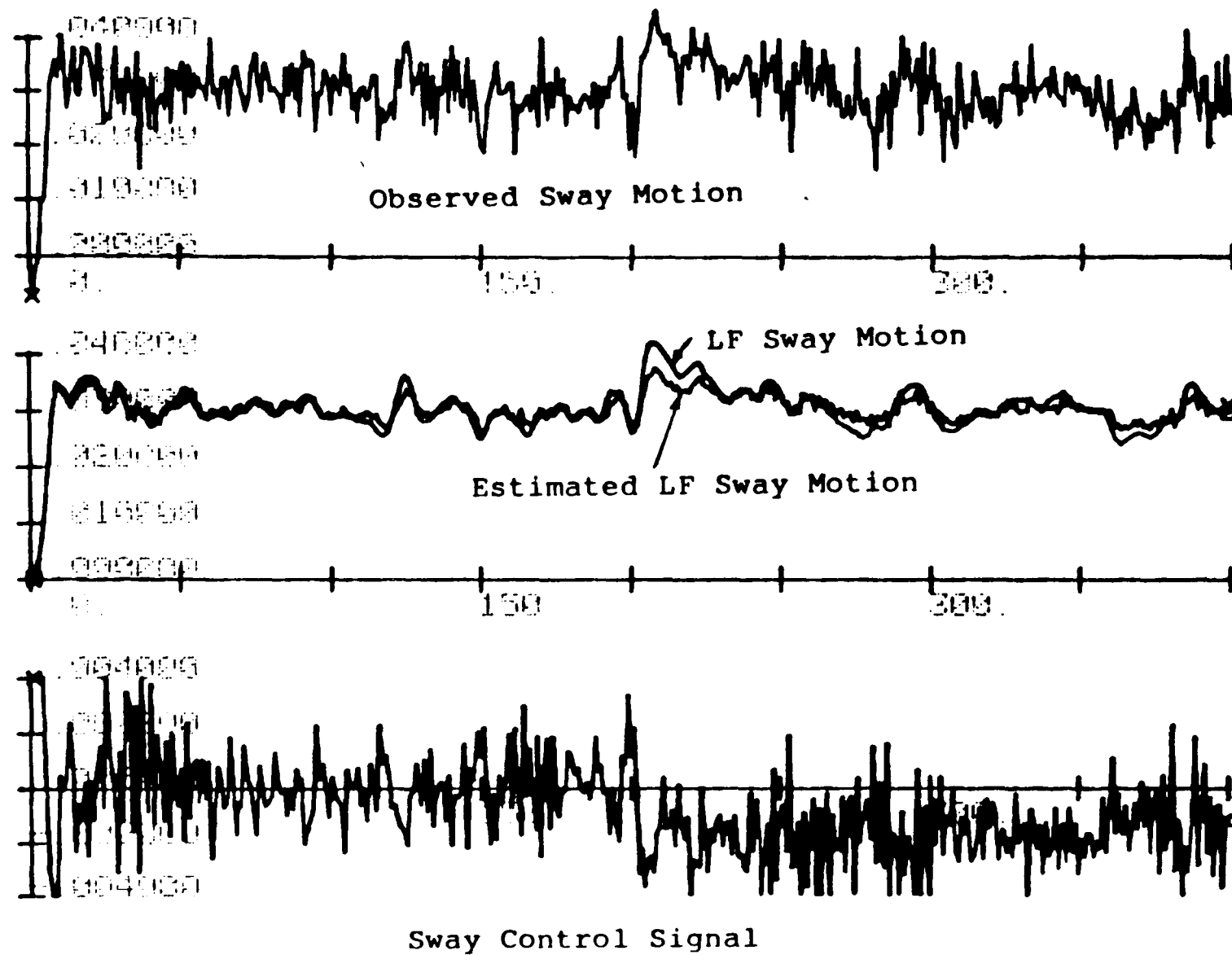


FIGURE 4-11 Ship Motions (Design Two) with Stochastic Disturbances

(Beaufort No. 5). A self-tuning Kalman filter (to be discussed in Chapter 5) was used.

4.4.4 Control System Design Three

In Design 2, position errors are fed back into the integrators through block A_I [28]. This is not found in some designs [50]. In their methods, only the innovations are fed back into the integrators [Figure 4-12]. The step responses of this control scheme were found to be similar to those results obtained in Design 2. This was because the innovations also included the steady state position errors and these signals were also fed back into the integral controllers, therefore the steady state errors would be zero in both designs. However, in Design 1 and Design 2 there is a unique procedure to compute the controller gains, whereas in Design 3, because the elements of A_I are all zero, the controller gains calculated using Riccati equation may cause the system to become unstable.

4.5 SUMMARY OF RESULTS

An optimal stochastic controller was designed for dynamic ship positioning of Wimpey Sealab. The controller included integral action which drove the steady state position error

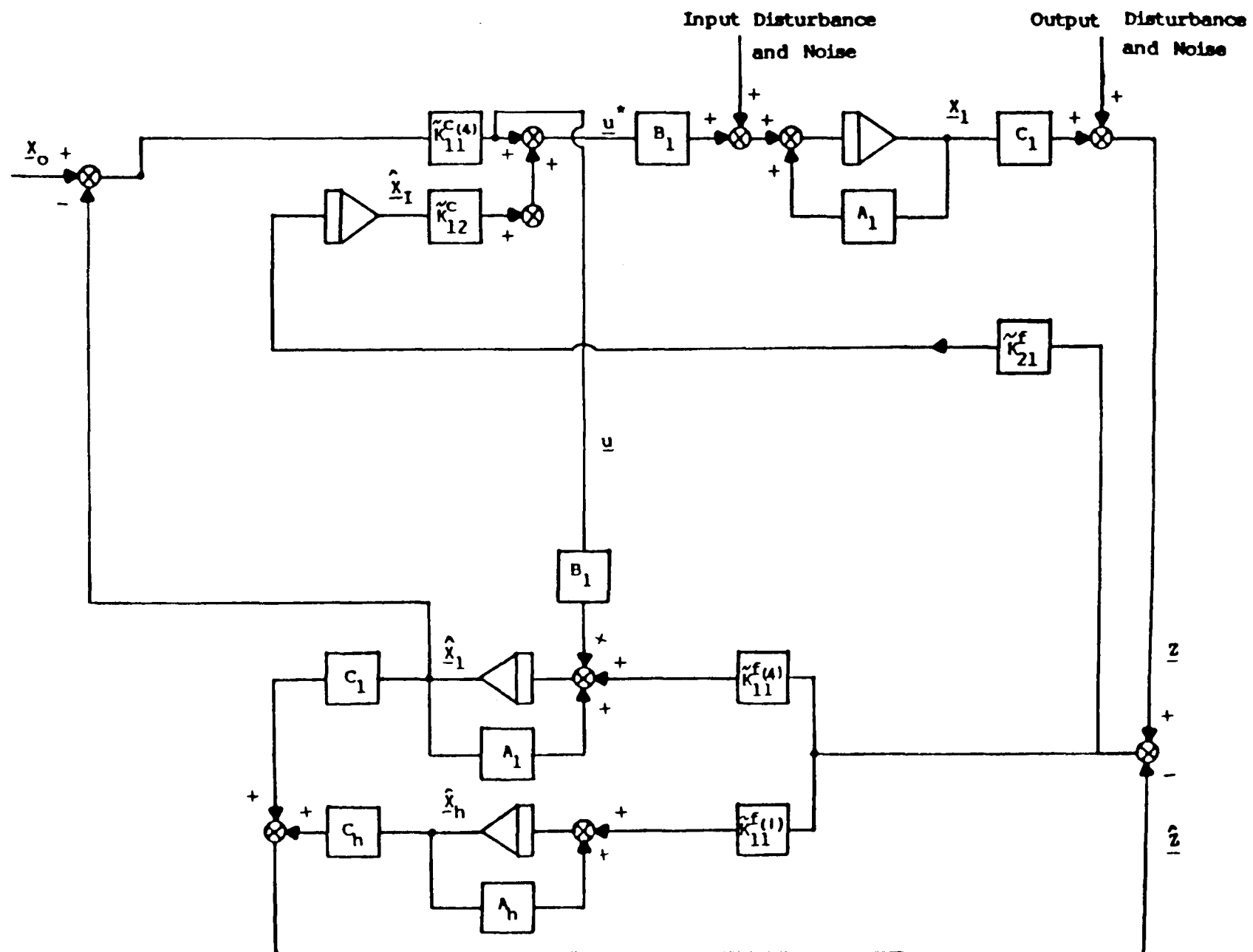


FIGURE 4-12 DP Regulating System with Integral Control (Design Three)

to zero. The position errors in DP systems are due to steady current force and steady wind force. The Kalman filter was used to estimate the states. Three simplified schemes, which did not include the estimation of the input constant disturbances, were used and simulation results were given. Because the Kalman filter did not have an input from the constant disturbances, the estimated states were biased from the real states.

A technique was developed to remove the bias by disconnecting the integral feedback from the filter. It was found to be quite successful.

A comparison between the technique which feedback only the innovations and that feedback both innovations and position errors (through A_I matrix) to the integral controllers was performed.

Because the position errors selected through A_I matrix to pass the integral controllers, and the innovations also included the steady state position errors, therefore, the results in both designs were found to be similar. However, a non-zero A_I matrix provides a unique procedure for computing controller gains using Riccati equation.

CHAPTER FIVE

SELF-TUNING KALMAN FILTER

5.1 INTRODUCTION

In this chapter, a novel adaptive filtering technique is developed for a class of systems with unknown disturbances. The estimator includes both a self-tuning filter and a Kalman filter. The approach was initially developed for application to the dynamic ship positioning control problem and has the advantage that existing non-adaptive Kalman filtering systems may easily be modified to include the self-tuning feature. However, the theory can be extended to apply to any system which has an output containing low frequency components and high frequency components provided the low frequency model is known. Many engineering and economical processes have this feature.

The extended Kalman filtering technique was first applied to dynamic ship positioning systems by Balchen, Jenssen and Saelid [17]. A simpler but non-adaptive constant gain Kalman filtering solution was also proposed by Grimbale, Patton and Wise [5]. In both cases, a linearized model was used for the estimation of the low frequency motions and

optimal control feedback was employed from these estimates. Balchen assumed, in this and subsequent schemes [18], that the high frequency motions were purely oscillatory and could be modelled by a second order sinusoidal oscillator with variable center frequency.

Grimble et. al. [5, 6, 7] used a fourth order wave model in the specification of the high frequency motions. However, the dominant wave frequency varies with weather conditions and the corresponding Kalman filter gain must therefore be switched for different operating conditions. The extended Kalman filter of Balchen automatically adapted to these varying environmental conditions. The computational load resulting from the gain matrix calculation was reduced by making suitable approximations. An alternative extended Kalman filtering scheme proposed by Grimble, Patton and Wise [6, 7] employed the higher order wave model but suggested the use of fixed low frequency filter gains to achieve the necessary computational savings. These are all described in Chapter Three. The self-tuning filter described here is based upon a similar decomposition property. This approach was first proposed by Fung and Grimble [16] using a scalar example and without the theoretical justification given in the following.

The analysis begins with the system and problem description in Section 5.2. The fixed gain Kalman filter is then considered in Section 5.3 and the self-tuning filter is described in Section 5.4. The errors which are introduced using the self-tuning structure are discussed in Section 5.5 and the total estimation algorithm is presented in Section 5.6. Section 5.7 discusses the advantages and disadvantages of the technique. Finally, a summary of the results is given in Section 5.8.

5.2 THE SYSTEM DESCRIPTION

The environmental forces acting on a vessel induce motions in six degrees of freedom. In dynamic positioning only vessel motions in the horizontal plane (surge, sway and yaw) are controlled. To simplify the problem, the motions of the vessel in the sway and yaw directions only are considered. This is possible because the linearized ship equations for the surge motion are normally decoupled from these for the sway and yaw motions [11]. The assumption is also made that the low and high frequency motions can be determined separately and that the total motion is the sum of each of them. Marine engineers often make this assumption since the analysis is simplified and the low frequency motions can also be predicted with more accuracy than the high frequency motions.

The canonical structure of the system under consideration is shown in Figure 5-1. The model for a vessel can be separated into low (l) and high (h) frequency subsystems. The low frequency motions (subsystem S_l) are controllable via thruster action and the high frequency motions (subsystem S_h) are due to the first order wave forces and are oscillatory in nature. The ship positioning problem is to control the low frequency motions (output of S_l) given that the measured position of the vessel (\underline{z}) includes both \underline{y}_l and \underline{y}_h . The object in the following is to design a state estimator to provide estimates of the low frequency motions \underline{x}_l . The estimator must be capable of adapting to variations in the high frequency subsystem S_h which occur due to variations in the weather conditions.

The plant S_l can be assumed to be completely controllable and observable and to be represented by the following discrete, time-invariant, state equations:

$$S_l: \quad \begin{aligned} \underline{x}_l(t+1) &= A_l \underline{x}_l(t) + B_l \underline{u}(t) + D_l \underline{\omega}(t) \\ \underline{y}_l(t) &= C_l \underline{x}_l(t) \end{aligned} \quad (5.1)$$

$$\underline{z}_l(t) = \underline{y}_l(t) + \underline{v}(t) \quad (5.2)$$

where:

$$E \{ \underline{\omega}(t) \} = 0, \quad E \{ \underline{\omega}(k) \underline{\omega}^T(m) \} = Q \delta_{km} \quad (5.3)$$

$$E \{ \underline{v}(t) \} = 0, \quad E \{ \underline{v}(k) \underline{v}^T(m) \} = R \delta_{km} \quad (5.4)$$

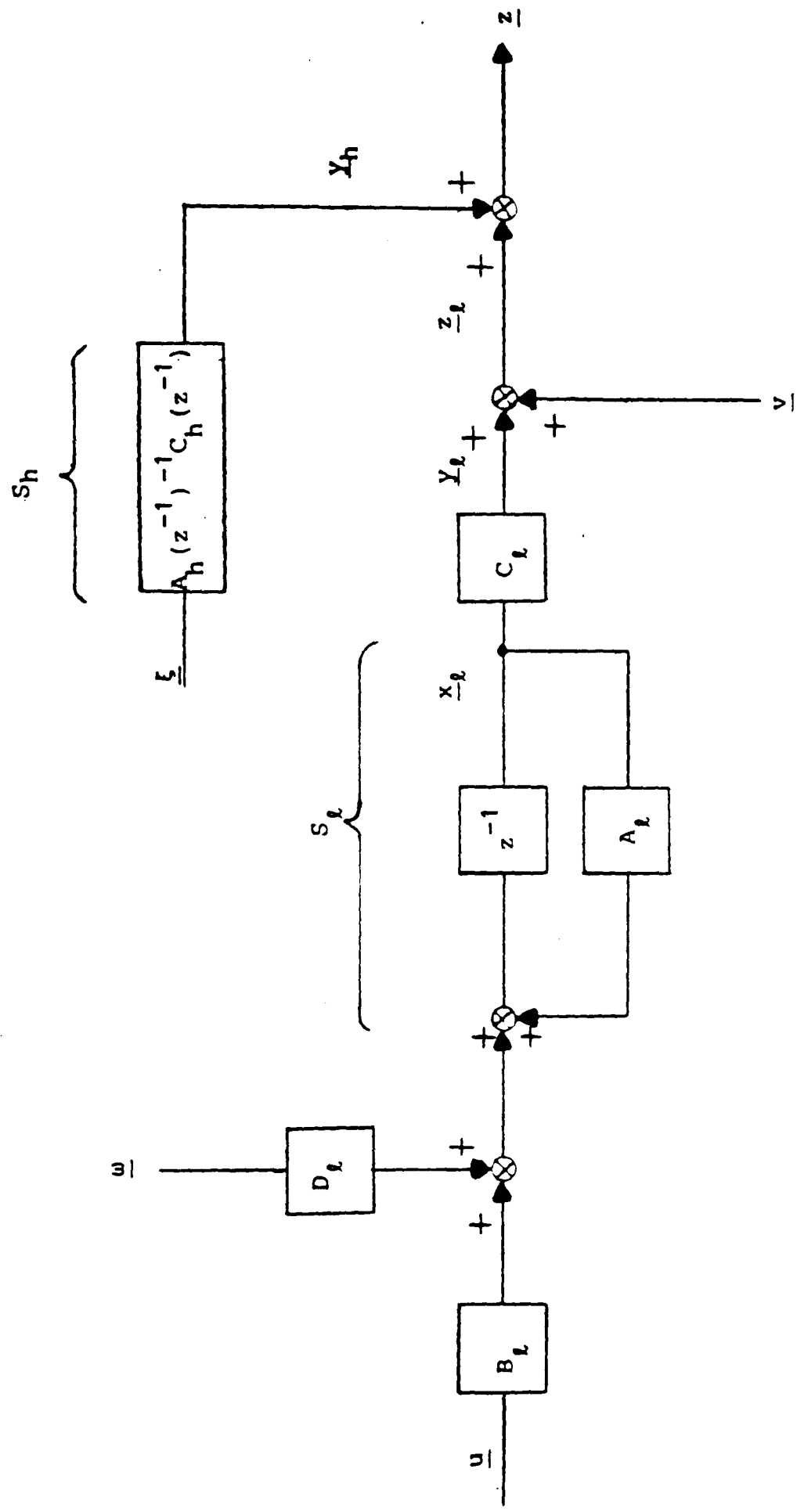


FIGURE 5-1 Low and High Frequency Subsystems

and δ_{km} is the Kronecker delta function, $\underline{x}_l(t) \in \mathbb{R}^n$, $\underline{u}(t) \in \mathbb{R}^m$, $\underline{\omega}(t) \in \mathbb{R}^q$ and $\underline{y}_l(t) \in \mathbb{R}^r$. The process noise $\underline{\omega}(t)$ is used to simulate the wind disturbance and $\underline{v}(t)$ represents a white measurement noise signal. The plant matrices A_l , B_l , C_l and D_l are assumed constant and known. The observed plant output includes the coloured noise (wave disturbance) signal $\underline{y}_h(t)$ and is given by:

$$\underline{z}(t) = \underline{z}_l(t) + \underline{y}_h(t) \quad (5.5)$$

The high frequency disturbance can be represented by the following multi-variable auto-regressive moving-average model:

$$S_h: \quad A_h(z^{-1})\underline{y}_h(t) = C_h(z^{-1})\underline{\xi}(t) \quad (5.6)$$

which is assumed to be asymptotically stable and $\underline{y}_h(t) \in \mathbb{R}^r$ and $\underline{\xi}(t) \in \mathbb{R}^r$. Here $\underline{\xi}(t)$ represents an independent zero mean random vector which is uncorrelated with $\underline{\omega}(t)$ and $\underline{v}(t)$ and has a diagonal covariance matrix Σ_{ξ} . The polynomial matrices $A_h(z^{-1})$ and $C_h(z^{-1})$ are assumed to be square and of the form:

$$A_h(z^{-1}) = I_r + A_1 z^{-1} + A_2 z^{-2} + \dots + A_n z^{-n} \quad (5.7)$$

$$C_h(z^{-1}) = C_1 z^{-1} + C_2 z^{-2} + \dots + C_n z^{-n} \quad (5.8)$$

where z^{-1} is the backward shift operator. The matrix $A_h(z^{-1})$ is assumed to be regular (that is A_{na} is non-singular). The zeros of $\det(A_h(x))$ and $\det(C_h(x))$ are assumed to be strictly outside the unit circle. The order of the polynomial matrices are known but the coefficient matrices $\{A_i\}$ and $\{C_j\}$, $i=1, \dots, na$, $j=1, \dots, nc$, are treated as unknowns, since in practice the wave disturbance spectrum varies slowly with weather conditions. It is also assumed [1] that the disturbances in each observed channel are uncorrelated so that the matrices $\{A_i\}$ and $\{C_j\}$ have diagonal form.

5.3 THE LOW FREQUENCY MOTION ESTIMATOR

Assume for the moment that the coloured noise signal \underline{y}_h can be measured, and thence \underline{z}_ℓ can be calculated. The plant states \underline{x}_ℓ can be estimated using a Kalman filter with input \underline{z}_ℓ , assuming the ship equations and noise covariances are known. It is reasonable to assume that a good time-invariant model for the low frequency motions is known and that the noise sources are stationary. This subsystem is stabilizable and detectable, and under these conditions the Kalman gain matrix is constant and may therefore be computed off-line. Thus, the solution to this part of the estimation problem is particularly simple.

The Kalman filter algorithm becomes:

Predictor:

$$\hat{\underline{x}}_l(t/t-1) = A_l \hat{\underline{x}}_l(t-1/t-1) + B_l \underline{u}(t-1) \quad (5.9)$$

$$\hat{\underline{y}}_l(t/t-1) = C_l \hat{\underline{x}}_l(t/t-1) \quad (5.10)$$

$$P(t/t-1) = A_l P(t-1/t-1) A_l^T + D_l Q_f D_l^T \quad (5.11)$$

$$\hat{\underline{x}}_l(t/t) = \hat{\underline{x}}_l(t/t-1) + \underline{K}_l(t) \underline{\xi}_l(t) \quad (5.12)$$

Corrector:

$$\hat{\underline{y}}_l(t/t) = C_l \hat{\underline{x}}_l(t/t) \quad (5.13)$$

$$P(t/t) = P(t/t-1) - \underline{K}_l(t) C_l P(t/t-1) \quad (5.14)$$

$$\underline{K}_l(t) = P(t/t-1) C_l^T [C_l P(t/t-1) C_l^T + R_f]^{-1} \quad (5.15)$$

where:

$$\underline{\xi}_l(t) = \underline{z}(t) - \hat{\underline{y}}_l(t/t-1) - \underline{y}_h(t) \quad (5.16)$$

$$= \underline{z}(t) - \hat{\underline{y}}_l(t/t-1) \quad (5.17)$$

and $\underline{K}_l(t)$ is the Kalman gain matrix, $P(\cdot)$ is the error covariance matrix. Q_f and R_f are the process noise covariance matrix and measurement noise covariance matrix respectively. Unfortunately $\underline{y}_h(t)$ cannot be separated from $\underline{z}(t)$ by measurement, and the signal $\underline{\xi}_l(t)$ cannot be

calculated. The way in which it is approximated will be discussed in Section 5.5.

5.4 High Frequency Motion Estimator

The wave spectrum is represented by the coloured noise model (5.6) and in this section, the high frequency motion estimator is constructed based upon this model. The assumption is made that the low frequency motions can be estimated via the technique of Section 5.3. For the present, the problem of generating $\hat{\underline{y}}_l(t/t-1)$ when $\underline{y}_h(t)$ is unmeasurable will be ignored.

Define the new variable $\underline{m}_h(t)$ as:

$$\underline{m}_h(t) = \underline{z}(t) - \hat{\underline{y}}_l(t/t-1) \quad (5.18)$$

and from (5.16):

$$\underline{m}_h(t) = \underline{\xi}_l(t) + \underline{y}_h(t) \quad (5.19)$$

The innovations signal $\underline{\xi}_l$ is white noise and \underline{m}_h can be treated as the measured output of a plant S_h with measurement noise $\underline{\xi}_l$. The covariance matrix for $\underline{\xi}_l$ is denoted by $\Sigma_{\xi l}$. The innovations signal model becomes:

$$A_h(z^{-1})\underline{m}_h(t) = D_h(z^{-1})\underline{\xi}_l(t) \quad (5.20)$$

where $\{\xi(t)\}$ is an independent random sequence with covariance matrix \sum_{ξ} .

The matrix polynomial $D_h(z^{-1})$ has the form:

$$D_h(z^{-1}) = I_r + D_1 z^{-1} + \dots + D_{nd} z^{-nd} \quad (5.21)$$

where the zeros of $\det(D_h(x))$ lie strictly inside the unit circle. The parameters of $D_h(z^{-1})$ are determined by the following spectral factorization:

$$D_h(z^{-1}) \sum_{\xi} D_h^T(z) = C_h(z^{-1}) \sum_{\xi} C_h^T(z) + A_h(z^{-1}) \sum_{\xi} A_h^T(z) \quad (5.22)$$

Note that $nd=na$ (since normally $na>nc$) and that by multiplying both sides of equation (5.22) by z^{nd} and taking the limit as $z \rightarrow 0$:

$$D_{nd} \sum_{\xi} = A_{na} \sum_{\xi} \quad (5.23)$$

Since $A_h(z^{-1})$ is regular, that is A_{na} is non-singular, the following identity holds:

$$A_{na}^{-1} D_{nd} = \sum_{\xi} \sum_{\xi}^{-1} \quad (5.24)$$

Hagander and Wittenmark [54] (for the scalar case) and Moir and Grimble [55] (for the multi-variable case) have shown that the optimal estimate of $y_h(t)$ can be calculated using:

$$\hat{\underline{y}}_h(t/t) = \underline{m}_h(t) - \sum_{\underline{e}} \sum_{\underline{\epsilon}}^{-1} \underline{\xi}(t) \quad (5.25)$$

where:

$$\underline{\xi}(t) = \underline{m}_h(t) - \hat{\underline{y}}_h(t/t-1) \quad (5.26)$$

Using the identity in equation(5.24), $\hat{\underline{y}}_h(t/t)$ becomes:

$$\hat{\underline{y}}_h(t/t) = \underline{m}_h(t) - A_{na}^{-1} D_{nd} \underline{\xi}(t) \quad (5.27)$$

The estimate of $\underline{y}_h(t)$ is not needed for control purposes but is required for updating $\hat{\underline{x}}_l(t/t)$. The wave frequency model changes with environmental conditions and these variations are accounted for in (5.27) by on-line estimation of A_{na} , D_{nd} and the innovations $\underline{\xi}(t)$ (Section 5.6).

5.5 MODIFIED ESTIMATION EQUATIONS

The signal $\underline{y}_h(t)$ is not measurable and must be replaced in the low frequency Kalman filter by $\hat{\underline{y}}_h(t/t)$. This substitution causes a difference in the state estimates (denoted $\hat{\underline{x}}_l(t/t)$) and in the calculated innovations:

$$\begin{aligned} \bar{\underline{\xi}}(t) &\triangleq \underline{z}(t) - \hat{\underline{y}}_l(t/t-1) - \hat{\underline{y}}_h(t/t) \\ &= \underline{\xi}_l(t) + \underline{n}_h(t) \end{aligned} \quad (5.28)$$

where $\underline{n}_h(t) = \underline{y}_h(t) - \hat{\underline{y}}_h(t/t)$. The signal $\underline{n}_h(t)$ for the high frequency motion estimator has a zero mean value if the errors in calculating $\hat{\underline{y}}_h(t/t)$ are neglected. Notice from (5.16) and (5.26), the innovations $\bar{\underline{\epsilon}}(t)$ is identical to the signal $\underline{\xi}_h(t)$ where:

$$\underline{\xi}_h(t) \triangleq \underline{m}_h(t) - \hat{\underline{y}}_h(t/t) \quad (5.29)$$

If the above substitution is made, the new low frequency filter has the form:

$$\hat{\underline{x}}_l(t/t) = A_l \hat{\underline{x}}_l(t-1/t-1) + B_l \underline{u}(t-1) + K_l(t) \bar{\underline{\epsilon}}(t) \quad (5.30)$$

but this equation may be decomposed into two parts:

$$\begin{aligned} \hat{\underline{x}}_l(t/t) &= A_l \hat{\underline{x}}_l(t-1/t-1) + B_l \underline{u}(t-1) \\ &\quad + K_l(t) \underline{\xi}_l(t) \end{aligned} \quad (5.31)$$

$$\hat{\underline{x}}_l(t/t) = A_l \hat{\underline{x}}_l(t-1/t-1) + K_l(t) \underline{n}_h(t) \quad (5.32)$$

where:

$$\hat{\underline{x}}_l(t/t) = \hat{\underline{x}}_l(t/t) + \tilde{\underline{x}}_l(t/t) \quad (5.33)$$

and $\tilde{\underline{x}}_l(t/t)$ represents the change brought about by replacing $\underline{y}_h(t)$ by $\hat{\underline{y}}_h(t/t)$ in (5.27). The change in the predicted output:

$$\tilde{\underline{y}}_l(t/t-1) = \hat{\underline{y}}_l(t/t-1) - \hat{\underline{y}}_l(t/t-1) \quad (5.34)$$

where:

$$\hat{\underline{y}}_l(t/t-1) = C_l \hat{\underline{x}}_l(t/t-1) \quad (5.35)$$

but from (5.9) and (5.33)

$$\begin{aligned}\tilde{\underline{y}}_l(t/t-1) &= C_l(\hat{\underline{x}}_l(t/t-1) - \underline{\hat{x}}_l(t/t-1)) \\ &= C_l A_l \hat{\underline{x}}_l(t-1/t-1)\end{aligned}\quad (5.36)$$

For later reference, note that $\tilde{\underline{y}}_l(t/t-1)$ is generated from the output of the low frequency subsystem (see (5.32)) driven by the zero mean signal \underline{n}_h . The resulting position variations are relatively slow in comparison with the high frequency motions.

The high frequency motion estimator is also modified because the signal $\underline{m}_h(t)$ in (5.18) cannot be calculated but instead $\bar{\underline{m}}_h(t)$ can be found where:

$$\bar{\underline{m}}_h(t) \triangleq \underline{z}(t) - \hat{\underline{y}}_l(t/t-1) \quad (5.37)$$

The basis of the parameter estimation equation (Section 5.6) follows from (5.19) and (5.34) as:

$$\begin{aligned}\bar{\underline{m}}_h(t) &= \underline{m}_h(t) - \hat{\underline{y}}_l(t/t-1) \\ &= A_h(z^{-1})^{-1} D_h(z^{-1}) \underline{\xi}(t) - \hat{\underline{y}}_l(t/t-1)\end{aligned}\quad (5.38)$$

Assuming that $\underline{\xi}$ and \underline{y}_l can be calculated the estimate of $\underline{y}_h(t)$ can be generated using (5.27) and (5.38):

$$\hat{\underline{y}}_h(t/t) = \bar{\underline{m}}_h(t) - A_{na}^{-1} D_{na} \underline{\xi}(t) + \hat{\underline{y}}_l(t/t-1) \quad (5.39)$$

The signal $\bar{\underline{x}}$ must be calculated to obtain the desired state estimates $\bar{\underline{x}}_l(t/t)$ and this can be found using (5.18), (5.27) and (5.28):

$$\bar{\underline{x}}(t) = A_{na}^{-1} D_{nd} \underline{x}(t) \quad (5.40)$$

Recall that the gain $K_l(t)$ is calculated based upon the low frequency subsystem rather than the total system model. This has the advantage that the gain is fixed and independent of variations in the high frequency subsystem. The optimal low frequency position estimate should therefore be calculated from (5.31) but this is not possible since $\underline{x}_l(t)$ cannot be computed directly. The state estimates are therefore obtained via (5.30) but are corrected using the estimated $\tilde{\underline{y}}_l(t/t-1)$. This can be achieved in the ship positioning problem because the position states are identical to the outputs of the system. Thus, let the corrected estimate

$$\begin{aligned} \hat{\underline{y}}_l(t/t) &= \hat{\underline{y}}_l(t/t) - \tilde{\underline{y}}_l(t/t-1) \\ &= \text{position states in } \hat{\underline{x}}_l(t/t) \end{aligned} \quad (5.41)$$

In the application of Kalman filters, it is unavoidable that errors will arise from incorrect models for the plant and noise signals. The signal $\tilde{\underline{y}}_l(t/t-1)$ will include such errors, but in the following section it is shown how this

quantity can be estimated and may be used to correct the low frequency state estimates.

5.6 KALMAN AND SELF-TUNING FILTER ALGORITHMS

The Kalman and self-tuning filter algorithms are combined below to produce the desired low frequency motion estimator. The Kalman filter to estimate $\hat{\underline{x}}_l(t/t)$ becomes:

Algorithms 5.1

Predictor:

$$\hat{\underline{x}}_l(t/t-1) = A_l \hat{\underline{x}}_l(t-1/t-1) + B_l(\underline{u}(t-1)) \quad (5.42)$$

$$\hat{\underline{y}}_l(t/t-1) = C_l \hat{\underline{x}}_l(t/t-1) \quad (5.43)$$

Corrector:

$$\hat{\underline{x}}_l(t/t) = \hat{\underline{x}}_l(t/t-1) + K_l(t) \bar{\underline{\epsilon}}(t) \quad (5.44)$$

$$\hat{\underline{y}}_l(t/t) = C_l \hat{\underline{x}}_l(t/t) \quad (5.45)$$

The signal $\bar{\underline{\epsilon}}$ is required in the above algorithms but this can be computed from (5.40) given the innovations signal and the matrices A_{n_d} and D_{n_d} . These matrices may be estimated as described in the following. Note that at time $t-1$, the predicted output $\hat{\underline{y}}_l(t/t-1)$ is known (from (5.42), (5.43)) so that $\bar{\underline{m}}_h(t)$ can be computed from (5.37). From (5.39):

$$A_h(z^{-1})\bar{m}_h(t) = D_h(z^{-1}) \underline{\xi}(t) - A_h(z^{-1})\tilde{y}_\ell(t/t-1) \quad (5.46)$$

The quantity \tilde{y}_ℓ is a slowly varying signal (from Section 5.5) and can be treated as a constant over a short time interval. Let $s(t)=A_h(z^{-1})\tilde{y}_\ell(t/t-1)$ (where using the final value theorem z may be replaced by unity) then (5.46) becomes:

$$A_h(z^{-1})\bar{m}_h(t) = D(z^{-1}) \underline{\xi}(t) - \underline{s}(t) \quad (5.47)$$

The innovations signal model can be represented in the usual form for parameter estimation:

$$\bar{m}_h(t) = \psi(t)\underline{\theta} + \underline{\xi}(t) \quad (5.48)$$

and the algorithm due to Panuska [56] can be employed to estimate the unknown parameters.

In the ship positioning problem, the high frequency disturbances can be assumed to be decoupled, so that $A_h(z^{-1})^{-1}D_h(z^{-1})$ is a diagonal matrix and the parameters for each channel can be estimated separately. Thence, standard extended recursive least squares or maximum likelihood parameter identification algorithms may be used. For the i th channel:

$$\bar{m}_{hi}(t) = \psi_i(t)\underline{\theta}_i + \xi_i(t) \quad (5.49)$$

where:

$$\begin{aligned} \psi_i(t) = & [-\bar{m}_{hi}(t-1)], \dots, \bar{m}_{hi}(t-n_a); \\ & \xi_i(t-1), \dots, \xi_i(t-n_d); 1] \end{aligned} \quad (5.50)$$

$$\theta_i^T = [a_i, \dots, a_{ina}; d_{i1}, \dots, d_{ind}, s_i] \quad (5.51)$$

Past values of the innovations signal are approximated by:

$$\hat{\xi}_i(t) = \bar{m}_{hi}(t) - \hat{\psi}_i(t) \hat{\theta}_i \quad (5.52)$$

where $\hat{\psi}_i(t)$ is given by (5.50) with $\xi_i(t-j)$ replaced by $\hat{\xi}_i(t-j)$ $j=1, 2, \dots, n_d$ and $\hat{\theta}_i$ represents the estimated parameter vector.

The recursive Kalman/self-tuning filter algorithm now becomes:

Algorithm 5.2

1. Initialize: θ_i , initial parameter covariance for each channel and assign the forgetting factor β .
Initialize state estimates.
2. Generate the Kalman filter estimates $\hat{\underline{x}}_l(t/t-1)$ and $\hat{\underline{y}}_l(t/t-1)$ using (5.42) and (5.43).
3. Calculate $\bar{m}_{hi}(t)$ using (5.37) and form $\hat{\psi}_i(t)$.

4. Parameter update:

$$\hat{\underline{\theta}}_i(t) = \hat{\underline{\theta}}_i(t-1) + K_i^P(t)(m_{hi}(t) - \hat{\psi}_i(t) \hat{\underline{\theta}}_i(t-1)) \quad (5.53)$$

5. Covariance and gain update:

$$P_i^P(t) = \left\{ P_i^P(t-1) - K_i^P(t) (\beta + \hat{\psi}_i(t) P_i^P(t-1) \hat{\psi}_i^T(t)) K_i^P(t)^T \right\} / \beta$$

$$K_i^P(t) = P_i^P(t-1) \hat{\psi}_i(t) (\beta + \hat{\psi}_i(t) P_i^P(t-1) \hat{\psi}_i^T(t))^{-1} \quad (5.54)$$

where $0.95 \leq \beta \leq 1$.

6. Innovations update:

$$\hat{\underline{\epsilon}}_i(t) = \bar{m}_{hi}(t) - \hat{\psi}_i(t) \hat{\underline{\theta}}_i(t) \quad (5.55)$$

7. Calculate $\hat{\underline{\tilde{\epsilon}}}_i(t)$ for channel i using (5.40):

$$\hat{\underline{\tilde{\epsilon}}}_i(t) = \hat{a}_{na}^{-1} \hat{d}_{nd} \hat{\underline{\epsilon}}_i(t) \quad (5.56)$$

8. If $i < \text{number of channels } (r)$, go to step 3.9. Generate the state $\hat{\underline{x}}_l(t/t)$ (using equations (5.44) and (5.45)).10. Calculate the estimated $\tilde{\underline{y}}_l(t/t-1)$ as:

$$\hat{\tilde{\underline{y}}}_{li}(t/t-1) = \hat{\underline{s}}_i(t) / A_{hi}(1) \quad (5.57)$$

$$\hat{\tilde{\underline{y}}}_{si}(t) = \alpha \hat{\tilde{\underline{y}}}_{si}(t-1) + (1-\alpha) \hat{\tilde{\underline{y}}}_{li}(t/t-1)$$

$$0 \leq \alpha \leq 1$$

11. Correct the position estimates using (5.41). Return to step 2.

The signal $\hat{\tilde{y}}_{li}(t/t-1)$ in step 10 may be processed, to produce the smoothed estimate $\hat{\tilde{y}}_{si}(t)$, before it is used to correct the state estimates. The algorithm described in Appendix D can predict the velocity as well as smoothing the estimation of $\tilde{y}_{li}(t)$.

The structure of the self-tuning/Kalman filtering scheme for the dynamic positioning system is shown in Figure 5-2. The surge motions are decoupled from the sway and yaw motions and thus these are normally estimated by separate filters.

5.7 DISCUSSION

The self-tuning Kalman filtering technique is the alternative scheme for a dynamic ship positioning control system. The advantages and disadvantages are listed below. Most of the advantages are also its advantages over harmonic wave model and fourth order wave model extended Kalman filtering approaches.

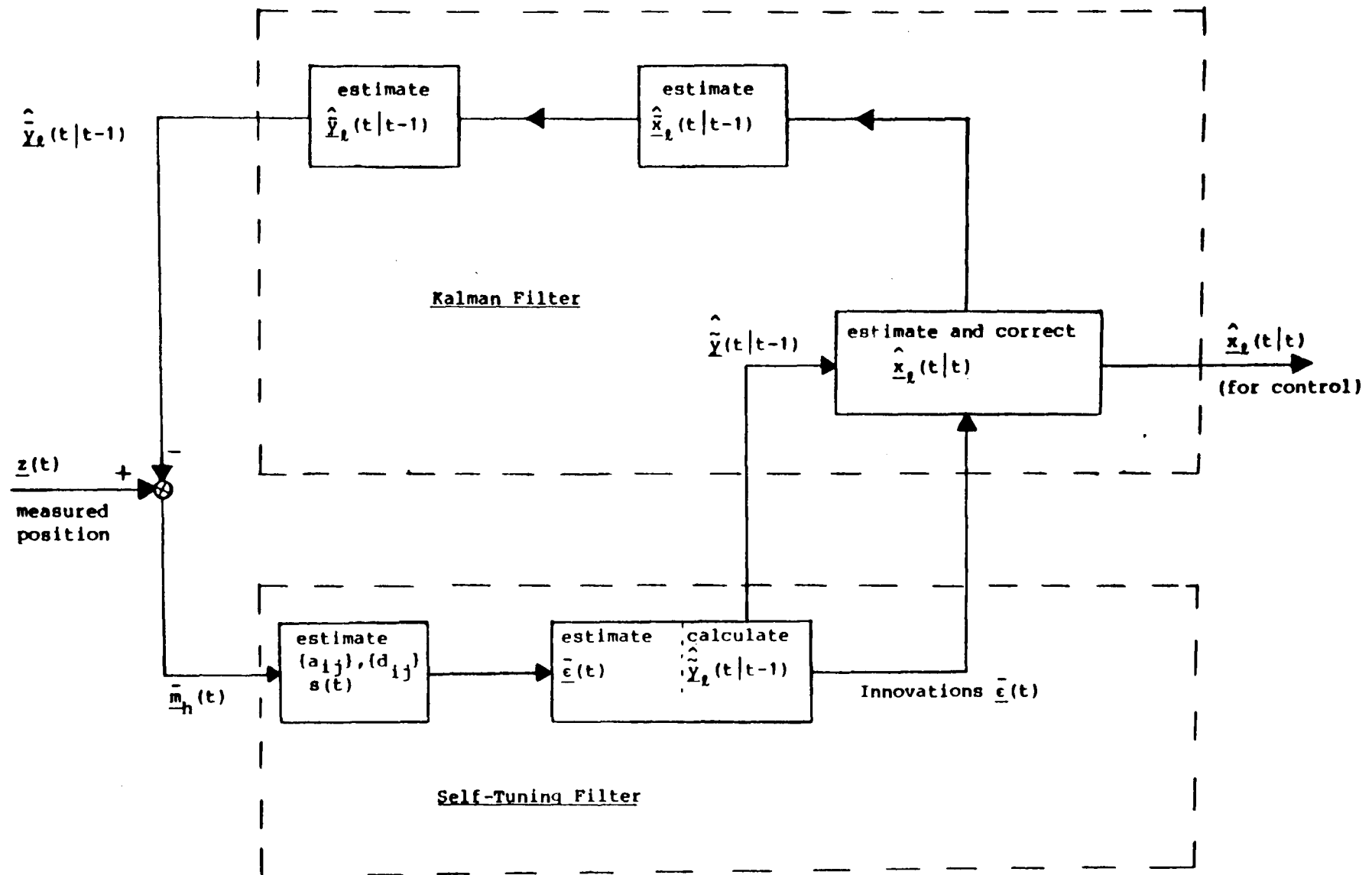


FIGURE 5-2 Structure of Filtering Scheme.

5.7.1 Advantages

- (a) The varying wave disturbance is represented by single-input single-output channels and thus the adaptive filter is not multi-variable in nature.
- (b) The high frequency adaptive filter forms a separate subsystem to the low frequency Kalman filter and thus the gain calculations are simplified and the system may be commissioned more easily.
- (c) The filter gains for the low frequency estimator are fixed and can be computed off-line whereas all of the gains in an extended Kalman filter must be computed on-line unless approximations are made [17, 18].
- (d) Existing constant gain linear Kalman filtering DP systems [5] may easily be modified to include the self-tuning features described here.
- (e) There is no need to specify the process noise covariance or the form of the high frequency model. Only the total order of the model is assumed known.

- (f) The high frequency model states which are not needed for control purposes, are not estimated in the self-tuning approach.

5.7.2 Disadvantages

The full extended Kalman filter in which all of the gains are computed on-line can be classed as being locally optimal (if the linearizations are correct) whereas the self-tuning scheme is sub-optimal unless the low frequency estimator gains are calculated on-line using knowledge of the changing high frequency model.

In fact, the harmonic wave model extended Kalman filtering approach is not an optimal extended Kalman filter. The fourth order wave model [6, 7] extended Kalman filter approach involves too many states and is therefore very difficult to implement for it may easily cause numerical problems and the stability problem is difficult to analyze.

5.8 SUMMARY OF RESULTS

A self-tuning technique has been developed to replace the usual fixed high frequency estimator in Kalman filtering

dynamic positioning systems. Thus, systems which do not currently have automatic adaption to varying environmental conditions can be provided with such a feature. The approach has the advantage of simplicity over extended Kalman filtering dynamic positioning systems. In addition:

- (a) There is no need to specify the process and measurement noise for the high frequency model.
- (b) High frequency model states which are not needed for control are not estimated.
- (c) The structure of the multi-variable estimator which involves separate adaptive and non-adaptive subsystems simplifies both implementation and fault finding.

The technique can also be applied to other engineering and economical processes which have the same features as the dynamic positioning systems.

CHAPTER SIX

THE USE OF SELF-TUNING KALMAN FILTERING TECHNIQUES IN DYNAMIC SHIP POSITIONING SYSTEMS

6.1 INTRODUCTION

In Chapter Five, the theory of a self-tuning Kalman filter was developed. Originally, the theory was inspired by the Dynamic Ship Positioning (DSP) problem. In DSP systems, the controlled ship motions are due to the current, wind and second order wave disturbances. These motions are slow compared with the high frequency oscillatory first order wave disturbances. The control problem and system modelling are fully described in Chapter One and Chapter Two. The self-tuning Kalman filter has several advantages over the more usual extended Kalman filter [7, 17, 18]. The separation of the LF and HF estimation functions is convenient for both fault analysis and error detection. The existing constant gain Kalman filtering DSP system [5] can easily be modified to include the self-tuning section. Most of all, the self-tuning filter subsystem is adaptive to the weather condition changes.

The application of self-tuning Kalman filter to DSP is tested in four conditions. In the linear case, both single input, single output (SISO) system and multi-input, multi-output (MIMO) system are used to test the filtering and control scheme. The results are given in Section 6.2. In the next test, instead of using a linear model to simulate the low frequency ship motions, the original non-linear differential equations are used. The estimation of states still remains the same, that is, a linear Kalman filter is employed. In the above three cases, no integral action is included in the controller. The final test is to demonstrate a special feature of the self-tuning Kalman filter when integral control is employed. The MIMO system is used in non-linear cases. The filter and controller parameters are given in each section. These parameters may vary among the tests, since the model used for the design may not be the same for each test.

6.2 LINEAR SYSTEM IMPLEMENTATION

6.2.1 Single Input - Single Output Systems

Low Frequency Model

In this study, the sway model of Wimpey Sealab [11] is considered with Beaufort No. 8 sea condition (equivalent to

a mean wind speed of 19 m sec^{-1}). The normalized linear model is:

$$\begin{aligned}\dot{\underline{x}}_l(t) &= A_l \underline{x}_l(t) + B_l u(t) + D_l \omega(t) \\ y_l(t) &= C_l \underline{x}_l(t) \\ z_l(t) &= y_l(t) + v(t)\end{aligned}\tag{6.1}$$

The system matrices are:

$$\begin{aligned}A_l &= \begin{bmatrix} -0.0546 & 0 & 0.5435 \\ 1 & 0 & 0 \\ 0 & 0 & -1.55 \end{bmatrix} \\ B_l^T &= \begin{bmatrix} 0 & 0 & 1.55 \end{bmatrix} \\ C_l &= \begin{bmatrix} 0 & 1 & 0 \end{bmatrix} \\ D_l^T &= \begin{bmatrix} 0.5435 & 0 & 0 \end{bmatrix}\end{aligned}\tag{6.2}$$

$$\underline{x}_l(t) = \begin{bmatrix} x_{l1}(t) \\ x_{l2}(t) \\ x_{l3}(t) \end{bmatrix} = \begin{bmatrix} \text{sway velocity} \\ \text{sway position} \\ \text{thruster state} \end{bmatrix}\tag{6.3}$$

Here $u(t) \in R^1$ represents the control input to the thruster, $\omega(t) \in R^1$ is a white noise sequence representing the random force on the vessel. Other disturbances, such as wave drift and current forces cannot be measured and can be considered to produce an unknown mean value on the signal $\omega(t)$. Let $y_l(t) \in R^1$ denote the low frequency motion, $v(t) \in R^1$ the measurement noise and $z_l(t) \in R^1$ is the measurement noise and

LF sway motion respectively. For Wimpey Sealab, the estimated standard deviation for $\omega(t)$ is $\sigma_p=0.00228$, and that for $v(t)$ is $\sigma_m=0.0033$.

High Frequency Model

The simulation model used is described in Method (1) in Section 2.8.4.

For the self-tuning filter subsystem, it is assumed the HF motion can be modelled by a second order transfer function.

$$y_h(t) = \frac{C_h(z^{-1})}{A_h(z^{-1})} \xi(t) \quad (6.4)$$

where:

$$C_h(z^{-1}) = c_1 z^{-1} \quad (6.5)$$

$$A_h(z^{-1}) = 1 + a_1 z^{-1} + a_2 z^{-2}$$

The parameters of the polynomials $A_h(z^{-1})$ and $C_h(z^{-1})$ are unknown and $\xi(t)$ is an independent random sequence.

The total measured output is:

$$z(t) = z_\ell(t) + y_h(t)$$

Filtering Problem and Results

A steady state Kalman gain matrix is used in the LF state estimation subsystem. For Wimpey Sealab, the process noise and measurement noise covariances are $\sigma_p^2 = 5.1984 \times 10^{-6}$ and $\sigma_m^2 = 10^{-5}$ respectively. The computed steady state Kalman gains are given as:

$$K_{SS}^f = \begin{bmatrix} 0.301351 \\ 0.776339 \\ 0.0 \end{bmatrix} \quad (6.6)$$

The thruster state has zero gain because the process noise is not fed into this state.

The estimated parameters are shown in Figure 6-1. The parameters converged to steady values after 350 seconds. It is, of course, well known that the convergence rate of any technique, where the innovations must be approximated, is very slow. Figure 6-2 shows the total sway motion, and the estimated LF motion is shown in Figure 6-3. When the uncontrolled vessel was drifting away from the station, the estimator tracked the position well even though the parameters had not reached steady state (see Figure 6-1). The high frequency estimation is shown in Figure 6-4. The HF estimator started to track accurately the HF motion after

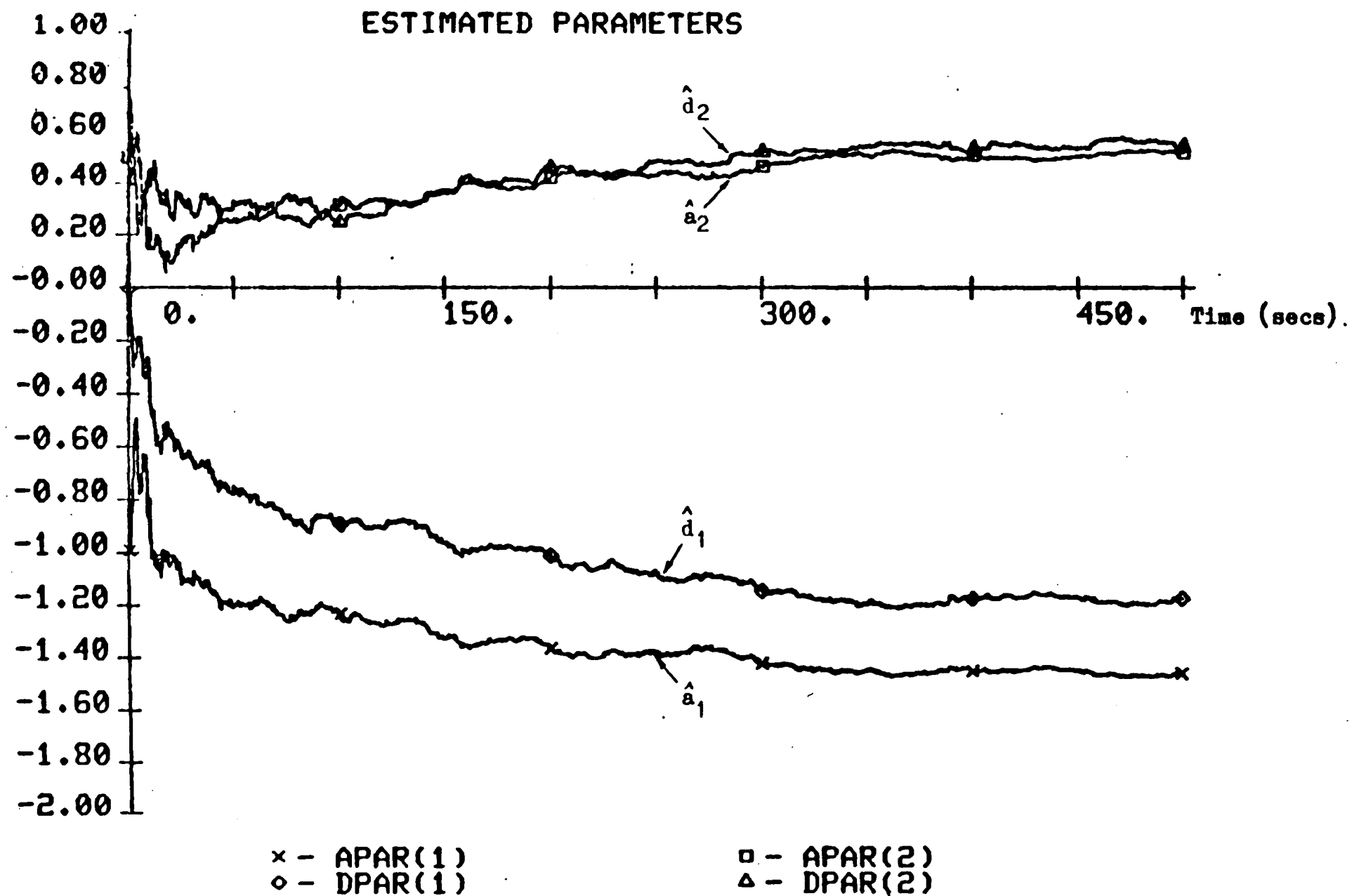


FIGURE 6-1 Estimated Parameters of Self-Tuning Filter (SISO)

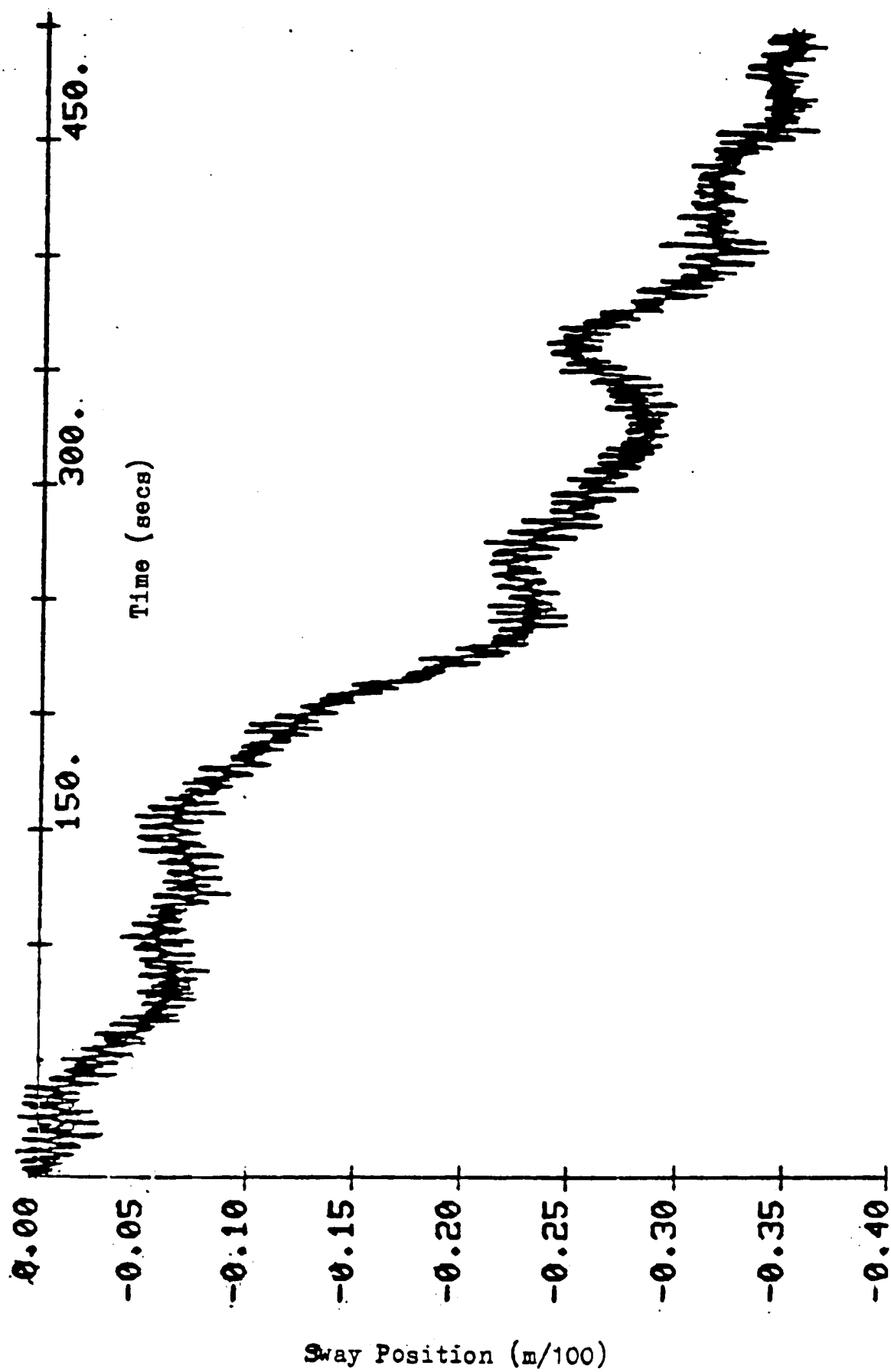


FIGURE 6-2 Total Sway Motion (SISO)

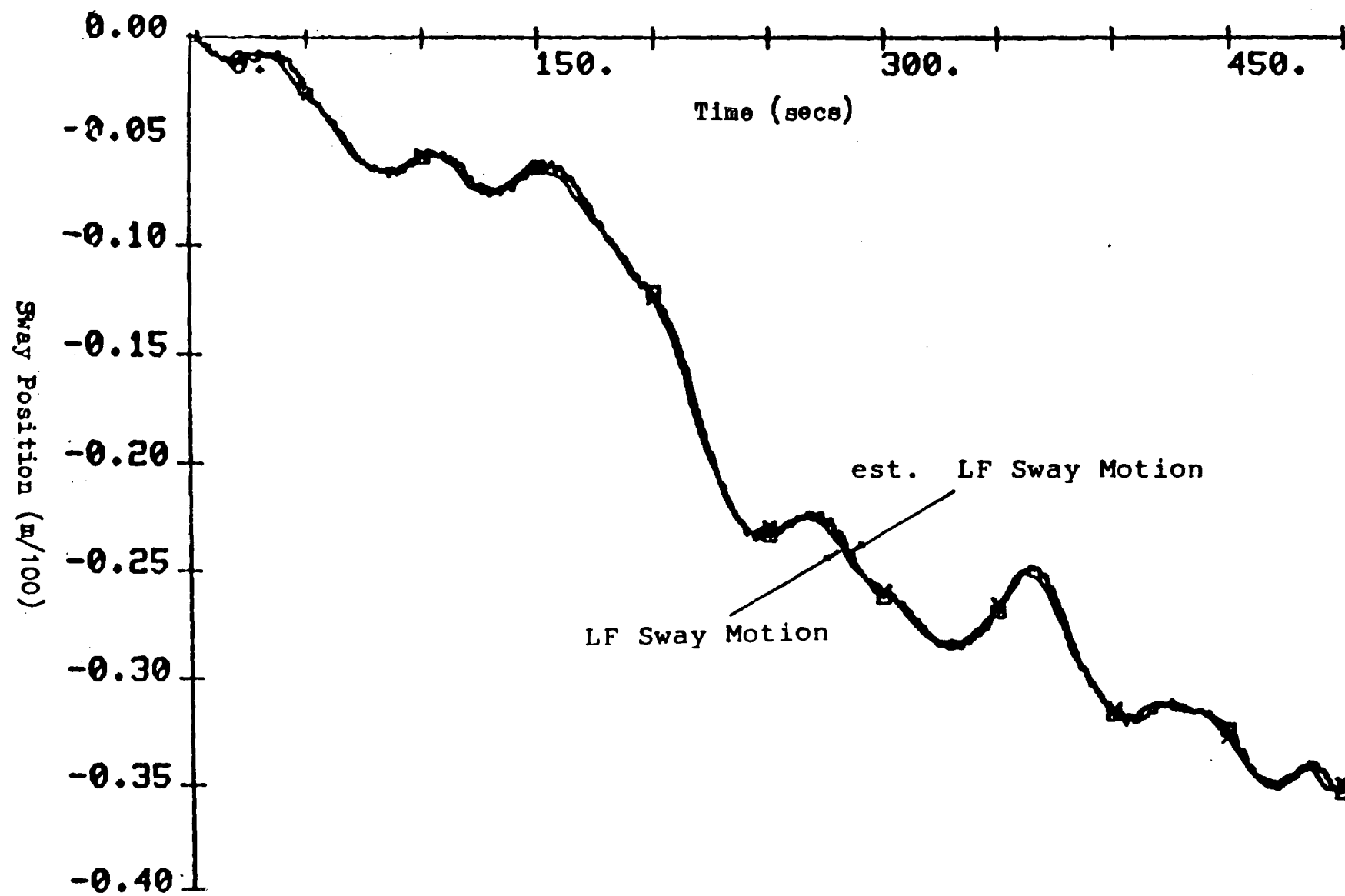


FIGURE 6-3 Simulated and Estimated LF Motion (SISO)

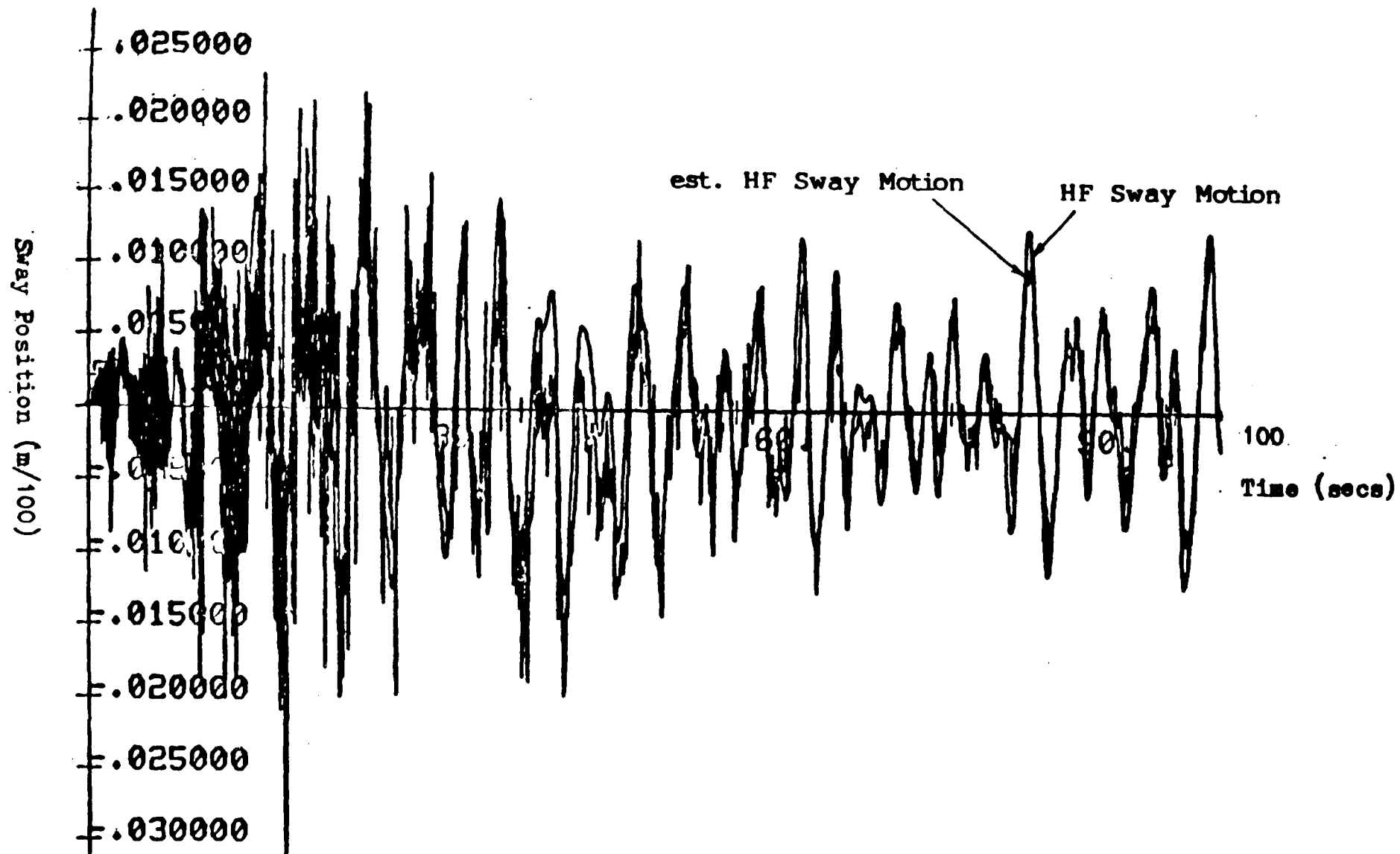


FIGURE 6-4 Simulated and Estimated LF Motion (SISO)

20 seconds. Before this time, it tracked reasonably well except for a noisy envelope.

For the innovation process equation (5.20) to be stable, the parameters a_1 and d_1 should lie in the interval $[0, -2]$, and a_2 and d_2 should lie in the interval $[0, 1]$. Thus, the best guess of the initial values for a_1 and d_1 are both -1.0 and those for a_2 and d_2 are 0.5. When using the extended least square algorithm, the parameter gains and the estimation errors should be restricted so that $\{a_i\}$ and $\{d_i\}$ lie in the stable region, otherwise, it has been observed that the estimated parameters may blow up in the initial estimation.

It is important to consider how the filters behave in steady state. Figures 6-5 to 6-7 show the motions between 400 to 500 seconds. Both LF estimator and HF estimator behaved well. The cumulative losses are shown in Figure 6-8. These tests were based on Beaufort No. 8 ($h_{1/3}=7.47\text{m}$) sea condition. Figure 6-9 shows the parameter estimation when the sea condition was changed to Beaufort No. 5 ($h_{1/3}=2.7\text{ m}$). As the Beaufort number decreases, the natural frequency of the wave spectrum increases, therefore, the absolute values of the parameters $\{a_i\}$ should increase. The absolute values of the parameters $\{a_i\}$ do increase at the time when sea condition is changed, and they converge to new steady state values. This demonstrated that, as required,

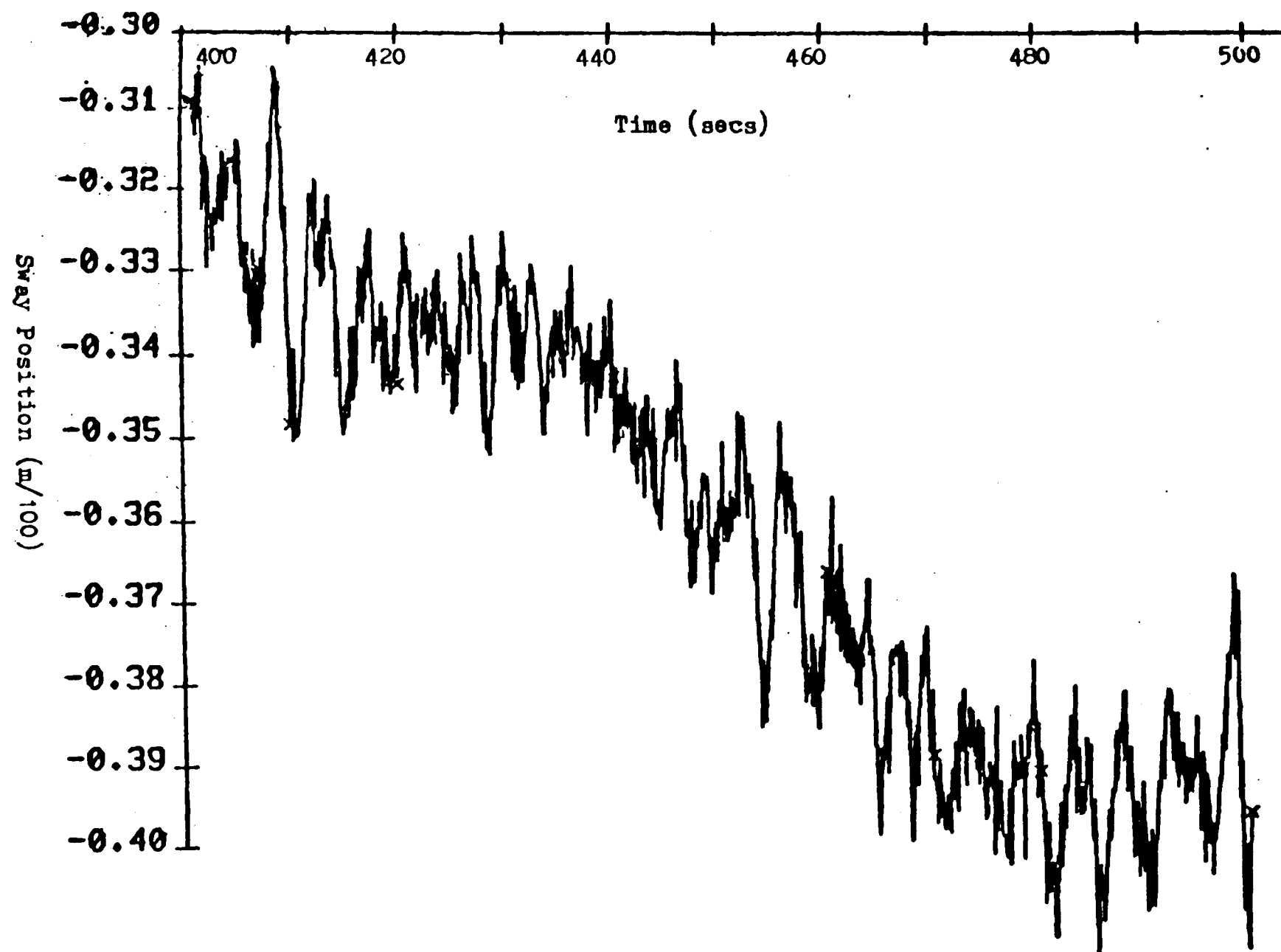


FIGURE 6-5 Total Sway Motion (400-500 secs., SISO)

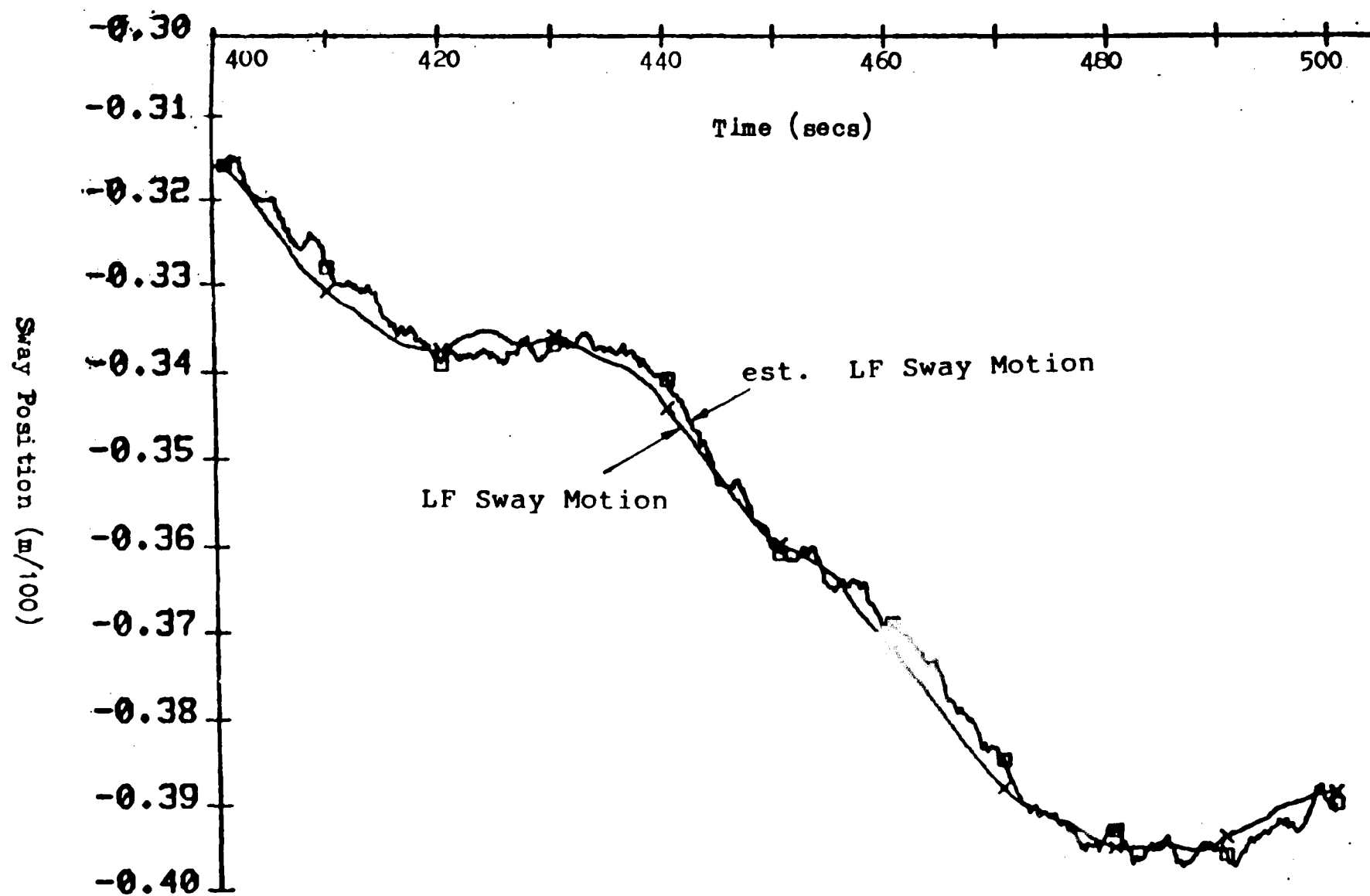


FIGURE 6-6 Simulated and Estimated LF Motion (400-500 secs. SISO)

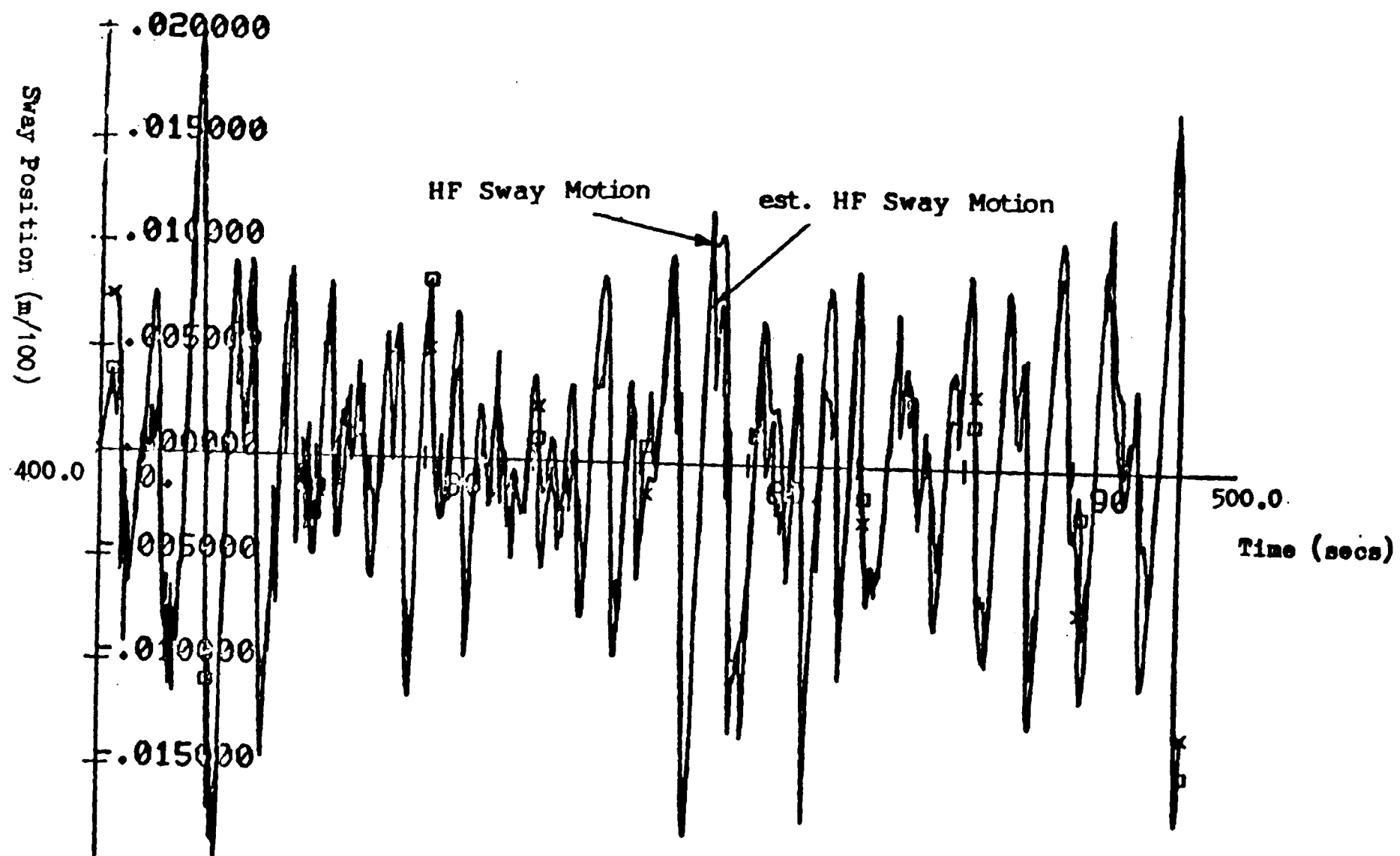


FIGURE 6-7 Simulated and Estimates HF Motion (400-500 secs. SISO)

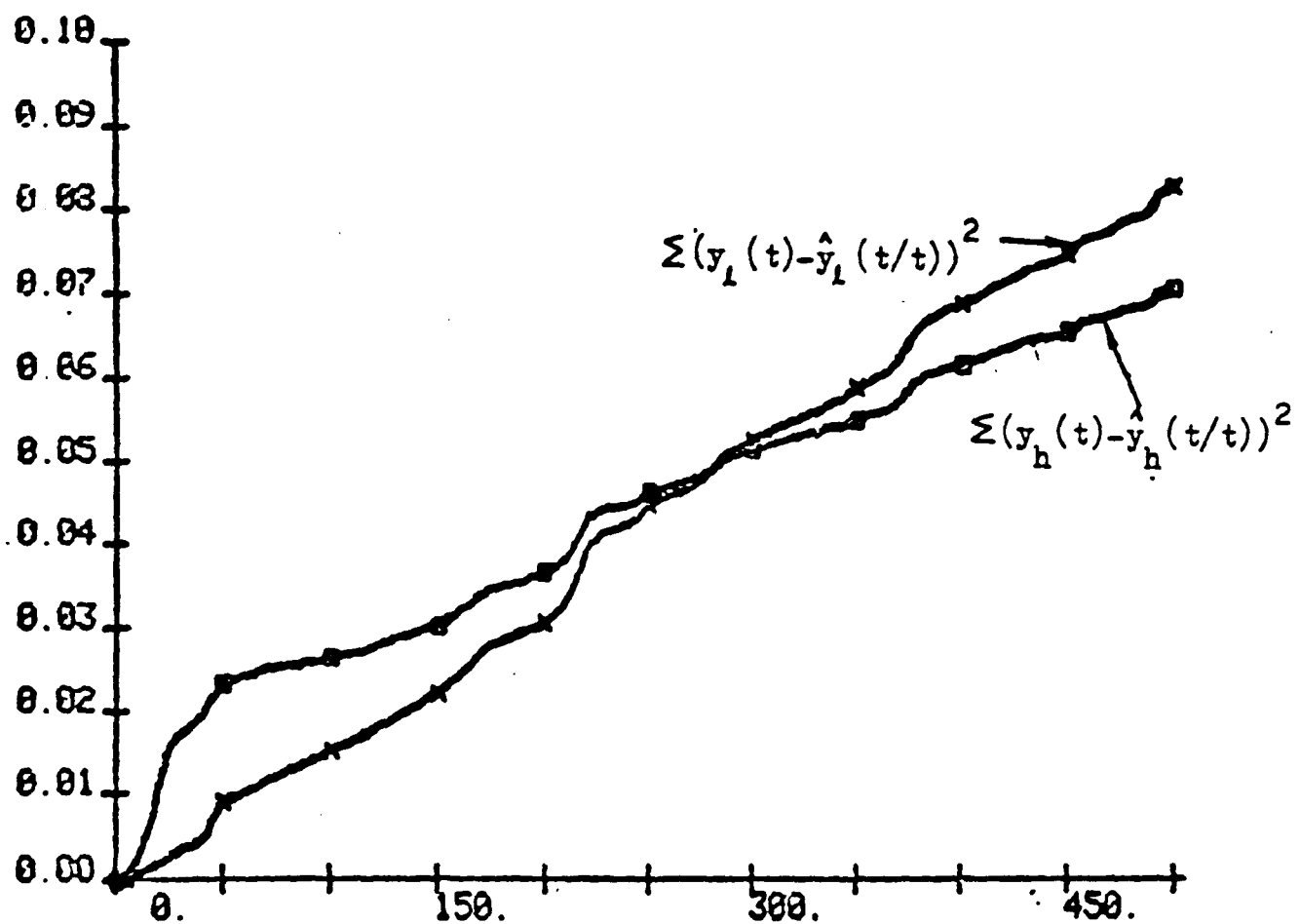


FIGURE 6-8 Accumulative loss Functions (SISO)

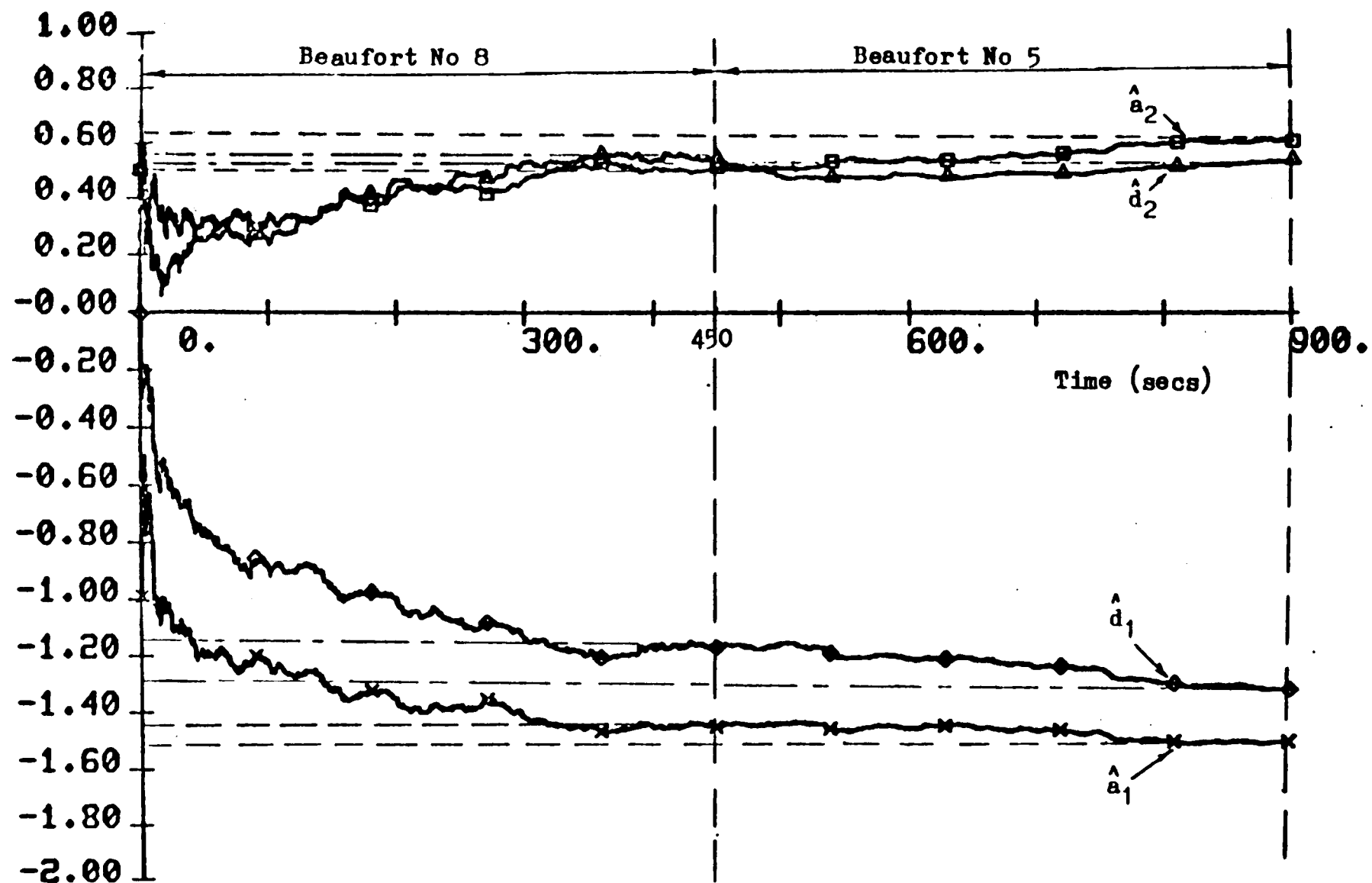


FIGURE 6-9 Estimated Parameters of Self-Tuning Filter with Sea Condition Changed (SISO)

the self-tuning scheme adapted to different weather conditions. The simulated frequency range of HF motion at Beaufort No. 8 is 0.3 to 1.2 radians per second, and that at Beaufort No. 5 is 0.5 to 1.9 radians per second.

In this simulation test, the quantity of $s(t)$ equation (5.66) was not estimated. This was based on the assumption that if the variance of the measurement noise was sufficiently high, the signal $n_h(t)$ in equation (5.51) was almost negligible compared with $\xi_l(t)$. Thence, the estimation of $s(t)$ may be dropped. The results have verified this assumption. However, if the variance of the measurement noise was unable to suppress the effect of $n_h(t)$ in the system, significant error in the LF estimation was found. Therefore, it is recommended that the estimation of $s(t)$ should always be included. On the other hand, if the variance of the HF disturbance is low (the variance of $n_h(t)$ is low), this will give better estimation in LF motion (see equation (5.32) and (5.33)).

6.2.2 Multi-Input - Multi-Output Systems Low Frequency Model

The DSP system to be considered here is a two-input and two-output system. The controlled variables are sway and yaw motions. The LF linear ship model is given in Section 2.7

(Wimpey Sealab). Model A was used in this simulation. The LF state vector is defined as:

$$\underline{x}_l(t) = \begin{bmatrix} x_1(t) \\ x_2(t) \\ x_3(t) \\ x_4(t) \\ x_5(t) \\ x_6(t) \end{bmatrix} \begin{array}{l} \text{sway velocity} \\ \text{sway position} \\ \text{yaw angular rate} \\ \text{yaw angle} \\ \text{thruster one} \\ \text{thruster two} \end{array} \quad (6.7)$$

High Frequency Model

The HF wave motions were simulated using Method [2] described in Section 2.8.4.

The high frequency model for the self-tuning filter is a second order ARMA model which is described in Section 2.8.2. The order of $D_h(z^{-1})$ is identical to that of the $A_h(z^{-1})$.

Filtering Problem and Results

The steady state Kalman filter gain matrix is computed based on the process noise variances (LF only) defined in equation (2.18) but the measurement noise covariance matrix (2.19) is inflated to $\text{diag} [5 \times 10^{-5}, 1.22 \times 10^{-4}]$. The first and second diagonal elements are five and ten times the

simulated measurement noise variances equation (2.19) respectively. The computed Kalman gain matrix is:

$$K^f = \begin{bmatrix} 0.1263 & 0.0031 \\ 0.5023 & 0.0086 \\ 0.0170 & 0.2201 \\ 0.0210 & 0.6633 \\ 0.0 & 0.0 \\ 0.0 & 0.0 \end{bmatrix} \quad (6.8)$$

The filter gains corresponding to thruster states are zero because the process noises are not fed to these states.

The simulation results presented below were obtained using the above high frequency model to generate the wave motions. The tests were based on sea states corresponding to Beaufort No. 8 and 5 (wind speeds 19 m/sec. and 9.3 m/sec., respectively), which correspond to typical rough and calm seas respectively. The first set of the filtering results (Figure 6-10 and Figure 6-15 are for Beaufort No. 8 without closed loop control.

The total sway motion is shown in Figure 6-10 and the estimated and modelled low frequency sway motions are shown in Figure 6-11. The estimate of the low frequency motion is required for control purposes and it is clear the estimate is good throughout the time interval (even after initial

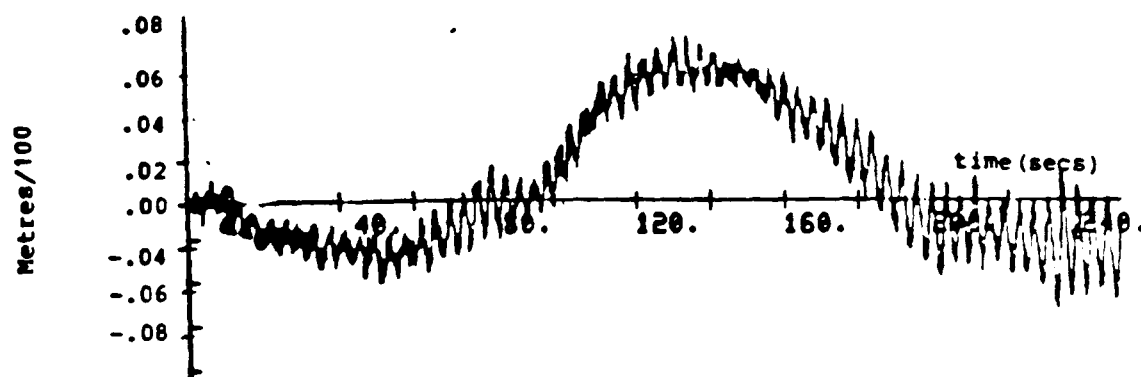


FIGURE 6-10 Observed Total Sway Motion (Beau.8, MIMO)

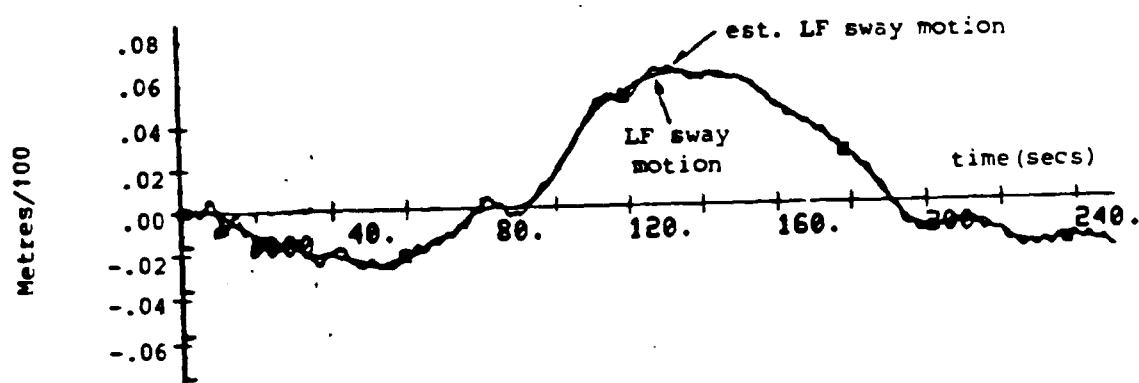


FIGURE 6-11 Estimated and Modelled LF Sway Motion (Beau.8 MIMO)

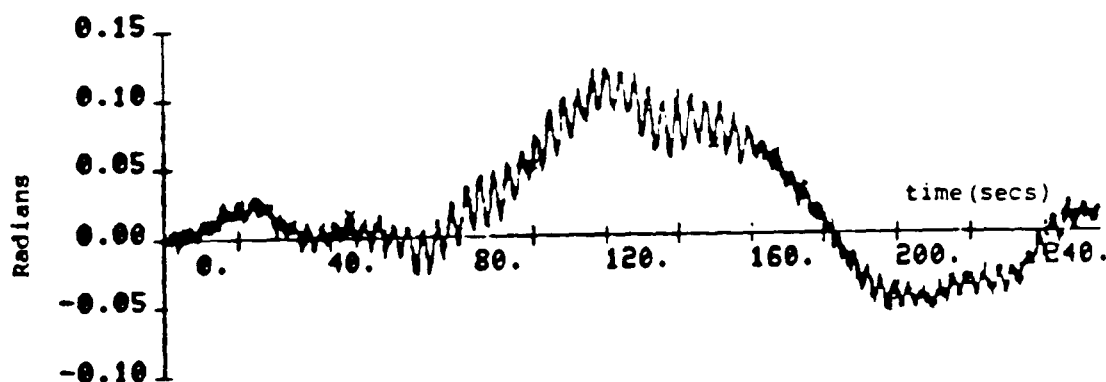


FIGURE 6-12 Observed Total Yaw Motion (Beau.8, MIMO)

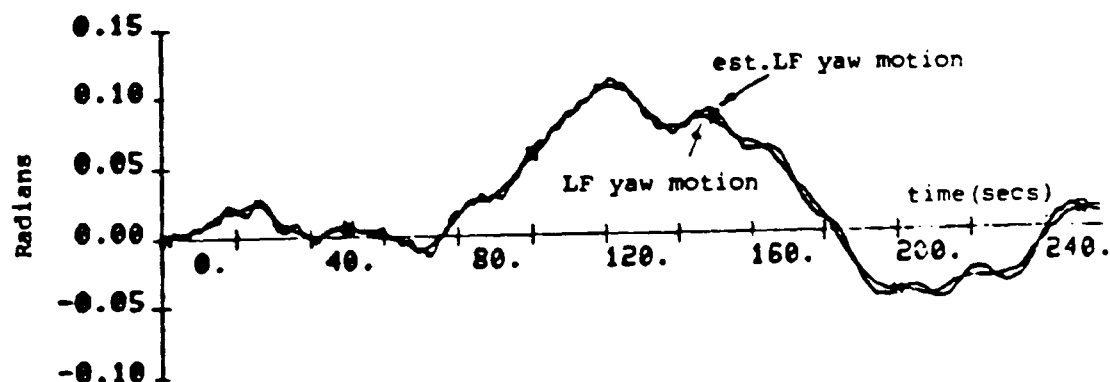


FIGURE 6-13 Estimated and Modelled LF Yaw Motion (Beau.8, MIMO)

start up). The high frequency sway motion estimates are not needed for feedback control and are not shown. The total and the low frequency yaw motions are shown in Figure 6-12 and Figure 6-13 respectively. It is important that the LF motion estimates are relatively smooth to reduce the consequential variations in the control action. The major role of the combined estimator is indeed to separate the HF and LF motion estimates. Since the LF Kalman filter does not have \underline{z}_l as an input, but rather:

$$\underline{z}(t) - \hat{\underline{y}}_h(t/t) = \underline{z}_l(t) + n_h(t) \quad (6.9)$$

the predicted measurement noise covariance should be increased if the LF estimates contain an HF component. Since the HF wave conditions are slowly varying, the amount by which R_f should be increased is not known exactly, but the system is not oversensitive to such an adjustment (factors of 5 on sway and 10 on yaw were used for the results shown here).

The cumulative loss functions for the position estimation errors in sway and yaw (both HF and LF) are shown in Figure 6-14. The LF loss function for sway is defined is:

$$J = \sum_{t=1}^N (y_l^s(t) - \hat{y}_l^s(t/t))^2 \quad (6.10)$$

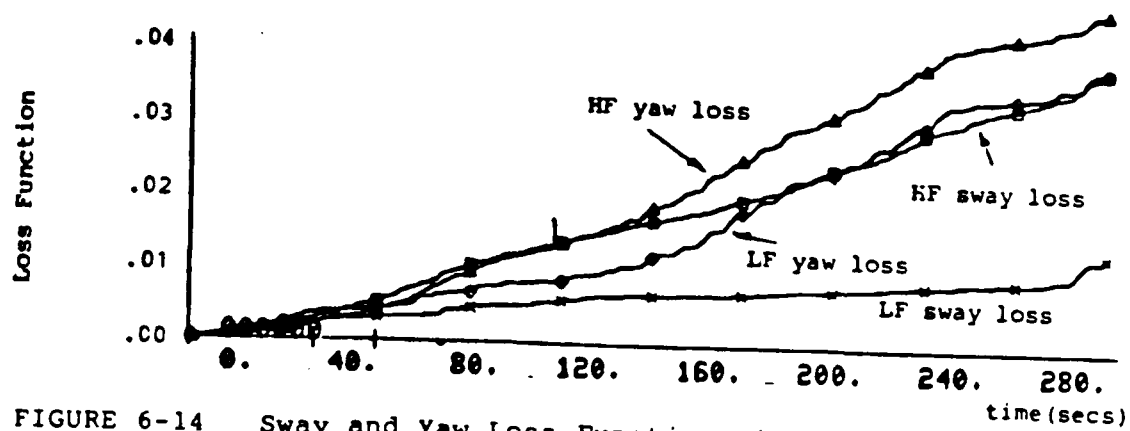


FIGURE 6-14 Sway and Yaw Loss Functions (Beau.8, MIMO)

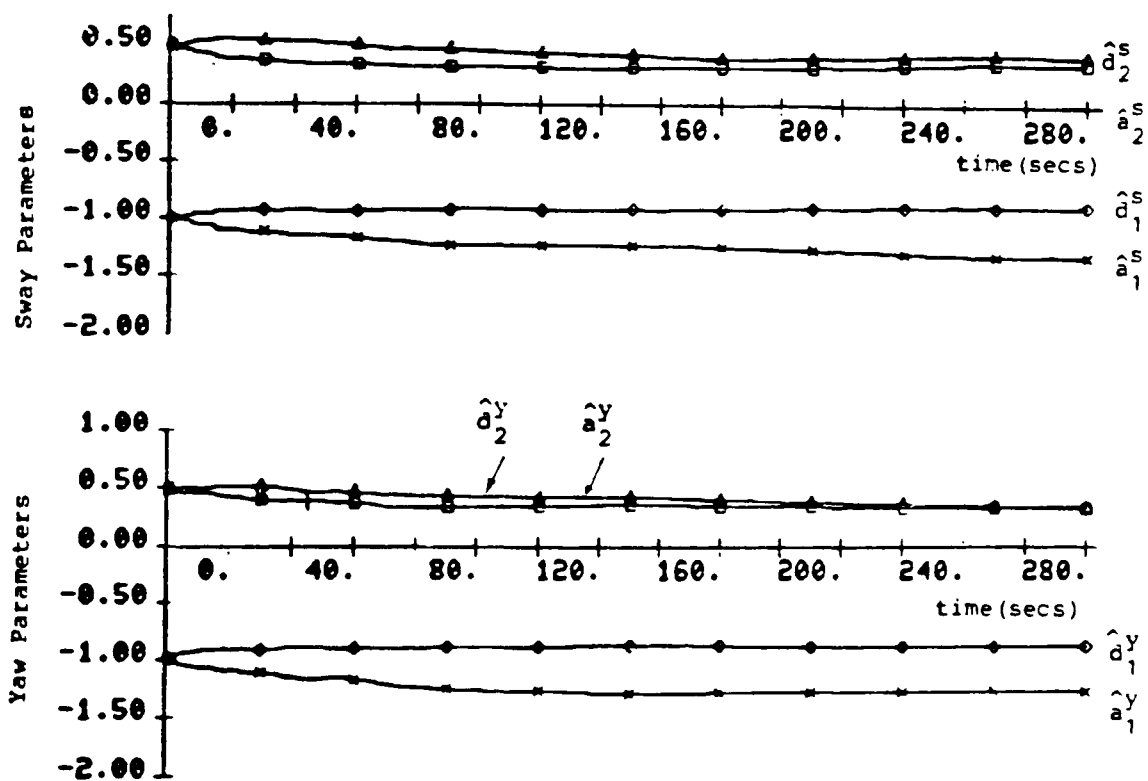


FIGURE 6-15 Sway and Yaw Estimated Parameters (Beau.8, MIMO)

If the measurement noise were not artificially increased when calculating the Kalman filter gain, the HF and LF loss functions for yaw would be found to be similar. This is an indication of optimal performance which has been sacrificed to some extent to obtain smoother position elements. The parameter estimates for the high frequency model are shown in Figure 6-15 where:

$$A_h(z^{-1}) = I_2 + \begin{bmatrix} a_1^s & 0 \\ 0 & a_1^y \end{bmatrix} z^{-1} + \begin{bmatrix} a_2^s & 0 \\ 0 & a_2^y \end{bmatrix} z^{-2} \quad (6.11)$$

$$D_h(z^{-1}) = I_2 + \begin{bmatrix} d_1^s & 0 \\ 0 & d_1^y \end{bmatrix} z^{-1} + \begin{bmatrix} d_2^s & 0 \\ 0 & d_2^y \end{bmatrix} z^{-2} \quad (6.12)$$

Note that even before the estimated parameters have converged, the position estimates are still accurate (see Figure 6-11 and Figure 6-13). The initial parameter estimates for the matrices A_h and D_h can be based upon the knowledge that these have stable inverses. The polynomials are all of the form $a = 1 + a_1 z^{-1} + a_2 z^{-2} = (m_1 z^{-1} + 1)(m_2 z^{-1} + 1)$ and since $|m_1| < 1$, $|m_2| < 1$ then $-2 < m_1 + m_2 < 2$, $-1 < m_1 m_2 < 1$. Assuming $m_1, m_2 < 0$ implies that good initial estimates are $a_2 = 0.5$ and $a_1 = -1$. It was found that the

initial error covariance for $s(t)$ should be small (e.g. 0.1 in this test) but the initial covariance for the other parameters should be high (e.g. 100). The estimate of $s(t)$ may contain a high frequency component and this may be smoothed by use of a simple first order lag filter.

The filtering results for a calm sea (Beaufort No. 5) are shown in Figures 6-16 to 6-21. The state estimates are much better for this case. This is consistent with the theory of Section 5 that shows that when the modelling errors are negligible, the term $\tilde{y}_l(t/t-1)$ is caused by the estimation error of the high frequency motion (see (5.22) and (5.33)) which is reduced in a calm sea.

Control Problem and Results

The controller design is based on the well known separation principle of stochastic optimal control theory. The controller with input \underline{x}_l and output \underline{u} is chosen to minimize the performance criterion:

$$J = \lim_{T \rightarrow \infty} \frac{1}{2T} E \left\{ \int_{-T}^T (\underline{x}_l - \underline{r}_l)^T Q_c (\underline{x}_l - \underline{r}_l) + \underline{u}^T R_c \underline{u} dt \right\} \quad (6.13)$$

where Q_c and R_c are positive definite weighting matrices. The optimal control signal is generated from a Kalman filter

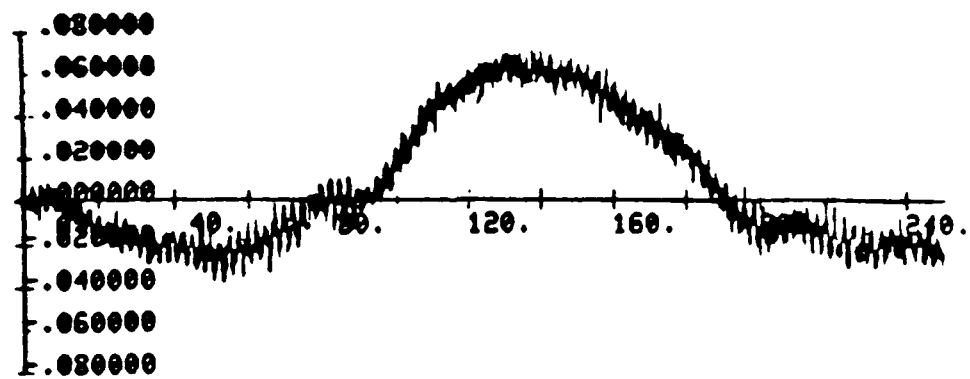


FIGURE 6-16 Observed Total Sway Motion (Beau.5, MIMO)

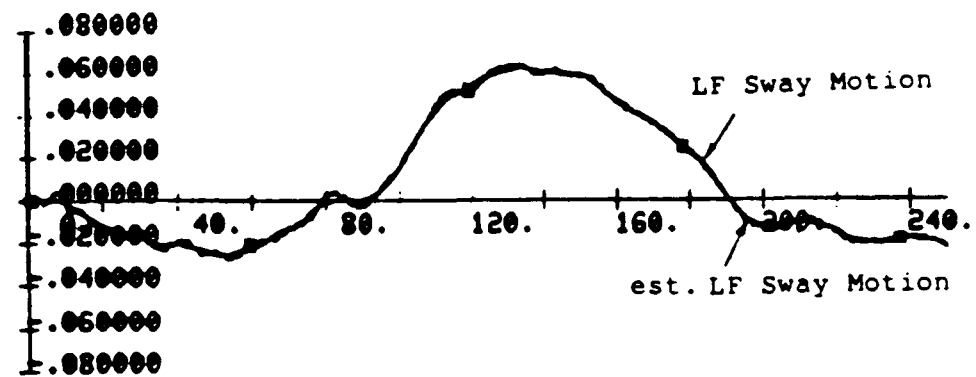


FIGURE 6-17 Estimated and Modelled LF Sway Motion (Beau.5, MIMO)

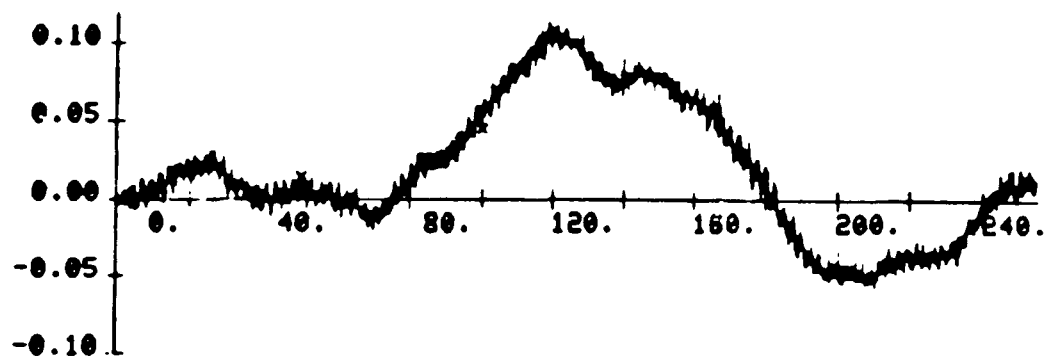


FIGURE 6-18 Observed Total Yaw Motion (Beau.5, MIMO)

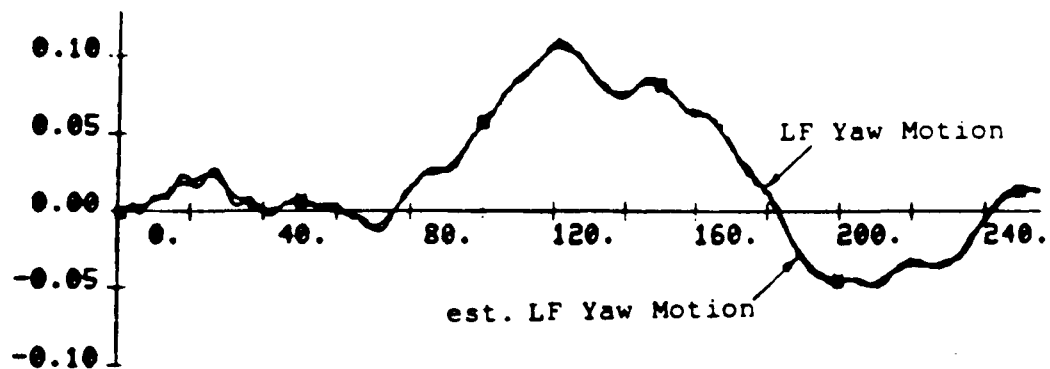


FIGURE 6-19 Estimated and Modelled LF Yaw Motion (Beau.5, MIMO)

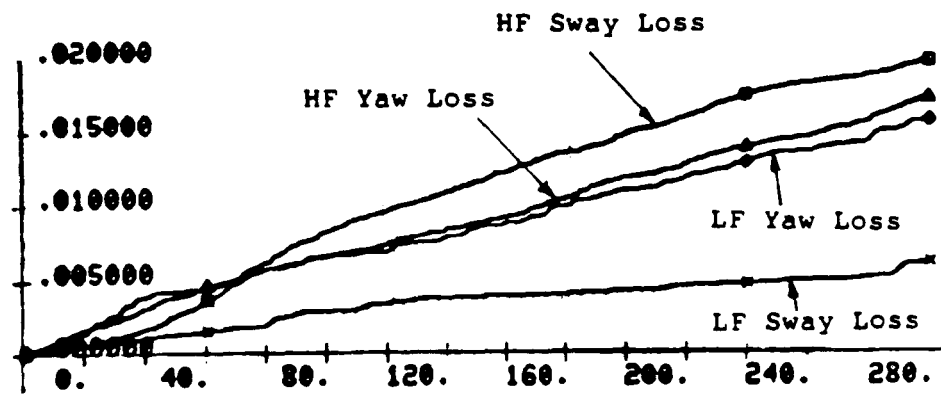


FIGURE 6-20 Sway and Yaw Loss Functions (Beau. 5, MIMO)

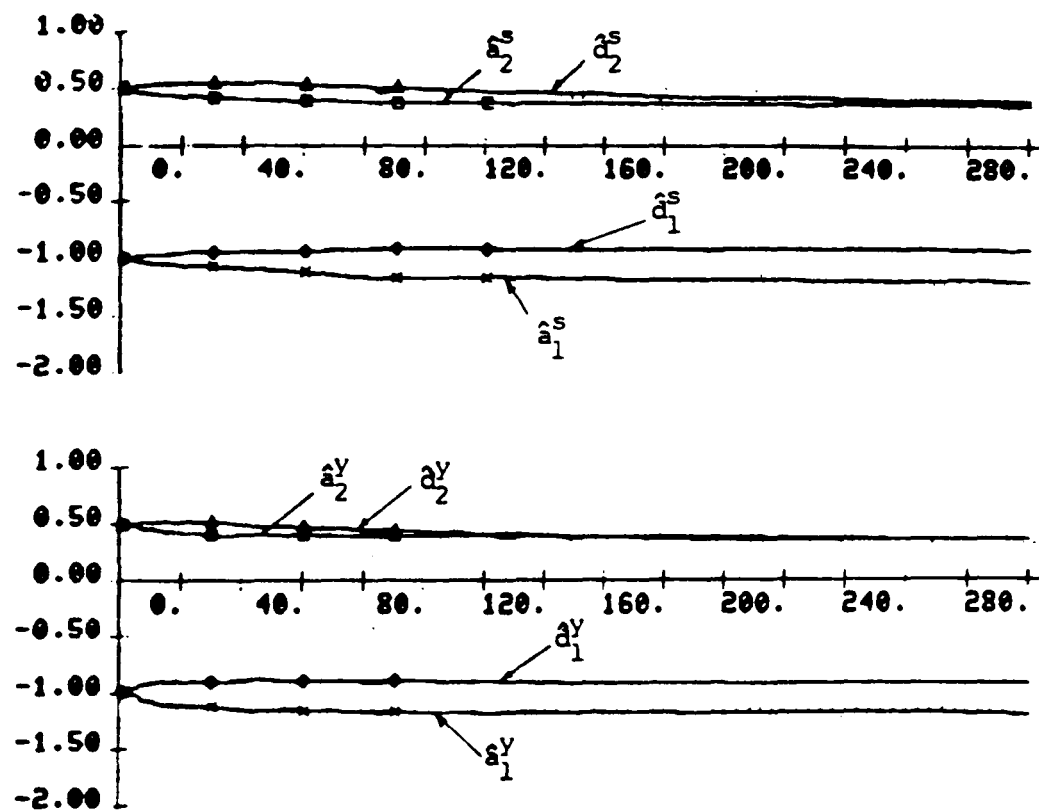


FIGURE 6-21 Sway and Yaw Estimated Parameters (Beau 5, MIMO)

cascaded with a control gain matrix K_C :

$$\underline{u}(t) = -K_C \hat{\underline{x}}_l(t/t) \quad (6.14)$$

The control gain matrix may be calculated from the steady state Riccati equation in the usual way. The closed loop control system is shown in Figure 6-22.

The optimal control weighting matrices were chosen to penalize the position error corresponding to the low frequency motions (states 2 and 4) and to give an appropriate step response. These were found as:

$$\begin{aligned} Q_C &= \text{diag}[5, 60, 5, 60, 1, 1] \\ R_C &= \text{diag}[400, 400] \end{aligned} \quad (6.15)$$

The computed optimal steady state gain matrix is:

$$K_C = \begin{bmatrix} 1.2907 & -0.0475 \\ 0.3873 & 0.0030 \\ 0.0116 & -0.8371 \\ 0.0030 & -0.3873 \\ 0.3815 & -0.0095 \\ -0.0095 & 0.6635 \end{bmatrix} \quad (6.16)$$

The saturation limits on the control signals were set at ± 0.002 per unit. These represented the actual saturation which can occur when thrusters are at full load. The

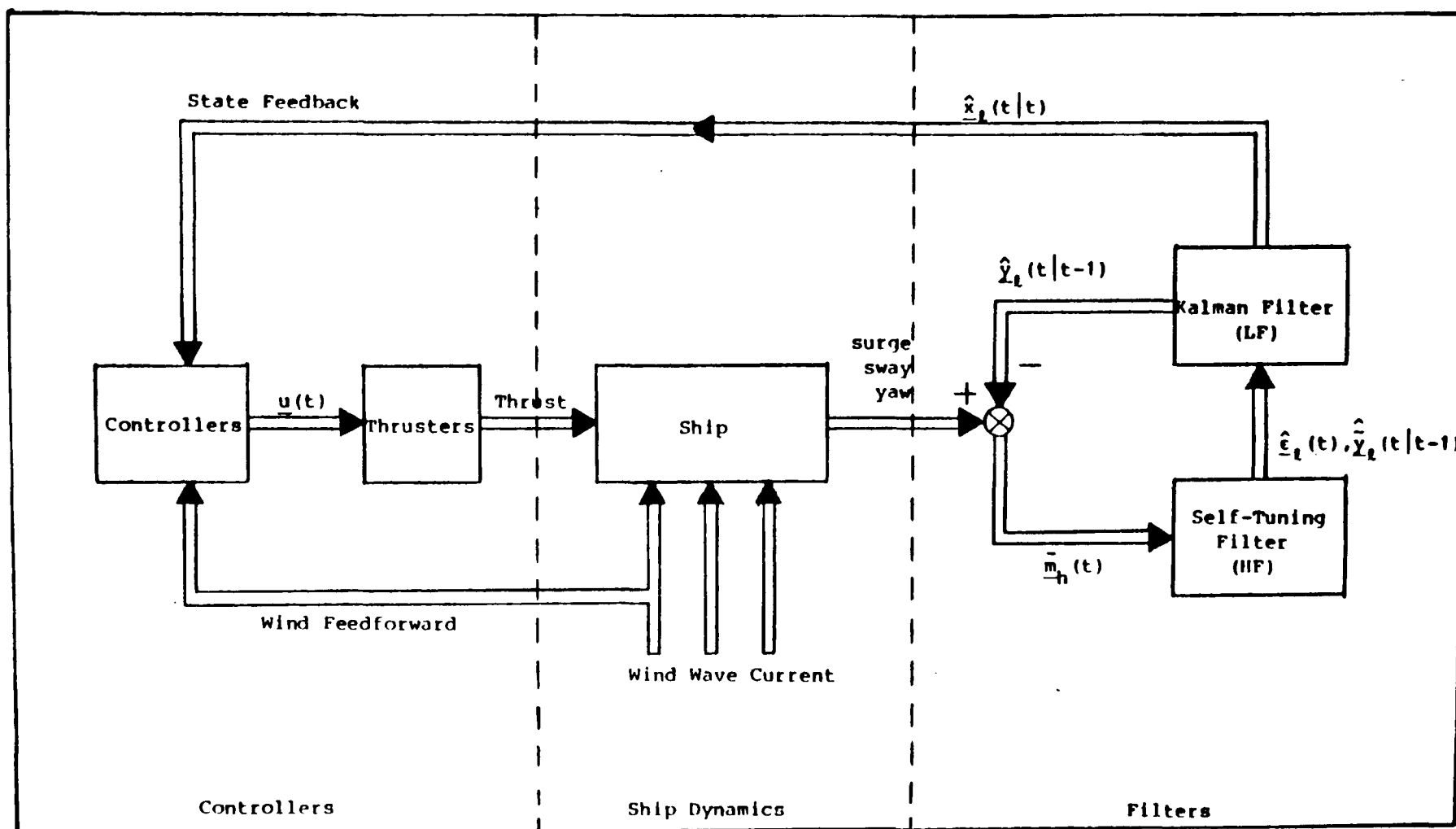


FIGURE 6-22 Kalman and Self-Tuning Filter State Estimate Feedback Control Scheme

details of the controller design is described in Chapter Four. Integral control is not included in this test, it is shown in Section 6.3.3.

Closed Loop Control

The first set of results are again for the rough sea (Beaufort No. 8) condition. To allow the parameter estimates to converge (as will be possible in practice) the step response of the system is measured over the time interval 150 to 300 seconds. A step reference of 0.06 per unit is input to the system at $t=150$ seconds. The sway and yaw responses are shown in Figures 6-23 to 6-26. The low frequency variations, due to wind and current disturbances, are much reduced under closed loop control but the high frequency motions are, as required, almost unchanged. The rise time for the step response can be reduced if larger control signal variations are allowed. These are shown in Figures 6-27 and 6-28 and it is clear the sway control enters the saturation limit for a few seconds when the step demand is entered. This is not a problem, since in practice position reference changes are not made in steps. One of the main design objectives is to reduce "thruster modulation", that is, a variation of the thrusters in sympathy with the wave motions. That this objective has been achieved is clear from the control signals shown in

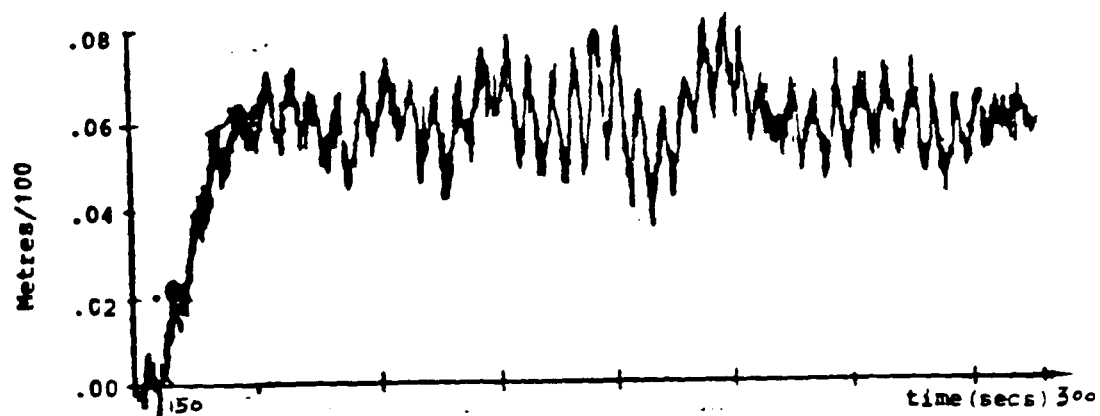


FIGURE 6-23 Controlled Total Sway Motion (Beau. 8, MIMO)

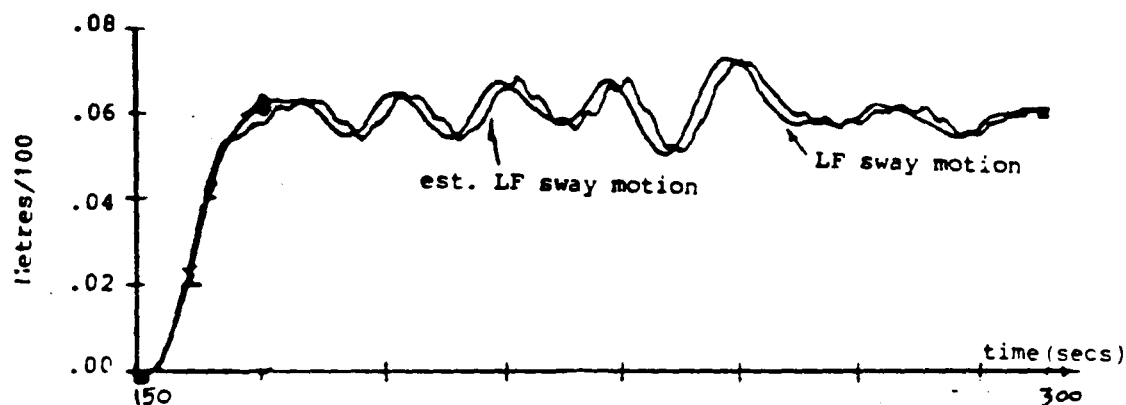


FIGURE 6-24 Controlled and Estimated LF Sway Motion (Beau. 8, MIMO)



FIGURE 6-25 Controlled Total Yaw Motion (Beau. 8, MIMO)

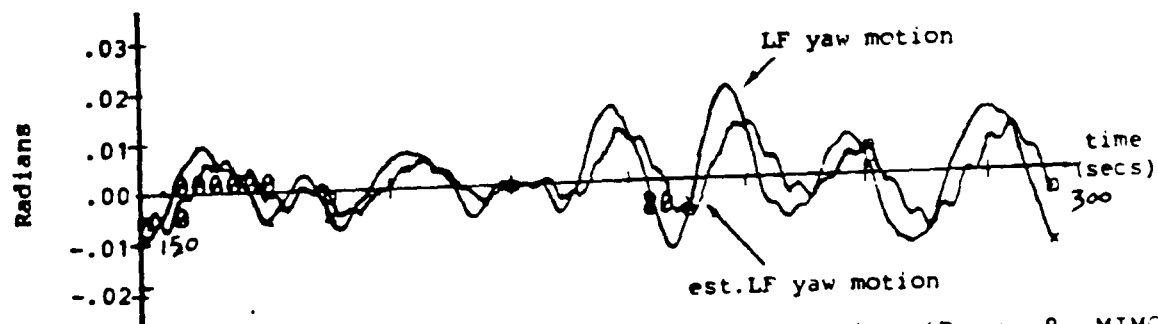


FIGURE 6-26 Controlled and Estimated LF Yaw Motion (Beau. 8, MIMO)

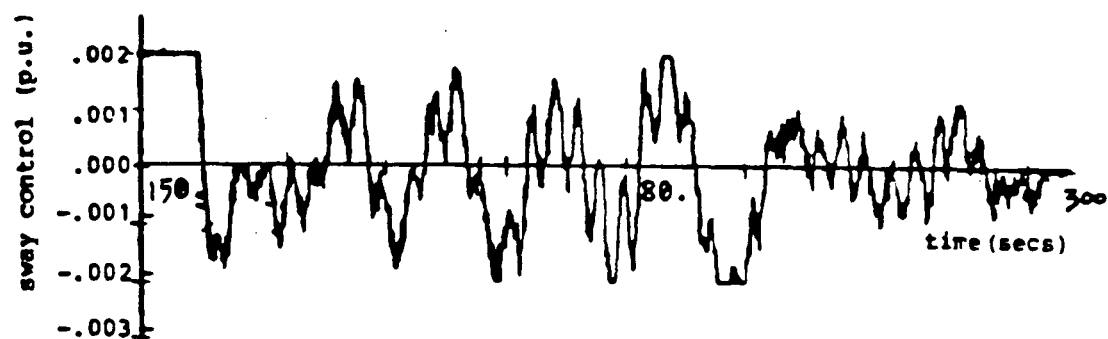


FIGURE 6-27 Sway Control Signal (Beau 8, MIMO)

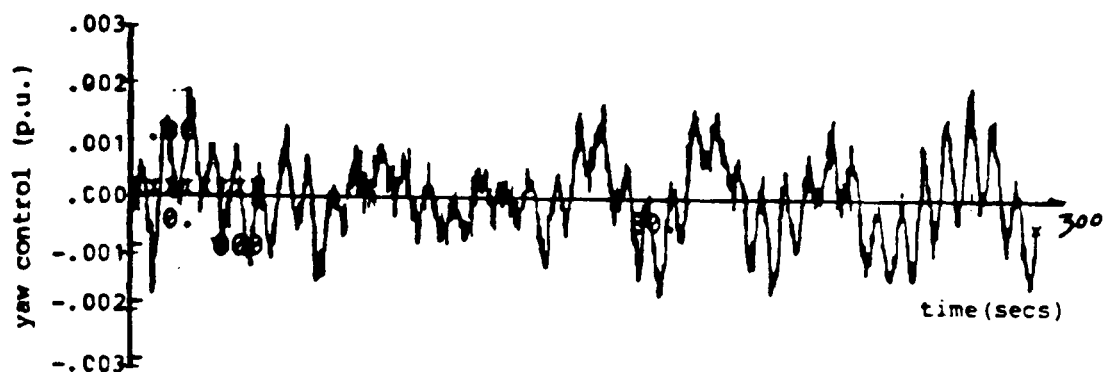


FIGURE 6-28 Yaw Control Signal (Beau. 8, MIMO)



FIGURE 6-29 Controlled Total Sway Motion (Beau. 5, MIMO)

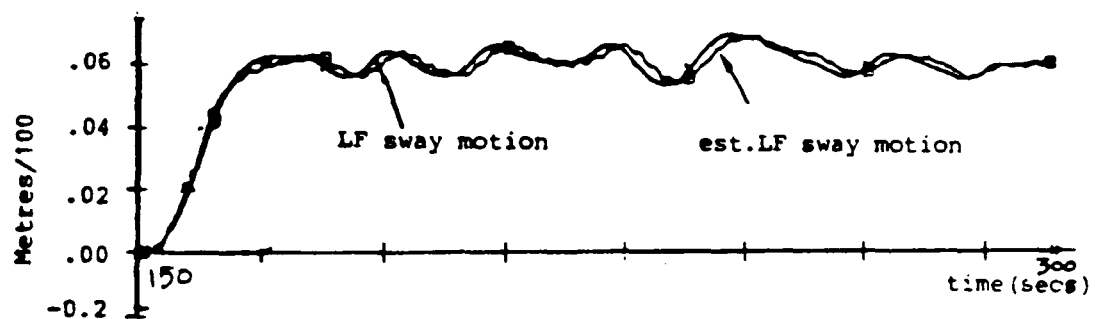


FIGURE 6-30 Controlled and Estimated LF Sway Motion (Beau. 5, MIMO)

Figures 6-27 and 6-28.

The equivalent results for the calm sea (Beaufort No. 5) condition are shown in Figures 6-29 to 6-34. The parameter estimates are improved and the control signal variations are reduced in this case, as would be expected. Note that in comparing the high frequency motions in Figures 6-23 and 6-29 the magnitude of the HF motion is reduced in the calm sea but the frequency of the wave motion is higher. The sway motion is less than the allowed limit of 3 metres for both sea states.

The estimated quantities of $\hat{y}_{si}(t)$ ($i=1,2$) shown in Chapter 5, algorithm 5.2, step 10 are illustrated in Figures 6-35 and 6-36. In Beaufort No. 5, this signal $\hat{y}_{si}(t)$ is much smoother than it is in Beaufort No. 8. These results are consistent with the theory. The argument is: $\hat{y}_{si}(t)$, a smoothed signal of \hat{y}_{i} , has been shown to be driven by the estimation error, \underline{n}_h , of the HF motion. In calm sea, the variance of the estimation error (driven noise) is small, thence, this noise is attenuated by the ship dynamics. As a result of this, $\hat{y}_{si}(t)$ is smoother in calm sea than it is in rough sea.

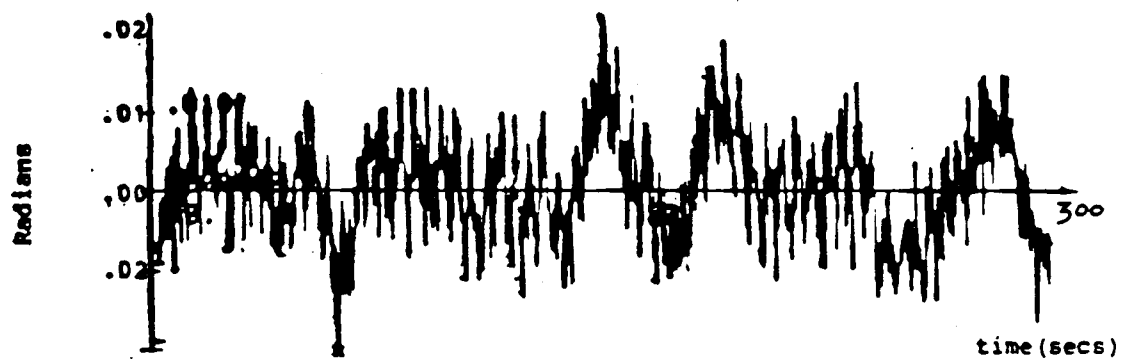


FIGURE 6-31 Controlled Total Yaw Motion (Beau. 5, MIMO)

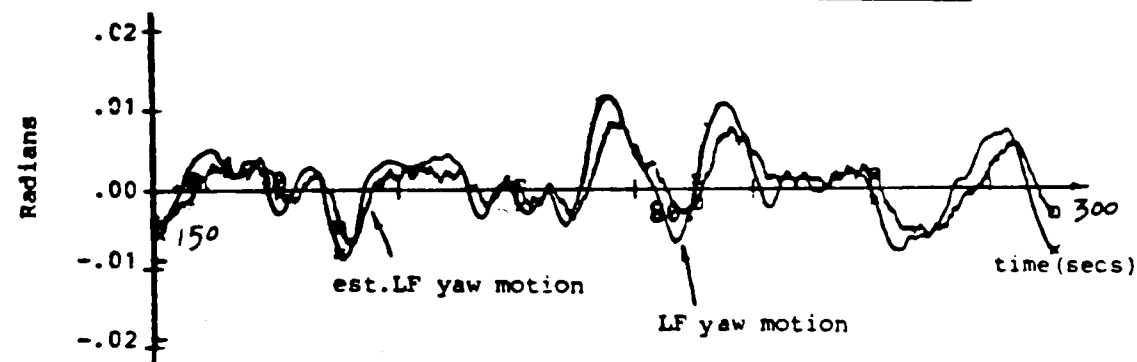


FIGURE 6-32 Controlled and Estimated LF Yaw Motion (Beau.5, MIMO)

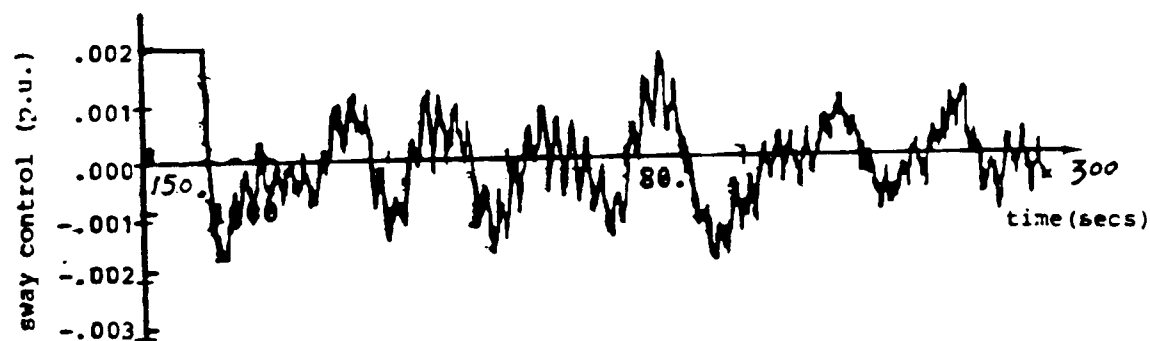


FIGURE 6-33 Sway Control Signal (Beau. 5, MIMO)

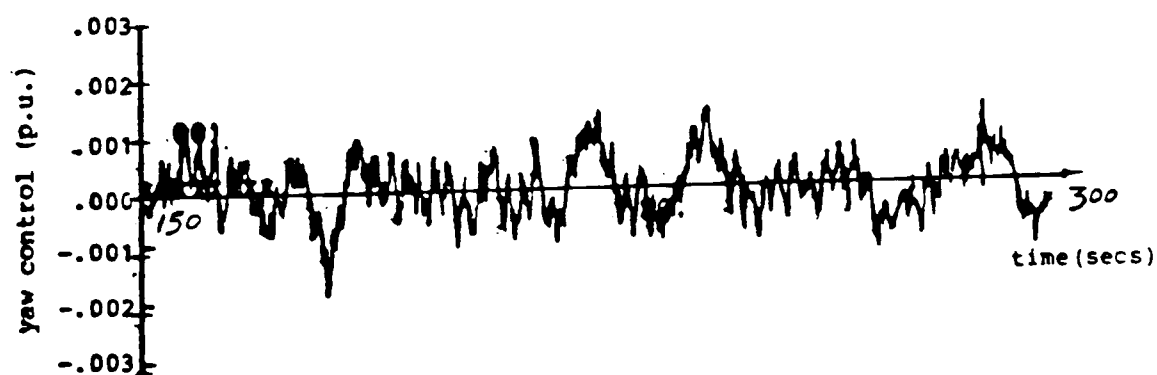


FIGURE 6-34 Yaw Control Signal (Beau. 5, MIMO)

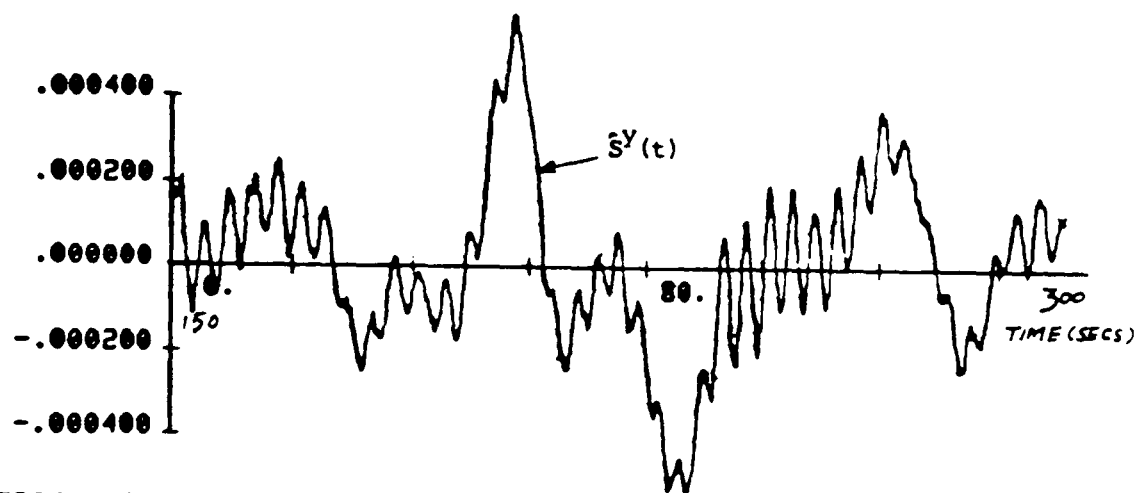
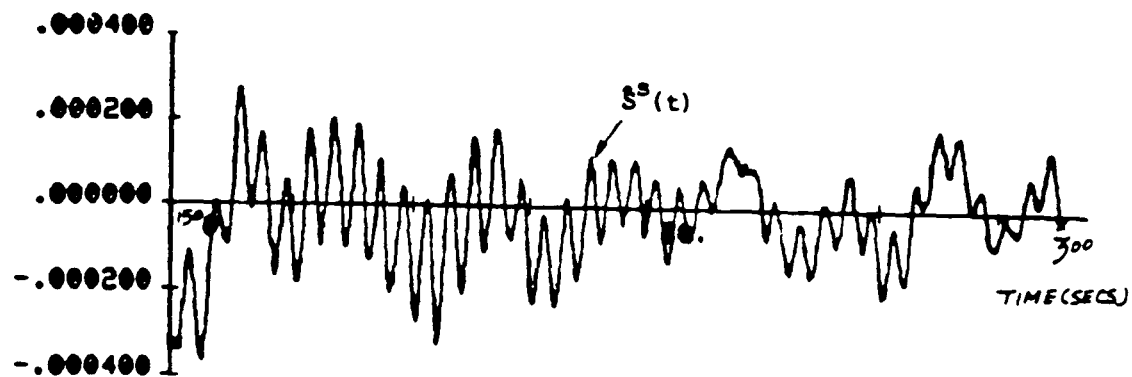


FIGURE 6-35 Estimated $s(t)$ Parameters for Sway and Yaw Motions (Beau. 8, MIMO)

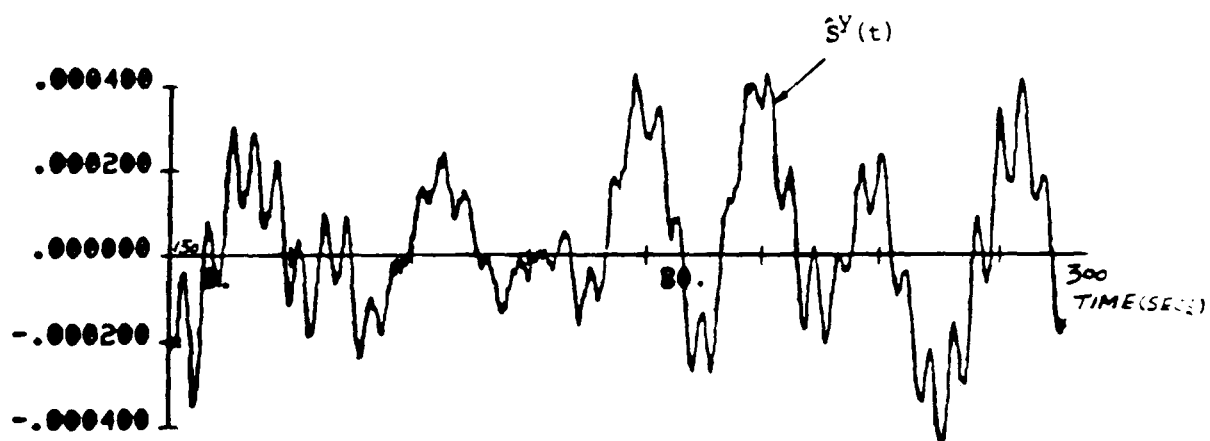
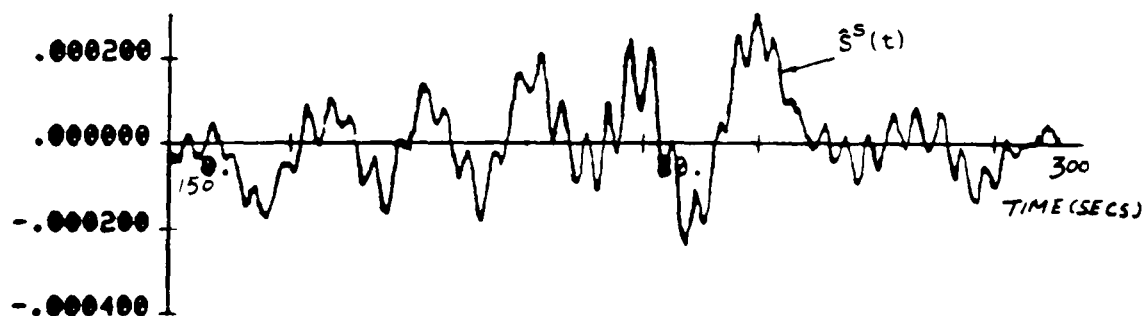


FIGURE 6-36 Estimated $s(t)$ Parameters for Sway and Yaw Motions (Beau. 5, MIMO)

6.3 NON-LINEAR SYSTEM IMPLEMENTATION

In the last section, the self-tuning Kalman filter has been applied to linear DSP systems and was found to be successful. Practically all physical systems in one way or another, are non-linear. To extend the study on the application of the self-tuning Kalman filter to DSP systems, a non-linear dynamic ship model is used to investigate the filtering and control problems. A non-linear thruster model is also included in the LF dynamics. The Kalman filter, however, is based upon the linearized version of the models. The thruster subsystem of the filter is a second order model (Section 2.6.2). The high frequency model is basically the same as in the linear case.

Low Frequency Model

The non-linear model for the thrusters is shown in Figure 2-6.

The LF equations of motion for the vessel Wimpey Sealab have been derived from tank tests and are non-linear (Section 2.7.1):

$$\begin{aligned}
\dot{x}_1 &= -2.4022 |x_1| x_1 + 0.03696 |x_3| x_3 \\
&\quad - 0.5435 |x_1| x_3 + 0.535 u_1 + 0.05435 \omega_1 \\
\dot{x}_2 &= x_1 \\
\dot{x}_3 &= 2.5245 |x_1| x_1 - 1.585 |x_3| x_3 - 1.634 u_2 \\
&\quad + 9.785 \omega_2 \\
\dot{x}_4 &= x_3
\end{aligned} \tag{6.17}$$

where x_1 =sway velocity, x_2 =sway position, x_3 =yaw velocity, x_4 =yaw angle, u_1 =thruster 1 output, u_2 =thruster 2 output, ω_1 , ω_2 =process noise. The ship simulation is based upon the above model.

The LF linear ship model B described in Section 2.7.1 was used for the Kalman filter and controller design.

$$\begin{aligned}
x_1 &= \text{sway velocity} \\
x_2 &= \text{sway position} \\
x_3 &= \text{yaw angular rate} \\
x_4 &= \text{yaw angle} \\
x_5 &= \text{thruster one state one} \\
x_6 &= \text{thruster one state two} \\
x_7 &= \text{thruster two state one} \\
x_8 &= \text{thruster two state two}
\end{aligned} \tag{6.18}$$

High Frequency Model

The simulation of high frequency motions and the self-tuning filters are identical to the linear system case described in Section 6.2.2.

Filtering and Control Problems and Results

The system matrices for the Kalman filter are identical to the linear system except that the thrusters are represented by second order models. The process noise covariance matrix Q_f (LF only) for the calculation of the Kalman gain is given in equation (2.18). The first and second diagonal elements of the modelled measurement noise covariance matrix, are increased by a factor of 4 and a factor of 10 respectively, which gives [c.f. equation (2.19)]

$$R_f^* = [4 \times 10^{-5}, 1.22 \times 10^{-4}] \quad (6.19)$$

The adjustment will allow the Kalman filter to accommodate the errors due to the estimation of the HF motions which though not computed directly, do affect the Kalman filter as additional measurement noise.

The computed Kalman gain matrix is:

$$K_F^* = \begin{bmatrix} 0.1427 & 0.003191 \\ 0.5341 & 0.008514 \\ 0.01829 & 0.2453 \\ 0.02129 & 0.7003 \\ 0 & 0 \\ 0 & 0 \\ 0 & 0 \end{bmatrix} \quad (6.20)$$

The optimal controller design criterion is similar to the linear system case (Section 6.2.2) but the state vector in the non-linear system has two additional thruster states. This requires the weighting matrices to be redefined. They are:

$$Q_C = \text{diag} [3 \ 500 \ 3 \ 500 \ 0 \ 10 \ 0 \ 10] \quad (6.21)$$

$$R_C = \text{diag} [500 \ 200] \quad (6.22)$$

By solving the Riccati equation, the steady state solution of the optimal feedback gain matrix was found to be:

$$K_C^T = \begin{bmatrix} 3.048 & -0.1742 \\ 1.0 & 0.002396 \\ 0.01137 & -3.049 \\ 0.001463 & -1.581 \\ 0.6652 & -0.01277 \\ 1.892 & -0.05395 \\ -0.005076 & 1.315 \\ -0.0164 & 4.322 \end{bmatrix} \quad (6.23)$$

The optimal control signal, based on the separation theorem, becomes:

$$u^*(t) = -K_c \hat{\underline{x}}_l(t/t) \quad (6.24)$$

where $\hat{\underline{x}}_l(t/t)$ is the estimated state vector of the LF motions. The stochastic control scheme is illustrated in Figure 6-37.

Simulation Results

The performance of the optimal state estimation scheme is illustrated in the first set of results (Beaufort No. 8) shown in Figure 6-38 to 6-41. The system has a step reference input of 0.03 per unit to the sway subsystem at $t=50$ seconds. (N.B. real time = 3.104 x simulated time). The results demonstrate that the system remains stable even in the non-linear case. The estimates of the LF motions (Figures 6-39 and 6-41) are needed for control purposes and are good even in this non-linear situation. The parameter estimates of the HF subsystem (Figure 6-42) converge rapidly. The initial parameter estimates for the matrices A_h and D_h are similar to the linear situation described in Section 6.2. The accumulative loss functions for the LF estimator (Figure 6-43) increase steadily after the parameters have settled down. The estimated thrusts, shown in Figure 6-44 and 6-45, are as expected varying more than

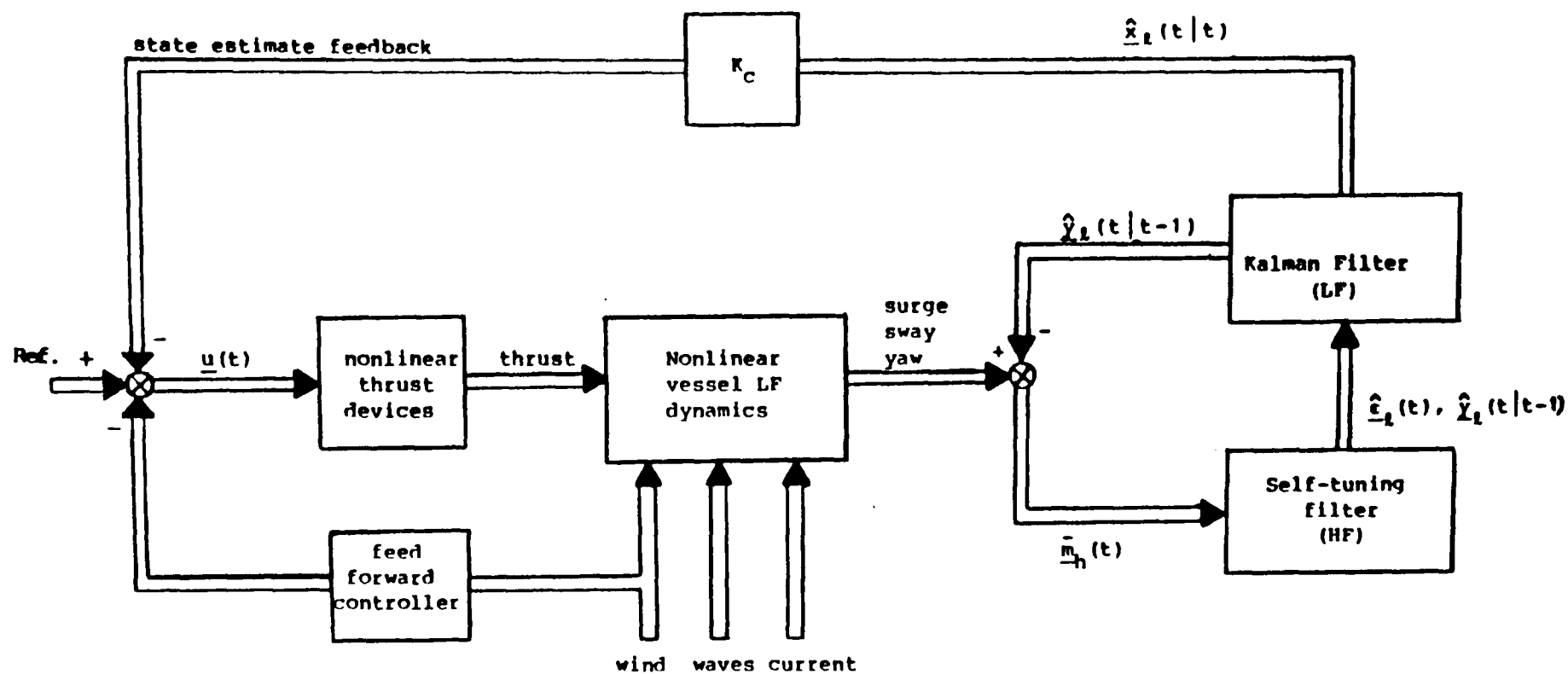


FIGURE 6-37

Kalman and Self-Tuning Filter State Feedback Control Scheme for Non-Linear System.

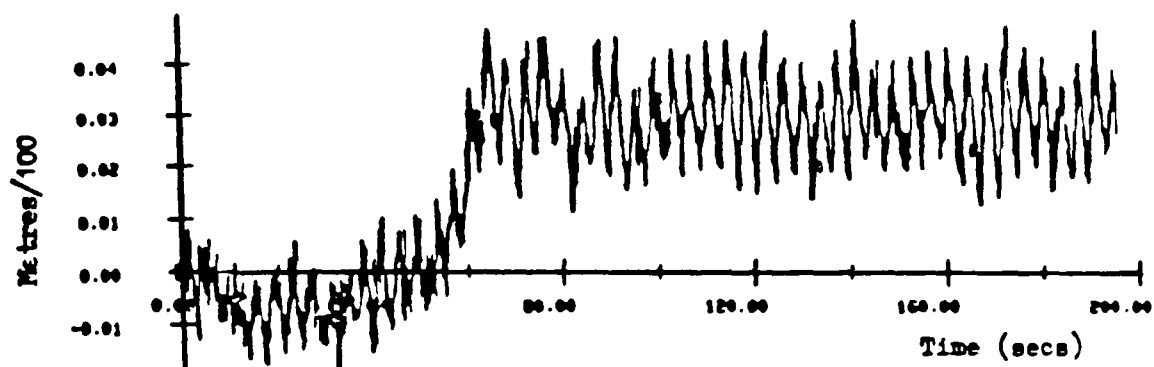


FIGURE 6-38 Total Observed Sway Motion (Beau. 8, NL, MIMO)

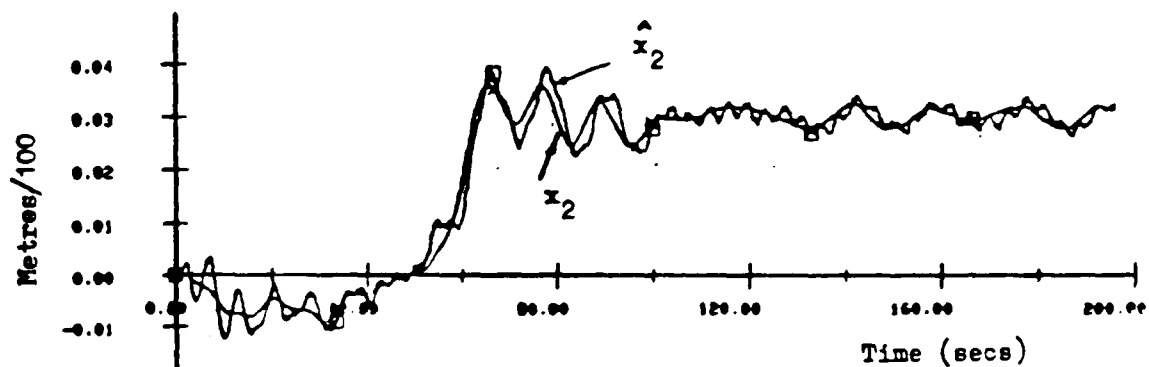


FIGURE 6-39 Modelled and Estimated LF Sway Motion (Beau.8, NL, MIMO)



FIGURE 6-40 Total Observed Yaw Motion (Beau. 8, NL, MIMO)

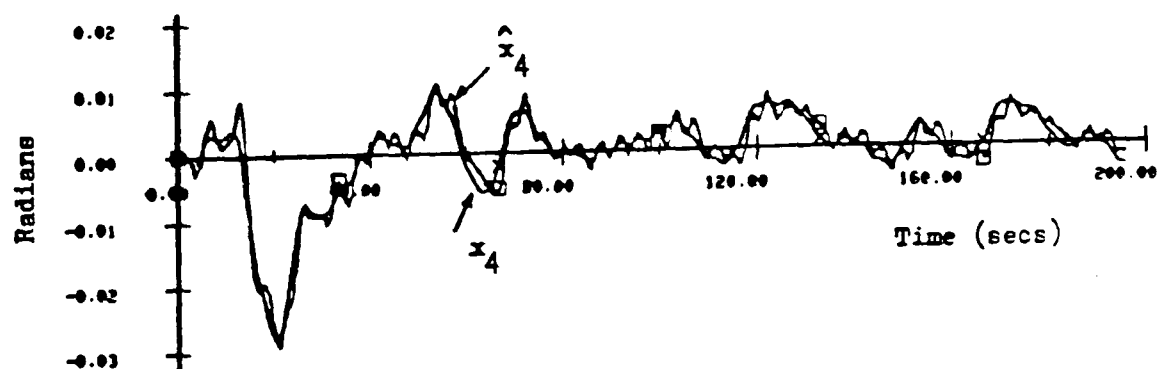


FIGURE 6-41 Modelled and Estimated LF Yaw Motion (Beau. 8, NL, MIMO)

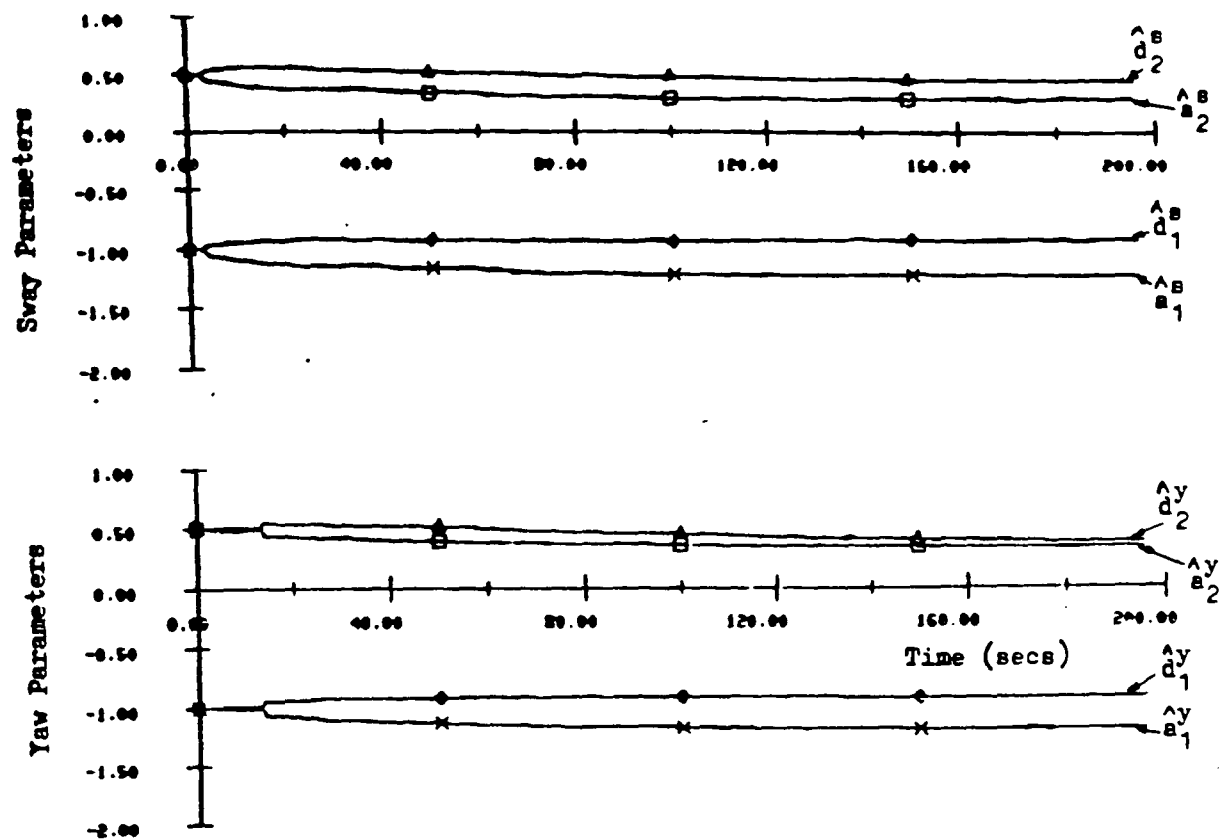


FIGURE 6-42 Sway and Yaw Self-Tuning Filter Parameters
(Beau. 8, NL, MIMO)

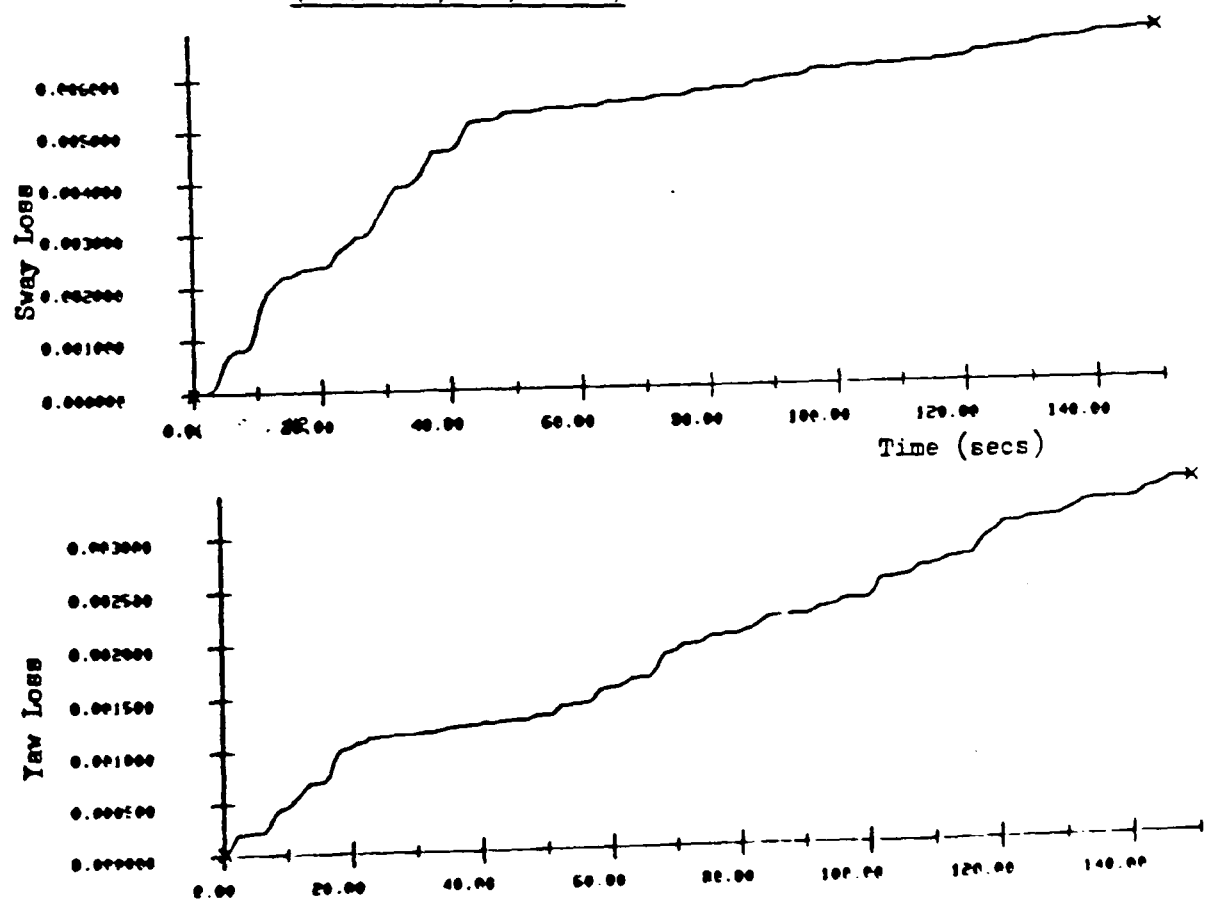


FIGURE 6-43 Accumulation Losses (Beau. 8, NL, MIMO)

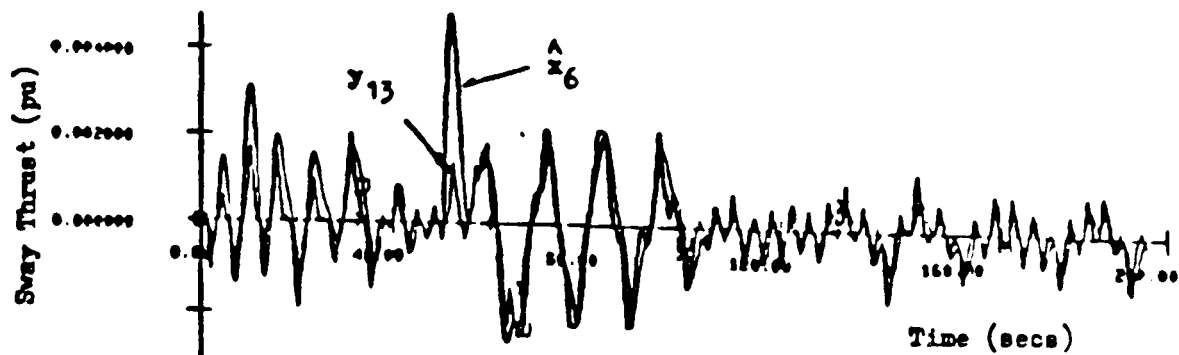


FIGURE 6-44 Estimated (\hat{x}_6) and Modelled (y_{13}) Sway Thrust (Beau. 8, NL, MIMO)

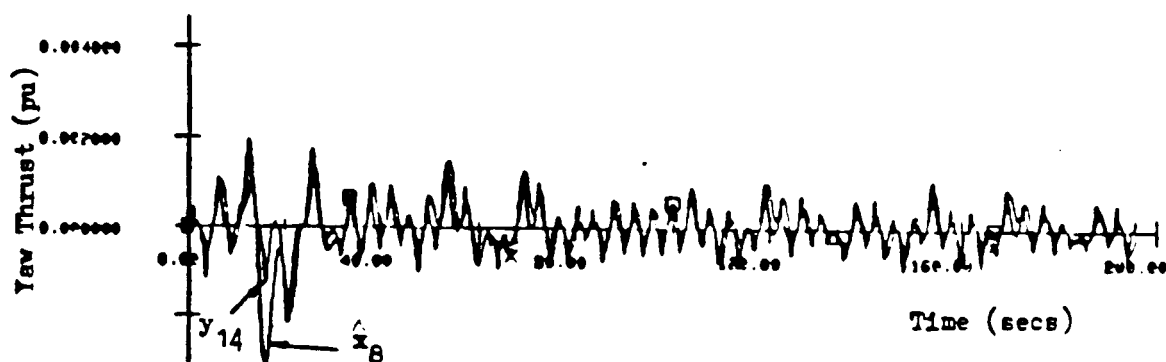


FIGURE 6-45 Estimated (\hat{x}_8) and Modelled (y_{14}) Yaw Thrust (Beau. 8, NL, MIMO)

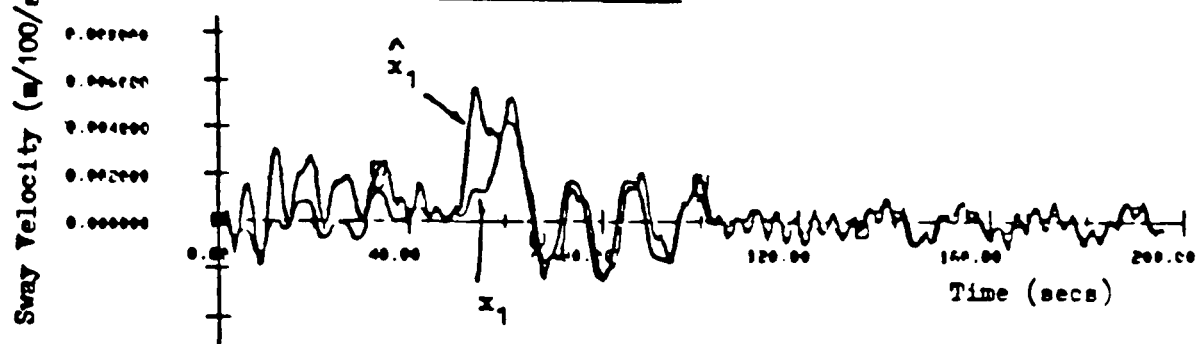


FIGURE 6-46 Sway Velocity and Estimate (Beau. 8, NL, MIMO)

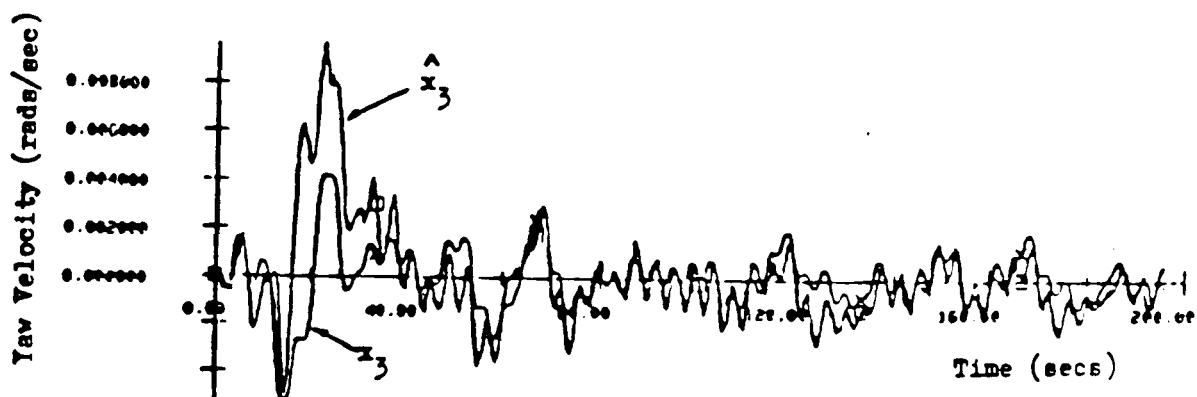


FIGURE 6-47 Yaw Velocity and Estimate (Beau. 8, NL, MIMO)

the thrusts generated from the modelled non-linear thrusters. This also applies to the estimated and modelled velocities shown in Figures 6-46 and 6-47. The estimates of the self-tuning parameter $\underline{s}(t)$ for sway and yaw (Figure 6-48 and 6-49) show higher frequency variations than are obtained with linear ship models (recall that $\underline{s}(t)$ is related to the error term $\tilde{\underline{y}}_f(t)$). Note that the amplitudes of these signals are very small. Also note that at $t=50$ seconds, $\underline{s}(t)$ for sway has a significant over shoot. This over shoot indicates that $\underline{s}(t)$ can detect the modelling errors when a step input is applied to the non-linear system while a linear filter is being used. The response shown in Figure 6-39 indicates that, when a step input is applied, the linear estimator reacts faster than the non-linear system response, and so gives a significant estimation error. When this error is detected in $\underline{s}(t)$, the estimation is upgraded to follow the actual system output.

The second set of results for Beaufort No. 5 is shown in Figure 6-50 to Figure 6-59. As expected, better results are obtained. The $\underline{s}(t)$ signals (Figures 6-58 and 6-59) are less oscillatory and the amplitudes are lower in Beaufort No. 5 than in Beaufort No. 8. This is consistent with the theory that $\underline{s}(t)$ is caused by the HF estimation error.

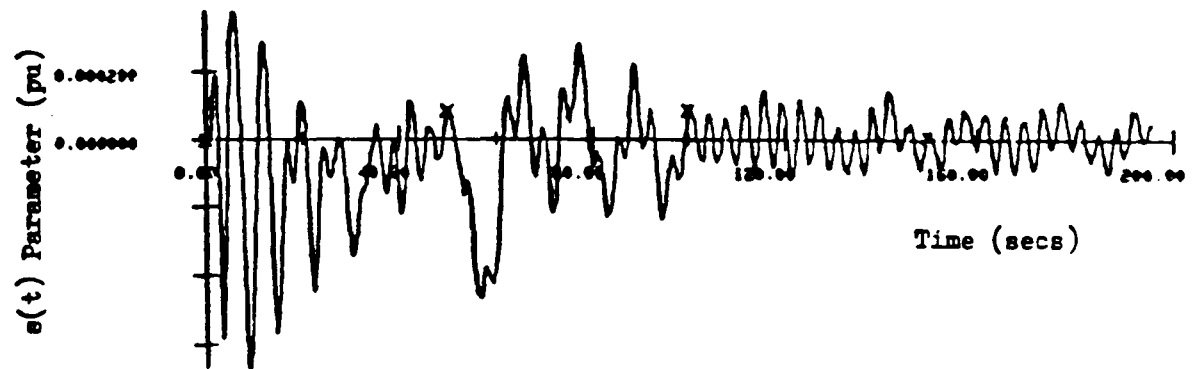


FIGURE 6-48 Estimated $s(t)$ Parameter for Sway (Beau. 8, NL, MIMO)

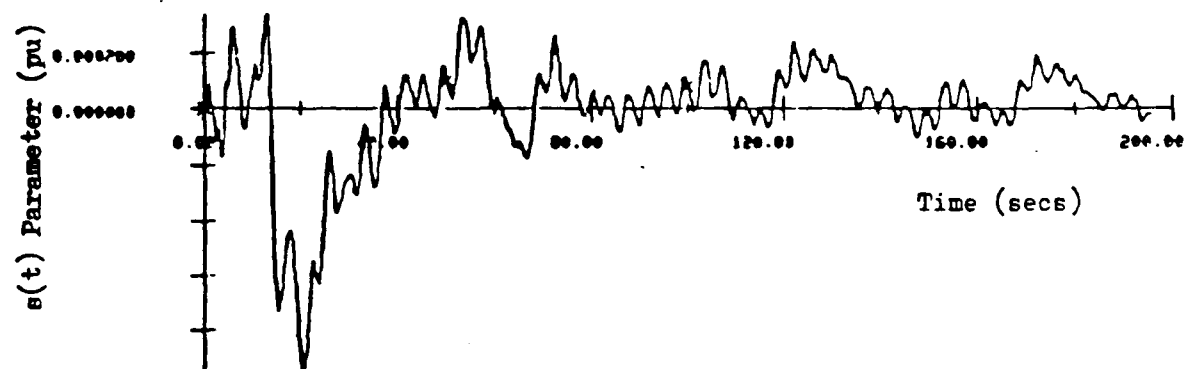


FIGURE 6-49 Estimated $s(t)$ Parameter for Yaw (Beau. 8, NL, MIMO)

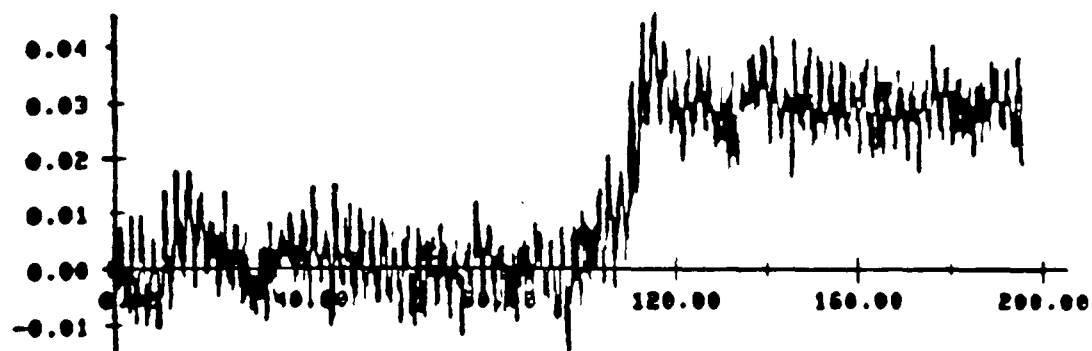


FIGURE 6-50 Total Observed Sway Motion (Beau. 5, NL, MIMO)

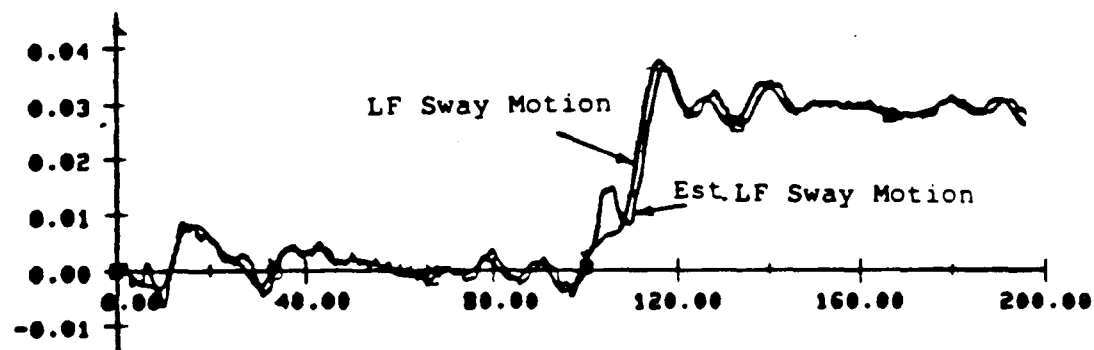


FIGURE 6-51 Modelled and Estimated LF Sway Motion (Beau. 5, NL, MIMO)

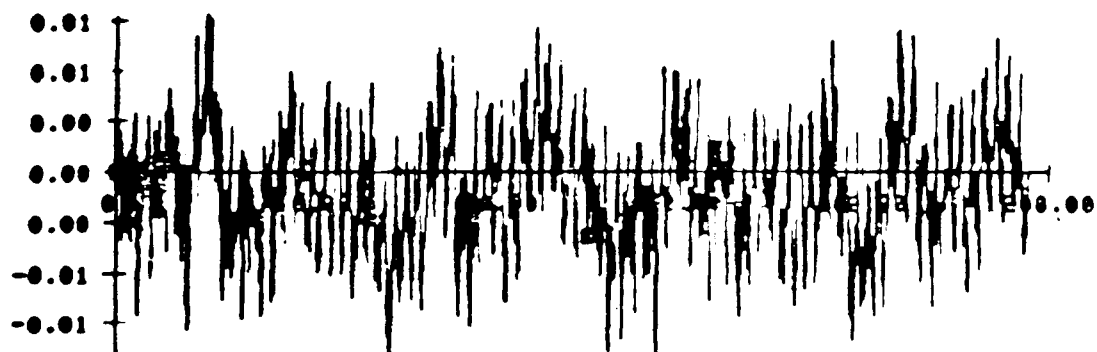


FIGURE 6-52 Total Observed Yaw Motion (Beau. 5, NL, MIMO)

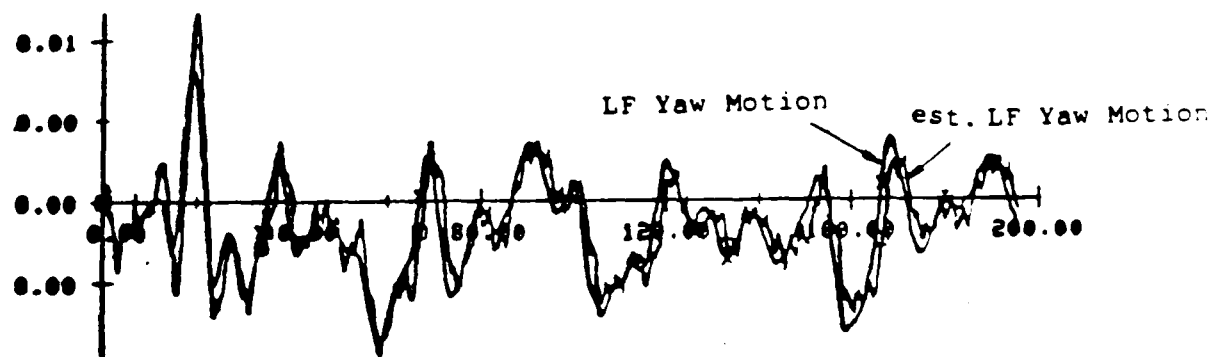


FIGURE 6-53 Modelled and Estimated LF Yaw Motion (Beau. 5, NL, MIMO)

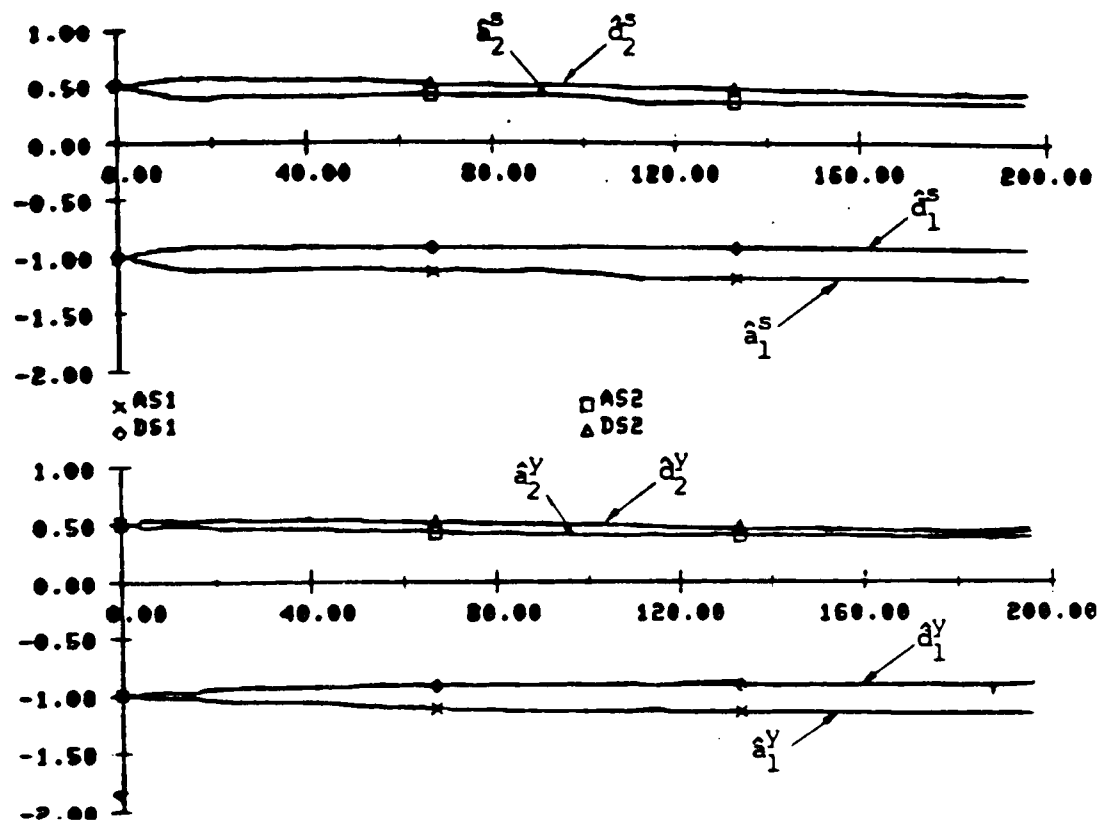


FIGURE 6-54 Sway and Yaw Self-Tuning Filter Parameters (Beau. 5, NL, MIMO)

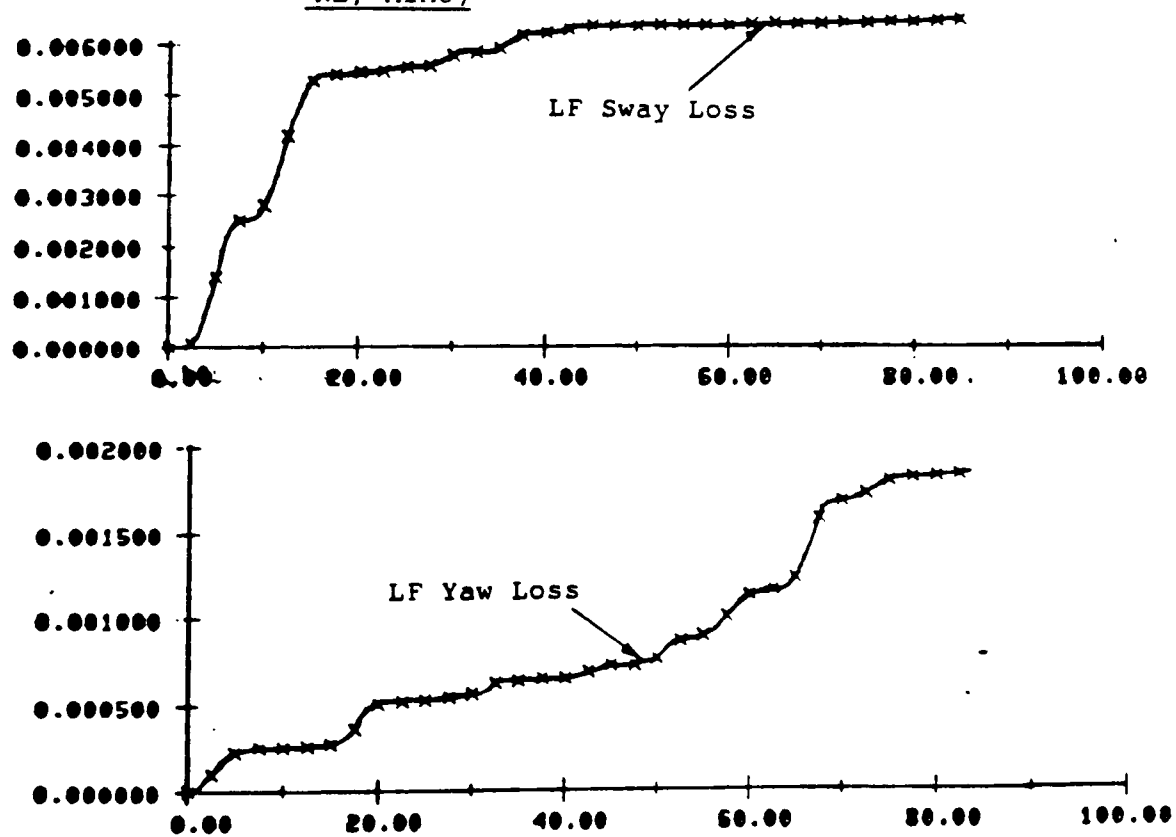


FIGURE 6-55 Accumulating Loss Functions (Beau. 5, NL, MIMO)

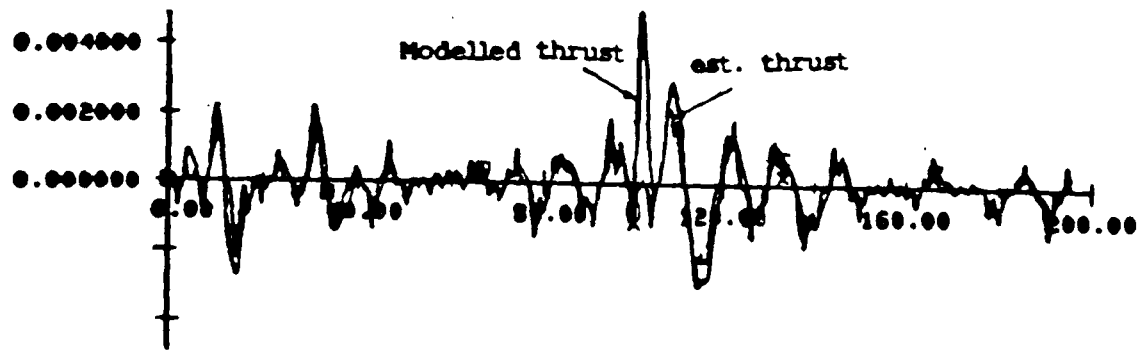


FIGURE 6-56 Estimated and Modelled Sway Thrust (Beau.5, NL, MIMO)

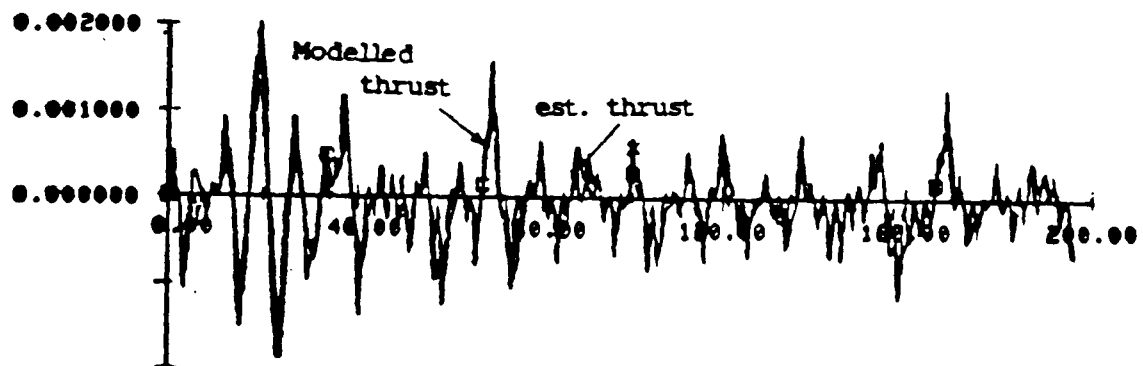


FIGURE 6-57 Estimated and Modelled Yaw Thrust (Beau. 5, NL, MIMO)

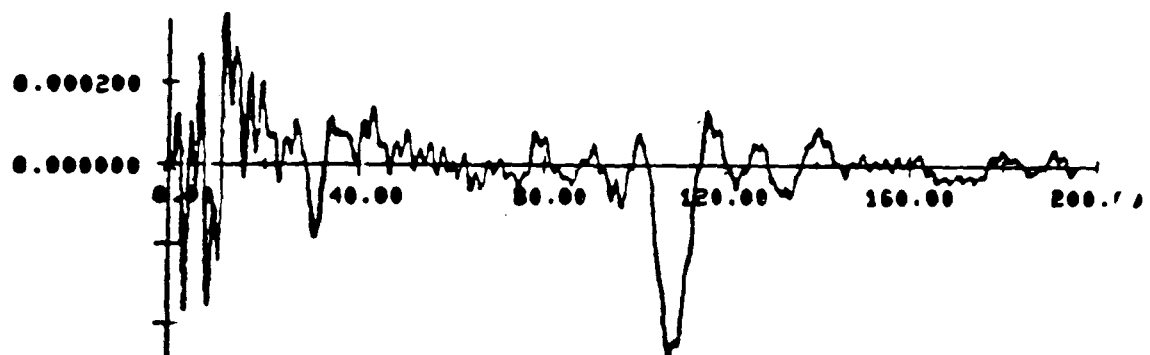


FIGURE 6-58 Estimated $s(t)$ Parameter for Sway (Beau. 5, NL, MIMO)



FIGURE 6-59 Estimated $s(t)$ Parameter for Yaw (Beau.5, NL, MIMO)

6.4 SELF-TUNING KALMAN FILTER WITH INTEGRAL CONTROL

The ship positioning system with integral action has been discussed extensively in Chapter 4. A simplified scheme was proposed for practical application purposes in Section 4.4.2 design 1. The simulation results show that the overall control system is stable and well damped (Figure 4-8). The plant output states have zero steady state error, but the drawback is that there are constant errors $\underline{e}^C(t)$ in the position estimation. In this section it will be shown that these constant errors due to constant disturbances, can be estimated, and therefore, the output state estimation will have no constant errors.

In Section 4.4.2, it has been shown that the constant estimation error is $\underline{e}^C(t) = \underline{y}_l^C(t) - \hat{\underline{y}}_l^C(t)$. Since $\underline{e}^C(t)$ appears in the usual Kalman filter estimation (because the constant disturbances are not modelled), these quantities will be included in the variable $\underline{m}_h(t)$ defined in equation (5.5.10). Thus, $\underline{m}_h(t)$ can be redefined as:

$$\underline{\bar{m}}_h(t) \triangleq \underline{z}(t) - \hat{\underline{y}}_l(t/t-1) - \underline{e}^C(t) \quad (6.25)$$

where $\underline{z}(t)$ is the measured output and $\hat{\underline{y}}_l(t/t-1)$ is the predicted output generated from the Kalman filter at time $t-1$. Assuming $\underline{e}^C(t)$ can be estimated, the total output

estimated positions using equation (5.41) can easily be shown to be:

$$\hat{\underline{y}}_l(t/t) = \hat{\underline{y}}_l(t/t) - \{ \tilde{\underline{y}}_l(t/t-1) - \underline{e}^c(t) \} \quad (6.26)$$

It is clear in equation (6.26) that compensation signals $\tilde{\underline{y}}_l(t/t-1)$ and $\underline{e}^c(t)$ need not be separated. Thence, these two quantities can be combined into one parameter. From equation (6.26) and equation (5.46), the equation for parameter estimation can be rewritten as:

$$\begin{aligned} A_h(z^{-1})\bar{\underline{m}}_h(t) &= D_h(z^{-1})\underline{x}(t) \\ &\quad - A_h(z^{-1})\{ \tilde{\underline{y}}_l(t/t-1) - \underline{e}^c(t) \} \end{aligned} \quad (6.27)$$

To estimate the sum of $\tilde{\underline{y}}_l(t/t-1)$ and $\underline{e}^c(t)$, the only change in algorithm 5.2 is to redefine the variable $s(t)$ as:

$$s(t) = A_h(z^{-1})\{ \tilde{\underline{y}}_l(t/t-1) - \underline{e}^c(t) \} \quad (6.28)$$

This is the theoretical analysis of estimating the error term $\underline{e}^c(t)$. In practice, the algorithm 5.2 does not require to be changed at all. In general, the variable $s(t)$ can represent any slowly varying and/or constant errors as well as errors due to linearization of non-linearity. The algorithm will automatically feed the estimate of $\underline{s}(t)$ through a filter $A_h^{-1}(z^{-1})$ to yield a signal for correcting the position output estimate.

Simulation Results

The simulation of the non-linear low frequency motions and high frequency motions are identical to those described in Section 6.3. Due to the introduction of integral states, the system matrices for the linear Kalman filter and for the calculation of the optimal feedback gain matrix are defined as follows:

$$\dot{\underline{\bar{x}}}_l(t) = \begin{bmatrix} A_l & 0 \\ A_I & 0 \end{bmatrix} \underline{\bar{x}}_l(t) + \begin{bmatrix} B_l \\ 0 \end{bmatrix} u(t) \quad (6.29)$$

where matrices A_l , B_l and D_l are defined in equation (6.27). The matrix E_l (steady state wind disturbance) is defined in equation (2.13).

$$A_I = \begin{bmatrix} 0 & 1 & 0 & 0 & 0 & 0 & 0 & 0 \\ 0 & 0 & 0 & 1 & 0 & 0 & 0 & 0 \end{bmatrix}$$

$$\underline{\bar{x}}_l(t) = \begin{bmatrix} x_1 \\ x_2 \\ x_3 \\ x_4 \\ x_5 \\ x_6 \\ x_7 \\ x_8 \\ x_9 \\ x_{10} \end{bmatrix} \begin{array}{l} \text{sway velocity} \\ \text{sway position} \\ \text{yaw angular velocity} \\ \text{yaw angle} \\ \text{thrust velocity of thruster 1} \\ \text{thrust of thruster 1} \\ \text{thrust velocity of thruster 2} \\ \text{thrust of thruster 2} \\ \text{integral state for sway motion} \\ \text{integral state for yaw motion} \end{array} \quad (6.30)$$

$$\underline{z}(t) = \begin{bmatrix} z_1 \\ z_2 \end{bmatrix} \begin{array}{l} \text{observed sway position} \\ \text{observed yaw angle} \end{array} \quad (6.31)$$

The state weighting matrix Q_C and control weighting matrix R_C are the same as those defined in equation (6.21) and (6.22) except for an extra A_I . The weighting factors corresponding to the integral term are:

$$Q_I = \begin{bmatrix} 0.5 & 0.25 \\ 0.25 & 0.5 \end{bmatrix} \quad (6.32)$$

When the steady state Kalman gain matrix was computed, the measurement noise covariances of sway and yaw motions were inflated by twice and three times respectively.

The performance of the entire stochastic control system is shown in Figures 6-60 to 6-63. The system has a constant current disturbance input of 0.002 per unit to the sway subsystem at $t=50$ seconds. The disturbance is much larger than would occur in practice since it would involve the thrusters acting continuously at full load to counteract the effect. However, the results demonstrate that the system remains stable even in this extreme situation. The steady state error can be reduced to zero by the use of integral action. The estimate of the LF motions which are needed for control purposes are good even in this non-linear situation.

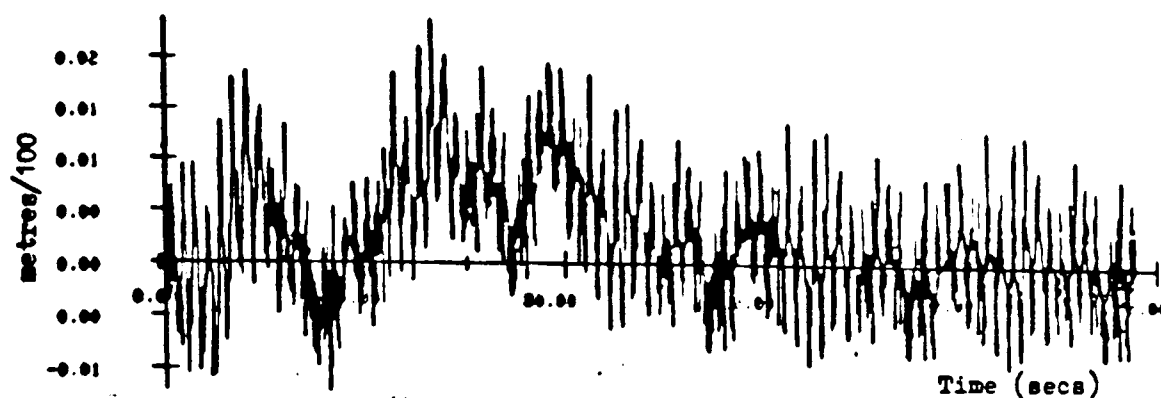


FIGURE 6-60 Total Observed Sway Motion with Integral Control (Beau. 5, NL, MIMO)

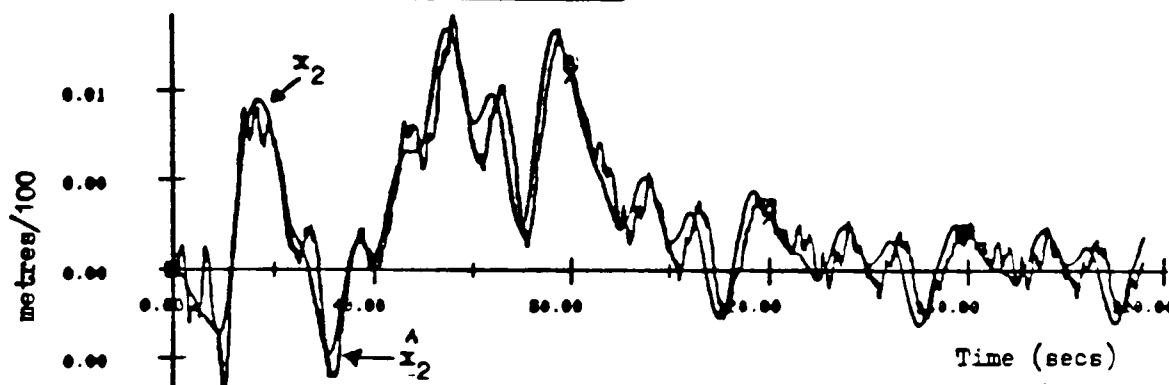


FIGURE 6-61 Modelled and Estimated LF Sway Motion with Integral Control (Beau. 5, NL, MIMO)



FIGURE 6-62 Total Observed Yaw Motion with Integral Control (Beau. 5, NL, MIMO)

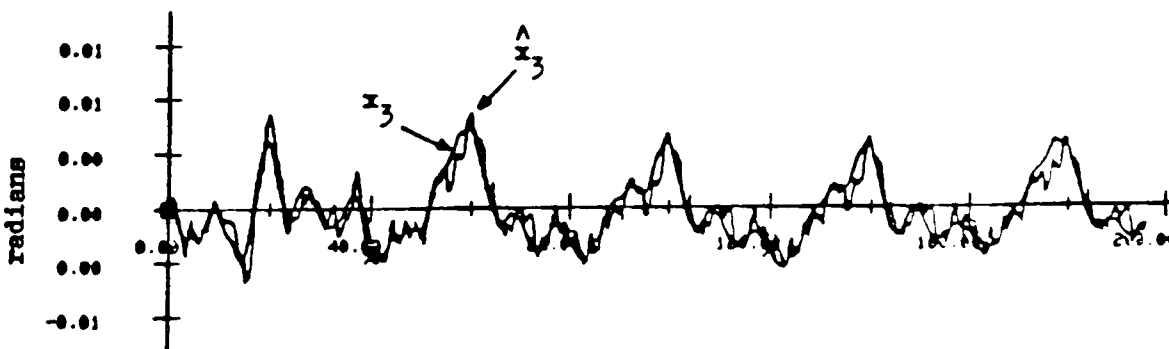


FIGURE 6-63 Modelled and Estimated LF Yaw Motion with Integral Control (Beau. 5, NL, MIMO)

6.5 SUMMARY OF RESULTS

The self-tuning Kalman filter has been shown to be successfully applicable in DSP systems in both calm and rough sea conditions. The filter and control scheme worked very well in single-input single-output, linear multi-variable and non-linear multi-variable cases. It was also shown that the self-tuning filter could estimate the errors due to linearization of non-linearities and the constant error due to constant disturbances, in the position output estimation.

CHAPTER SEVEN

THE ADAPTIVE TRACKING OF SLOWLY VARYING PROCESSES WITH COLOURED NOISE DISTURBANCES

7.1 INTRODUCTION

In many industrial processes and communication systems the low frequency signals of interest are corrupted by high frequency disturbances. The conventional technique to remove these disturbances is to use low pass filters. It is well known that the filtered output will contain a significant phase lag especially when the filter has been designed to produce very smooth estimates. If the signal model and the noise covariances of a process are known, an extended Kalman filter can be used to adapt to the varying coloured noise disturbances. However, if the model of the plant and disturbances are unknown, it is very difficult to use this approach. In this chapter, an adaptive estimation technique is developed to deal with slowly varying processes where the process model is unknown. The adaptive estimator is divided into two parts, namely a primary estimator and a vernier estimator. The primary estimator is a low pass filter or its equivalent. The vernier estimator is self-tuning and is adaptive to varying disturbances. The terms

primary and vernier were borrowed from the space shuttle orbital control system where primary jets are used to control large errors and vernier jets to correct small errors.

The adaptive estimator can be used to track constant, ramp, step and sine wave signals. It is well known that the motion of a ship at sea consists of low and high frequency motion components. The low frequency motion is due to wind, current, second order wave and propulsion forces. The high frequency motion is caused by the first order wave forces. The adaptive tracker can be employed to estimate the low frequency motions, and simulation results for this are presented.

The theory of the adaptive tracking problem was originally inspired by the self-tuning Kalman filter theory developed in Chapter Five.

7.2 SYSTEM DESCRIPTION

The canonical structure of the single-input/single-output system to be considered is shown in Figure 7-1.

The slowly varying process is modelled by:

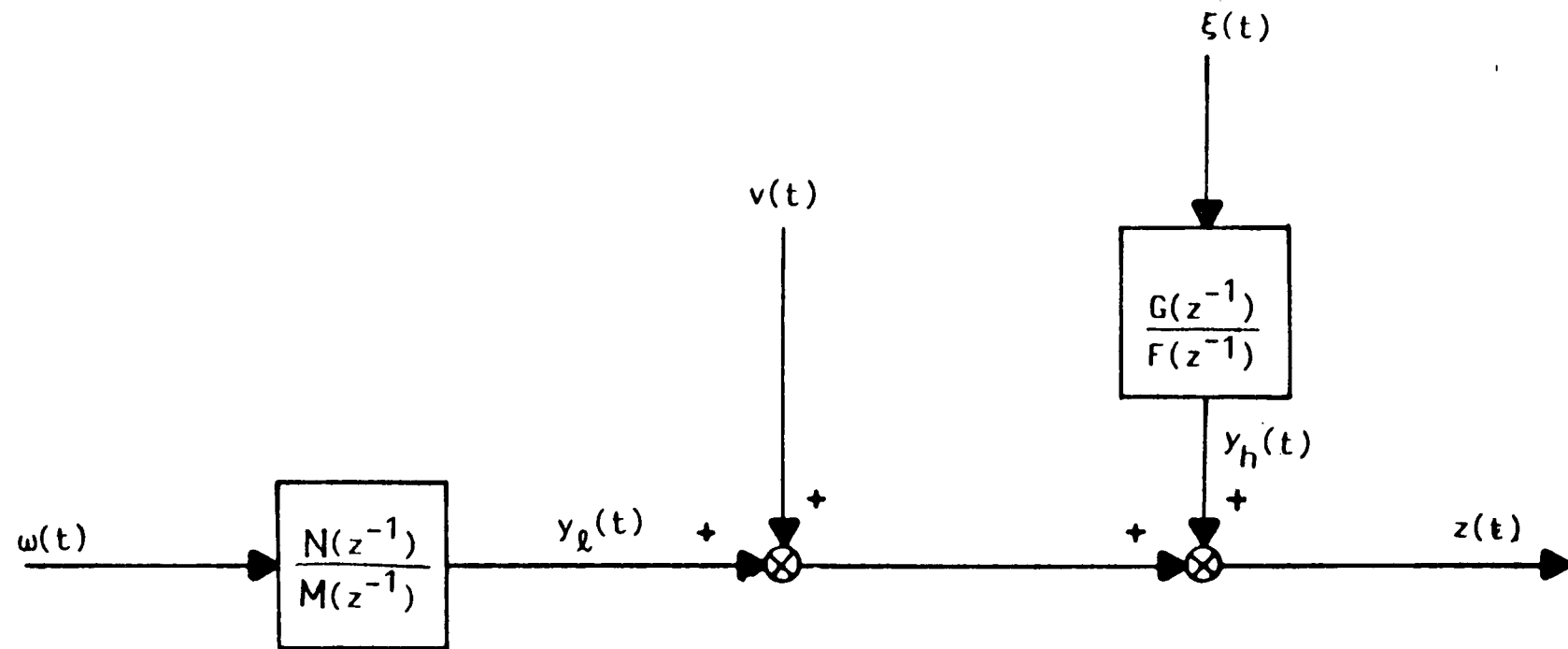


FIGURE 7-1 A Single Input - Single Output Stochastic System

$$S_l: y_l(t) = \frac{N(z^{-1})}{M(z^{-1})} \omega(t) \quad (7.1)$$

and the high frequency disturbance is modelled by:

$$S_h: y_h(t) = \frac{G(z^{-1})}{F(z^{-1})} \xi(t) \quad (7.2)$$

$$\text{and } E\{y_h(t)\} = 0 \quad (7.3)$$

where z^{-1} is the backward shift operator, $v(t)$ and $\xi(t)$ are independent random variables with variances σ_v^2 and σ_ξ^2 , respectively. The signal $\omega(t)$ is also an independent random variable with variance σ_ω^2 but not necessarily zero mean value. $M(z^{-1})$ and $N(z^{-1})$ represent the unknown plant polynomials. The plant can be a non-linear system or a linear system. The polynomials $F(z^{-1})$ and $G(z^{-1})$ are defined as:

$$F(z^{-1}) = 1 + f_1 z^{-1} + f_2 z^{-2} + \dots + f_{n_f} z^{-n_f} \quad (7.4)$$

$$G(z^{-1}) = 1 + g_1 z^{-1} + g_2 z^{-2} + \dots + g_{n_g} z^{-n_g}$$

The parameters of the polynomials $F(z^{-1})$, $G(z^{-1})$ are unknown. Only the order n_f is assumed known. The process output $y_l(t)$ is corrupted by the high frequency disturbance $y_h(t)$ and measurement noise $v(t)$. The measured output is given by:

$$z(t) = y_l(t) + y_h(t) + v(t) \quad (7.5)$$

where $v(t)$ usually represents measurement noise.

An example of this process is a vessel's motions at sea. The motion due to current, wind and second order waves is slowly varying and the motion due to first order wave forces is of high frequency.

7.3 TRACKING AND FILTERING PROBLEMS

In many applications, the observation $z(t)$ is not the desired signal for feedback. It is essential that the process output $y_l(t)$ is estimated. The conventional method is to design a low pass filter. However, this will give significant phase lag in the system response, particularly when the filter is of high order. With the knowledge of the polynomials $M(z^{-1})$, $N(z^{-1})$, $F(z^{-1})$, $G(z^{-1})$ and the variances of the disturbances, a Kalman filter may be suitable. If these parameters are unknown the Kalman filter can only be based on rough estimates which may not be adequate. For the analysis here it is assumed that the order n_f of the polynomial $F(z^{-1})$ is known. In most cases, n_f can be obtained from knowledge of the physics of the process. Generally, $n_f = 2$ is adequate for most disturbance models. In the next section, an adaptive filter is developed to estimate $y_l(t)$ which has a small time lag relative to fixed parameters filters. The adaptive filter can adapt to the range of parameters in the polynomials as well as to change in the variances of the random disturbances.

7.4 THE DESIGN OF ADAPTIVE ESTIMATOR

It is assumed the signal $y_l(t)$ can be decomposed into two components $\bar{y}_l(t)$ and $\tilde{y}_l(t)$:

$$y_l(t) = \bar{y}_l(t) + \tilde{y}_l(t) \quad (7.6)$$

where $\tilde{y}_l(t)$ represents the component which varies within a boundary of $\pm\delta$, that is:

$$-\delta \leq \tilde{y}_l(t) \leq \delta \quad (7.7)$$

Here δ is a constant which is close to the maximum amplitude of the sum of $y_h(t)$ and $v(t)$. That is,

$$\delta \simeq (\max |y_h(t) + v(t)|) \times k, \quad k > 1 \quad (7.8)$$

In the present discussion $\bar{y}_l(t)$ represents the output from a primary estimator. There are several ways to design such a coarse estimator.

A. Averaging Method

$$\bar{y}_l(t) = E\{y_l(t)\} \quad (7.9)$$

The expectation of both sides in equation (7.5):

$$E\{z(t)\} = E\{y_l(t)\} + E\{y_h(t)\} + E\{v(t)\} \quad (7.10)$$

$$= E\{y_l(t)\} \quad (7.11)$$

The expectation of the last two terms on the RHS are zero.

Thence,

$$\bar{y}_l(t) = E\{z(t)\} \quad (7.12)$$

The result in equation (7.12) is useful because $\bar{y}_l(t)$ can be generated from the measured output $z(t)$.

B. Conventional Low Pass Filter

$$\bar{y}_l(t) = W(z^{-1})z(t) \quad (7.13)$$

where $W(z^{-1})$ is a low pass filter in which $\bar{y}_l(t)$ can be generated directly from the output.

C. Innovation Disturbance Model

Define a new variable $n(t)$:

$$n(t) = z(t) - \bar{y}_l(t) \quad (7.14)$$

Using equations (7.5) and (7.6):

$$n(t) = y_l(t) + y_h(t) + v(t) - \bar{y}_l(t) \quad (7.15)$$

$$= y_h(t) + v(t) + \tilde{y}_l(t) \quad (7.16)$$

The variable $y_h(t)$ and the disturbance $v(t)$ can be represented by a new process called an innovation model, defined as:

$$y_h(t) + v(t) = \frac{H(z^{-1})}{F(z^{-1})} \mathcal{E}(t) \quad (7.17)$$

where the polynomial $H(z^{-1})$ and the variance of $\mathcal{E}(t)$ satisfy the spectral factorization:

$$H(z^{-1})H^*(z^{-1})\sigma_{\mathcal{E}}^2 = G(z^{-1})G^*(z^{-1})\sigma_{\xi}^2 + F(z^{-1})F^*(z^{-1})\sigma_v^2 \quad (7.18)$$

and $\mathcal{E}(t)$ is an independent random sequence. The polynomial $H(z^{-1})$ is of the form

$$H(z^{-1}) = 1 + h_1 z^{-1} + \dots + h_{nh} z^{-nh} \quad (7.19)$$

If $n_f > n_g$ then from equation (7.18) $n_h = n_f$. $D^*(z^{-1})$ represents the reciprocal of polynomial $D(z^{-1})$, which is defined as:

$$D^*(z^{-1}) = z^{-nh}(D(z)) \quad (7.20)$$

Substitute equation (7.17) into (7.16) to yield:

$$n(t) = \frac{H(z^{-1})}{F(z^{-1})} \mathcal{E}(t) + \tilde{y}_l(t) \quad (7.21)$$

D. Adaptive Tracking of $\tilde{y}_l(t)$ (Vernier Estimator)

Equations (7.12) and (7.13) show that the quantity $\bar{y}_l(t)$ can be generated from the measured output $z(t)$. The conditions set in equation (7.7) can easily be fulfilled by using either the averaging method or a conventional low pass filter. In order to obtain a good estimation of $y_l(t)$, there is still a quantity $\tilde{y}_l(t)$ to be estimated (equation 7.6). The variable $\tilde{y}_l(t)$ varies within the envelope of $\pm\delta$ (equation 7.7). Therefore, if $y_l(t)$ varies slowly, the quantity $\tilde{y}_l(t)$ can be treated as a constant within a few sampling intervals. Hence equation (7.21) can be represented as:

$$n(t) = x^T(t-1) \underline{\theta}(t) + \xi(t) \quad (7.22)$$

where

$$x^T(t-1) = [-n(t-1), \dots, -n(t-n_f), \xi(t-1), \dots, \xi(t-n_h), 1] \quad (7.23)$$

$$\theta^T = [f_1, \dots, f_n, h_1, \dots, h_n, s(t)] \quad (7.24)$$

where $s(t) = F\tilde{y}_l(t)$

The commonly used methods for estimating the parameter vector $\theta(t)$ are (1) recursive extended least square, (2)

recursive maximum likelihood and (3) recursive generalized least squares. Suppose the recursive extended least squares technique is used. The unmeasurable innovation signal $\varepsilon(t)$ is approximated by:

$$\hat{\varepsilon}(t) = n(t) - \hat{X}^T(t-1)\hat{\theta}(t) \quad (7.25)$$

where $\hat{\theta}(t)$ is the estimate of vector $\theta(t)$.

The quantity $\tilde{y}_l(t)$ is assumed to be varying slowly, and the parameters of the disturbances may also be varying. It is essential that the identification algorithm has a forgetting factor β of slightly less than unity. This will enable the recently observed output to be weighted more heavily than past information. The value of β should be within the range of 0.98 to 1.0. There are methods for varying the forgetting factor β but most of them are intuitively based. A more detailed analysis of such an algorithm was done by Osomio Cordero and Mayne [113]. They modified the algorithm so that the trace of the error covariance was divided by β . They claimed that it may prevent the algorithm from diverging but care must be taken when choosing the constants σ and λ in the algorithm. It was found that the algorithm is sensitive to these parameters. Collecting the above results the desired adaptive tracking algorithm becomes:

E. Adaptive Tracking Algorithm

- (1) Initialize data: $P(0), \hat{\theta}(0), \beta(0), \sigma, \lambda$
- (2) Measure output $z(t)$

Primary Estimation

- (3) Generate $\bar{y}_l(t) = M(z^{-1})z(t)$ or

$$= E\{z(t)\}$$
- (4) Generate $n(t) = z(t) - \bar{y}_l(t)$

Vernier Estimation

- (5) $\xi(t) = n(t) - \hat{X}^T(t-1)\hat{\theta}(t-1)$
- (6) $K(t) = [1 + X^T(t-1)P(t-1)X(t-1)]^{-1}P(t-1)X(t-1)$
- (7) $\hat{\theta}(t) = \hat{\theta}(t-1) + K(t)\xi(t)$
- (8) $N(t) = \sigma/[1 - X^T(t-1)K(t)]\xi^2(t)$
- (9) $\beta(t) = 1 - 1/N(t)$
- (10) $W(t) = [I - K(t)X^T(t-1)]P(t-1)$
 If $\text{trace } W(t)/\beta(t) < \lambda$ set $P(t) = W(t)/\beta(t)$
 Else set $P(t) = W(t)$
- (11) $\hat{\xi}(t) = n(t) - \hat{X}^T(t-1)\hat{\theta}(t)$
- (12) $\hat{\tilde{y}}_l(t) = \hat{s}(t)/\hat{F}(z^{-1}), z = 1$

Total Estimated Output

- (13) $\hat{y}_l(t) = \bar{y}_l(t) + \hat{\tilde{y}}_l(t)$
- (14) Go to Step 2

It may be necessary to smooth $\hat{\tilde{y}}_l(t)$ in step (12) using the following algorithm:

$$\hat{\tilde{y}}_l(t) = \alpha \hat{\tilde{y}}_l(t-1) + (1-\alpha) \hat{s}(t) / \hat{F}(z^{-1}), \quad z = 1$$

where α should be less than 0.5, otherwise it will introduce too much lag and deteriorate the performance of the vernier estimator.

7.5 SIMULATION RESULTS

In order to test the stability of the adaptive estimator under the condition where there is a severe change in the plant output, the adaptive estimator was used to track a square wave which was corrupted by high frequency noises.

The measured output, primary estimate and final estimate are shown in Figure 7-2. The primary estimator alone is quite insensitive to the step changes. This is the well known lag problem in the low pass filter. However, with the vernier estimator being activated, the lags observed at step changes are much reduced. When the plant output becomes constant the final estimate settles very well to the plant's constant value.

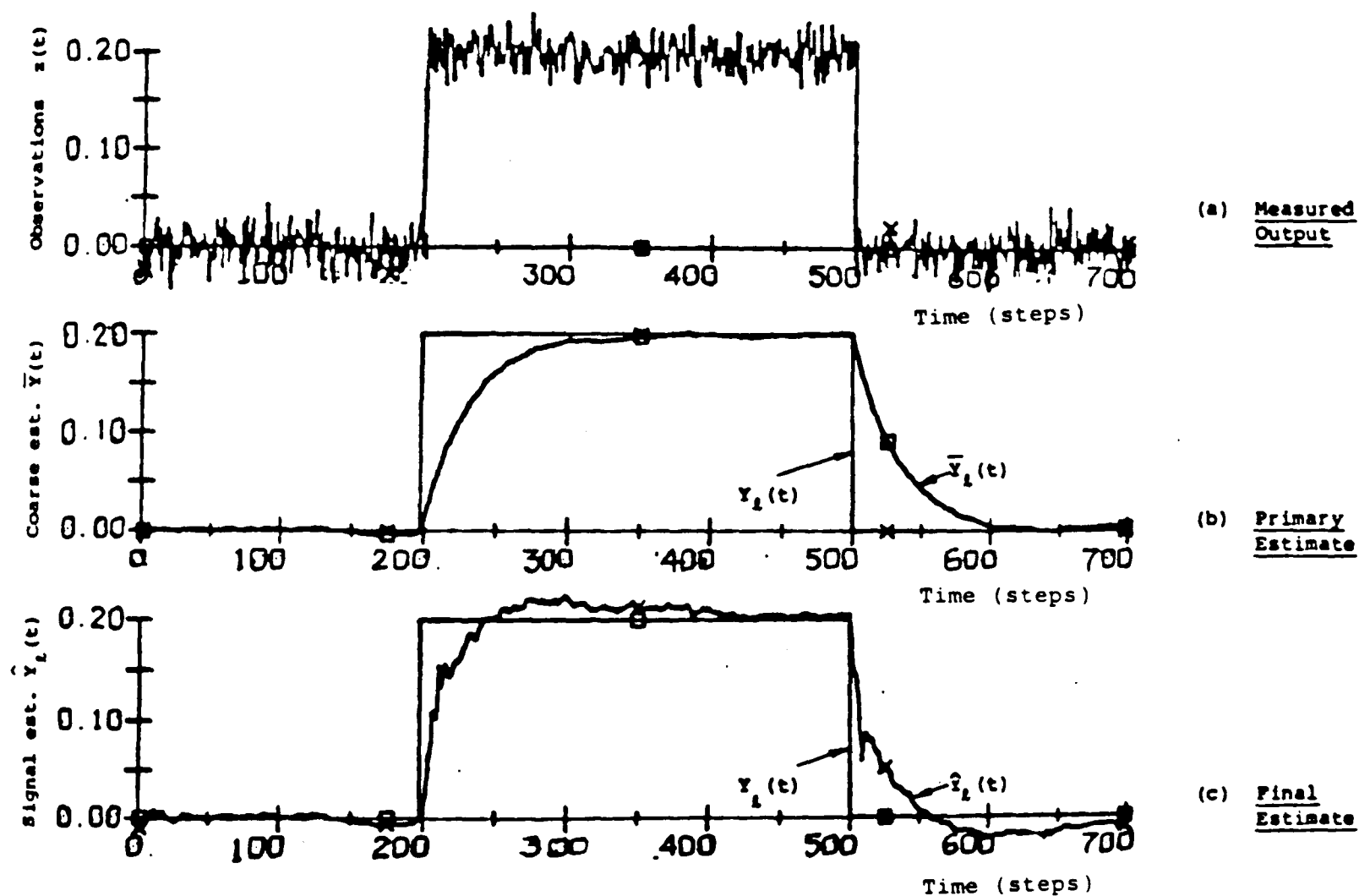


FIGURE 7-2 Estimation of a Square Signal

The second test is to demonstrate the adaptive tracker's capability in following trapezoidal (ramp and constant) signal. The results are shown in Figure 7-3. It is found that the significant lag in the primary estimate when following a ramp signal is quickly eliminated by the vernier estimator. The difference between the cumulative losses of the primary estimate and of the final estimate shown in the Figure 7-3(d) have justified the contribution of the vernier self-tuning estimator to the accuracy of the estimation. The estimated parameters of the disturbance model are shown in Figure 7-3(e).

The disturbance consists of high frequency oscillatory noise (simulated using the method described in Section 2.8.4, method one) and white noise component. The disturbance model was assumed to be of second order. Four parameters, $\{f_i\}$, $\{h_i\}$, $i = 1, 2$, and $\tilde{y}_l(t)$ were estimated in the self-tuning vernier estimator. The initial parameters are $\{f_1, f_2\} = \{h_1, h_2\} = \{-1, 0.5\}$. These initial guesses ensure the disturbance model is stable and that the parameters lie at the mid-point of their maximum range of values.

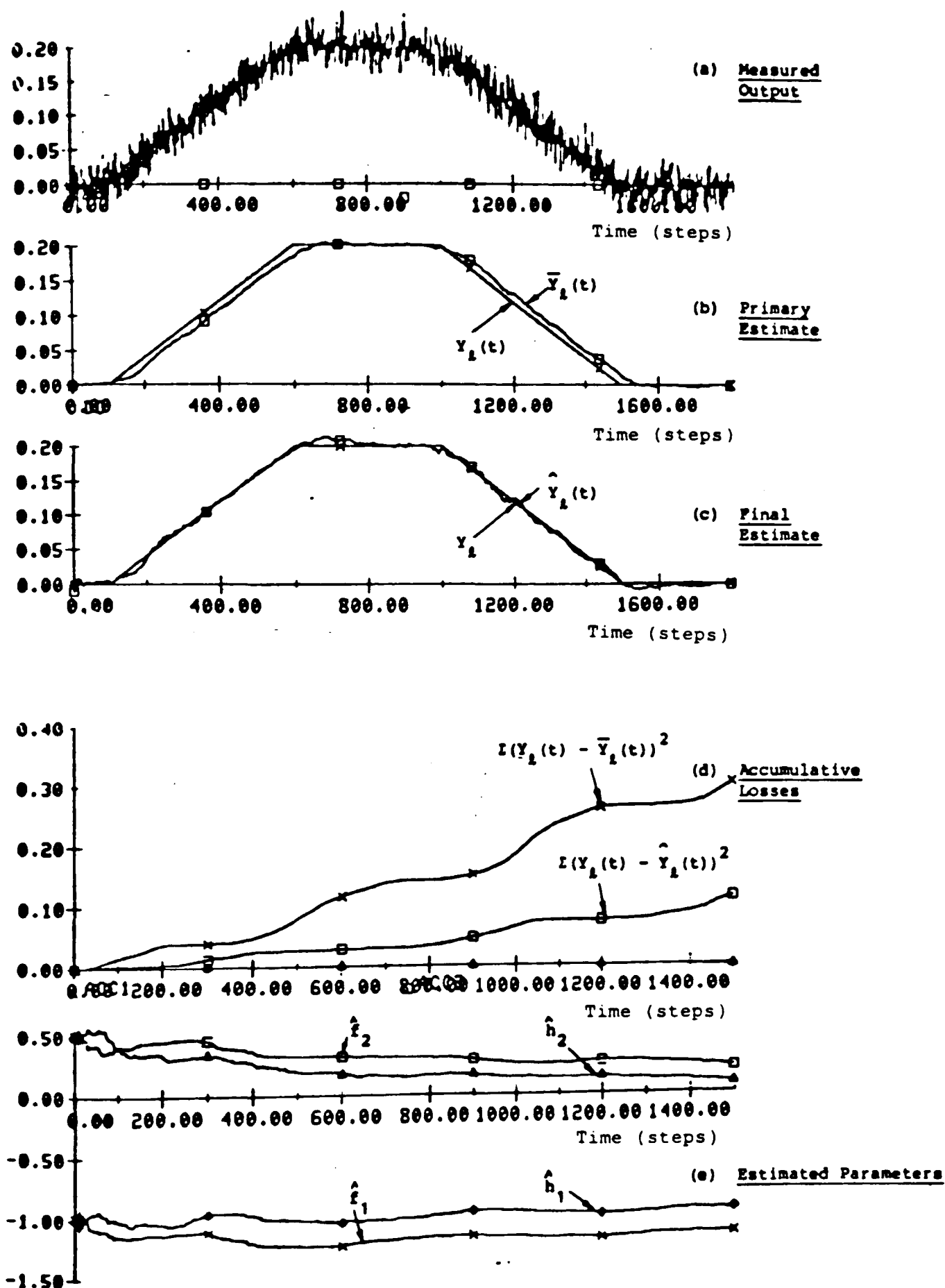


FIGURE 7-3 Estimation of a Trapezoidal Signal

The third test is the tracking of a sinusoidal signal which is corrupted by a high frequency oscillatory disturbance and white noise. The measured output is shown in Figure 7-4(a). The vernier estimate shown in Figure 7-4(b) varies consistently with the error, $\tilde{y}_l(t)$, between the primary estimate and the true signal (shown in Figure 7-4(c)). The vernier self-tuning estimator performs very well even when it crosses the zero value. However, the estimate fluctuates whenever the gradient of $\tilde{y}_l(t)$ changes sign, but the magnitude of this fluctuation is small compared with the output disturbances. The fluctuation observed in the vernier estimate was due to the fact that the forgetting factor in those regions was small. Notice that the small forgetting factor enables the vernier estimator to adapt to any the change faster than in normal operation. The final estimate is shown in Figure 7-4(d).

The last test is to track the sway motion of a vessel on sea. The measured output is shown in Figure 7-5(a). The primary estimate and the final estimate are shown in Figure 7-5(b) and 7-5(c) respectively. The final tracking lag was found to be smaller than the primary tracking lag, particularly when the velocity of the ship varied slowly.

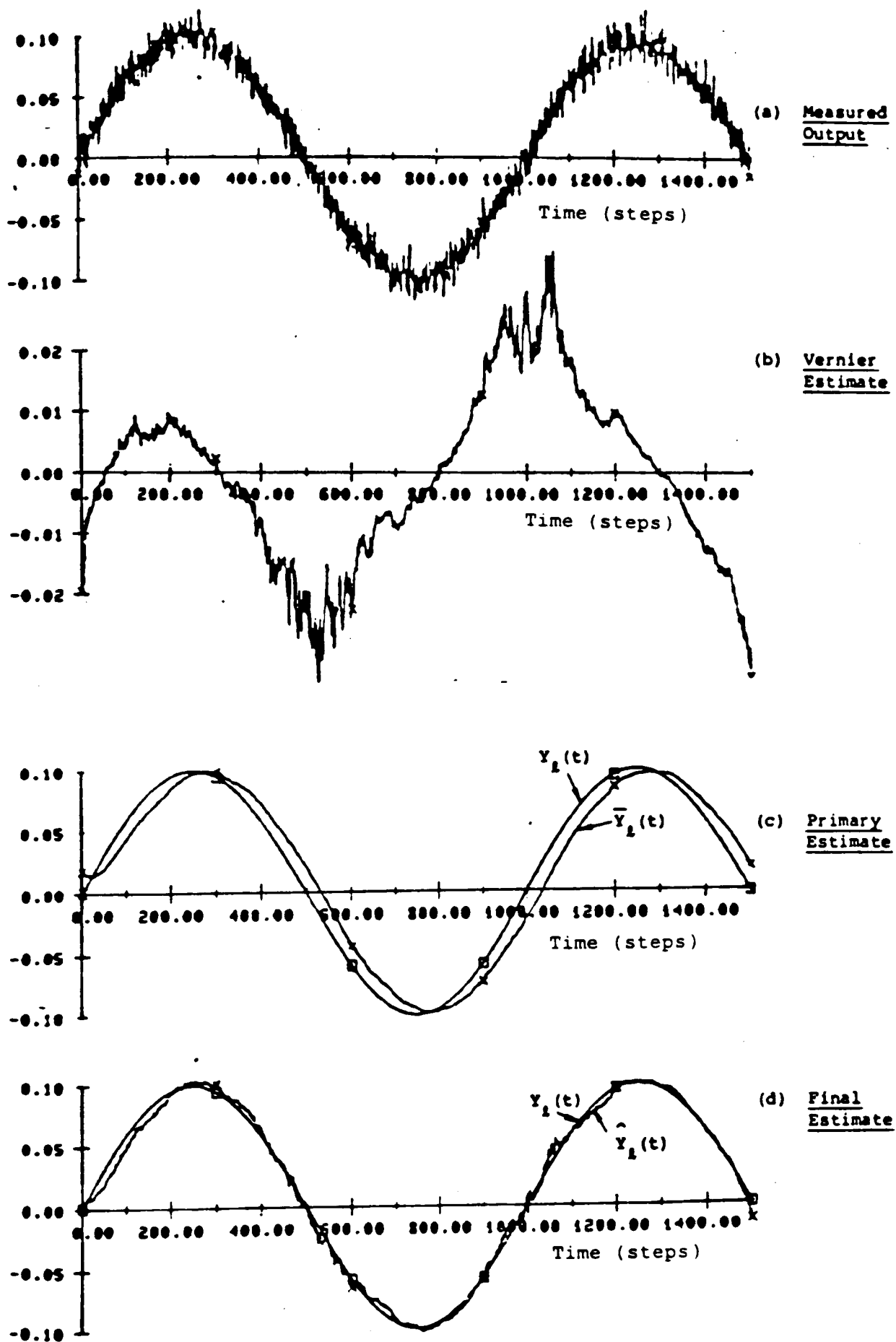


FIGURE 7-4 Estimation of a Sinusoidal Signal

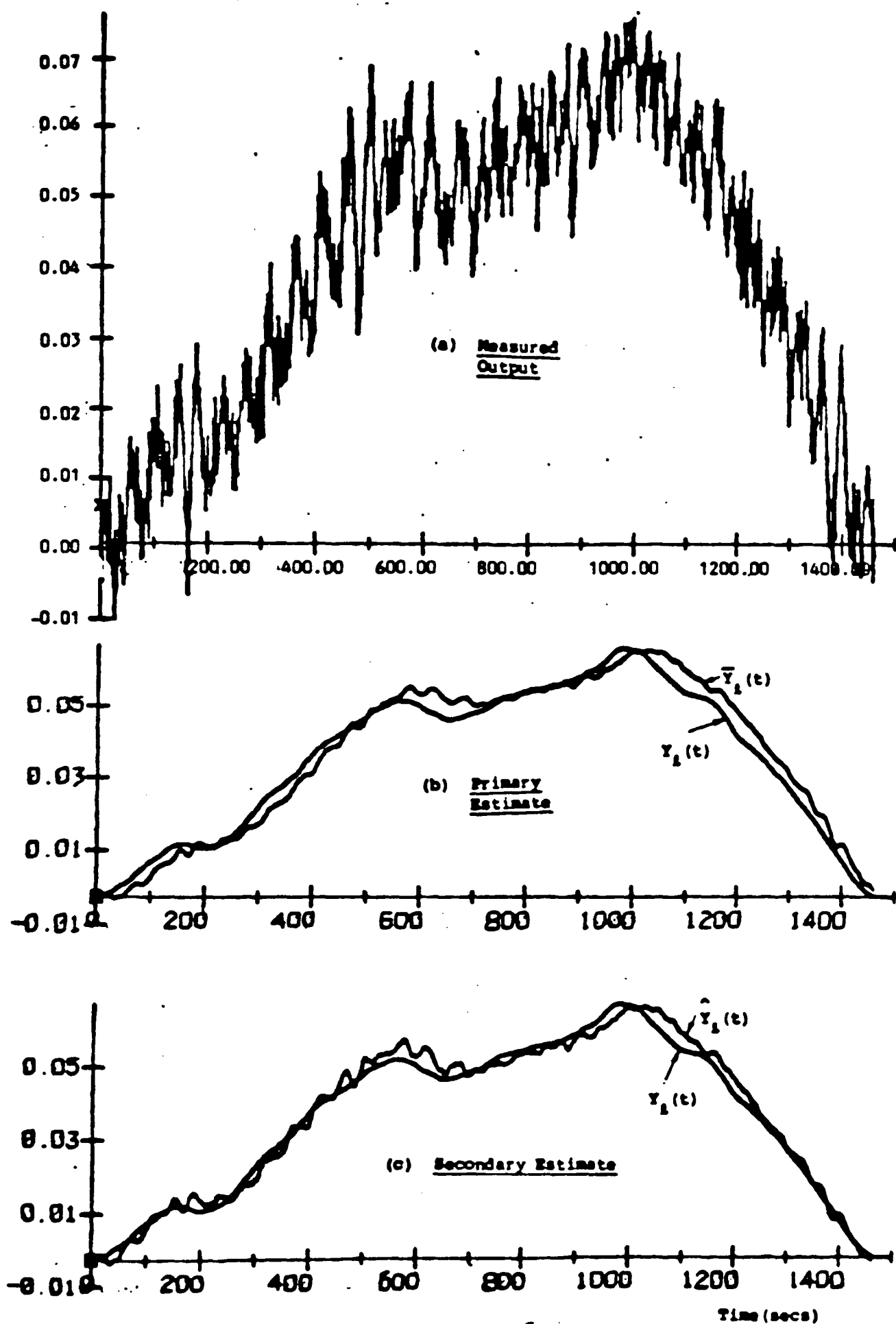


FIGURE 7-5

Estimation of Low Frequency Ship Sway Motion

7.6 SUMMARY OF RESULTS

An adaptive tracking technique has been developed to estimate the output of a slowly varying process which is corrupted by a coloured noise disturbance. No assumption was made on the plant model and the noise covariances. The only assumption made in the disturbances is that they are modelled by a second order process and the parameters are treated as unknowns. The estimator consists of a primary estimation subsystem and a vernier estimation subsystem. The primary estimator is simply a low pass filter or its equivalent. The vernier estimator is self-tuning and is adaptive to varying disturbances. A variable forgetting factor technique is employed in the parameter estimation algorithm. The adaptive estimator was used to track a square signal, trapezoidal signal, sinusoidal signal and the sway motion of a vessel at sea.

It was shown in the simulation results that the vernier self-tuning estimator is capable of reducing or eliminating (depending on the variation of the signal being tracked) the lag caused by the primary estimator.

CHAPTER EIGHT

SELF-TUNING CONTROL AND WEIGHTED MINIMUM VARIANCE SELF-TUNER

8.1 INTRODUCTION

There are two objectives in this chapter. The first is to overview the self-tuning control techniques which have become popular since the early seventies. The self-tuning methods developed in the previous chapters were originally inspired by this methodology. The second objective is to develop a class of self-tuning controllers called Weighted Minimum Variance (WMV) self-tuning controllers. An explicit WMV self-tuner for multivariable systems and an implicit algorithm for single input-single output systems are proposed. The robustness of these self-tuners suggests further development may be possible in the future.

8.2 SELF-TUNING CONTROL OVERVIEW

8.2.1 The Self-Tuning Control

Self-tuning Control is a Direct Digital Control (DDC) technique. The objective is to achieve a high performance

system in which conventional Proportional-Integral-Derivative (PID) control may have difficulty in fulfilling the requirements. Self-tuning begins when the identification procedures are combined with control strategy. One approach is to perform a plant identification and then to calculate the control action directly from the estimated parameters. This is called self-tuning control with explicit identification. A more subtle approach is to set up the control and identification problems so that the plant parameters are incorporated into the controller gains and to identify the latter. This route is known as self-tuning control with implicit identification. The basic assumptions made on self-tuning control are: (a) the parameters of the plant are constant or varying slowly; (b) the order of the plant is known; (c) the time delay is known. However, some self-tuning techniques are able to identify the time delay on-line.

In a wider context than self-tuning, the class of control systems known as "optimally adaptive" incorporate on-line process identification with optimal control action. In particular, the system input signal provides data for parameter estimation and executes the control strategy giving rise to the term "dual control". A categorization due to Jacob and Patchell [58] breaks down the control signal into three components:

- (a) Certainty Equivalent Control: The control which would be exercised if the estimated parameters were the actual ones.
- (b) Caution: The component which recognizes that errors in parameter estimates may cause excessive deviations in the control signal. This component takes account of uncertainties in the parameters estimated and is a function of estimated parameters and their accuracies.
- (c) Probing: This component is used to inject an optimal testing signal into the process to improve the estimates of uncertain parameters.

The optimal self-tuning theory approximates the optimal signal via the first component. Identification and control are regarded as separate operations so that the control law is derived under the assumption that the plant parameters are known. In this respect, the self-tuning controllers [74] may be classified as a certainty equivalent control law. Thence it is not optimal in the dual sense [59]. The pole and zero placement self-tuner [87], which is based on conventional control theory, does not fall in either category.

8.2.2 The Development

Self-adaptive control is always a challenging subject for control theoreticians and engineers. It is very much like non-linear control system theory, and though many techniques have been proposed, the application to a particular system is usually unique. The ad hoc tuning was the earliest technique in this field. This method developed in the early fifties is based on conventional control theory.

In 1958 Kalman [60] developed a simplified algorithm of a self-optimizing control system. However, the theory was inadequate and the digital computer technology at that time was unable to perform the adaptive feature.

In 1970, Peterka [63] revised and strengthened the minimum variance (MV) control law. The hundred flowers blossom period began when Astrom and Wittenmark [65] developed a Peterka type minimum variance self-tuning regulator in 1973. The MV control law suffers two drawbacks in application: (a) the control signal cannot be shaped or weighted, therefore it may exceed the hardware limitations, and; (b) it can only be applied to a non-minimum phase system. It often happens that a continuous time minimum phase system becomes a non-minimum phase system after discretization. Later work of Astrom and Wittenmark [66] employed the spec-

tral factorization technique to eliminate the unstable poles from the closed loop transfer function. The use of the spectral factorization technique means more computing is required, and increases the complexity of the self-tuning algorithm. It also requires that the number of unstable zeros must be known exactly.

In 1975, Clarke and Gawthrop [74] extended Astrom and Wittenmark's theory to produce a more general self-tuning controller which is based on the generalized minimum variance control (GMV) law proposed by Clarke and Hastings-James [72] in 1971. The cost function of this control law has weighting transfer functions on the system output and the control signal. Similar to LQG control law, designers can select these weightings according to the desired responses. Gawthrop [75] has found a few interpretations of the control law based on these weighting functions. One typical example is its relation to model adaptive control. The GMV controller can overcome the two drawbacks in the MV controller. The control is stable in a non-minimum phase systems if the weighting function on the control is properly selected. This weighting function can also be used to shape the control signal within the hardware limits. Because of its generalized feature, the GMV self-tuner has received greater attention in application than the MV self-tuner. Astrom [163] claimed that the excess in the control signal

may be improved by adjusting the sampling rate. However, the sampling rate is a very critical parameter in many aspects systems [166], and it may not be freely selectable in many applications.

The MV self-tuner is not optimal in a dual sense [59], but is optimal in the principal of certainty equivalent. The GMV self-tuner, because of the weighting on the control, is only optimal based upon the conditional expectation on all the acquired input/output data [61]. These self-tuners require the time delay and the order of the plant to be known.

In 1977, Wellstead, et al [86] proposed an alternative self-tuning technique called the pole placement self-tuner. The latter version [87] of this class of self-tuner was extended to include zero placement. The original concept should be dated back to Edmund's work in this area in 1976 [62]. The closed loop pole/zero placement theory is well established in classical control theory. The designer can place the pole/zero of the closed loop transfer function to achieve the desired response. It was shown that by solving the diophantine equation using the estimated plant parameters identified explicitly, the controller has the self-tuning property. A controller is self-tuning if the parameter estimates are unbiased and converge to the true

values. Because of its explicit feature, this self-tuner may allow the time delay to be estimated on-line.

Since the appearance of Astrom and Wittenmark's paper in 1973 [65] followed by Clarke and Gawthrop's article in 1975 [74], the number of reports in this field has multiplied greatly. The articles can be divided into the following categories:

- (a) MV Self-tuner [65-71]
- (b) GMV Self-tuner [72-83]
- (c) Pole/zero Placement Self-tuner [84-87]
- (d) Multivariable Self-tuners [88-95]
- (e) PID Self-tuners [96-98]
- (f) State Feedback Self-tuners [99-102]
- (g) Hybrid Self-tuning Control [103-104]
- (h) Self-tuning filters [105-107]
- (i) Self-tuning Predictors [108-109]
- (j) Non-linear Self-tuners [110-111]
- (k) Stability Study and Identification Algorithms [112-132]
- (l) Applications [133-160]

A comprehensive review on self-tuning control by experts from the United Kingdom is given in Reference [161].

In 1981, Grimble [164] proposed a weighted minimum variance (WMV) controller which fills the gap between the MV controller and the GMV controller. When the GMV controller encounters a non-minimum phase system, the closed loop system may become unstable if the control weighting factor is not suitably chosen. Whereas for the MV regulator (non-minimum phase version), since there is no weighting on the control, the control may be excessive. WMV control does not suffer from the above problems. However, to modify a WMV controller to become self-tuning involves complicated algorithms which may be difficult to realize in complex systems. In Section 8.3, an explicit multivariable WMV self-tuner will be described. An implicit version for a single input-single output system is given in Section 8.4.

Recently, Koivo and Guo [160] have applied the self-tuning concept to robotic control. A robotic system is time varying because the moment of inertia is dependent on the configuration of the arm. Therefore, the adaptive controller may not achieve the self-tuning property. Nevertheless, the simulation results have demonstrated that this adaptive controller is a potential candidate for highly time-varying manipulator systems.

Indeed, self-tuning control is the first offspring of the marriage between parameter identification and control design

in this digital computer age. The reason that the self-tuning control has received much attention in this decade is mainly due to its practical features. Although many fruitful implementation results have been reported, many engineers still do not have confidence in self-tuning techniques for various reasons. The implementation aspects will be discussed in the next section.

8.2.3 Implementation, Advantages and Disadvantages

It is not uncommon that engineers in industry, due to the 'generation gap' mainly in mathematics, have the impression that modern control theory is only an academic fashion and that it is of little use in practical problems. It is certainly true that modern control theory is strongly mathematically based. Since the mathematical model often idealizes a practical problem, it is not suprising that control theory based solely on the model may not be appropriate for practical purposes. For example, an optimal controller with a time delay may not perform as well as a Smith predictor type controller [162]. Recently, control engineering research has tended strongly towards solution of practical problems. The self-tuning control is highly regarded as a major achievement in this aspect.

Self-tuning control is an alternative control design technique. The self-tuner is usually only a small part of a control system and should only be used when the problem is appropriate and only then in its most computationally efficient form.

The percentage of success in the application of self-tuners to chemical processes is far higher than those applied to any other dynamic systems. The result is not surprising because chemical processes are often complex and slow and so plant parameters are either constant or varying slowly. These characteristics are the basic assumptions in the development of the self-tuning theory. The use of a MV self-tuner in a paper machine is the first successful application of the self-tuner reported in the literature [134]. Surprisingly, the PID controller was used again in the same plant [163] later. Two possible simple reasons are: (a) engineers have a lack of confidence in the robustness of the self-tuner, and (b) the MV self-tuner in particular, or self-tuning in general, is not appropriate for the process. To conclude, the advantages and disadvantages of implementing a self-tuning control solution based on experience to date are listed below:

Advantages

- (a) The self-tuner can be applied to a plant which contains unknown or slowly varying parameters.
- (b) It may be possible to improve the control of certain non-linear systems by treating the gains of the non-linear elements as variables.
- (c) Existing controllers may be adjusted by self-tuning techniques, by monitoring the controller performance online.

Disadvantages

- (a) The number of parameters to be estimated depends upon the order of the plant polynomials. In practice, most system constants are usually known approximately, but no advantage is taken, in the basic self-tuners of the information structure of the plant parameters. This is in direct contrast to the extended filtering methodology in which only the unknown or varying parameters are estimated.
- (b) If the uncontrolled system is unstable or non-minimum phase it is possible for self-tuning controllers based

upon a single-stage cost function to yield unstable controllers. Grimble [164] has recently introduced a weighted minimum-variance controller which has advantages in this situation.

- (c) The time-delay must be known for the Clarke/Gawthrop and Astrom/Wittenmark self-tuners. The Wellstead algorithm has the advantage that it leaves the leading coefficient of the $B(z^{-1})$ polynomial as an unknown and can be used for systems with unknown delays. However, this is a non-optimal technique which is not so appropriate for more complex stochastic systems having several noise and disturbance inputs (the controller is independent of the noise intensities). For this situation a method of weighting the importance of the noise is required which is available with LQG controllers [165], although such controllers are necessarily more complex.

An optimal control system can be proposed based upon an extended Kalman filter and a state-estimate feedback gain matrix. Unknown parameters can then be estimated using the extended filter. This type of controller seems to be more robust than the equivalent self-tuning system, but it is not called upon to do as much as in the self-tuning problems. In self-tuning control no knowledge of the plant parameters

or of the noise sources is assumed. In extended filtering, however, only a few system parameters are normally to be estimated. There is, therefore, a difference in the assumptions made for these two types of control system.

One unknown parameter in a state-space model can affect many of the coefficients in a transfer-function plant model. Thus, in such cases if only one parameter is to be estimated, an extended Kalman-filter scheme may be appropriate. Conversely, the plant may be modelled in z-transfer-function form with one unknown coefficient. In this case, the basic self-tuners can be modified so that this parameter only is identified.

8.3 EXPLICIT MULTIVARIABLE WEIGHTED MINIMUM VARIANCE SELF-TUNING CONTROLLER

8.3.1 Introduction

An explicit self-tuning controller is described based upon the weighted minimum variance control law. The controller has the advantage that a non-minimum phase system can be stabilized under conditions where other minimum variance control laws fail. The system can be multivariable and can include unknown transport delay terms which are different in each loop.

The weighted minimum variance controller for single input-single output systems was recently introduced (Grimble [164]) to overcome some of the problems in the control of non-minimum phase systems. For example, the generalized minimum variance controller employed by Clarke and Gawthrop [74] in their successful self-tuning controller is unstable when the control weighting tends to zero. Since small control weighting corresponds to tight control action this is an unfortunate feature of this controller. The weighted minimum variance controller is stable in this situation.

The controller also has advantages in comparison with the minimum variance regulator employed by Astrom and Wittenmark [66]. The cost function includes control weighting and control signal variations can be much reduced. The penalty to be paid for the improvement in performance characteristics is that the controller is more complicated than the foregoing. A multivariable version of the weighted minimum variance controller is derived in the following and this is used as an explicit self-tuning controller.

8.3.2 System Description

The multivariable linear constant plant is given as:

$$A(z^{-1})\underline{y}(t) = B(z^{-1})\underline{u}(t) + C(z^{-1})\underline{\xi}(t) \quad (8.1)$$

where the polynomial matrices are m -squared. The disturbance $\underline{\xi}(t)$ is a sequence of independent zero mean random vectors with covariance $E\{\underline{\xi}(t)\underline{\xi}(t)\} = Q$. The polynomial matrices $A(z^{-1}) = I_m + A_1z^{-1} + \dots + A_nz^{-n}$, $B(z^{-1}) = (B_0 + B_1z^{-1} + \dots + B_{n-k}z^{-n+k})z^{-k}$ and $C(z^{-1}) = I_m + C_1z^{-1} + \dots + C_nz^{-n}$. The delay $k \geq 1$ and if this is unknown k is assumed to be unity and the actual delay can be estimated. Notice that B_0 is not necessarily full rank as assumed in most of the work on self-tuning. This implies that different loops in the multivariable system may contain different transport delay terms.

The matrix $B(z^{-1})$ is assumed to be of normal full rank and $B = B_2B_1$ where B_2 and B_1 represent the non-minimum and minimum phase spectral factors, respectively. The B_2 term includes the delay k and without loss of generality $B_1(0)$ can be chosen to be full rank, (the factorization is performed via the Smith form). The orders of B_1 and B_2 are denoted by n_1 and n_2 , respectively.

For greater generality the system will include a reference input $\underline{r}(t) = A(z^{-1})^{-1}E(z^{-1})\underline{\omega}(t)$ and a set point $\underline{w}(t)$. The covariance matrix for the white noise signal $\underline{\omega}(t)$ is denoted

Q_0 . The stochastic tracking error $\underline{e}(t) \triangleq \underline{r}(t) - \underline{y}(t)$. The innovations form of the system equation becomes:

$$A\underline{e}(t) = D\underline{\xi}(t) - B\underline{u}(t) \quad (8.2)$$

where the matrix D follows from the spectral factorization:

$$\begin{aligned} D(z^{-1})D^T(z) &= E(z^{-1})Q_0E^T(z) \\ &\quad + C(z^{-1})QC^T(z) \end{aligned} \quad (8.3)$$

and $D(z^{-1})^{-1}$ is stable. It will be necessary to write $D^{-1}B$ in the form:

$$D^{-1}B_2 = B_2^0 D_0^{-1}$$

where $\det D_0 = \det D$, $D_0(0) = I_m$ and $n_{d0} = n_d$. The polynomial matrices B_2^0 and D_0 are right coprime and always exist but are not unique.

8.3.3 Cost Function

The feedback control law is required to minimize the cost function:

$$J = E\left\{\underline{\phi}_1(t+K)^T \underline{\phi}_1(t+K)/t\right\} \quad (8.4)$$

where the expectation is conditional upon all observations up to time t . The signal

$$\begin{aligned} \phi_1(t+k) \triangleq & P_0(z^{-1})\underline{e}(t) + P_1(z^{-1})\underline{w}(t) \\ & - P_2(z^{-1})\underline{u}(t) \end{aligned} \quad (8.5)$$

and the transfer function matrices P_0 , P_1 and P_2 can be specified to achieve given performance specifications. The transfer function matrix

$$P_0(z^{-1}) \triangleq d_1(z^{-1})(A_C(z^{-1})B_C(z^{-1}))^{-1} \quad (8.6)$$

where $d_1(z^{-1})$ is a minimum phase scalar polynomial and $A_C(z^{-1})^{-1}$ is a stable matrix. The matrix $B_C(z^{-1})$ is related to $B_2(z^{-1})$ and is defined in the following. Assume that $d_1(0) = 1$, $A_C(0) = I_m$ and $P_2(0) \geq 0$, and let $A_1(z^{-1}) \triangleq A(z^{-1})A_C(z^{-1})$.

8.3.4 Multivariable Weighted Minimum Variance Controller

The weighted minimum variance controller is defined in the following theorem:

Theorem 8.1 Weighted Minimum Variance Controller

The optimal control for the plant (8.1) and the performance criterion (8.4) is given as:

$$\begin{aligned} \underline{u}^0(t) = & (B_1 + D_0 P_2)^{-1} (G H^{-1} \underline{e}'(t) \\ & + D_0 P_1 \underline{w}(t)) \end{aligned} \quad (8.7)$$

where $\underline{e}'_1(t) = A_C^{-1}\underline{e}(t)$, G and H satisfy:

$$A_1 H + B_2 G = d_1 D \quad (8.8)$$

$$n_h = n_2 - 1 \text{ and } n_g = \max(n_{a1} - 1, n_{d1} + n_d - n_2)$$

The proof follows that for the single-input, single-output case given by Grimble, 1981 [164], and is summarized briefly below.

Proof: Let $\underline{\phi}(t + k) \triangleq P_O \underline{e}(t)$ then from (8.2):

$$\underline{\phi}(t + k) = B_C^{-1} d_1 A_1^{-1} (D \underline{\xi}(t) - B \underline{u}(t)) \quad (8.9)$$

and from (8.2) and (8.8):

$$\begin{aligned} \underline{\phi}(t + k) = B_C^{-1} (H \underline{\xi}(t) + A_1^{-1} B_2 G D^{-1} A_1 \underline{e}'_1(t) \\ - H D^{-1} B \underline{u}(t)) \end{aligned} \quad (8.10)$$

but from (8.8):

$$A_1^{-1} B_2 G D^{-1} A_1 = H D^{-1} B_2 G H^{-1} \quad (8.11)$$

thence

$$\begin{aligned} \underline{\phi}(t + k) = B_C^{-1} (H \underline{\xi}(t) + H D^{-1} B_2 (G H^{-1} \underline{e}'_1(t) \\ - B_1 \underline{u}(t))) \end{aligned} \quad (8.12)$$

The term $D^{-1} B_2$ may be written in terms of the right coprime polynomial matrices B_2^O and D_O as:

$$D^{-1}B_2 = B_2^O D_O^{-1} \quad (8.13)$$

where $\det D_O = \det D$ and $D_O(0) = I_m$. The term D_O^{-1} is stable but

$$\begin{aligned} (B_2^O(z^{-1}))^{-1} &= z^{n_2} (B_{2n_0}^O + B_{2(n_0-1)}^O z + \dots \\ &+ B_{20}^O z^{n_0})^{-1} \end{aligned} \quad (8.14)$$

represents a non-causal transfer function ($n_2 - n_0 = k \geq 1$).

The term B_C in the cost function may now be defined as:

$$B_C = H B_2^O \quad (8.15)$$

so that

$$B_C^{-1} H D^{-1} B_2 = D_O^{-1} \quad (8.16)$$

and

$$B_C^{-1} H = (B_2^O)^{-1}$$

From (8.12) and using the above relationships:

$$\begin{aligned} \phi(t+k) &= (B_2^O)^{-1} \underline{\xi}(t) + D_O^{-1} (G H^{-1} \underline{e}_1'(t) \\ &\quad - B_1 \underline{u}(t)) \end{aligned} \quad (8.18)$$

and from (8.5):

$$\begin{aligned}\phi_1(t+k) &= (B_2^0)^{-1}\underline{\xi}(t) + D_0^{-1}(GH^{-1}\underline{e}_1'(t) \\ &\quad + D_0P_1\underline{w}(t) - (B_1 + D_0P_2)\underline{u}(t))\end{aligned}\quad (8.19)$$

From these results it follows that a least squares predictor $\hat{\phi}_1(t+k/t)$ and prediction error $\tilde{\phi}_1(t+k/t)$ may be defined as:

$$\begin{aligned}\hat{\phi}_1(t+k/t) &= D_0^{-1}(GH^{-1}\underline{e}_1'(t) + D_0P_1\underline{w}(t) \\ &\quad - (B_1 + D_0P_2)\underline{u}(t))\end{aligned}\quad (8.20)$$

$$\tilde{\phi}_1(t+k/t) = (B_2^0)^{-1}\underline{\xi}(t) \quad (8.21)$$

The prediction error is uncorrelated with the signal $\hat{\phi}_1(t+k/t)$ which is known at time t .

The cost function (8.4) may now be expressed as:

$$J = E\left\{\tilde{\phi}_1(t+k/t)^T \tilde{\phi}_1(t+k/t) + \hat{\phi}_1(t+k/t)^T \hat{\phi}_1(t+k/t)\right\} \quad (8.22)$$

and it follows by the usual arguments that the optimal control gives $\hat{\phi}_1(t+k/t) = 0$ or

$$(B_1 + D_0P_2)\underline{u}^0(t) - (GH^{-1}\underline{e}_1'(t) + D_0P_1\underline{w}(t)) = 0 \quad (8.23)$$

This completes the proof of (8.7).

The stability of the closed-loop system can be ascertained from the characteristic equation. This follows via:

$$\det(A^{-1}(A_1H+B(B_1+D_0P_2)^{-1}G)H^{-1}A_C^{-1}) = 0 \quad (8.24)$$

and in the limiting case as $P_2 \rightarrow 0$ the characteristic equation becomes $\det d_1D = 0$ and the system is stable. Similarly, if the plant is open loop stable the closed loop system is stable when $p_2 \rightarrow \infty$.

Special Cases:

- (a) Assume the model for \underline{e} is autoregressive ($D = I_m$) then $D_0 = D$.
- (b) Assume that the time-delay and non-minimum phase behaviour is the same in each signal path for the plant, thus $B_2 = b_2I_m$ where b_2 is a scalar, and $D_0 = D$. The calculation of b_2 is also simplified in this case.

8.3.5 Explicit Self-tuning Control

An explicit self-tuning algorithm may be constructed in the usual manner and this is illustrated for the plan considered by Koivo [91]. The plant polynomial matrices are defined as:

$$A(z^{-1}) = I_2 + \begin{bmatrix} -0.9 & 0.5 \\ 0.5 & -0.2 \end{bmatrix} z^{-1} \quad (8.25)$$

$$B(z^{-1}) = \begin{bmatrix} 0.2 & 1.0 \\ 0.25 & 0.2 \end{bmatrix} z^{-1} + \begin{bmatrix} 1.0 & 0 \\ 0 & 1.0 \end{bmatrix} z^{-2} \quad (8.26)$$

$$C(z^{-1}) = I_2$$

Let the performance criterion polynomials be defined as:

$$d_1(z^{-1}) = 1 - \lambda_1 z^{-1}, \lambda_1 = 0.5$$

$$A_C(z^{-1}) = I_2, P_1(z^{-1}) = I_2 \text{ and } P_2(z^{-1}) = \lambda I_2$$

where λ is a real positive scalar. For this system $\underline{r} = 0$,

$$B_2(z^{-1}) = B(z^{-1}) \text{ and } B_1(z^{-1}) = I_2$$

In this case the expressions for the optimal control simplify and the following simple explicit self-tuning algorithm may be employed.

1. Estimate A and B_2 using $A\underline{y}(t) = B_2\underline{u}(t) + \underline{\xi}(t)$
2. Solve $AH + B_2G = d_1I_2$ for H and G where $n_h = n_2 - 1 = 1$
and $n_g = n_a - 1 = 0$
3. Calculate $\underline{u}^o(t) = \frac{1}{1+\lambda} (GH^{-1}\underline{y}(t) + \underline{w}(t))$
Return to 1.

To evaluate the diophantine equation note that it may be expressed in the form:

$$\begin{bmatrix} I_2 & B_0 \\ A_1 & B_1 \end{bmatrix} \begin{bmatrix} H_1 \\ B_0 \end{bmatrix} = \begin{bmatrix} -A_1 - \lambda_1 I_2 \\ 0 \end{bmatrix} \quad (8.27)$$

where $A(z^{-1}) = I_2 + A_1 z^{-1}$, $B_2(z^{-1}) = z^{-1}(B_{20} + B_{21} z^{-1})$, $G(z^{-1}) = G_0$ and $H(z^{-1}) = I_2 + H_1 z^{-1}$. Assuming the inverse exists during self-tuning:

$$\begin{bmatrix} H_1^* \\ G_0^* \end{bmatrix} = \begin{bmatrix} I & B_0^* \\ A_1^* & B_1^* \end{bmatrix}^{-1} \begin{bmatrix} -A_1 - \lambda_1 I_2 \\ 0 \end{bmatrix} \quad (8.28)$$

where the * denotes the estimated value.

The system is open loop unstable and non-minimum phase and thence the closed-loop system may be unstable for some values of λ . In the approach by Clarke and Gawthrop [74] (or Koivo [91] for the multivariable case) λ cannot be either too large or too small if the system is to be closed-loop stable. The advantage of the weighted minimum variance controller is that λ can be set to zero (as in the simulation results) and stability is maintained.

Simulation results for both output regulator and servomechanism are given. The estimated parameters for the

regulator problem are shown in Figure 8-2 and the outputs and control signals are shown in Figure 8-1. The time delay can be estimated on-line provided an upper order on B is known. In the servomechanism results, different unknown delays in different loops were simulated. This was achieved by replacing $b_{11}^0 = 0.2$ in (8.26) by zero. The time delay in loop 1 is $k_1 = 2$ and in loop 2, $k_2 = 1$. The estimated parameters are shown in Figure 8-4 (notice that $\hat{b}_{11}^0 = 0$) and compare with Figure 8-2. The controlled outputs are shown in Figure 8-3 and these demonstrate the effect of a step change in the set-point signal.

8.3.6 Discussion

A weighted minimum variance control law has been derived for multivariable systems and has been combined with an estimation algorithm to produce an explicit self-tuning controller. This approach has the disadvantage that the matrix polynomial B must be spectrally factored. Recent work has been concerned with the development of an implicit scheme which does not involve this spectral factorization stage. The advantages of this approach are: (a) the range of stability is extended over that normally found for non-minimum phase plants; (b) the performance criterion includes control weighting; (c) stochastic reference or known set point signals may be included; (d) the transport

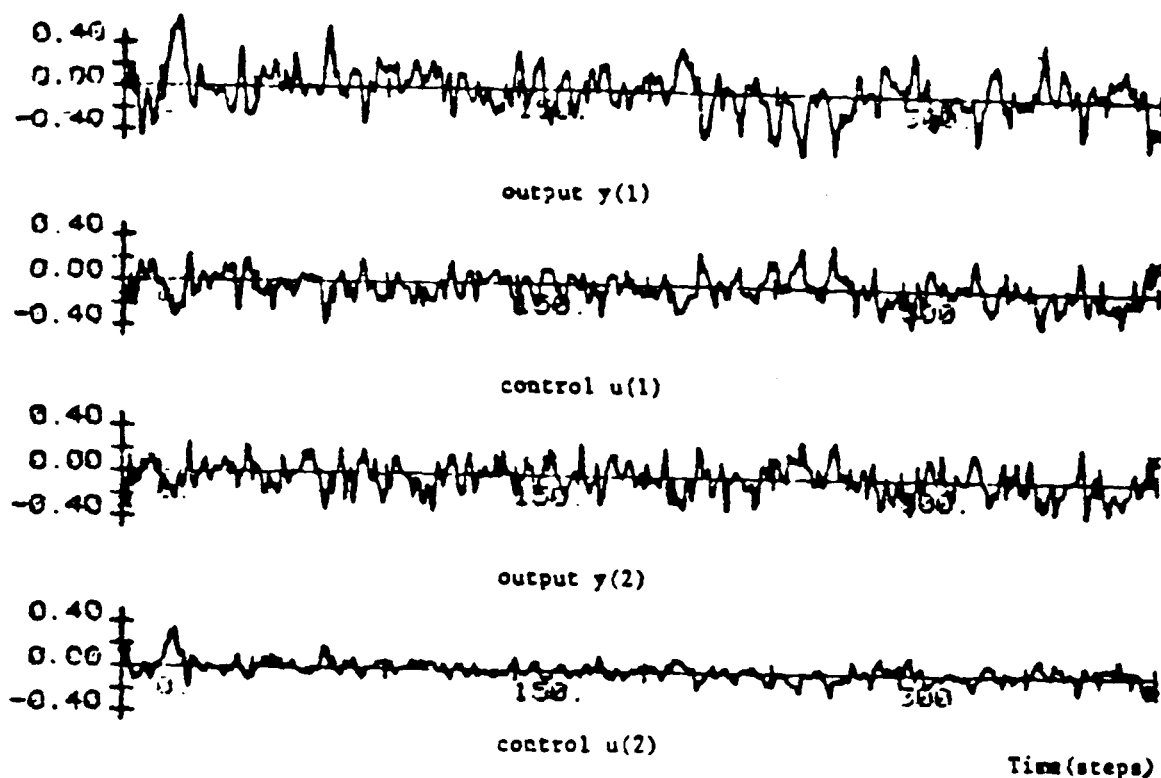


FIGURE 8-1 Outputs and Control Signals (Regulation)

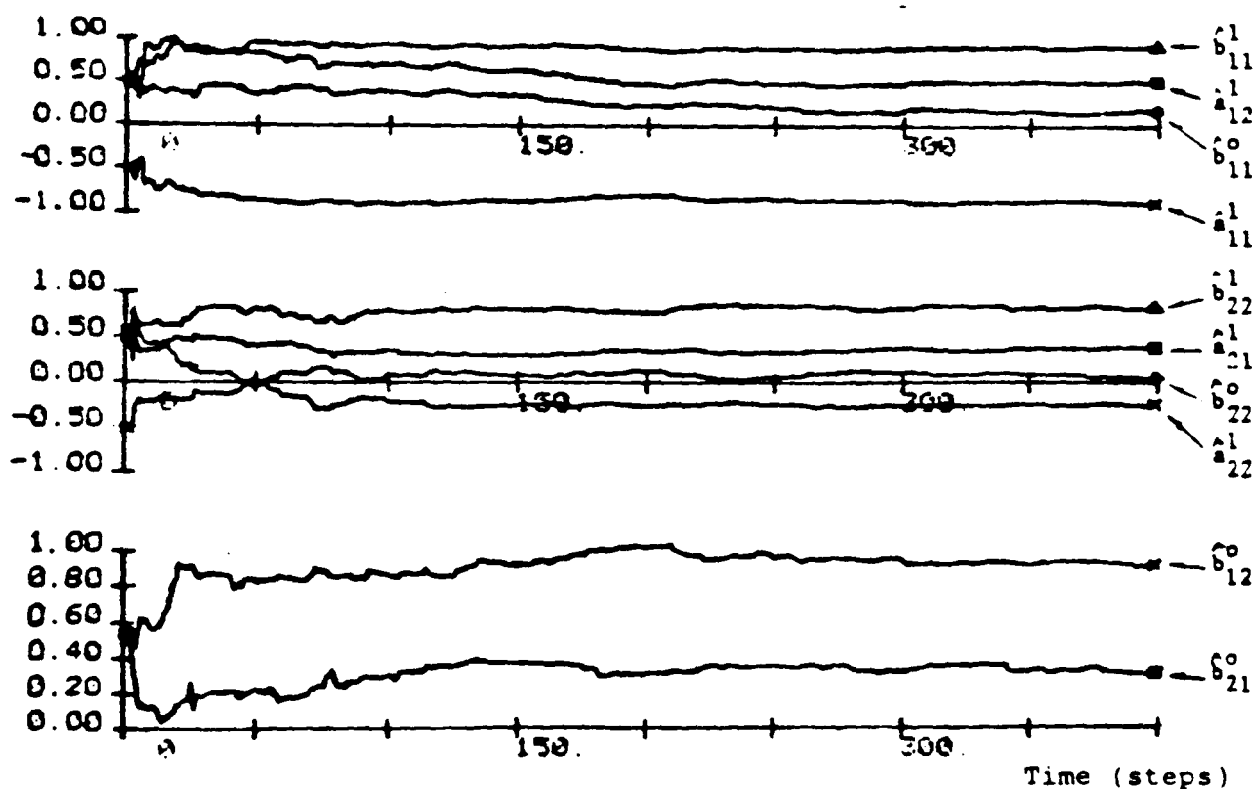


FIGURE 8-2 Estimated Parameters (Regulation)

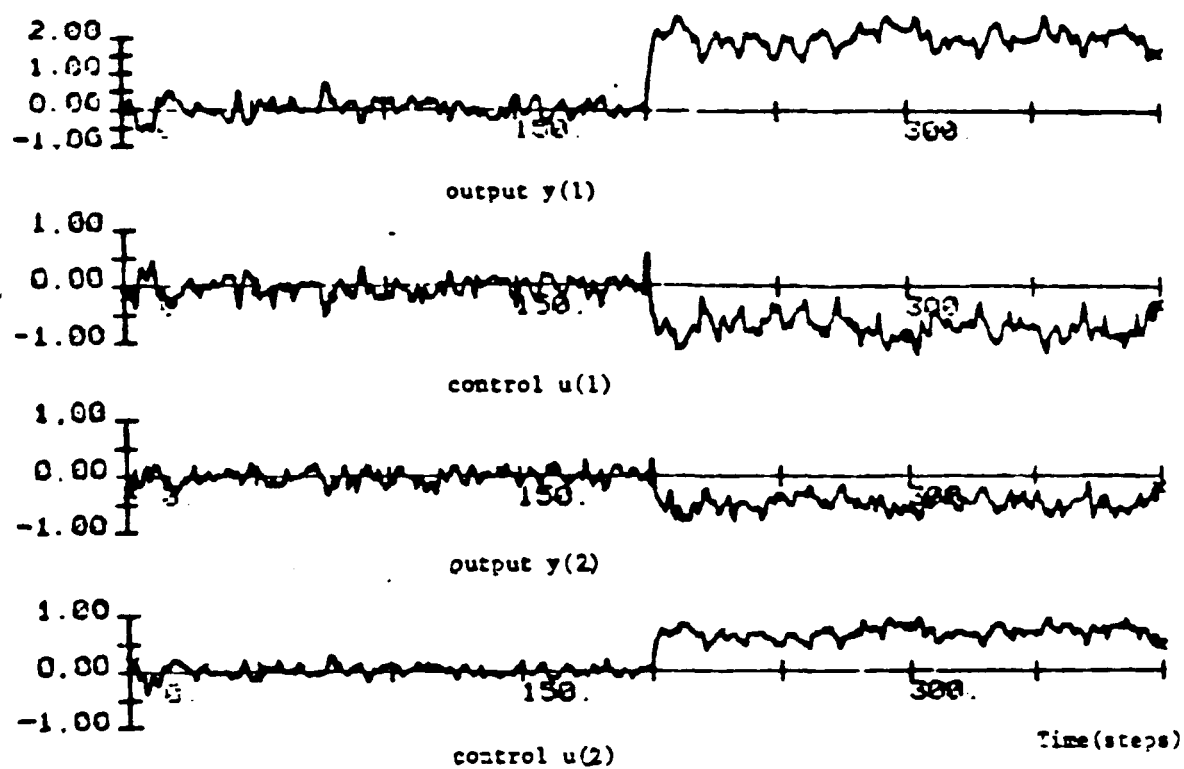


FIGURE 8-3 Outputs and Control Signals (Tracking)

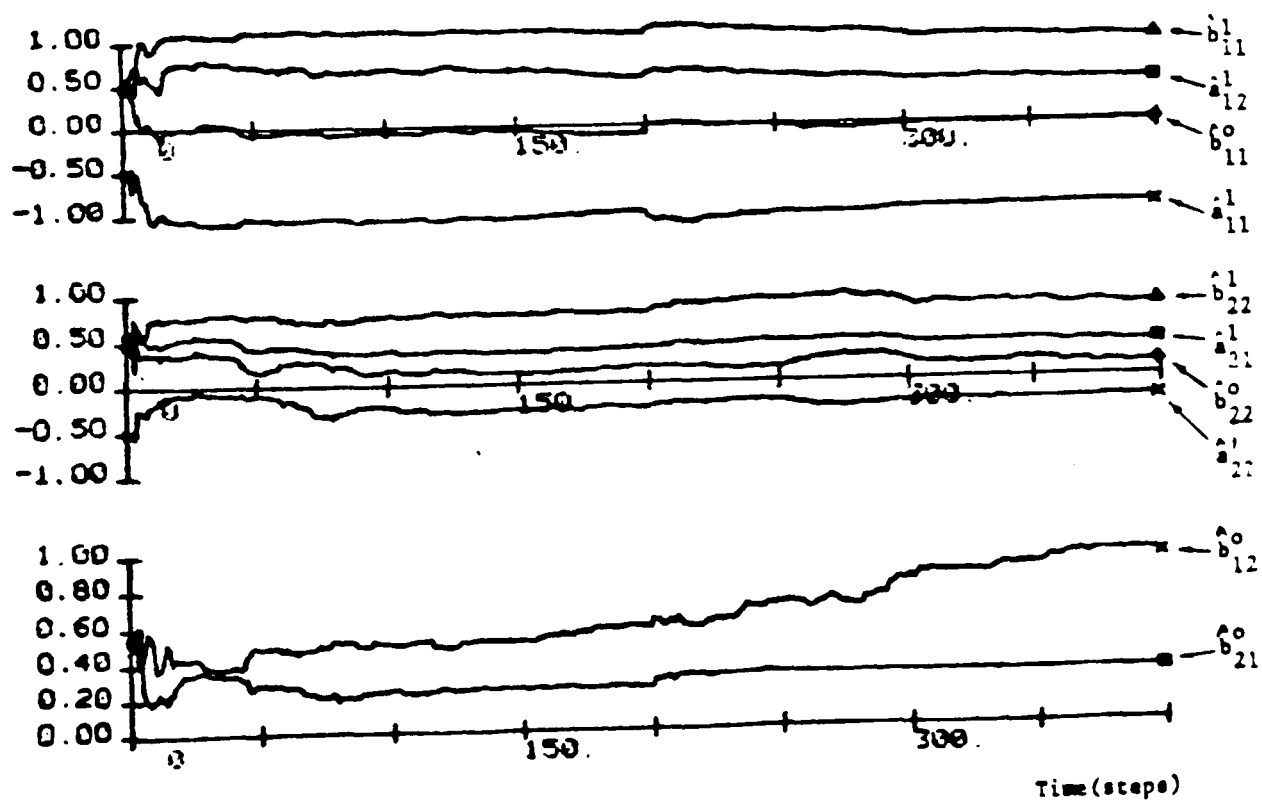


FIGURE 8-4 Estimated Parameters (Tracking)

delay may be estimated since the controller does not depend upon knowledge of k ; and (e) the delay can be different in each signal path.

8.3.7 Industrial Application

It is often true that the simplest solution to a control problem is the best in an industrial situation. The engineer would therefore choose the self-tuning regulator of Astrom and Wittenmark [65] if the discrete plant were minimum phase and the output variance was of major importance. If say the control energy was important, then the self-tuning controller of Clark and Gawthrop [74], which could involve a minor increase in complexity, could be used. Varying time delays would suggest the use of a pole placement type of self-tuner due to Wellstead, Prager and Zanker [84].

The WMV self-tuner involves greater computational complexity, however, several problems might justify its use. The control problem might be basically stochastic and multivariable in nature, as in a marine application. The optimal types of self-tuner have advantages here, particularly when the cost function has some physical significance [75]. The minimum variance types of self-tuner described above can have problems on non-minimum phase and

open loop unstable plants, as was demonstrated in the simple example. These problems are due to the control laws which form the basis of the self-tuning schemes. The WMV control law has the property of better stability. There may of course be computational and numerical difficulties in implementing more complex control laws, but although important these are not fundamental limitations.

8.4 IMPLICIT WEIGHTED MINIMUM VARIANCE SELF-TUNER

8.4.1 Introduction

An implicit self-tuning controller based on the weighted minimum variance control law, by Grimble [164], is developed for the single-input single-output non-minimum phase systems. This self-tuner has the advantages of identifying the controller parameters directly and it does not need any spectral factorization. The robustness study of this self-tuner and simulation work are possible areas for future work.

8.4.2 Plant Description

The single-input/single-output linear time invariant system is assumed to be represented by the following difference equation:

$$A(z^{-1})y(t) = z^{-k}B(z^{-1})u(t) + C(z^{-1})\xi(t) \quad (8.29)$$

The polynomials A , B and C (z^{-1} are dropped for clarity) are assumed to be of known degree n_a , n_b and n_c respectively. The zeros of $C(x)$ are strictly outside the unit disc in the x -plane. k is the known time delay (or estimated on-line). $y(t)$ is the system output, $u(t)$ is the control signal and $\xi(t)$ is the disturbance signal. The disturbance $\xi(t)$ is a sequence of normally distributed independent random sequence with zero mean and covariance $E\{\xi(t)\xi(t)\} = \sigma_\xi^2$. Polynomial B is factorized into minimum B^+ and non-minimum phase B^- spectral factors. The factorization $B = B^+B^-$ may now be defined as:

$$B^+ = b_0^+ + b_1^+z^{-1} + \dots + b_{n1}^+z^{-n1} \quad (8.30)$$

$$B^- = 1 + b_1^-z^{-1} + \dots + b_{n2}^-z^{-n2} \quad (8.31)$$

and the other polynomials are defined as:

$$A = 1 + a_1z^{-1} + \dots + a_{na}z^{-na} \quad (8.32)$$

$$C = 1 + c_1z^{-1} + \dots + c_{nc}z^{-nc} \quad (8.33)$$

8.4.3 Weighted Minimum Variance Controller

The weighted minimum variance (WMV) controller [164] which minimizes the cost function (Appendix E)

$$J = E \left\{ \psi^2(t+k)/t \right\} \quad (8.34)$$

is

$$u_0(t) = \frac{CRw(t) - Gy(t)/Pd}{(FB^+ + QC)} \quad (8.35)$$

where

$$\psi(t+k) = P'y(t+k) + Qu(t) - Rw(t) \quad (8.36)$$

where P' is defined as

$$P' = P/B^- \quad (8.37)$$

P , Q and R are weighting transfer functions, that is:

$$P = P_n/P_d \text{ etc.}$$

The polynomials F and G are determined by the diophantine equation:

$$P_n C = P_d A F + z^{-k} B^- G \quad (8.38)$$

Where F and G are of degree $n_f = k-1 + n_2$, $n_g = n_a + n_{pd}-1$ respectively, and are of the form in (8.32) and (8.33).

w is the reference signal.

It may be shown that the controller also minimizes the following equivalent function:

$$I_2 = E \left\{ (P'y(t+k) - Rw(t))^2 + (Q'u(t))^2 \right\} \quad (8.39)$$

where Q' is related to Q by a scalar [74].

The main results of WMV control are:

(a) The prediction:

$$\hat{\psi}_y(t/t-k) = \frac{H}{C} u(t-k) + \frac{G}{C} y_p(t-k) \quad (8.40)$$

(b) The remnant:

$$\psi_y(t) = \hat{\psi}_y(t/t-k) + \mathcal{E}(t) \quad (8.41)$$

(c) The control strategy:

$$\begin{aligned} \hat{\psi}(t/t-k) &= \hat{\psi}_y(t/t-k) + Qu(t-k) - Rw(t-k) \\ &= 0 \end{aligned} \quad (8.42)$$

(d) The generalized function:

$$\psi(t) = P'y(t) + Qu(t-k) - Rw(t-k) \quad (8.43)$$

where

$$\psi_Y(t) = P'y(t) = \frac{Py(t)}{B^-} \quad (8.44)$$

$$y_p(t) = y(t)/Pd \quad (8.45)$$

(e) The prediction error:

$$\xi(t/t-k) = \frac{F}{B^-} \xi(t) \quad (8.46)$$

The polynomials F and G are determined by the diophantine equation (8.38).

$$H = B^+F \quad (8.47)$$

$$= h_0 + h_1 z^{-1} + \dots + h_{nh} z^{-nh} \quad (8.48)$$

8.4.4 Implicit Self-Tuning Control

Assume the control signal $u_1(t)$, at time t , will set the prediction $\hat{\psi}_Y(t+k/t)$ equal to $Rw(t)$. Clarke and Gawthrop [76] have deduced the following results:

$$u(t) = \frac{h_0}{h_0 + Q} u_1(t) \quad (8.49)$$

where

$$\begin{aligned} h_0 &= B^+(o)F(o) \\ &= H(o) \end{aligned} \quad (8.50)$$

and

$$\hat{\psi}_Y(t/t-k) = R w(t-k) + h_0(u(t-k) - u_1(t-k)) \quad (8.51)$$

In self-tuning control, a suitable algorithm is required to be used for parameter estimation. Explicit self-tuning control identifies the plant parameters. Implicit control should identify the controller parameters directly. The equivalent form of $\psi_Y(t)$ in Clarke and Gawthrop's [76] self-tuning algorithm is used for parameter estimation. However, in this case, $\psi_Y(t)$ consists of an unstable polynomial B^- in the denominator. Furthermore, B^- is unknown. Thus, the expression in equation (8.41) is unsuitable for identification. The following technique is used instead:

Define

$$\varphi_Y(t) = B^- \psi_Y(t) \quad (8.52)$$

$$= P_Y(t) \quad (8.53)$$

From equation (8.41) and equation (8.46)

$$\varphi_Y(t) = B^- \hat{\psi}_Y(t/t-k) + B^- \varepsilon(t) \quad (8.54)$$

$$= B^- \hat{\psi}_Y(t/t-k) + \varepsilon'(t) \quad (8.55)$$

where

$$\varepsilon'(t) = F \xi(t) \quad (8.56)$$

~~$\varepsilon(t)$ in equation (8.55) is uncorrelated with the other two terms on the RHS. Hence define the prediction of $\varphi_Y(t)$ as:~~

$$\hat{\varphi}_Y(t/t-k) = B^- \hat{\psi}_Y(t/t-k) + \tilde{B}^- \varepsilon(t-1) \quad (8.57)$$

Substitute equation (8.40) for $\hat{\psi}_Y(t/t-k)$ into equation (8.55).

$$\varphi_Y(t) = B^- \left\{ \frac{H}{C} u(t-k) + \frac{G}{C} y_p(t-k) \right\} + \varepsilon'(t) \quad (8.58)$$

Multiply both sides by C and use equation (8.55) to yield:

$$\begin{aligned} \varphi_Y(t) &= B^- \left\{ Hu(t-k) + Gy_p(t-k) \right\} \\ &\quad - \tilde{C} B^- \hat{\psi}_Y(t-1/t-k-1) - \tilde{C} \varepsilon'(t-1) \\ &\quad + \tilde{C} \varepsilon'(t-1) + \varepsilon'(t) \\ &= B^- \left\{ Hu(t-k) + Gy_p(t-k) \right\} \\ &\quad - \tilde{C} B^- \hat{\psi}_Y(t-1/t-k-1) + \varepsilon'(t) \end{aligned} \quad (8.59)$$

where

$$C = 1 + z^{-1}\tilde{C} \quad (8.60)$$

or

$$\begin{aligned} \varphi_y(t) = & Hu(t-k) + Gy_p(t-k) - \tilde{C}\hat{\psi}_y(t-1/t-k-1) \\ & + \tilde{B}^- m(t-k-1) + \tilde{F}\xi(t) + \xi(t) \end{aligned} \quad (8.61)$$

where

$$\begin{aligned} \tilde{B}^- = & 1 + \tilde{B}^- z^{-1} \text{ and } F = 1 + \tilde{F}z^{-1} \\ m(t-k-1) = & Hu(t-k-1) + Gy_p(t-k-1) \\ & - \tilde{C}\hat{\psi}_y(t-2/t-k-2) \end{aligned} \quad (8.62)$$

From the control strategy (8.38)

$$\hat{\psi}_y(t/t-k) + Qu(t-k) - Rw(t-k) = 0 \quad (8.63)$$

which is equivalent to

$$\begin{aligned} Hu(t-k) + Gy_p(t-k) - \tilde{C}\hat{\psi}_y(t-1/t-k-1) \\ = Rw(t-k) - Qu(t-k) \end{aligned} \quad (8.64)$$

Thus

$$m(t-k-1) = Rw(t-k-1) - Qu(t-k-1) \quad (8.65)$$

Define

$$\hat{X}^T(t) = [u(t), y_p(t), \hat{\psi}_y(t+k-1/t-1), m(t-1), \xi(t-1)] \quad (8.66)$$

$$\underline{\theta}^T(t) = [H, G, -\tilde{C}, \tilde{B}^-, \tilde{F}] \quad (8.67)$$

Thus equation (8.58) can be written as:

$$\varphi_y(t) = X^T(t-k) \underline{\theta}(t-k) + \xi(t) \quad (8.68)$$

Similar to Clarke and Gawthrop's self-tuner, $\xi(t)$ is uncorrelated with $X(t-k)$, thence unbiased estimates are achieved.

Self-Tuning Algorithm

- Step 1: Select P, Q, R and $w(t)$. Assign n_h, n_g, n_c, n_2 (order of B^-), k and initialize the self-tuner with initial parameters and parameter error covariance matrix.
- Step 2: Calculate $\varphi_y(t) = Py(t)$, and form the information vector $X(t-k)$.
- Step 3: Identify the controller parameters using:

$$\varphi_y(t) = X^T(t-k) \underline{\theta}(t-k) + \xi(t)$$

by extended recursive least squares technique or recursive maximum likelihood technique.

Step 4: Calculate the control signal $u_1(t)$ from

$$u_1(t) = -\frac{\hat{G}}{\hat{H}} y_p(t) + \frac{\hat{C}}{\hat{H}} \hat{\psi}_Y(t+k-1/t-1)$$

Step 5: Calculate the control signal $u(t)$ from:

$$u(t) = \frac{\hat{h}_0}{\hat{h}_0 + Q} u_1(t)$$

Step 6: Approximate:

$$\hat{\xi}(t) = \varphi_Y - \hat{x}^T(t-k) \hat{\theta}(t-k)$$

Step 7: Calculate:

$$m(t-k) = R w(t-k) - Q u(t-k) + \hat{\xi}(t)$$

Step 8: Calculate $\hat{\psi}_Y(t+k/t)$ from:

$$\hat{\psi}_Y(t+k/t) = R w(t) + \hat{h}_0(u(t) - u_1(t))$$

Step 9: Return to step 2.

Special Cases:

- i) If $B^- = 1$ then $B^-m(t) = 0$, $\varphi_Y(t) = \psi_Y(t)$. This is the implicit self-tuning control developed by Clarke and Gawthrop [76]. In this case, \tilde{F} needs not to be estimated because $\tilde{F}\xi(t) = 0$.

ii) If $Q=0$, $R=0$ then $\hat{\psi}_Y(t+k-1/t-1) = \hat{\psi}(t+k-1/t-1) = 0$.

This is the implicit version of the minimum variance self-tuning controller for the non-minimum phase system which was developed by Astrom and Wittenmark [66].

iii) If $B^- = 1$, $Q=0$, $R=0$ then $B^-m(t) = 0$, $\varphi_Y(t) = \psi_Y(t)$, $\hat{\psi}_Y(t+k-1/t-1) = \hat{\psi}(t+k-1/t-1) = 0$. This class of self-tuning control is called Minimum Variance Regulator developed by Astrom and Wittenmark [65].

8.4.5 Discussion

The implicit WMV self-tuner is complex compared with Clarke and Gawthrop's GMV self-tuner. The WMV control law, in the deterministic case, is more robust than the GMV control law. However, its self-tuning version is very much dependent on the robustness of the identification algorithm. The robustness of the GMV self-tuner has been investigated extensively by Gawthrop [129] and Gawthrop and Lam [132]. The WMV self-tuner needs similar investigation in the future.

CHAPTER NINE

OVERALL CONCLUSIONS AND SUGGESTIONS FOR FUTURE WORK

9.1 OVERALL CONCLUSIONS

The work presented in this thesis is divided into two parts. Part One (Chapter One to Chapter Six) was to develop an adaptive control system for dynamically positioned vessels. Part Two (Chapter Seven and Chapter Eight) consists of a few contributions to the self-adaptive control theory.

In Part One, the control problems and the basic components of the ship positioning system were first defined, followed by the development of dynamic models for controller and filter design purposes. The models are: low frequency ship model, thruster model and high frequency wave model. The dynamic positioning control system consists of two parts: control and filtering. A LQG (Linear Quadratic Gaussian) optimal controller with integral action was developed. However, this controller requires the detailed models of the disturbances, so it may not be easily implemented. For this reason, the control scheme was simplified and the simulation results were still found to be good.

The previous contributions to the filtering problem of the dynamic positioning system were mainly from Balchen [17,18], Grimble [5,6] and their co-workers. It was found that their adaptive filtering approaches either cumbersome or the assumption on the wave model is oversimplified and the adaptive algorithm is complicated. The author has developed a novel self-tuning Kalman filter to estimate the low frequency states for feedback purposes. The scheme is relatively insensitive to the to the presence of non-linear ship dynamics and thruster non-linearities. The self-tuning filter is able to estimate implicitly the offsets between the low frequency position states and their estimates due to the constant disturbance when using the simplified LQG controller with integral action. The structure of this adaptive scheme is simple compared with those developed by the Balchen and by Grimble.

In Part Two, an adaptive technique was developed for tracking slowly varying processes which are corrupted by coloured noises. The technique has the advantage of not requiring the specification of the noise properties except the order of the noise model. Usually a second order noise model is sufficient for most applications. The adaptive tracker was found to be successful in estimating square, trapezoidal, sinusoidal and low frequency ship motion. The

results were extremely good when the process output varied linearly or near linearly.

Lastly, the published self-tuning control theory and applications were over-viewed. A multivariable explicit and single input-single output weighted minimum variance (WMV) self-tuning controller were also developed. The WMV control is stable over a wide range of control weightings in non-minimum phase systems. However, its structure is more complex compared with some other popular self-tuners. Nevertheless, it does offer an alternative in certain applications.

9.2 Suggestions for Future Work

1. It has been shown that the self-tuning Kalman filter is able to estimate the offset between position states and their estimates due to the absence of a constant disturbance model in the Kalman filter. Theoretically, this can be extended to estimate the slowly varying position estimation errors due to the low frequency model mismatch. This property needs further investigation.

2. The weighted minimum variance self-tuners require further investigation. It should be compared with LQG controllers regarding their computational efficiency and robustness. Usually, complex self-tuning control algorithms will give additional uncertainty to a control system. Simplification of the algorithms should be one of the important activities in the future.

REFERENCES

- 1 BALL, A.E. & BLUMBERG, J.M., 1975, "Development of a Dynamic Ship Positioning System", GEC J. Sci. and Technology, Vol. 42, No.1, p.29-36.
- 2 ENGLISH, J.W. & WISE, D.A., 1975, "Hydrodynamic Aspects of Dynamic Positioning", Transactions, North East Coast Inst. of Engineers and Shipbuilders, Vol. 92, No.3, p.53-72.
- 3 COMSTOCK, J.P. (Ed.), 1967, "Principles of Naval Architecture", The Soc. of Naval Architects and Marine Engineers.
- 4 URRY, P., 1981, "Internal Communication", GEC & Strathclyde University.
- 5 GRIMBLE, M.J., PATTON, R.J. & WISE, D.A., 1980, "The Use of Kalman Filtering Techniques in Dynamic Ship Positioning Systems", Proc. IEE, Vol.172, Pt.D, No.3.
- 6 GRIMBLE, M.J., PATTON, R.J. & WISE, D.A., 1980, "The Design of Dynamic Ship Positioning Control Systems Using Stochastic Optimal Control Theory", Optimal Control Applications and Methods, Vol. 1, p.167-202.

- 7 GRIMBLE, M.J., PATTON, R.J. & WISE, D.A., 1979, "The Design of Dynamic Ship Positioning Control Systems Using Extended Kalman Filtering Techniques", IEEE Oceans '79 Conference, San Diego, California, U.S.A.
- 8 FUNG, P.T.K., CHEN, Y.L., & GRIMBLE, M.J., "Dynamic Ship Positioning Control Systems design Including Non-Linear Thrusters and Dynamics", NATO Advanced study Institute on Non-Linear Stochastic Problems, May 1982 Algarve, Portugal.
- 9 CHEN, Y.L., 1981, "Internal Communication", University of Strathclyde.
- 10 GEWAY, R.P., de MULDER, E.P.H.M., & WESSELINK, A.F. "The Behaviour of the Controllable Pitch Propeller Mechanism".
- 11 WISE, D.A. & ENGLISH, J.W., 1975, "Tank and Wind Tunnel Tests for a Drill Ship with Dynamic Position Control", 7th Annual Offshore Technology Conference, Houston, Texas.
- 12 NEVILLE, E.J., 1971, "Standard Wave Spectra", National Physical Lab., Ship Division, Ship T.M. 301, p.1-5.

- 13 PIERSON, W.J. & MOSKOWITZ, L., 1964, "A Proposed Spectral Form for Fully Developed Wind Seas Based on Similarity Theory of S.A. Kitagarodskii", J. Geophysical Research, Vol. 69.
- 14 KOSTECKI, M., 1975, "About One-and-Two Dimension Stochastic Sea Surface Simulation Method", Benken-Model Symposium, London.
- 15 PATTON, R.J. & GRIMBLE, M.J., 1978, "An Investigation Into the Uses of Kalman Filtering in Dynamic Ship Positioning", Sheffield Polytechnic Research Report EEE/14/1978.
- 16 FUNG, P.T.K. & GRIMBLE, M.J., 1981, "Self-Tuning Control of Ship Positioning Systems", IEE Workshop on Theory and Application of Adaptive & Self-Tuning Control, Oxford University, also published by Peter Peregrinus Ltd., edited by C.J. Harris & S.A. Billings, 1981.
- 17 BALCHEN, J.H., JENSSEN, N.A., SAELID, S. & SINTEF, 1976, "Dynamic Positioning Using Kalman Filtering and Optimal Control Theory", Automation in Offshore Oil Field Operation, p.183-188.

- 18 BALCHEN, J.G., JENNSSEN, N.A., MATHISEN, E. & SÆLID, S., 1980, "A Dynamic Positioning System Based on Kalman Filtering and Optimal Control", Modelling, Identification and Control, Vol.1, No.3, p.135-163.
- 19 MORGAN, M.J., "Dynamic Positioning of Offshore Vessels", Appendix B, A Method of Approximating the Wave Spectrum. Division of the Petroleum Publishing Company, Tulsa, Oklahoma, (book).
- 20 JAZWINSKI, A.H., 1970 "Stochastic Processes and Filtering Theory", Academic Press, (book).
- 21 ANDERSON, B.D.O. & MOORE, J.B., 1979, "Optimal Filtering", Prentice-Hall, (book).
- 22 SORHEIM, H.R. & GALTUNG, F.L., 1977, "Wave Filter Performance Evaluation", Paper No. OTC 2869, 9th Annual Offshore Technology Conference, Houston, Texas.
- 23 CHANG, S.S.L., 1961, "Synthesis of Optimum Control Systems", McGraw Hill Book Company, (book).

- 24 TYLER, J.S. & TUTEUR, F.B., 1966, "The Use of a Quadratic Performance Index to Design Multivariable Control Systems", IEEE Trans. on Auto. Const., Vol. AC-11, No.1, Jan., pp.84-92.
- 25 CHEN, R.T.N., & SHEN, D.W.C., 1969, "Sensitivity Analysis and Design of Multivariable Regulators Using a Quadratic Performance Criterion", Pro. JACC, pp.229-238.
- 26 SOLHEIM, O.A., 1972, "Design of Optimal Control Systems with Prescribed Eigenvalues", Int. J. Control, Vol.15, No.1, pp.243-160.
- 27 GRIMBLE, M.J., 1981, "Design of Optimal Output Regulators Using Multivariable Root Loci", IEE Proc., Vol.128, Pt.D, No.2, p.41-49.
- 28 GRIMBLE, M.J., 1979, "Design of Optimal Stochastic Resulting Systems Including Integral Action", Proc. IEE, Vol.126, No.9, p.841-848.
- 29 KWAKERNAAK, H. & SIVAN, R., 1972, "Linear Optimal Control System", Wiley Interscience, (book).

- 30 MEDITCH, J.G., 1969, "Stochastic Optimal Linear Estimation and Control, McGraw Hill, (book).
- 31 KUCERA, V., 1972, "A Contribution to Matrix Quadratic Equations", IEEE Trans. AC-17, pp.344-347.
- 32 NOBLE, B., 1969, "Applied Linear Algebra", Prentice Hall, p.407, (book).
- 33 DRESSLER, R.M. & LARSON, R.E., 1969, "Computation of Optimal Control in Partially Controlled Linear Systems", IEEE Trans. Automatic Control AC-14 p.575-578.
- 34 GANTMACHER, F.R., 1959, "The Theory of Matrices, Chelsea Publishing Co., (book).
- 35 LANCASTER, P., 1969, "Theory of Matrices", Academic Press, (book).
- 36 POWER, H.M. & PORTER, B., 1970, "Necessary and Sufficient Conditions for Controllability of Multivariable Systems Incorporating Integral Feedback", Electronics Letters, Vol.6, No.25, p.815-816.

- 37 PORTER, B., & POWER, H.M., 1970, "Mode-Controllability Matrices of Multivariable Linear Systems Incorporating Integral Feedback", Electronics Letters, Vol.6, No.25, p.809-810.

- 38 PORTER, B. & POWER, H.M., 1970, "Controllability of Multivariable Systems Incorporating Integral Feedback", Electronics Letters, Vol.6, No.22, p.689-690.

- 39 PORTER, B., 1971, "Optimal Control of Multivariable Linear systems Incorporating Integral Feedback", Electronics Letters, Vol.7, No.8, p.170-172.

- 40 NEWELL,, R.B. & FISHER, D.G., 1972, "Experimental Evaluation of Optimal, Multivariable Regulatory Controllers With Model-Following Capabilities", Automatica, Vol.8, p.247-262.

- 41 PORTER, B., 1969, "Synthesis of Asymptotically Stable Linear Time-Invariant Closed-Loop Systems Incorporating Multivariable 3-term Controllers", Electronics Letters, Vol.5, No.22, p.557-558.

- 42 PORTER B., 1970, "Synthesis of Asymptotically Stable Linear Time-Invariant Closed-Loop Systems Incorporating Multivariable 3-term Controllers", Electronics Letters, Vol.6, No.8, p.251-253.
- 43 FULLER, A.T., 1976, "Feedback Control Systems With Low Frequency Stochastic Disturbances", Int. J. Control, 24 p.165-207.
- 44 KALMAN, R.E., 1960, "A New Approach to Linear Filtering and Prediction Problems", J. Basic Engineering Trans. American Society of Mechanical Engineers, Series D., Vol.82, p.35-45.
- 45 SIMPSON, A., 1970, "Linear Systems With Multivariable 3-term Controllers: Use of Matrix Pseudoinverse in Their Synthesis", Electronics Letters, Vol.6, No.12, p.374-375.
- 46 SIMPSON, A., 1970, "Synthesis of Asymptotically Stable Linear Time-Invariance Closed-Loop Systems Incorporating Multivariable 3-term Controllers", Electronics Letters, Vol.6, No.8, p.251-252.

- 47 GRIMBLE, M.J., 1978, "Relationship Between Kalman and Notch Filters Used in Dynamic Positioning Systems, *ibid*, 14, p.399.

- 48 KLEINMAN, D.L., 1969, "Optimal Control of Linear Systems With Time Delay and Observation Noise", *IEEE Trans. Automatic Control*, AC-14, p.524-527.

- 49 GRIMBLE, M.J., 1979, "Solution of the Stochastic Optimal Control Problem in the S-Domain for Systems with Time Delay", *Proc. IEE*, v.126, No.7, p.697-703.

- 50 BELANGER, R.B., 1970, "Observation and Control of Linear Systems with Constant Disturbances", *IEEE Trans. AC-15 on Automatic Control*, p.695-696.

- 51 JOHNSON, C.D., 1968, "Optimal Control of the Linear Regulator with Constant Disturbances", *IEEE Trans. on Automatic Control*, AC-13, p.416-421.

- 52 SMITH, H.W. & DAVISON, E.J., 1972, "Design of Industrial Regulators, Integral Feedback", *Proc. IEE*, Vol.119, No.8, p.1210-1216.

- 53 DAVISON, E.J. & SMITH, H.W., 1974, "A Note on the Design of Industrial Regulators: Integral Feedback and Feedforward Controllers", Automatica, Vol.10, p.329-332.
- 54 HAGANDER, P. & WITTENMARK, B., 1977, "A Self-Tuning Filter for Fixed-Lag Smoothing", IEEE Trans. on Information Theory, Vol.IT23, No.3, p.377-384.
- 55 MOIR, T.J. & GRIMBLE, M.J., 1981, "Optimal Self-Tuning Filtering, Prediction and Smoothing for Discrete Multivariable Processes", Submitted to IEEE Trans. Automatic Control, July.
- 56 PANUSKA, V., 1980, "A New Form of the Extended Kalman Filter for Parameter Estimation in Linear Systems With Correlated Noise", IEEE Trans. on Automatic Control, Vol. AC-25, No.2, p.229-235.
- 57 FUNG, P.T.K. & GRIMBLE, M.J., 1982, "Dynamic Ship Positioning Using a Self-Tuning Kalman Filter", University of Strathclyde Research Report No. EE/8/March, also appeared in IEEE Trans. Automatic Control, Special Issue on Applications of Kalman Filtering, AC-28, March 1983, p.339-350.

- 58 JACOBS, O.L.R. & PATCHELL, J.W., 1972, "Caution and Probing in Stochastic Control," Int. J. Control, Vol.16, p.189-199.
- 59 FELDBAUM, A.A., 1960, "Dual-Control Theory, I&II", Translated from Avtomatika i Telemekhamika, (Automation & Remote Control), Vol.21, No.9, p.1240-1249; Vol.21, No.11, P.1453-1464.
- 1961, "Dual-Control Theory, III & Iv", Translated from Avtomatika i Telemekhanika, Vol.22, No.1, p.3-16; Vol.22, No.2, p.129-142.
- 60 KALMAN, R.E., 1958, "Design of a Self-Optimizing Control System", Am. Soc. Mech. Engr. Trans., Vol.80, p.468-478.
- 61 MACGREGOR, J.F. & TIDWELL, P.W., 1977, "Discrete Stochastic Control with Input Constraints", Proc. IEE, Vol.124, No.8, p.732-734.
- 62 EDMUNDS, J., 1976, PhD Thesis, Control System Centre, UMIST.

- 63 PETERKA, V., 1970, "Adaptive Digital Regulation of Noisy Systems", 2nd Prague IFAC Symposium on Identification and Process Parameter Estimation.
- 64 PETERKA, V., 1972, "On Steady State Minimum Variance Control Strategy", Kybernetika, Vol.8, No.3, p.219-231.
- 65 ASTROM, K.J. & WITTENMARK, B., 1973, "On Self-Tuning Regulators", Automatica, Vol.9, p.185-199.
- 66 ASTROM, K.J. & WITTENMARK, B., 1974, "Analysis of a Self-Tuning Regulator for Non-Minimum Phase System", IFAC Symposium on Stochastic Control, Budapest.
- 67 ASTROM, K.J., BORISSON, U., LJUNG, L. & WITTENMARK, B., 1977, "Theory and Applications of Self-Tuning Regulators", Automatica, Vol.13, p.457-476.
- 68 GOODWIN, G.C., RAMADGE, P.J. & GAINES, P.E., 1979, "Discrete Time Stochastic Adaptive Control", IEEE CDC p.736-739.
- 69 ALAM, M.A. & BURHANDT, K.K., 1979, "Future Work on Self-Tuning Regulators", IEEE CDC, p.616-619.

- 70 KEVICKSKY, L., & VAJK, I., 1979, "A Self-Tuning Extremum Regulator", IEEE CDC p.69-72.

- 71 HANGOS, K.M., 1980, "Investigation of the Peterka-Type Self-Tuning Regulator by Simulation", 6th IFAC/IFIP Conference, Dusseldorf, F.R. German.

- 72 CLARKE, D.W., & HASTINGS-JAMES, R., 1972, "Design of Digital Controllers for Randomly Disturbed Systems", Proc. IEE, Vol.118, No.10, p.1503-1505.

- 73 GAWTHROP, P.J. & CLARKE, D.W., 1975, "Generalization of the Self-Tuning Regulator", Electronics Letters, Vol.11, No.2, p.40-42.

- 74 CLARKE, D.W. & GAWTHROP, P.J., 1975, "Self-Tuning Controller", Proc. IEE, Vol.122, No.9, p.929-934.

- 75 GAWTHROP, P.J., 1977, "Some Interpretations of the Self-Tuning Controller" proc. Iee, Vol.124, No.10, p.889-894.

- 76 CLARK, D.W. & GAWTHROP, P.J., 1979, "Self-Tuning Control", Proc. IEE, Vol.126, No.6, p.633-638.

- 77 ALLIDINA, A.Y. & HUGHES, F.M., 1979, "Self-Tuning Controller Steady-State Error", Electronics Letters, Vol.15, No.12, p.346-347.
- 78 GAWTHROP, P.J., 1979, "Smith's Method and Self-Tuning Control", IEE Colloquim on Smith Predictor.
- 79 ALLIDINA, A.Y. & HUGHES, F.M., 1980, "Generalized Self-Tuning Controller with Pole Assignment", Proc. IEE, Vol.127, Pt.D., No.1, p.13-18.
- 80 FUCHS, J.J., 1980, "Explicit Self-Tuning Methods", Proc. IEE, Vol.127, pt.D, No.6, p.259-264.
- 81 GRIMBLE, M.J., JOHNSON, M.A. & FUNG, P.T.K., 1980, "Optimal Self-Tuning Control Systems" Theory and Application. Part I - Introduction and Controller Design", Inst. MC Vol.2, No.3, p.115-120.
- 82 GRIMBLE, M.J., FUNG, P.T.K. & JOHNSON, M.A., 1982, "Optimal Self-Tuning Control Systems: Theory and Application", Part II: Identification and Self-Tuning", Trans. Inst. MC, Vol.4, No.1, p.25-36.

- 83 ALLIDINA, A.Y., HUGHES, F.M. & TYE, C., 1981,
"Self-Tuning Control for Systems Employing
Feedforward", Pro. IEE 128, Pt.D., p.283-291.

- 84 WELLSTEAD, P.E., PRAGER, D. & ZANKER, P., 1977, "Pole
Assignment Self-Tuning Regulator", Proc. IEE, Vol.126,
No.8, p.781-787.

- 85 WELLSTEAD, P.E., EDMUNDS, J.M. PRAGER, D. & ZANKER, P.,
1979, "Self-Tuning Pole/Zero ASSignment Regulators,
Int. J. Control, Vol.3, No.1, p.1-26.

- 86 ASTROM, K.J. & WITTENMARK, B., 1980, "Self-Tuning
Controllers Based On Pole/Zero Placement", Proc. IEE,
Vol.127, PtD., No.2, P.120-130.

- 87 WELLSTEAD, P.E. & SANOFF, S.P., 1981, "Extended
Self-Tuning Algorithm", Int. J. Control, Vol.34, No.3,
p.433-455.

- 88 KEVICZKY, L., & HETTHESSY, J., 1977, "Self-Tuning
Minimum Variance Control of IMO Discrete Time Systems",
Automatic Control Theory & Applications, Vol.5, No.1,
p.11-17.

- 89 BORISON, U., 1979, "Self-Tuning Regulators for a Class of Multivariable Systems", Automatica, Vol.15, p.209-215.
- 90 HESKETH, T., 1980, "Disturbance Rejection and Multivariable Self-Tuning Controllers", Electronics Letters, Vol.16, No.11, p.404-406.
- 91 KOIVO, H.N., 1980, "A Multivariable Self-Tuning Controller", Automatica, Vol.16, p.351-366.
- 92 PENTTINEN, J. & KOIVO, H.N., 1980, "Multivariable Tuning Regulators for Unknown Systems", Automatica, Vol.16, p.393-398.
- 93 BAYOUMI, M.M., WONG, K.Y. & EL-BAGOURY, M.A., 1981, "A Self-Tuning Regulator for Multivariable Systems", Automatica, Vol.12, No.4, p.575-592.
- 94 KEVICZKY, L., & KUMAR, K.S.P., 1981, "Multivariable Self-Tuning Regulator with Generalized Cost-Function", Int. J. Control, Vol.33, No.5, p.913-921.
- 95 LU, G.Z. & YUAN, Z.Z., 1980, "Self-Tuning Controller of IMO Discrete Time Systems", 6th IFAC/IFIP Conference, Dusseldorf, F.R. Germany.

- 96 WITTENMARK, B. & ASTROM, K.J., 1980, "Simple Self-Tuning Controllers", International Symposium on Adaptive Systems, Ruhr University, Bochum, Germany.

- 97 GAWTHROP, P.J., 1982, "Self-Tuning PI and PID Controllers", IEEE Conference on "Applications of Multivariable and Adaptive Control" at Hull University, United Kingdom.

- 98a GAWTHROP, P.J., 1982, "Using the Self-Tuning Controller to Tune PID Regulators", School of Engineering & Applied Sci. University of Sussex, Brighton, United Kingdom.

- 98b YUAN, Z.Z., 1983 "Self-Tuning PID Regulators", IFAC/IFIP Symposium on Real Time Digital Control Applications, Guadalajara, Mexico, January.

- 99 MCGREAVY, C. & GILL, P.J., 1975, "Self-Tuning State Variable Methods for D.D.C.", IEE Conference Publication No.127, Trends in On-Line Computer Control Systems, Sheffield, p.214-221.

- 100 LAM, K.P., 1980, "Implicit and Explicit Self-Tuning Controllers", D. Phil Thesis, Oxford University.

- 101 TSAY, Y.T. & SHIEH, L.S., 1981, "State-Space Approach for Self-Tuning Feedback Control with Pole Assignment", Proc. IEE, Vol.128, Pt.D., No.3, p.93-101.

- 102 WARWICK, K., 1981, "Self-Tuning Regulators - A State Space Approach", Int. J. Control, Vol.33, No.5, p.839-858.

- 103 GAWTHROP, P.J. & CLARKE, D.W., 1980, "Hybrid Self-Tuning Control and Its Interpretation", University of Oxford, Dept. of Engineering Sci. Report No. 1331/80. Presented at 3rd IMA Conference on Control Theory, University of Sheffield, Sept. 1980.

- 104 GAWTHROP, P.J., 1980, "Hybrid Self-Tuning Control", Proc. IEE, Vol.127, Pt.D, No.5, p.229-236.

- 105 HAGANDER, P. & WITTENMARK, B., 1977, "A Self-Tuning Filter for Fixed-Lag Smoothing", IEEE Trans. on Automatic Theory, Vol. IT-23, No.3, p.377-384.

- 106 LEDWICH, G. & MOORE, J.B., 19 , "Multivariable Self-Tuning Filters", University of Newcastle, Newcastle, New South Wales, Australia, p.345-375.

- 107 MOIR, T.J., 1981, "On Self-Tuning Smoothing for Discrete Linear Multivariable Processes", Sheffield City Polytechnic Report No. EEE/78/1981.
- 108 WITTENMARK, B., 1974, "A Self-Tuning Predictor", IEEE Trans. on Automatic Control, Vol. AC-19, No.6, p.48-51.
- 109 TANTTU, J.T., 1980, "A Self-Tuning Predictor for a Class of Multivariable Stochastic Processes", Int. J. Control, Vol.32, No.2, p.359-370.
- 110 HAMZA, M.H. & SHIERAH, M.A., 1978, "A Self-Tuning Regulator for Distributed Parameter Systems", Automatica, Vol.14, p.453-463.
- 111a ANBUMANI, K., SARMA, I.G. & PATNAIK, L.M., 1981, "Self-Tuning Control of Non-Linear Systems Characterized by Hammerstein Models", Proceedings, IFAC Congress, Kyoto, Japan.
- 111b KEVICZKY L. & VAJK, I., 1979, " A Self-Tuning Extremal Controller for Generalized Hammerstein Model", 5th IFAC Symp. on System Identification, p.1147-1151.

- 112 FORTESCUE, T.R., KERSHENBAUM, L.S. & YDSTIE, B.E.,
1981, "Implementation of Self-Tuning regulators with
Variable Forgetting Factors", Automatica, 17 p.831-835.

- 113 OSORIO CORDERO, A. & MAYNE, D.Q., 1981, "Deterministic
Convergence of a Self-Tuning Regulator with Variable
Forgetting Factor", Proc., IEE, Vol.128, Pt.D, No.1,
p.19-23.

- 114 LOZANO LEAL R., 1981, "Adaptive Control with Forgetting
Factor", Proceedings, IFAC Congress, Kyoto, Japan.

- 115 GOODWIN, G.C., ELLIOTT, H. & TEOH, E.K., 1983,
"Deterministic Convergence of a Self-Tuning Regulator
with Covariance Resetting", Proc. IEE, Vol.130, Pt.D,
No.1, p.6-8.

- 116 WIESLANDER, J. & WITTENMARK, B., 1971, "An Approach to
Adaptive Control Using Real Time Identification",
Automatica, Vol.7, p.211-217.

- 117 LJUNG, L. & WITTENMARK, B., 1974, "Asymptotic
Properties of Self-Tuning Regulators", Report T404,
Div. of Automatic Control, Lund Inst. of Technology.

- 118 LJUNG, L. & WITTENMARK, B., 1974, "Analysis of a Class of Adaptive Regulators", proceedings IFAC Stochastic Control Symposium, Budapest.
- 119 LJUNG, L., SODERSTROM, T. & GUSTAVSSON, I., 1975, "Counter Examples to General Convergence of a Commonly Used Recursive Identification Method", IEEE Trans. on Automatic Control, Vol. AC-20, No.5, p.643-652.
- 120 LJUNG, L., 1977, "Analysis of Recursive Stochastic Algorithms", IEE Trans. on Automatic Control, Vol. AC-22, No.4, p.551-575.
- 121 LJUNG, L., 1977, "On Positive Real Transfer Functions and the Convergence of Some Recursive Schemes", IEEE Trans. on Automatic Control, Vol AC-22, No.4, p.539-550.
- 122 LJUNG, L. & WITTENMARK, B., 1978, "On a Stabilizing Property of Adaptive Regulators", Identification and System Parameter Estimation, Rajbman (ed.) North-Holland Publishing Co.
- 123 SODERSTROM, T., LJUNG, L. & GUSTAVSSON, I., 1978, "A Theoretical Analysis of Recursive Identification Methods", Automatica, Vol.14, p.231-244.

- 124 MORSE, A.S., 1979, "Global Stability of Parameter-Adaptive Control Systems", IEEE, CDC, p.1041-1045.

- 125 LANDAU, I.D., 1976, "Unbiased Recursive Identification Using Model Reference Adaptive Techniques", IEEE Transactions on Automatic Control, Vol.AC-21, No.2, p.194-202.

- 126 LANDAU, I.D., 1978, "An Addendum to Unbiased Recursive Identification Using Model Reference Adaptive Techniques", ibid AC-23, p.97-99.

- 127 KURZ, H., ISERMANN, F. & SCHUMANN, R., 1980, "Experimental Comparison and Application of Various Parameter - Adaptive Control Algorithms", Automatica, Vol.16, p.117-133.

- 128 ASTROM, K.J., 1980, "Robustness of a Design Method Based on Assignment of Poles and Zeros", IEEE Trans. on Automatic Control, Vol. AC-25, No.3, p.588-591.

- 129 GAWTHROP, P.J., 1980, "On the Stability and Convergence of a Self-Tuning Controller", Int. J. Control, Vol.31, No.5, p.973-998.

- 130 TSYPKIN, Y.Z., AVEDYAN, E.D. & GULINSKIY, O.V., 1981, "On Convergence of the Recursive Identification Algorithms", IEEE Trans. on Automatic Control, Vol.AC-26, No.5, p.1009-1017.

- 131 FUCHS, J.J.J., 1981, "Recursive Least-Squares Algorithm Revisited", Proc. IEE, Vol.128, Pt.D, No.2, p.74-76.

- 132 GAWTHROP, P.J. & LIM, K.W., 1982, "Robustness of Self-Tuning Controllers", Proc. IEEE Vol.129, Pt.d, No.1, p.21-29.

- 133 JENSEL L. & HANSEL, R., 1974, "Computer Control of an Enthalpy Exchanger", Report 7417, Lund Institute of Technology, Sweden.

- 134 CEGRELL, T. & HEDQVIST, T., 1975, "Successful Adaptive Control of Paper Machines", Automatica, Vol.11, p.53-59.

- 135 BORISSON, U. & SYDING, R., 1976, "Self-Tuning Control of an Ore Crusher", Automatica, Vol.12, p.1-17.

- 136 SASTRY, V.A., SEBORG, D.E. & WOOD, R.K., 1977, "Self-Tuning Regulator Applied to a Binary Distillation Column", Automatica, Vol.13, p.417-424.

- 137 MORRIS, A.J., FENTON, T.P. & NAZER, Y., 1977,
"Application of Self-Tuning Regulators to the Control
of Chemical Processes", Digital Computer Applications
to Process Control, Van Nauta Lemke, ed., IFAC and
North-Holland Publishing Co., p.447-455.
- 138 ASTROM, K.J., 1978, "Applications of Self-Tuning
Regulators", SRC Summer Vacation School, Warwick, U.K.
- 139 AMARAL, W.C., MAGALHAES, L.P. & MENDES, M.J., 1978,
"Implementation of Self-Tuning Regulators in a
Mini-Computer", Dept. of Electrical Engineering,
Unicamp, Brazil.
- 140 DUMONT, G.A. & BELANGER, P.R., 1978, "Self-Tuning
Control of a Titanium Dioxide Kiln", IEEE Trans. on
Automatic Control, Vol. AC-23, No. 4, p.532-538.
- 141 KALLSTROM, C.G., ASTROM, K.J., THORELL, N.E., ERIKSSON,
J. & STEN, L., 1978, "Adaptive Autopilots for Large
Tankers", Proc. IFAC World Congress, Helsinki.
- 142 KEVICZKY, L., HETTHESSY, J., HILGER, M. &
KOLOSTORI, J., 1978, "Self-Tuning Adaptive Control of
Cement Raw Material Blending", Automatica, Vol.14,
p.525-532.

- 143 ZANKER, P.M. & WELLSTEAD, P.E., 1978, "On Self-Tuning Diesel Engine Governors", Control Systems Centre Report No.422, Control Systems Centre, UMIST.

- 144 BAYOUMI, M.M. & EL-BAGOURY, M.A., 1979, Comments on "Self-Tuning Adaptive Control of Cement Raw Material Blending", Automatica, Vol.15, p.693-694.

- 145 BUCHHOLT, F. & KUMMEL, M., 1979 "Self-Tuning Control of a pH-Neutralization Process", Automatica, Vol.15, p.665-671.

- 146 CLARKE, D.W., & GAWTHROP, P.J., 1979, "Implementation and Application of Microprocessor-Based Self-Tuners", IFAC, Darmstadt, p.1-12.

- 147 SEBORG, D.E. & WOOD, R.K., 1979, A Reply to "Comments on Self-Tuning Regulator Applied to a Binary Distillation Column", Automatica, Vol.15, p.225.

- 148 TOIVONEN, H. & WESTERLUND, T., 1979, "Comments on Self-Tuning Regulator Applied to a Binary Distillation Column", Automatica, Vol.15, p.223-224.

- 149 TOIVONEN, H. & WESTERLUND T., 1979, "Reply by Toivonen and Westerlund", Automatica, Vol.15, p.226.

- 150 ZANKER, P.M. & WELLSTEAD, P.E., 1979, "Practical Features of Self-Tuning", Trends On-Line Computer Control Systems Conference", Sheffield, p.160-164.

- 151 ASTROM, K.J., 1980, "Self-Tuning Control of a Fixed-Bed Chemical Reactor System", Int. J. Control, Vol.32, No.2, p.221-256.

- 152 CLARKE, D.W., 1980, "Some Implementation Considerations of Self-Tuning Controllers", Numerical Techniques for Stochastic System, edited by F. Archetti and M. Cugiani, North-Holland.

- 153 KAHLQVIST, S.A., 1980, "Application of Self-Tuning Regulators to the Control of Distillation Columns", 6th IFAC/IFIP Conference, Dusseldorf, F.R. Germany.

- 154 HARRIS, T.J. & MACGREGOR, J.F., 1980, "Self-Tuning and Adaptive Controllers - An application to Catalytic Reactor Control", Techometrics, Vol.22, No.2, p.153-164.

- 155 YUAN, Z.Z., LU, G.Z. & WANG, X.F., 1980, "Self-Tuning Adaptive Control of Two Installations in Chemical Industry", 6th IFAC/IFIP Conference, Dusseldorf, F.R. Germany.
- 156 ALLIDINA, A.Y., HUGHES, F.M. & TYP, C., 1981, "Self-Tuning Control of a Nuclear Reactor", International Conference on Control and its Applications, University of Warwick, IEE Conference Publication No.194
- 157 BUCHHOLT, F. & KUMMEL, M., 1981, "A Multivariable Self-Tuning Regulator to Control a Double Effect Evaporator", Automatica, Vol.17, No.5, p.737-743.
- 158a DEXTER, A.L., 1981, "Self-Tuning Optimum Start Control of Heating Plant", Automatica, Vol.17, No.3, p.483-492.
- 158b LU, G.Z., 1981, "Self-Tuning Controller with Application to a Distillation Column", Triennial World Congress, Kyoto, Japan, August.
- 158c YUAN, Z.Z., LU, G.Z., & WANG, X.F., 1981, "Application of Self-Tuning Regulators to Chemical and Cement Industry, IFAC 8th Triennial World Congress, Kyoto, Japan, August.

- 159 MORRIS, A.J. & NAZER, Y., 19 , "Multivariable Self-Tuning Control Theory and Experimental Evaluation".
- 160 KOIVO, A.J. & GUO, T.H., 1983, "Adaptive Linear Controller for Robotic Manipulators", IEEE Trans. on Automatic Control, Vol.AC-28, No.2, p.162-171.
- 161 HARRIS, C.J. & BILLINGS, S.A., 1981, "Self-Tuning and Adaptive Control: Theory and Application", Peter Peregrinus Ltd.
- 162 DONGHUE, J.F., 1977, "A Comparison of the Smith Predictor and Optimal Design Approaches for Systems with Delay in the Control", IEEE Trans. on Industrial Electronics and Control Instrumentation, Vol.IECI-24, No.1.
- 163 ASTROM, K.J., 1980, "Private Communication"
- 164 GRIMBLE, M.J., 1981, "A Control Weighted Minimum-Variance Control for Non-Minimum Phase Systems", Int. J. Control, Vol.33, No.4, p.751-762.

- 165 GRIMBLE, M.J., MOIR, T.J. & FUNG, P.T.K., 1982,
"Comparison of WMV and LQG Self-Tuning Controllers",
IEEE Symposium on Multivariable Stochastic Control
Theory, Hull, U.K.

- 166 FUNG, P.T.K., 1978, "PID Tuning and Simulation", MSC
Design Report, Control Systems Centre, UMIST.

- 167 CADZOW, J.A., 1973, "Discrete Time Systems: An
Introduction with Inter-Disciplinary Applications",
Englwood Cliffs, N.J., Prentice Hall, (book).

- 168 BOZIC, S.M., 1979, "Digital and Kalman Filtering",
London" Arnold, p.8, (book).

- 169 ASTROM, K.J., 1970, "Introduction to Stochastic Control
Theory", Academic Press, 1970, (book).

APPENDIX ATRANSFER FUNCTION WAVE MODELS FOR VARIOUS SEA CONDITIONSTABLE A-1

Beaufort No.	$h_{1/3}(m)$	K	ζ_1	β_1	ζ_2	β_2	ω_{n1}	ω_{n2}
5	2.74	0.52	0.50	0.77	0.24	0.70	0.93	0.74
6	4.24	0.92	0.41	0.61	0.18	0.57	0.73	0.58
7	5.73	1.38	0.36	0.54	0.15	0.48	0.65	0.51
8	7.47	1.95	0.31	0.49	0.14	0.42	0.58	0.49
9	9.24	2.60	0.28	0.45	0.13	0.37	0.54	0.38

$h_{1/3}$ - significant wave height (metres)*

- * The significant wave height $h_{1/3}$ is defined by taking 99 waves, choosing the 33 largest waves and then calculating one-third of the peak-to-peak magnitude of these waves.

The fourth order model transfer function is:

$$G(s) = \frac{4 \zeta_1 \zeta_2 K^2 s^2}{(s^2 + 2 \zeta_1 s + \omega_{n1}^2) (s^2 + 2 \zeta_2 s + \omega_{n2}^2)}$$

or

$$G(s) = \frac{K' s^2}{(s^4 + \alpha_1 s^3 + \alpha_2 s^2 + \alpha_3 s + \alpha_4)}$$

where

$$\alpha_1 \triangleq 2(\zeta_1 + \zeta_2), \alpha_2 \triangleq (\omega_{n1}^2 + \omega_{n2}^2)$$

$$\alpha_3 \triangleq 2(\zeta_1 \omega_{n2}^2 + \zeta_2 \omega_{n1}^2), \alpha_4 \triangleq \omega_{n1}^2 \omega_{n2}^2$$

$$\text{and } K' = 4 \zeta_1 \zeta_2 K^2$$

The signal flow graph for the system in companion form is shown in Figure A-1.

The characteristic polynomial of the companion form state-space representation is the fourth order s polynomial of the scalar transfer function $G(s)$ above, so that the frequency system F_h matrix is given by:

$$F_h = \begin{bmatrix} 0 & T_b & 0 & 0 \\ 0 & 0 & T_b & 0 \\ 0 & 0 & 0 & T_b \\ -\alpha_4 & -\alpha_3 & -\alpha_2 & -\alpha_1 \end{bmatrix} \quad \text{where } T_b = 3.104 \text{ secs}$$

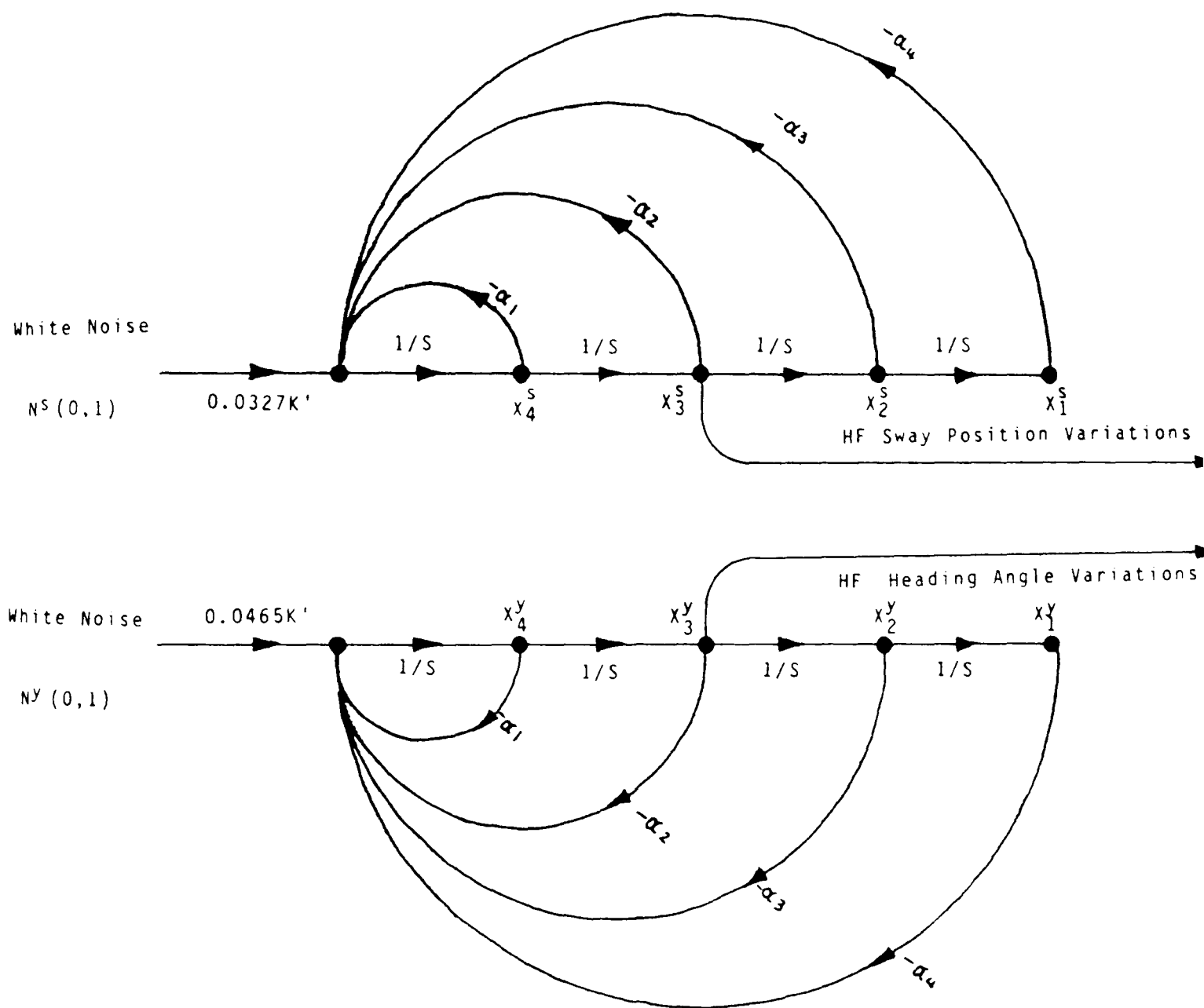


FIGURE A-1 Sway and Yaw High Frequency Model Flow Graphs

The coefficients α and overall gain constants K' may be tabulated as follows (Table A-2) for the range of sea state conditions corresponding to Beaufort scale numbers 5 to 9 and for time scale factor of 3.104:

TABLE A-2

Beaufort No.	1	2	3	4	K
5	4.594	4.384	2.988	1.470	0.403
6	3.663	2.698	1.452	0.556	0.776
7	3.166	2.119	0.974	0.341	1.277
8	2.794	1.789	0.754	0.251	2.049
9	2.545	1.353	0.486	0.131	3.055

It is convenient to transfer the scalar gain K' into the D_h matrix so that the overall matrix H_h for both sway and yaw is:

$$H_h = \begin{bmatrix} 0 & 0 & 1.0 & 0 & 0 & 0 & 0 & 0 \\ 0 & 0 & 0 & 0 & 0 & 0 & 1.0 & 0 \end{bmatrix}$$

The G_h matrix must then contain the gain K' divided by suitable scaling factors.

The normalizing factor for sway position measurement is L_{pp} (see Appendix B). Thus the noise input to sway motion has unit variance, but is scaled by the factor:

$$K'/L_{pp} = K'/94.49 \text{ (for Wimpey Scalab)}$$

The output of this high frequency yaw angle motions must be in per-unit of angle, that is in radians. The approximation is also made that the vessel dynamics have a constant attenuation of 0.885 at the high frequencies considered, so that the yaw scaling factor is:

$$K'(0.855)/57 = 0.0465K'$$

where it must be noted that K' has previously been normalized with respect to time.

The resulting G_h matrix for the combined high frequency sway and yaw motions is:

$$G_h = \begin{bmatrix} 0 & 0 \\ 0 & 0 \\ 0 & 0 \\ K'L_{pp} & 0 \\ 0 & 0 \\ 0 & 0 \\ 0 & 0 \\ 0 & 0.0465K' \end{bmatrix}$$

An alternative 4th order approximate HF model can be derived which has the following companion form:

$$F_h = \begin{bmatrix} 0 & 1 & 0 & 0 \\ 0 & 0 & 1 & 0 \\ 0 & 0 & 0 & 1 \\ -\epsilon^4 & -2\sqrt{2}\epsilon^3 & -4\epsilon^2 & -2\sqrt{2}\epsilon \end{bmatrix}$$

The corresponding transfer function is:

$$G(s) = \frac{K's^2}{(s^2 + \sqrt{2}\epsilon s + \epsilon^2)(s^2 + \sqrt{2}\epsilon s + \epsilon^2)}$$

$$\text{where } K' = 25.33 \left\{ \frac{A}{B^{1/4}} \right\}^{1/2}$$

$$\text{and } \epsilon = 5B^{1/4}$$

Table A-3 shows the variation of gain K' and parameter ϵ for Beaufort numbers 5 to 9. The corresponding significant wave height ($h_{1/3}$) and Pierson-Moskowitz parameters A and B are also shown.

TABLE A-3

Beaufort No.	$h_{1/3}$ (M)	K'	A	B	ϵ
5	2.74	1.58	5×10^{-4}	2.66×10^{-4}	0.640
6	4.24	1.77	5×10^{-4}	1.11×10^{-4}	0.513
7	5.73	1.91	5×10^{-4}	6.08×10^{-5}	0.441
8	7.47	2.04	5×10^{-4}	3.58×10^{-5}	0.386
9	9.24	2.15	5×10^{-4}	2.34×10^{-5}	0.347

Table A-4 shows the resulting time scaled state-space coefficients for the model for time scale factor of 3.104.

TABLE A-4

Beaufort No.	α_1	α_2	α_3	α_4	K'
5	5.60	5.09	2.30	0.51	1.58
6	4.50	3.27	1.18	0.21	1.77
7	3.87	2.41	0.75	0.12	1.91
8	3.39	1.85	0.51	0.07	2.04
9	3.05	1.49	0.37	0.05	2.15

The system eigenvalues for this model are all complex conjugate and given by:

$$\begin{aligned}\lambda_{1,2} = \lambda_{3,4} &= -\frac{\sqrt{2}}{2} \alpha \pm 1/2 \left\{ 2\alpha^2 - 4\alpha^2 \right\}^{1/2} \\ &= -\frac{\sqrt{2}}{2} \alpha \left\{ 1 \pm j^1 \right\}\end{aligned}$$

APPENDIX B

WIMPEY SEALAB PER UNIT SYSTEM SPECIFICATIONS

Mass $m = 5670$ tonne

Length L_{pp} (between perpendiculars) = 94.49 m

Acceleration $g = 9.81 \text{ m}\cdot\text{sec}^{-2}$

Time $\sqrt{\frac{L_{pp}}{g}} = 3.104 \text{ sec.}$

Velocity $\sqrt{L_{pp}g} = 30.44 \text{ m}\cdot\text{sec}^{-1}$

Force $Mg = 5670(9.81) = 55,620 \text{ KN}$

Moment $MgL_{pp} = 5,256,000 \text{ KN}\cdot\text{m}$

Angular Velocity $\sqrt{\frac{g}{L_{pp}}} = 0.3222 \text{ rad}\cdot\text{sec}^{-1}$

Radius of gyration in yaw $k_{zz} \simeq 0.25 L_{pp}$
 $\simeq 0.243 \text{ p.u.}$

0/5/mcl749/51

Vessel's attenuation to high frequency motions in yaw =
0.855.

$$\begin{aligned} &\approx \frac{0.855}{57} (3.104) \text{ p.u.} \\ &= 0.0466 \text{ p.u.} \end{aligned}$$

per unit scale factor

$$\text{for sway HF noise} = \frac{3.104}{L_{pp}} = \frac{3.104}{94.49} = 0.0327 \text{ p.u.}$$

APPENDIX CDISCRETE KALMAN GAIN MATRIX COMPUTATION

The position measurements are not defined in continuous form but are sampled at regular intervals. The system simulation and the Kalman filter have both been modelled using their discrete forms. The resulting discrete equations are as follows:

$$\underline{x}(k+1) = \underline{\Phi}(k+1, k) \underline{x}(k) + \underline{\Psi} \underline{u}(k) + \underline{\Gamma} \underline{\omega}(k) \quad (C-1)$$

$$\underline{z}(k) = C \underline{x}(k) + \underline{v}(k) \quad (C-2)$$

with

$$E\{\underline{\omega}(k)\} = 0 \quad E\{\underline{\omega}(k) \underline{\omega}^T(m)\} = Q \delta_{km} \quad (C-3)$$

$$E\{\underline{v}(k)\} = 0 \quad E\{\underline{v}(k) \underline{v}^T(m)\} = R \delta_{km} \quad (C-4)$$

and where δ_{km} is the Kronecker delta function. The matrices $\underline{\Psi}$ and $\underline{\Gamma}$ are related to their continuous-time counterparts by:

$$\underline{\Psi} = \int_0^{\tau_1} \underline{\Phi}(\tau) B \, d\tau \quad (C-5)$$

$$\underline{\Gamma} = \int_0^{\tau_1} \underline{\Phi}(\tau) D \, d\tau \quad (C-6)$$

and

$$\underline{\Phi}(k+1, k) \triangleq \underline{\Phi}(\tau_1) = e^{A\tau_1} \quad (C-7)$$

where τ_1 is the sampling interval, matrices A, B and D are the continuous time counterparts of $\underline{\Phi}$, $\underline{\Psi}$ and $\underline{\Gamma}$.

The state estimate is given by calculating the predicted state

$$\hat{\underline{x}}(k+1/k) = \underline{\Phi}(k+1, k) \hat{\underline{x}}(k/k) \quad (C-8)$$

and then calculating the estimated state at the instant (k+1), using

$$\hat{\underline{x}}(k+1/k+1) = \hat{\underline{x}}(k+1/k) + K(k+1)(z(k+1) - C\hat{\underline{x}}(k+1/k)) \quad (C-9)$$

The Kalman gain matrix $K(k+1)$ can be obtained, first by calculating the predicted error covariance matrix:

$$P(k+1/k) = \underline{\Phi}(k+1, k) P(k/k) \underline{\Phi}^T(k+1, k) + \underline{\Gamma} Q \underline{\Gamma}^T \quad (C-10)$$

for some initial error covariance $P(k/k)$, and then calculating

$$K(k+1) = P(k+1/k) C^T [C P(k+1/k) C^T + R]^{-1} \quad (C-11)$$

Finally, the error covariance matrix is obtained using

$$P(k+1/k+1) = (I-K(k+1)C)P(k+1/k) \quad (C-12)$$

The above equations can be used iteratively to obtain the state estimate at any future sampling time, given the initial state and covariance.

APPENDIX DA RECURSIVE ALGORITHM FOR SMOOTHING AND
PREDICTION OF A SIGNAL

The Algorithm for tracking the error $y_1(t)$ based on the estimated position error $y_1(t/t-1)$, for the i th channel [167,168] becomes

$$\tilde{y}_{1i}^p(t) = \tilde{y}_{1i}^*(t-1) + T\dot{\tilde{y}}_{1i}^*(t-1) \quad (D-1)$$

$$\tilde{y}_{1i}^*(t) = \tilde{y}_{1i}^p(t) + k_{1i} [\hat{y}_{1i}(t/t-1) - \tilde{y}_{1i}^p(t)] \quad (D-2)$$

$$\dot{\tilde{y}}_{1i}^*(t) = \dot{\tilde{y}}_{1i}^*(t-1) + \frac{k_{2i}}{T} [\hat{y}_{1i}(t/t-1) - \tilde{y}_{1i}^p(t)] \quad (D-3)$$

where

T sampling interval

k_{1i} constant less than unity

k_{2i} constant less than unity

$\tilde{y}_{1i}^p(t)$ predicted position

$\tilde{y}_{1i}^*(t)$ updated position error

0/5/mcl749/56

$\dot{\tilde{y}}_{1i}^*(t)$ updated velocity error

$\hat{\tilde{y}}_{1i}(t/t-1)$ estimated position error from the self-tuning
filter.

APPENDIX EWEIGHTED MINIMUM VARIANCE CONTROLLER DERIVATIONDiscrete-Time Plant

The time-invariant single-input/single-output plant is assumed to be represented either by the control autoregressive moving average equation:

$$A(z^{-1})y(t) = z^{-k}B(z^{-1})u(t) + C(z^{-1})\xi(t) \quad (E-1)$$

where z is the forward shift operator $z^k y(t) = y(t+k)$ and t is the sampling state. The order of the system is n and the time-delay is an integer number of sample intervals ($k \geq 1$). This definition of k implies that b_0 is non-zero. The polynomials A , B and C have the form:

$$A(z^{-1}) = 1 + a_1 z^{-1} + \dots + a_n z^{-n_a} \quad (E-2)$$

$$B(z^{-1}) = b_0 + b_1 z^{-1} + \dots + b_n z^{-n_b}, \quad (b_0 \neq 0) \quad (E-3)$$

$$C(z^{-1}) = 1 + c_1 z^{-1} + \dots + c_n z^{-n_c} \quad (E-4)$$

The disturbance $\xi(t)$ is a weak stationary sequence of uncorrelated random variables with zero mean. The delay k and an upper bound n to the orders of A , B and C (denoted

n_a, n_b, n_c) are assumed known. Owing to the physical realizability, the discrete closed-loop system must contain at least one step delay; thus $k \geq 1$. The delay k is equal to the magnitude of the pole excess $k - n_a - n_b$ which appears explicitly when the backward shift operator is used. The polynomial C may, without loss of generality, be taken not to have roots outside or on the unit circle in the z -plane. This statement may be justified using the representation and spectral factorization theorems. z^{-1} will be dropped in the following polynomials for clarity.

Weighted Minimum-variance Controller

The controller derived below will be termed the weighted minimum-variance controller and must minimize the performance criterion:

$$J_1 = E \left\{ (Py(t+k) - Rw(t))^2 + (Q'u(t))^2/t \right\} \quad (E-5)$$

Let $y'(t) \triangleq P(z^{-1}y(t))$ where

$$P = \frac{\tilde{B}^- P_n}{B^- P_d} \quad (E-6)$$

Note that B^- and \tilde{B}^- are reciprocal polynomials and thus they do not affect the steady state variance of $Py(t+k)$. The

weighting polynomial P_d will always be chosen so that $1/P_d$ is stable. To define a predictor introduce the following diophantine equation:

$$\tilde{B}^- P_n C = P_d A F + z^{-k} B^- G \quad (E-7)$$

where F and G are of degree $k-1+n_b^-$ and $n_a+n_{pd}-1$, respectively (assuming $n_{pn} + n_c \leq n_{pd}+n_a+k-1$). Thus,

$$\begin{aligned} y'(t+k) &= \frac{PC}{A} \xi(t+k) + \frac{PB}{A} u(t) \\ &= \frac{F}{B} \xi(t+k) + \frac{G}{A} u(t) + \frac{G\xi(t)}{AP_d} \end{aligned}$$

but from (E-1)

$$\begin{aligned} y'(t+k) &= \frac{F}{B} \xi(t+k) + \frac{G}{P_d} y(t) \\ &\quad + \frac{B^+}{CP_d A} \left\{ \tilde{B}^- P_n - z^{-k} B^- G \right\} u(t) \end{aligned} \quad (E-8)$$

Recall that $z^k F/B^-$ may be expanded as a convergent series, $|z| < 1$, of the form:

$$z^k F/B^- = \alpha_1 z + \alpha_2 z^2 + \dots$$

Thus, the first term in (E-8) represents an unpredictable random sequence.

The k steps ahead predictor follows from (E-8) as:

$$\hat{y}'(t+k/t) = \frac{G}{P_d C} y(t) + \frac{B^+ F}{C} u(t) \quad (E-9)$$

The prediction error is given by

$$\xi'(t+k/t) = y'(t+k) - \hat{y}'(t+k/t) = \frac{F}{B^-} \xi(t+k) \quad (E-10)$$

where $\xi'(t+k/t)$ depends upon future values of the disturbance signal. It follows that $\xi'(t+k/t)$ is uncorrelated with all $y(t-i)$, and $u(t-i)$ values for $i \geq 0$. Since $\xi(t)$ is zero mean it also follows that the prediction error is uncorrelated with $w(t)$ which is known at time t . Let $\sigma_1^2 \triangleq E(\xi'(t+k/t)^2/t)$ then the performance criterion may be simplified as:

$$\begin{aligned} J_1 &= E \left\{ (\hat{y}'(t+k/t) + \xi(t+k/t) - R w(t))^2 + (Q' u(t))^2/t \right\} \quad (E-11) \\ &= E \left\{ (\hat{y}'(t+k/t) - R w(t))^2 + (Q' u(t))^2/t \right\} + \sigma_1^2 \end{aligned}$$

The necessary condition for optimality may be derived by noting that $(\hat{y}'(t+k/t) - R w(t))$ is known at time t ,

$$\frac{\partial J_1}{\partial u(t)} = 2(\hat{y}'(t+k/t) - R w(t)) \frac{\partial y'}{\partial u(t)} + 2Q' q'_0 u(t) = 0 \quad (E-12)$$

where q'_0 is the coefficient of z^0 in the power series expansion of Q' . Note that

$$\frac{\partial y'}{\partial u(t)} = \left(\frac{B^+ F}{C} \right)(0) = b_0 \quad (E-13)$$

since $B^+(0) = b_0, F(0) = 1$ and $C(0) = 1$. Define the transfer function $Q = Q'q/b_0$ then the condition for optimality becomes:

$$\hat{y}'(t+k/t) + Qu(t) - Rw(t) = 0 \quad (E-14)$$

The second partial derivative of J_1 with respect to $u(t)$ is always positive which confirms that (E-14) is also a sufficient condition for optimality. The optimal control law follows as:

$$u_0(t) = -(\hat{y}'(t+k/t) - Rw(t))/Q \quad (E-15)$$

An alternative expression for the optimal control may be derived as follows. From (E-9) and E-14):

$$(1 + \frac{B^+F}{CQ})u(t) = \frac{-G}{P_d CQ} y(t) + \frac{R}{Q} w(t)$$

or

$$u_0(t) = \frac{CRw(t) - Gy(t)/P_d}{(FB^+ + QC)} \quad (E-16)$$

It may easily be shown that this controller also minimizes the following equivalent cost function:

$$J = E \left\{ \phi_1(t+k)^2/t \right\} \quad (E-17)$$

where

$$\phi_1(t+k) = Py(t+k) + Qu(t) - Rw(t) \quad (E-18)$$

The performance of the weighted minimum variance controller is compared with the generalized minimum variance controller using the example treated by both Astrom and Wittenmark [66] and Clarke and Gawthrop [74]. The results are shown in Figure E-1 and E-2.

$$(1 - 0.95z^{-1})y(t) = z^{-2}(1 + 2z^{-1})u(t) + (1 - 0.7z^{-1})\xi(t)$$

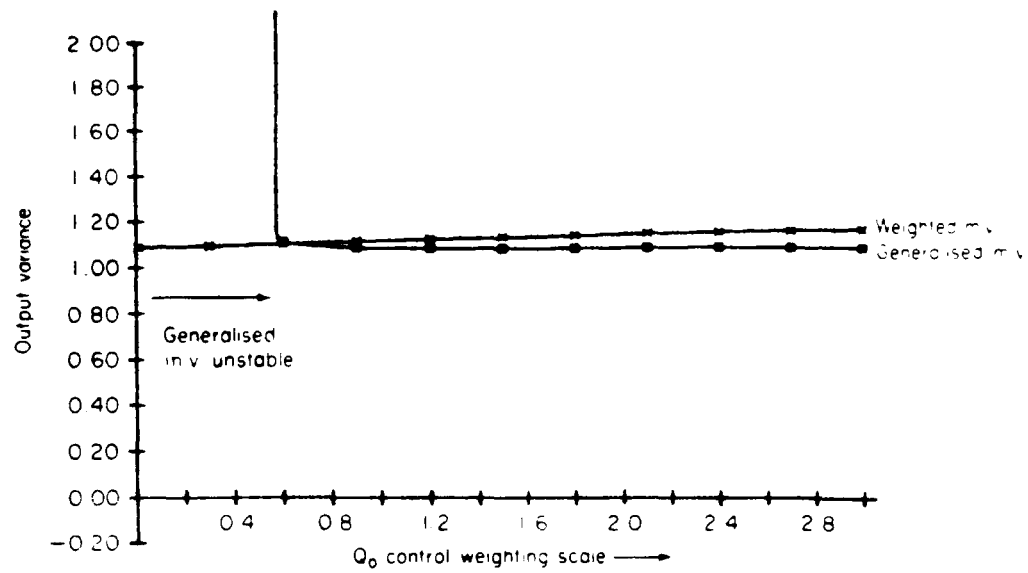


FIGURE E-1 Variance of the output for the generalized and weighted minimum-variance controllers.

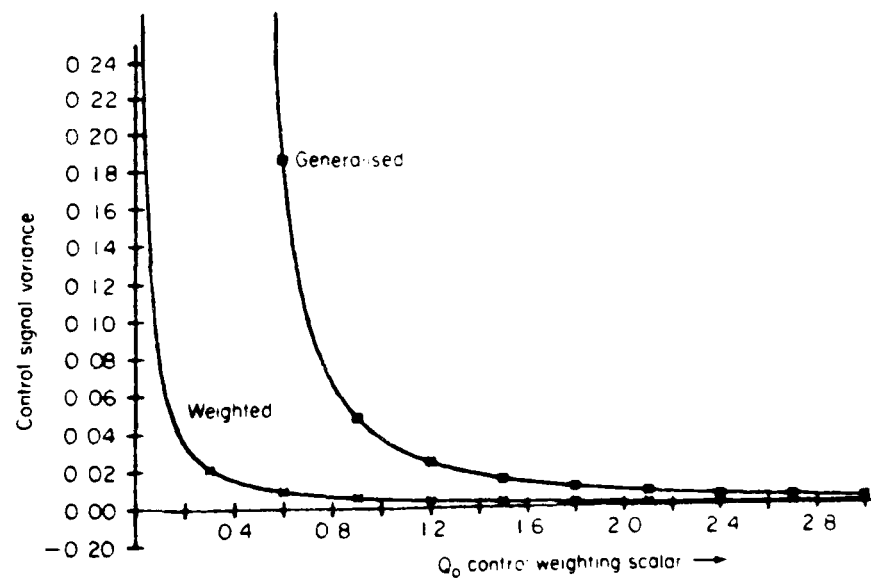


FIGURE E-2 Variance of the control signal for the generalized and weighted minimum-variance controllers.

Dynamic Ship Positioning Using a Self-Tuning Kalman Filter

PATRICK TZE-KWAI FUNG AND MIKE J. GRIMBLE, SENIOR MEMBER, IEEE

Abstract—A novel adaptive filtering technique is described for a class of systems with unknown disturbances. The estimator includes both a self-tuning filter and a Kalman filter. The state estimates are employed in a closed-loop feedback control scheme which is designed via the usual linear quadratic approach. The approach was developed for application to the dynamic ship positioning control problem and has the advantage that existing nonadaptive Kalman filtering systems may be easily modified to include the self-tuning feature.

Manuscript received April 21, 1982; revised September 27, 1982. This work was supported by GEC Electrical Projects Ltd., and the United Kingdom Science and Engineering Research Council.

P. T.-K. Fung was with the Department of Electrical Engineering, University of Strathclyde, Glasgow, Scotland. He is now with the Space and Electronic Group, Spar Aerospace Ltd., Weston, Ont., Canada.

M. J. Grumble is with the Department of Electrical Engineering, University of Strathclyde, Glasgow, Scotland.

I. INTRODUCTION

A DYNAMIC positioning (DP) system is used to maintain a floating vessel on a specified position and desired heading. The system involves a position/heading measurement system, a thruster control algorithm, and a set of thrusters (including the main propulsion units in some cases). This type of vessel is used for several applications in the survey and development of offshore mineral and oil resources. The number of countries involved in offshore exploration is increasing rapidly. For example, Saudi Arabia and the Sudan are preparing to dredge deposits of zinc, copper, and silver from the Red Sea. Manganese nodules of the highest grade have been found

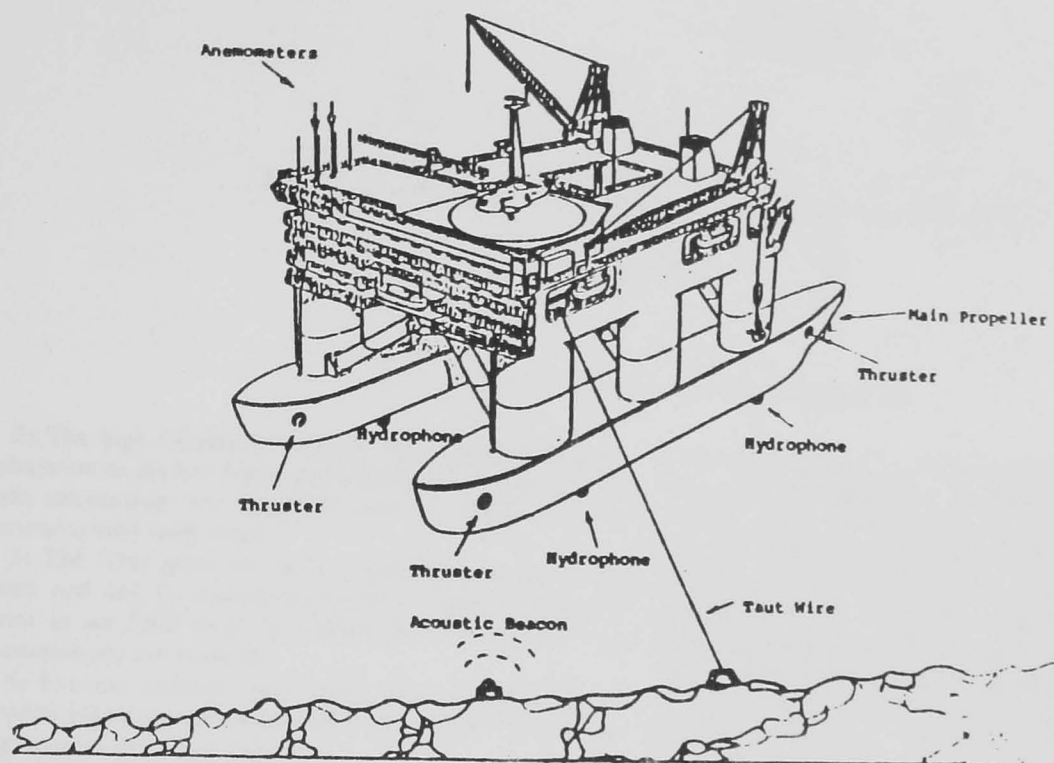


Fig. 1. Basic components in a dynamic positioning system.

in the international waters between Hawaii and California, and hence have become the subject of a prolonged debate at the United Nations Conference on the Law of the Sea.

The basic components in a DP system are illustrated in Fig. 1. Several types of position measurement systems can be used including taut wire [1], short range radio reference, and sonar systems. These measurements can be pooled and this gives rise to a combination of measurement problems. The heading measurement is given by a gyrocompass. Communication satellites are increasingly being used to provide a position fix and this enables vessels to be moved from a reference position in just a few minutes. A maximum allowable radial position error is normally specified, for example, 3 percent of water depth (under 100 m) [2].

The control loops for dynamically positioned vessels include filters to remove the wave motion signals. This is necessary because the thrust devices are not intended and are not rated to suppress the wave induced motions (greater than 0.3 rad/s). The position control system must only respond to the low frequency forces on the vessel. The filtering problem is one of estimating the low frequency motions so that control can be applied. Notice that even though the position measurement includes a noise component, this does not cause the filtering problem. If the total position of the vessel was known exactly there would still be a need to estimate the low frequency motions.

The extended Kalman filtering technique was first applied to dynamic ship positioning systems by Balchen, Jenssen, and Saelid [3]. A simpler, but nonadaptive, constant gain Kalman filtering solution was also proposed by Grimble, Patton, and Wise [4]. In both cases a linearized model was used for the estimation of the low frequency

motions and optimal control feedback was employed from these estimates [5]. Balchen assumed in this and subsequent schemes [6] that the high frequency motions were purely oscillatory and could be modeled by a second order sinusoidal oscillator with variable center frequency.

Grimble *et al.* used a fourth order wave model in the specification of the high frequency motions. However, the dominant wave frequency varies with weather conditions and the corresponding Kalman filter gain must therefore be switched for different operating conditions. The extended Kalman filter of Balchen automatically adapted to these varying environmental conditions. The computational load resulting from the gain matrix calculation was reduced by making suitable approximations. An alternative extended Kalman filtering scheme proposed by Grimble, Patton, and Wise [7], [8], employed the higher order wave model, but suggested the use of fixed low frequency filter gains to achieve the necessary computational savings. The self-tuning filter described here is based upon a similar decomposition property. This approach was first proposed by Fung and Grimble [18] using a scalar example and without the theoretical justification given in the following.

The advantages and disadvantages of the self-tuning approach in comparison with the usual extended Kalman filtering schemes can be listed as follows.

Advantages

- 1) The varying disturbance is represented by single-input single-output channels, and thus the adaptive filter is not multivariable in nature.

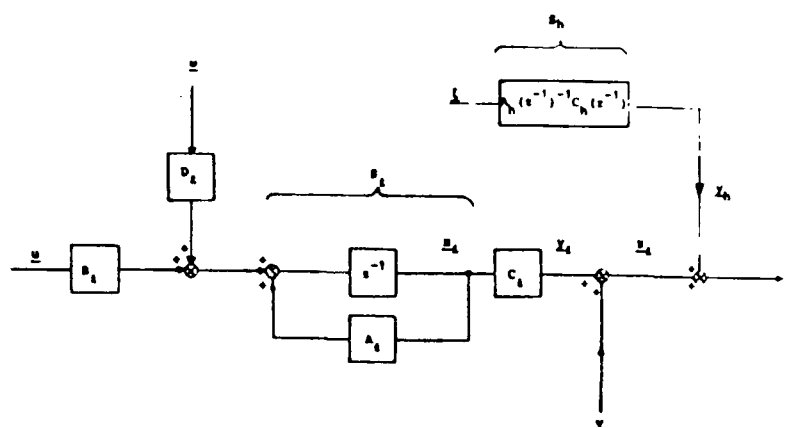


Fig. 2. Low and high frequency subsystems for a ship model.

2) The high frequency adaptive filter forms a separate subsystem to the low frequency Kalman filter, and thus the gain calculations are simplified and the system may be commissioned more easily.

3) The filter gains for the low frequency estimator are fixed and can be computed off-line, whereas all of the gains in an EKF must be computed on-line unless approximations are made [6].

4) Existing constant gain linear Kalman filtering DP systems [4] may easily be modified to include the self-tuning features described here.

5) There is no need to specify the process noise covariance or the form of the high frequency model. Only the total order of the model is assumed known.

6) The high frequency model states which are not needed for control purposes are not estimated in the self-tuning approach.

7) The scheme presented here is relatively insensitive to the presence of nonlinear ship dynamics and thruster nonlinearities [23].

Disadvantages

1) The full EKF in which all of the gains are computed on-line can be classified as being locally optimal (if the linearizations are correct), whereas the self-tuning scheme is suboptimal unless the low frequency estimator gains are calculated on-line using knowledge of the changing high frequency model.

The analysis begins with the system and problem description in Section II. The fixed gain Kalman filter is then considered in Section III and the self-tuning filter is described in Section IV. The errors which are introduced using the self-tuning structure are discussed in Section V and the total estimation algorithm is presented in Section VI. The controller design is considered in Section VII and the simulation and results are described in Sections VIII and IX, respectively.

II. THE SYSTEM DESCRIPTION

The environmental forces acting on a vessel induce motions in six degrees of freedom. In dynamic positioning

only vessel motions in the horizontal plane (surge, sway, and yaw) are controlled. To simplify the problem, the motions of the vessel in the sway and yaw directions only are considered. This is possible because the linearized ship equations for the surge motion are normally decoupled from those for the sway and yaw motions [9]. The assumption is also made that the low and high frequency motions can be determined separately and that the total motion is the sum of each of them. Marine engineers often make this assumption since the analysis is simplified and the low frequency motions can also be predicted with more accuracy than the high frequency motions.

The canonical structure of the system under consideration is shown in Fig. 2. The model for a vessel can be separated into low l and high h frequency subsystems. The low frequency motions (subsystem S_l) are controllable via thruster action and the high frequency motions (subsystem S_h) are due to the first order wave forces and are oscillatory in nature. The ship positioning problem is to control the low frequency motions (output of S_l) given that the measured position of the vessel (z) includes both y_l and y_h . The object in the following is to design a state estimator to provide estimates of the low frequency motions x_l . The estimator must be capable of adapting to variations in the high frequency subsystem S_h which occur due to variations in the weather conditions.

The plant S_l can be assumed to be completely controllable and observable and to be represented by the following discrete time-invariant state equations:

$$S_l: \quad x_l(t+1) = A_l x_l(t) + B_l u(t) + D_l \omega(t) \quad (1)$$

$$y_l(t) = C_l x_l(t) \quad (2)$$

$$z_l(t) = y_l(t) + v(t)$$

where

$$E\{\omega(t)\} = 0, \quad E\{\omega(k) \omega^T(m)\} = Q \delta_{k,m} \quad (3)$$

$$E\{v(t)\} = 0, \quad E\{v(k) v^T(m)\} = R \delta_{k,m} \quad (4)$$

and $\delta_{k,m}$ is the Kronecker delta function, $x_l(t) \in R^n$, $u(t) \in R^m$, $\omega(t) \in R^q$, and $y_l(t) \in R^r$. The process noise $\omega(t)$ is used to simulate the wind disturbance and $v(t)$ represents

using

$$\hat{y}_h(t|t) = m_h(t) - \Sigma_t \Sigma_t^{-1} \epsilon(t) \quad (25)$$

where

$$\epsilon(t) = m_h(t) - \hat{y}_h(t|t-1). \quad (26)$$

Using the identity in (24), $\hat{y}_h(t|t)$ becomes

$$\hat{y}_h(t|t) = m_h(t) - A_{n_h}^{-1} D_{n_h} \epsilon(t). \quad (27)$$

The estimate of $y_h(t)$ is not needed for control purposes, but is required for updating $\hat{x}_l(t|t)$. The wave frequency model changes with environmental conditions and these variations are accounted for in (27) by on-line estimation of A_{n_h} , D_{n_h} , and the innovations $\epsilon(t)$ (Section VI).

V. MODIFIED ESTIMATION EQUATIONS

The signal $y_h(t)$ is not measurable and must be replaced in the low frequency Kalman filter by $\hat{y}_h(t|t)$. This substitution causes a difference in the state estimates [denoted $\tilde{x}_l(t|t)$] and in the calculated innovations

$$\begin{aligned} \tilde{\epsilon}(t) &\triangleq z(t) - \hat{y}_l(t|t-1) - \hat{y}_h(t|t) \\ &= \epsilon_l(t) + n_h(t) \end{aligned} \quad (28)$$

where $n_h(t) \triangleq y_h(t) - \hat{y}_h(t|t)$. The signal $n_h(t)$ for the high frequency motion estimator has a zero mean value if the errors in calculating $\hat{y}_h(t|t)$ are neglected. Notice from (16) and (26) that the innovations $\tilde{\epsilon}(t)$ are identical to the signal $\epsilon_h(t)$ where

$$\epsilon_h(t) \triangleq m_h(t) - \hat{y}_h(t|t).$$

If the above substitution is made the new low frequency filter has the form

$$\hat{\tilde{x}}_l(t|t) = A_l \hat{\tilde{x}}_l(t-1|t-1) + B_l u(t-1) + K_l(t) \tilde{\epsilon}(t), \quad (29)$$

but this equation may be decomposed into the following two parts:

$$\hat{x}_l(t|t) = A_l \hat{x}_l(t-1|t-1) + B_l u(t-1) + K_l(t) \epsilon_l(t) \quad (30)$$

$$\hat{\tilde{x}}_l(t|t) = A_l \hat{\tilde{x}}_l(t-1|t-1) + K_l(t) n_h(t) \quad (31)$$

where

$$\hat{\tilde{x}}_l(t|t) = \hat{x}_l(t|t) + \hat{\tilde{x}}_l(t|t) \quad (32)$$

and $\hat{\tilde{x}}_l(t|t)$ represents the change brought about by replacing $y_h(t)$ by $\hat{y}_h(t|t)$ in (27). The change in the predicted output

$$\hat{y}_l(t|t-1) \triangleq \hat{\tilde{y}}_l(t|t-1) - \hat{y}_l(t|t-1) \quad (33)$$

where

$$\hat{\tilde{y}}_l(t|t-1) = C_l \hat{\tilde{x}}_l(t|t-1) \quad (34)$$

but from (9) and (32)

$$\begin{aligned} \hat{y}_l(t|t-1) &= C_l (\hat{\tilde{x}}_l(t|t-1) - \hat{x}_l(t|t-1)) \\ &= C_l A_l \hat{\tilde{x}}_l(t-1|t-1). \end{aligned} \quad (35)$$

For later reference note that $\hat{y}_l(t|t-1)$ is generated from the output of the low frequency subsystem [see (31)] driven by the zero mean signal n_h . The resulting position variations are relatively slow in comparison with the high frequency motions.

The high frequency motion estimator is also modified because the signal $m_h(t)$ in (18) cannot be calculated, but instead $\bar{m}_h(t)$ can be found where

$$\bar{m}_h(t) \triangleq z(t) - \hat{\tilde{y}}_l(t|t-1). \quad (36)$$

The basis of the parameter estimation equation (Section VI) follows from (19) and (33) as

$$\begin{aligned} \bar{m}_h(t) &= m_h(t) - \hat{y}_l(t|t-1) \\ &= A_h(z^{-1})^{-1} D_h(z^{-1}) \epsilon(t) - \hat{y}_l(t|t-1). \end{aligned} \quad (37)$$

Assuming that ϵ and \hat{y}_l can be calculated the estimate of $y_h(t)$ can be generated using (27) and (37)

$$\hat{y}_h(t|t) = \bar{m}_h(t) - A_{n_h}^{-1} D_{n_h} \epsilon(t) + \hat{y}_l(t|t-1). \quad (38)$$

The signal $\tilde{\epsilon}$ must be calculated to obtain the desired state estimates $\hat{\tilde{x}}_l(t|t)$ and this can be found using (18), (27), and (28)

$$\tilde{\epsilon}(t) = A_{n_h}^{-1} D_{n_h} \epsilon(t). \quad (39)$$

Recall that the gain $K_l(t)$ is calculated based upon the low frequency subsystem rather than the total system model [7]. This has the advantage that the gain is fixed and independent of variations in the high frequency subsystem. The optimal low frequency position estimate should therefore be calculated from (30), but this is not possible since ϵ_l cannot be computed directly. The state estimates are therefore obtained via (29), but are corrected using the estimated $\hat{y}_l(t|t-1)$. This can be achieved in the ship positioning problem because the position states are identical to the outputs of the system. Thus, let the corrected estimate

$$\begin{aligned} \hat{y}_l(t|t) &= \hat{\tilde{y}}_l(t|t) - \hat{y}_l(t|t-1) \\ &\equiv \text{(position states in } \hat{\tilde{x}}_l(t|t)). \end{aligned} \quad (40)$$

In the application of Kalman filters it is unavoidable that errors will arise from incorrect models for the plant and noise signals. The signal $\hat{y}_l(t|t-1)$ will include such errors, but in the following section it is shown how this quantity can be estimated and may be used to correct the low frequency state estimates.

VI. KALMAN AND SELF-TUNING FILTER ALGORITHMS

The Kalman and self-tuning filter algorithms are combined below to produce the desired low frequency motion estimator. The Kalman filter to estimate $\hat{x}_l(t|t)$ becomes

Algorithm 6.1:
predictor:

$$\hat{\bar{x}}_i(t|t-1) = A_i \hat{\bar{x}}_i(t-1|t-1) + B_i u(t-1) \quad (41)$$

$$\hat{\bar{y}}_i(t|t-1) = C_i \hat{\bar{x}}_i(t|t-1) \quad (42)$$

corrector:

$$\hat{\bar{x}}_i(t|t) = \hat{\bar{x}}_i(t|t-1) + K_i(t) \bar{\epsilon}(t) \quad (43)$$

$$\hat{\bar{y}}_i(t|t) = C_i \hat{\bar{x}}_i(t|t). \quad (44)$$

The signal $\bar{\epsilon}$ is required in the above algorithm, but this can be computed from (39) given the innovations signal ϵ and the matrices A_{n_s} and D_{n_s} . These matrices may be estimated as described in the following. Note that at time $t-1$ the predicted output $\hat{\bar{y}}_i(t|t-1)$ is known [from (41), (42)] so that $\bar{m}_h(t)$ can be computed from (36). From (38)

$$A_h(z^{-1}) \bar{m}(t) = D_h(z^{-1}) \epsilon(t) - A_h(z^{-1}) \hat{\bar{y}}_i(t|t-1). \quad (45)$$

The quantity $\hat{\bar{y}}_i$ is a slowly varying signal (from Section V) and can be treated as a constant over a short time interval. Let $s(t) \triangleq A_h(z^{-1}) \hat{\bar{y}}_i(t|t-1)$ (where using the final value theorem z may be replaced by unity) then (45) becomes

$$A_h(z^{-1}) \bar{m}_h(t) = D_h(z^{-1}) \epsilon(t) - s(t). \quad (46)$$

The innovations signal model can be represented in the usual form for parameter estimation

$$\bar{m}_h(t) = \psi(t) \theta + \epsilon(t) \quad (47)$$

and the algorithm due to Panuska [12] can be employed to estimate the unknown parameters.

In the ship positioning problem the high frequency disturbances can be assumed to be decoupled, so that $A_h(z^{-1})^{-1} D_h(z^{-1})$ is a diagonal matrix and the parameters for each channel can be estimated separately. Hence, standard extended recursive least squares or maximum likelihood parameter identification algorithms may be used. For the i th channel

$$\bar{m}_{h_i}(t) = \psi_i(t) \theta_i + \epsilon_i(t) \quad (48)$$

where

$$\psi_i(t) = [-\bar{m}_{h_i}(t-1), \dots, -\bar{m}_{h_i}(t-n_d); \epsilon_i(t-1), \dots, \epsilon_i(t-n_d); 1] \quad (49)$$

$$\theta_i^T = [a_{i,1}, \dots, a_{i,n_a}; d_{i,1}, \dots, d_{i,n_d}; s_i]. \quad (50)$$

Past values of the innovations signal are approximated by

$$\bar{\epsilon}_i(t) = \bar{m}_{h_i}(t) - \hat{\bar{y}}_i(t) \hat{\theta}_i \quad (51)$$

where $\hat{\bar{y}}_i(t)$ is given by (49) with $\epsilon_i(t-j)$ replaced by $\bar{\epsilon}_i(t-j)$ $j=1, 2, \dots, n_d$ and $\hat{\theta}_i$ represents the estimated parameter vector.

The recursive Kalman/self-tuning filter algorithm now becomes

Algorithm 6.2:

1) Initialize $\hat{\theta}_i$, initial parameter covariance for each channel and assign the forgetting factor β . Initialize state estimates.

2) Generate the Kalman filter estimates $\hat{\bar{x}}_i(t|t-1)$ and $\hat{\bar{y}}_i(t|t-1)$ using (41) and (42).

3) Calculate $\bar{m}_{h_i}(t)$ using (36) and form $\hat{\psi}_i(t)$.

4) Parameter update:

$$\hat{\theta}_i(t) = \hat{\theta}_i(t-1) + K_i^p(t) (\bar{m}_{h_i}(t) - \hat{\psi}_i(t) \hat{\theta}_i(t-1)). \quad (52)$$

5) Covariance and gain update

$$\begin{aligned} P_i^p(t) &= \{ P_i^p(t-1) - K_i^p(t) \\ &\quad \cdot (\beta + \psi_i(t) P_i^p(t-1) \psi_i^T(t)) K_i^p(t)^T \} / \beta \\ K_i^p(t) &= P_i^p(t-1) \psi_i(t) \\ &\quad \cdot (\beta + \psi_i(t) P_i^p(t-1) \psi_i^T(t))^{-1} \end{aligned} \quad (53)$$

where $0.95 \leq \beta \leq 1$.

6) Innovations update:

$$\bar{\epsilon}_i(t) = \bar{m}_{h_i}(t) - \hat{\psi}_i(t) \hat{\theta}_i(t). \quad (54)$$

7) Calculate $\bar{\epsilon}_{h_i}(t)$ for channel i using (39)

$$\bar{\epsilon}_{h_i}(t) = \hat{a}_{n_s}^{-1} \hat{d}_{n_s} \bar{\epsilon}_i(t). \quad (55)$$

8) If $i < \text{number of channels } (r)$ go to step 3).

9) Generate the state $\hat{\bar{x}}_i(t|t)$ [using (43) and (44)].

10) Calculate the estimated $\hat{\bar{y}}_i(t|t-1)$ as

$$\begin{aligned} \hat{\bar{y}}_i(t|t-1) &= \hat{f}_i(t) / \hat{A}_{h_i}(1) \\ \hat{\bar{y}}_i(t) &= \alpha \hat{\bar{y}}_i(t-1) + (1-\alpha) \hat{\bar{y}}_i(t|t-1), \\ 0 &< \alpha < 1. \end{aligned} \quad (56)$$

11) Correct the position estimates using (40). Return to step 2).

The signal $\hat{\bar{y}}_i(t|t-1)$ in step 10) may be processed to produce the smoothed estimate $\hat{\bar{y}}_i(t)$ before it is used to correct the state estimates. The algorithm described in the Appendix can predict the velocity as well as smooth the estimation of $\hat{\bar{y}}_i(t)$.

The structure of the self-tuning/Kalman filtering scheme for the dynamic positioning system is shown in Fig. 3. The surge motions are decoupled from the sway and yaw motions, and thus these are normally estimated by separate filters.

VII. CONTROLLER DESIGN

The controller design is based on the separation principle of stochastic optimal control theory [16]. The controller with input z and output u is chosen to minimize the

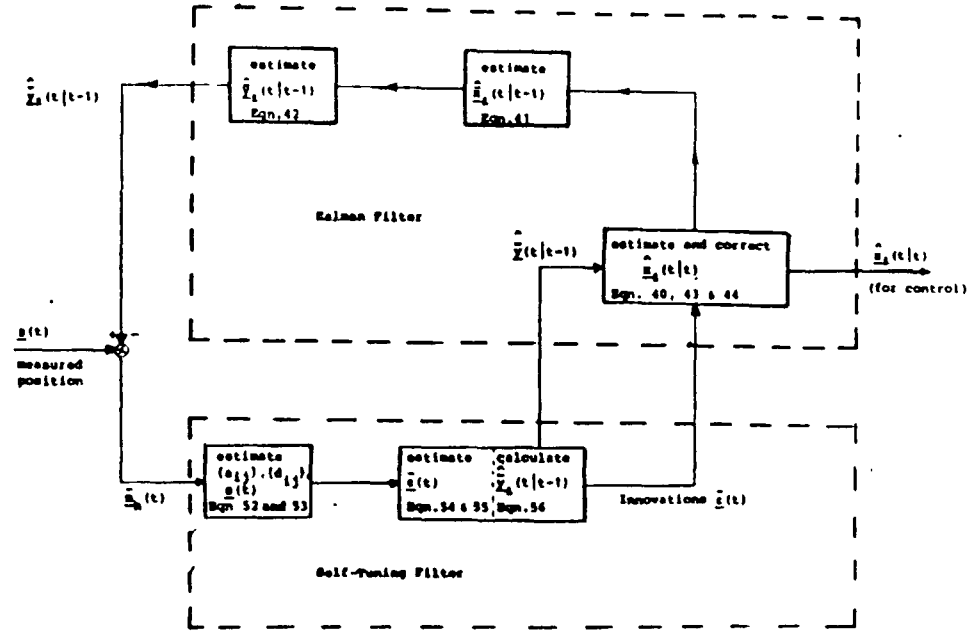


Fig. 3. Structure of the filtering scheme.

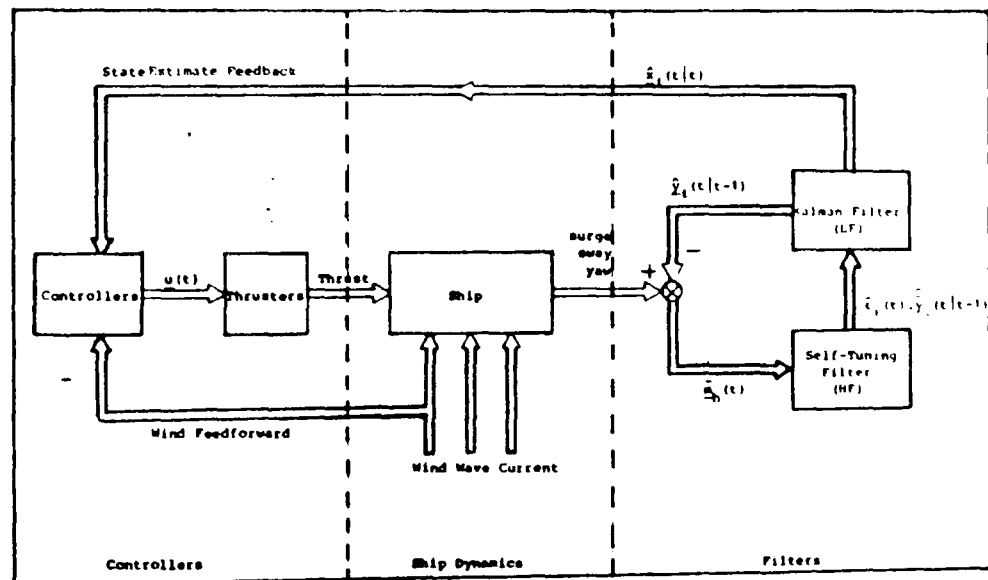


Fig. 4. Kalman and self-tuning filter state estimate feedback scheme.

performance criterion

$$J = \lim_{T \rightarrow \infty} \frac{1}{2T} E \left\{ \int_{-T}^T (x_t - r_t)^T Q_1 (x_t - r_t) + u^T R_1 u dt \right\} \quad (57)$$

where Q_1 and R_1 are positive definite weighting matrices. The optimal control signal is generated from a Kalman filter cascaded with a control gain matrix K_c .

$$u(t) = -K_c \hat{x}(t). \quad (58)$$

The control gain matrix may be calculated from the steady-state Riccati equation in the usual way. The closed loop control system is shown in Fig. 4.

The optimal control weighting matrices were chosen to penalize the position error corresponding to the low frequency motions (states 2 and 4) and to give an appropriate step response [17]. These were found as

$$Q_c = \text{diag}(5, 60, 5, 60, 1, 1)$$

$$R_c = \text{diag}(400, 400).$$

The saturation limits on the control signals were set at ± 0.002 per unit. These represented the actual saturation which can occur when the thrusters are at full load. The selection of the optimal control weighting matrices in the ship positioning problem can be based upon results from asymptotic root loci [17] since the system is uniform rank

VIII. SIMULATION AND SHIP EQUATIONS

A. Low Frequency Ship Motions

The low frequency motions of a vessel are determined by nonlinear equations [13] which are linearized for system analysis. The forces which produce the low frequency motions can be listed as follows: 1) forces generated by the thrusters and propellers; 2) wind forces; 3) wave induced forces; 4) hydrodynamic forces.

The linearized low frequency model of the vessel can be represented by (1) and (2) where the state vector is defined as

$$x_l(t) = \begin{bmatrix} x_1(t) \\ x_2(t) \\ x_3(t) \\ x_4(t) \\ x_5(t) \\ x_6(t) \end{bmatrix} \begin{array}{l} \text{) sway velocity} \\ \text{) sway position} \\ \text{) yaw angular velocity} \\ \text{) yaw angle} \\ \text{) thruster one} \\ \text{) thruster two.} \end{array} \quad (59)$$

The system matrices for Wimpey Sealab [4] corresponding to the zero current condition and the continuous time state equations become

$$A_l = \begin{bmatrix} -0.056 & 0 & 0.0016 & 0 & 0.5435 & 0 \\ 1.0 & 0 & 0 & 0 & 0 & 0 \\ 0.573 & 0 & -0.0695 & 0 & 0 & 9.785 \\ 0 & 0 & 1.0 & 0 & 0 & 0 \\ 0 & 0 & 0 & 0 & -1.55 & 0 \\ 0 & 0 & 0 & 0 & 0 & -1.55 \end{bmatrix}$$

$$B_l = \begin{bmatrix} 0 & 0 \\ 0 & 0 \\ 0 & 0 \\ 0 & 0 \\ 1.55 & 0 \\ 0 & 1.55 \end{bmatrix} \quad D_l = \begin{bmatrix} 0.5435 & 0 \\ 0 & 0 \\ 0 & 9.785 \\ 0 & 0 \\ 0 & 0 \\ 0 & 0 \end{bmatrix}$$

$$E_l = \begin{bmatrix} 0.384 & 0 \\ 0 & 0 \\ 0 & 6.92 \\ 0 & 0 \\ 0 & 0 \\ 0 & 0 \end{bmatrix} \quad C_l = \begin{bmatrix} 0 & 1 & 0 & 0 & 0 & 0 \\ 0 & 0 & 0 & 1 & 0 & 0 \end{bmatrix} \quad (60)$$

where E_l is the input matrix corresponding to the wind force disturbances. The above linearized equations are in per-unit form and have been time scaled (real time = 3.104 \times simulated time). The following simulation results are also in terms of per-unit quantities and scaled time.

The covariance of the process noise is dependent upon the wind force level and can be defined as

$$Q = \text{diag}(4 \times 10^{-6}, 9 \times 10^{-8}).$$

The standard deviation of the measurement noise (sonar position measurement device) is assumed to be 1/3 and 0.2 degrees, giving the normalized sway and yaw covariances

$$R = \text{diag}(10^{-5}, 1.22 \times 10^{-5}). \quad (61)$$

B. High Frequency Motions

The high frequency motions of the vessel are due to the first order wave forces. The worst case high frequency motion is determined by the sea wave spectrum alone and can be represented by the input-output vector difference (6). The order of the polynomial matrices $A_h(z^{-1})$ and $C_h(z^{-1})$ can be assumed to be second and first order, respectively. The parameters of these matrices vary with sea state.

It is usual to test the DP designs for real applications using simulated rather than measured sea wave data. This is partly due to the difficulty in collecting representative sea wave data, but also reflects the fact that tests over a range of different conditions must be made.

The high frequency motions were simulated using two fourth order coloring filters driven by white noise. In state space notation

$$\dot{x}_h = A_h x_h + D_h \xi \quad (62)$$

$$y_h = C_h x_h \quad (63)$$

where

$$A_h = \begin{bmatrix} A_h^1 & 0 \\ 0 & A_h^2 \end{bmatrix} \text{ and } D_h = \begin{bmatrix} D_h^1 & 0 \\ 0 & D_h^2 \end{bmatrix}$$

and the submatrices for the sway and yaw directions have the same form

$$A_h^1 = \begin{bmatrix} 0 & 1 & 0 & 0 \\ 0 & 0 & 1 & 0 \\ 0 & 0 & 0 & 1 \\ -a_4^1 & -a_3^1 & -a_2^1 & -a_1^1 \end{bmatrix} \quad D_h^1 = \begin{bmatrix} 0 \\ 0 \\ 0 \\ k^1 \end{bmatrix} \quad (64)$$

$$C_h^1 = [0 \ 0 \ 1 \ 0]. \quad (65)$$

The parameters of the system matrices are calculated to minimize the integral squared error between the modeled and Pierson Moskowitz sea spectra [8].

Tests on the Filters: The simulation results presented below were obtained using the above high frequency model to generate the wave motions. The tests were based on weather conditions corresponding to Beaufort numbers 8 and 5 (wind speeds 19 m/s and 9.3 m/s, respectively) which are typical examples of rough and calm seas, respectively. The first set of "filtering" results (Figs. 5-8) are for Beaufort 8, without closed loop control.

The total sway motion is shown in Fig. 5 and the estimated and modeled low frequency sway motions are shown in Fig. 6. The estimate of the low frequency motion is required for control purposes and it is clear that the estimate is good throughout the time interval (even after initial startup). The high frequency sway motion estimates are not needed for feedback control and are not shown. It is important that the LF motion estimates are relatively smooth to reduce the consequential variations in the control action. The major role of the combined estimator is indeed to separate the HF and LF motion estimates

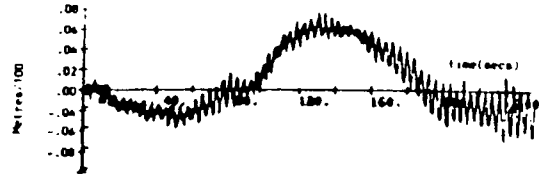


Fig. 5. Observed total sway motion (Beaufort 8).

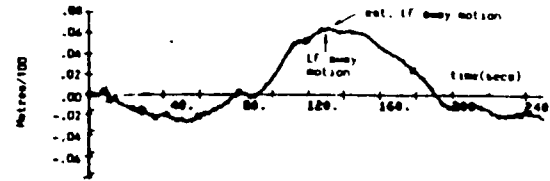


Fig. 6. Estimated and modeled low frequency sway motion (Beaufort 8)

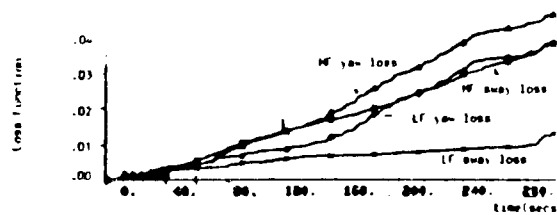


Fig. 7. Sway and yaw loss functions (Beaufort 8)

Because the LF Kalman filter does not have z_t as an input, but rather

$$z(t) - \hat{y}_h(t|t) = z_t(t) + n_h(t)$$

the predicted measurement noise covariance should be increased if the LF estimates contain an HF component. Since the HF wave conditions are slowly varying the amount by which R should be increased is not known exactly, but the system is not oversensitive to such an adjustment (factors of 5 on sway and 10 on yaw were used for the results shown here).

The accumulative loss functions for the position estimation errors in sway and yaw (both HF and LF) are shown in Fig. 7. The LF loss function for sway is defined as

$$J = \sum_{t=1}^N (y_t^s(t) - \hat{y}_t^s(t|t))^2.$$

If the measurement noise were not artificially increased, when calculating the Kalman filter gain, the HF and LF loss functions for yaw would be found to be similar. This is an indication of optimal performance which has been sacrificed to some extent to obtain smoother position estimates. The parameter estimates for the high frequency model are shown in Fig. 8 where

$$A_h(z^{-1}) = I_2 + \begin{bmatrix} a_1^s & 0 \\ 0 & a_1^y \end{bmatrix} z^{-1} + \begin{bmatrix} a_2^s & 0 \\ 0 & a_2^y \end{bmatrix} z^{-2} \quad (68)$$

$$D_h(z^{-1}) = I_2 + \begin{bmatrix} d_1^s & 0 \\ 0 & d_1^y \end{bmatrix} z^{-1} + \begin{bmatrix} d_2^s & 0 \\ 0 & d_2^y \end{bmatrix} z^{-2}. \quad (69)$$

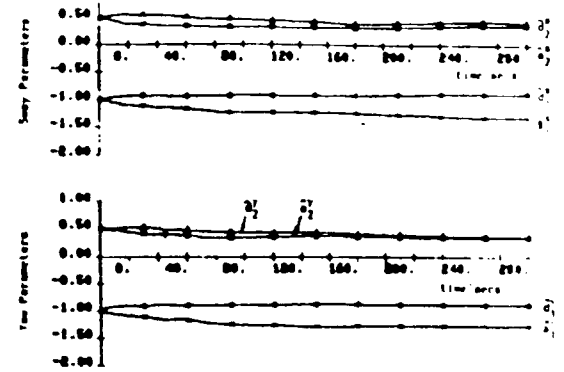


Fig. 8. Sway and yaw estimated parameters (Beaufort 8)

Note that even before the estimated parameters have converged the position estimates are still accurate (see Fig. 8). The initial parameter estimates for the matrices A_h and D_h can be based upon the knowledge that these have stable inverses. The polynomials are all of the form $a = a_1 z^{-1} + a_2 z^{-2} = (m_1 z^{-1} + 1)(m_2 z^{-1} + 1)$ and since $|m_1| < 1$, $|m_2| < 1$ then $-2 < m_1 + m_2 < 2$, $-1 < m_1 m_2 < 1$. Assuming $m_1, m_2 < 0$ implies that good initial estimates are $a_2 = 0.5$ and $a_1 = -1$. It was found that the initial error covariance for $\hat{s}(t)$ should be small (e.g., 0.1 in this test), but the initial covariance for the other parameters should be high (e.g., 100). The estimate of $s(t)$ may contain a high frequency component and thus this is smoothed by use of a simple first order lag filter.

The filtering results for a calm sea (Beaufort 5) are not shown since the parameter estimates are much better for this case. This is consistent with the theory of Section V that shows that when the modeling errors are negligible, the term $\hat{y}_t(t|t-1)$ is caused by the estimation error of the high frequency motion [see (35)] which is reduced in a calm sea.

Closed Loop Control: The first set of results are again for the rough sea (Beaufort 8) condition. To allow the parameter estimates to converge (as will be possible in practice) the step response of the system is measured over the time interval 240–360 s. A step reference of 0.06 per unit is input to the system at $t = 240$ s. The sway and yaw responses are shown in Figs. 9–12. The low frequency variations, due to wind disturbances, are much reduced under closed loop control, but the high frequency motions are, as required, almost unchanged. The rise time for the step response can be reduced if larger control signal variations are allowed. These are shown in Figs. 13 and 14 and it is clear the sway control enters the saturation limit for a few seconds when the step demand is entered. This is not a problem since in practice position reference changes are not made in steps. One of the main design objectives is to reduce "thruster modulation," that is, variation of the thrusters in sympathy with the wave motions. That this objective has been achieved is clear from the control signals in Figs. 13 and 14.

The equivalent results for the calm sea (Beaufort 5) conditions are not shown. The parameter estimates are

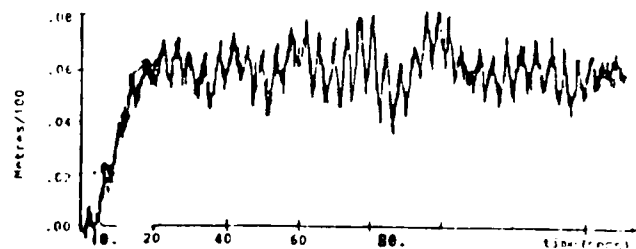


Fig. 9. Controlled total sway motion (sway reference = 0.08, Beaufort 8).

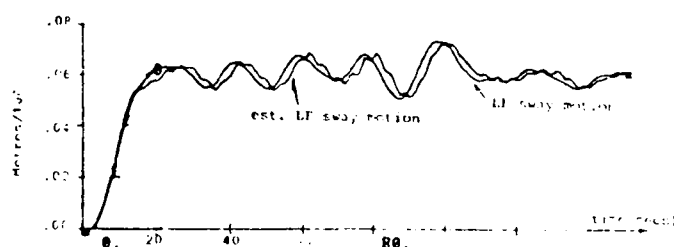


Fig. 10. Controlled LF sway and estimated sway motion (Beaufort 8).



Fig. 11. Controlled total yaw motion (Beaufort 8).

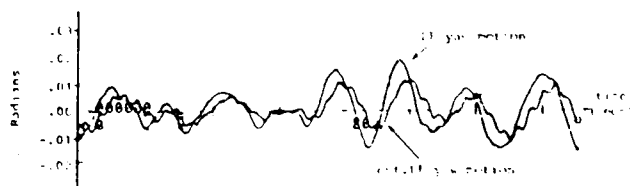


Fig. 12. Controlled LF yaw and estimated yaw motion (Beaufort 8).

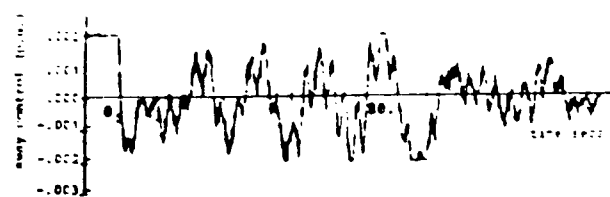


Fig. 13. Sway control signal (Beaufort 8).

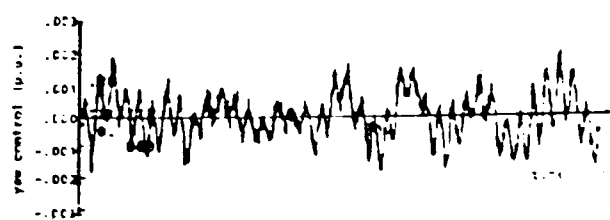


Fig. 14. Yaw control signal (Beaufort 8).

improved and the control signal variations are reduced in this case, as would be expected. Note that in comparing the high frequency motions the magnitude of the HF motion is reduced in the calm sea, but the frequency of the wave motion is higher. The sway motion is less than the allowed limit of the ± 3 for both sea states.

Rapid Weather Changes: The sea state will, relative to the system time constants, take a long time to change. It might therefore be expected that the self-tuning filter could easily track such variations and this has been demonstrated in [18]. If the weather direction changes or if the heading is changed the direction of the disturbances acting on the vessel will also vary. The magnitude of the wind and second-order wave forces will change according to the sine of the angle of incidence of these forces on the vessel and also according to the shape of the superstructure and hull exposed to these forces. The change in the angle of the current forces will be reflected in a change to the low frequency dynamics of the vessel, and hence to the linearized low frequency model [23]. These changes necessitate a variation in the drift estimator or integral action term, and the optimal control gain of this loop must be carefully chosen by posing an appropriate cost function [22]. This design problem is of course common to other Kalman filtering dynamic ship positioning schemes.

Comparison: A comparison between characteristic locus and optimal designs for dynamic ship positioning systems has recently shown [24] that the performance achievable is roughly the same in both cases. The differences lie more in the engineering implications and the relative ease of use of the different design procedures. Similar conclusions may be drawn when comparing the usual and self-tuning Kalman filtering solutions to this problem. The sway step response and control signal variations, shown in [24], for the usual fixed Kalman filtering solution, are very similar to those in Figs. 10 and 13, respectively. If the Kalman filter is matched to the sea state model (by using the same dynamics to the filter as in the wave model [8]) the Kalman filter gives a slightly lower mean square estimation error of about 10 percent. However, whenever the sea state model is significantly mismatched with the Kalman filter the self-tuning filter gives the best results. This is the situation in practice since the HF dynamical model structure is a poor representation of the nonlinear sea spectrum generator. Extended Kalman filtering schemes can also of course adapt the dominant wave frequency parameter, but these usually have a more restrictive structure than the self-tuning wave filter. A full EKF also involves a considerably larger computational burden.

IX. CONCLUSIONS

The self-tuning filter replaces the usual fixed high frequency estimator in Kalman filtering DP systems. Thus, systems which do not currently have automatic adaption to varying environmental conditions can be provided with such a feature. The approach has the advantage of simplicity over extended Kalman filtering DP systems. In addition

1) there is no need to specify the process and measurement noise covariances for the high frequency model, 2) high frequency model states which are not needed for control are not estimated, 3) the structure of the multivariable estimator which involves separate adaptive and nonadaptive subsystems simplifies both implementation and fault finding, and 4) recent simulation results using nonlinear ship models and thruster nonlinearities have demonstrated that the scheme is robust in the presence of such nonlinearities [23].

APPENDIX

The algorithm for tracking the error $\hat{y}_i(t)$ based on the estimated position error $\hat{y}_i(t|t-1)$, for the i th channel [19], [20], becomes

$$\hat{y}_i^p(t) = \hat{y}_i^*(t-1) + T\hat{y}_i^*(t-1) \quad (70)$$

$$\hat{y}_i^*(t) = \hat{y}_i^p(t) + k_{1i}[\hat{y}_i(t|t-1) - \hat{y}_i^p(t)] \quad (71)$$

$$\dot{\hat{y}}_i^*(t) = \dot{\hat{y}}_i^*(t-1) + \frac{k_{2i}}{T}[\hat{y}_i(t|t-1) - \hat{y}_i^p(t)] \quad (72)$$

where

T	sampling interval
k_{1i}	constant less than unity
k_{2i}	constant less than unity
$\hat{y}_i^p(t)$	predicted position error
$\hat{y}_i^*(t)$	updated position error
$\dot{\hat{y}}_i^*(t)$	updated velocity error
$\hat{y}_i(t t-1)$	estimated position error from the self-tuning filter.

ACKNOWLEDGMENT

The authors are grateful for the assistance and guidance of D. Wise of GEC Electrical Projects Ltd.

REFERENCES

- [1] A. E. Ball and J. M. Blumberg, "Development of a dynamic ship-positioning system," *GEC J. Sci. Technol.*, vol. 42, no. 1, pp. 29-36, 1975.
- [2] A. W. Brink, J. B. Van Den Brug, C. Ton, R. Wahab, and W. R. Van Wijk, "Automatic position and heading control of a drilling vessel," Inst. TNO for Mechanical Constructions, The Netherlands, Sept. 1972.
- [3] J. G. Balchen, N. A. Jenssen, and S. Saelid, "Dynamic positioning using Kalman filtering and optimal control theory," in *Automation in Offshore Oil Field Operation*, 1976, pp. 183-188.
- [4] M. J. Grimble, R. J. Patton, and D. A. Wise, "The use of Kalman filtering techniques in dynamic ship positioning systems," presented at the Oceanology Int. Conf., Brighton, England, Mar. 1978.
- [5] M. J. Grimble, "The application of Kalman filters to dynamic ship positioning control," GEC Eng. Memorandum EM188, Feb. 1976.
- [6] J. G. Balchen, N. A. Jenssen, E. Mathisen, and S. Saelid, "A dynamic positioning system based on Kalman filtering and optimal control," *Modeling, Ident. Contr.*, vol. 1, no. 3, pp. 135-163, 1980.
- [7] M. J. Grimble, R. J. Patton, and D. A. Wise, "The design of dynamic ship positioning control systems using extended Kalman filtering techniques," in *Proc. IEEE Oceans '79 Conf.*, San Diego, CA, Sept. 1979, pp. 488-498.
- [8] —, "The design of dynamic ship positioning control systems using stochastic optimal control theory," *Opt. Contr. Appl. Methods*, pp. 167-202, June 1980.
- [9] D. A. Wise and J. W. English, "Tank and wind tunnel tests for a drill-ship with dynamic position control," presented at the Offshore Technol. Conf., Dallas, TX, 1975, paper OTC 2345.
- [10] P. Hagander and B. Wittenmark, "A self-tuning filter for fixed-lag smoothing," *IEEE Trans. Inform. Theory*, vol. IT-23, pp. 377-384, May 1977.
- [11] T. J. Mor and M. J. Grimble, "Optimal self-tuning filtering prediction and smoothing for discrete multivariable processes," *IEEE Trans. Automat. Contr.*, to be published.
- [12] V. Panuska, "A new form of the extended Kalman filter for parameter estimation in linear systems with correlated noise," *IEEE Trans. Automat. Contr.*, vol. AC-25, pp. 229-235, Apr. 1980.
- [13] J. W. English and D. A. Wise, "Hydrodynamic aspects of dynamic positioning," *Trans. North East Coast Inst. Eng. Shipbuilders*, vol. 92, no. 3, pp. 53-72.
- [14] W. G. Price and R. E. D. Bishop, *Probabilistic Theory of Ship Dynamics*. London: Chapman and Hall, 1974, p. 159.
- [15] W. J. Pierson and W. Marks, "The power spectrum analysis of ocean wave records," *Trans. Amer. Geophys. Union*, vol. 33, pp. 834-844, Dec. 1952.
- [16] H. Kwakernaak and R. Sivan, *Linear Optimal Control Systems*. New York: Wiley Interscience, 1972.
- [17] M. J. Grimble, "Design of optimal output regulators using multivariable root loci," *Proc. IEE*, Part D, vol. 128, pp. 41-49, Mar. 1981.
- [18] P. T. -K. Fung and M. J. Grimble, "Self tuning control of ship positioning systems," in *IEE Workshop on Theory & Application of Adaptive & Self-Tuning Control*, Oxford University, Mar. 1981, also in C. J. Harris and S. A. Billings, Eds., London: Peregrinus, 1981, p. 322.
- [19] J. A. Cadzow, *Discrete Time Systems: An Introduction with Interdisciplinary Applications*. Englewood Cliffs, NJ: Prentice-Hall, 1973.
- [20] S. M. Bozic, *Digital and Kalman Filtering*. London: Arnold, 1979, p. 8.
- [21] M. J. Morgan, *Dynamic Positioning of Offshore Vessels*. Tulsa, OK: Petroleum, 1978.
- [22] M. J. Grimble, "Design of optimal stochastic, regulating systems including integral action," *Proc. IEE*, vol. 126, pp. 841-848, Sept. 1979.
- [23] P. T. -K. Fung, Y. L. Chen, and M. J. Grimble, "Dynamic ship positioning control systems design including nonlinear thrusters and dynamics," presented at the NATO Advanced Study Inst. on Non-linear Stochastic Problems, Algarve, Portugal, May 1982, paper 16818.
- [24] J. Fotakis, M. J. Grimble, and B. Kouvaritakis, "A comparison of characteristic locus and optimal designs for dynamic ship positioning systems," *IEEE Trans. Automat. Contr.*, vol. AC-27, Dec. 1982.



Patrick Tze-Kwai Fung received the B.Sc. degree from the University of Leeds in 1977 and the M.Sc. degree from UMIST in 1978.

He was a Research Assistant at Sheffield City Polytechnic from 1978 to 1981, and a Research Fellow in 1981. From 1981 to 1982 he was a Research Fellow at the University of Strathclyde, Glasgow, Scotland. Since April 1982 he has been an Engineer at Spar Aerospace, Weston, Ont., Canada. His research interests are in optimal stochastic control, self-tuning and adaptive control and filtering, Kalman filtering, and application of modern control theory to industrial processes.



Mike J. Grimble (S'75-SM'78) was born in Grimsby, England, on October 30, 1943. He received the B.Sc. degree from Rugby College of Engineering Technology in 1970 and the M.Sc. and Ph.D. degrees from the University of Birmingham, Birmingham, England, in 1971 and 1974, respectively.

In 1971 he served a student apprenticeship with GEC Electrical Projects Ltd., and was employed as a Systems Design Engineer, working upon analog and computer control of industrial systems, including steel processing lines. He was seconded to the In-

dustrial Automation Group, Imperial College, where he worked on the development of models for cold rolling mills using functional analytic and gradient techniques. He joined the Department of Electrical and Electronic Engineering, Sheffield City Polytechnic in 1976 as a Senior Lecturer responsible for research. He was promoted to a Reader in Control Engineering in 1979, responsible for an industrial control group. He is currently a Professor of Industrial Systems at the University of Strathclyde, Glasgow, Scotland, and his group is concerned with industrial

control problems, particularly in the marine and steel industries. He is interested in optimal control, estimation theory, self-tuning, and multi-variable control systems design.

Dr. Grimble is past Chairman of the UKRI chapter of the CSS and is the Associate Editor of the journal *Optimal Control Applications and Methods*. He serves upon the Control Theory Committees of the International Federation of Automatic Control, the Institution of Electrical Engineers, and the Institute of Mathematics and its Applications.